Agrociencia

eISSN: 2521-9766

VOLUME 59, NUMBER 3 | April 01 - May 15, 2025 | MEXICO

AGRICULTURA
SECRETARÍA DE AGRICULTURA Y DESARROLLO RURAL

The opinions expressed by the authors do not necessarily reflect the position of the editor of the publication.

All correspondence (subscription information, sales, advertising, author contributions, etc.) should be addressed to:

Central Office:

Agrociencia
Guerrero No. 9, Esquina con Avenida Hidalgo,
San Luis Huexotla, Texcoco 56220,
State of Mexico. MEXICO
Tel.: +52-595 92 84427

https://agrociencia-colpos.org/index.php/agrociencia

Disclaimer: Trade marks or any commercial representations cited on scientific articles, essays or notes do not imply nor should be inferred as Agrociencia endorsement. No criticism, disclosure or rejection should be assumed either. Likewise, statements or recommendations expressed by authors are solely their responsibility and may not totally agree with those of the Editor.

Cover: *Solanum lycopersicum* L.
Photography and credits: Designed by Freepik
www.freepik.es

AGRICULTURA
SECRETARÍA DE AGRICULTURA Y DESARROLLO RURAL

Contents

Volume 59, Number 3 | April 01 - May 15, 2025

Agrociencia

BOOSTING ANTIOXIDANT ACTIVITY AND PHENOLIC CONTENT IN HASSAWI DATE PALM CALLUS THROUGH CHELATED IRON

Wael **Shehata**[1]

[1]King Faisal University. College of Agriculture and Food Sciences. Department of Agricultural Biotechnology. Al-Ahsa, Saudi Arabia. 31982.
* Author for correspondence: wshehata@kfu.edu.sa

ABSTRACT

TThe date palm (*Phoenix dactylifera* L.) is a vital crop in Saudi Arabia, the Arabian Peninsula, and numerous Arab countries, valued for its exceptional resilience to harsh environmental conditions and its profound nutritional, economic, and cultural importance. Tissue culture techniques have been utilized to preserve plant genetic integrity and pass on desirable qualities, allowing for regulated growth of plant tissues to safeguard certain genetic traits. Chelated iron, which is made up of iron ions attached to organic molecules, makes iron more soluble and bioavailable. It is an important part of many physiological processes in plants, including the production of chlorophyll, metabolic activity, and the response to stress. This study investigates the influence of chelated iron on the production of phenolic compounds and the activation of antioxidants in date palm callus cultures, focusing on three elite cultivars native to the Al-Ahsa Oasis: Khalas, Ruziz, and Shishi. Statistical analysis using analysis of variance (ANOVA), coupled with heat map visualizations, revealed a strong correlation between chelated iron concentration and the enhancement of phenolic content and antioxidant activity. Results demonstrated that a double concentration of chelated iron significantly improved the formation of phenolic compounds and boosted antioxidant activity across all cultivars, with the Shishi cultivar exhibiting the highest response. Notable differences were observed between cultivars and treatment levels, emphasizing the critical role of cultivar-specific responses in optimizing tissue culture protocols. These findings underscore the importance of chelated iron in enhancing the biochemical properties of date palm callus cultures and provide a foundation for refining tissue culture practices to support sustainable agriculture and genetic preservation in date palm cultivation.

Keywords: *Phoenix dactylifera* L., antioxidants, oxidative stress, phenolic compounds, somatic embryogenesis.

Citation: Shehata W. 2025. Boosting antioxidant activity and phenolic content in Hassawi date palm callus through chelated iron. **Agrociencia** 59(3): 293-308. https://doi.org/ 10.47163/ agrociencia.v59i3.3397

Editor in Chief:
Dr. Fernando C. Gómez Merino

Received: January 02, 2025.
Approved: April 11, 2025.
Published in Agrociencia:
May 07, 2025.

INTRODUCTION

Al-Ahsa Oasis, located in Saudi Arabia, is the largest green oasis globally and serves as a cornerstone of food security for the Kingdom. It is home to over 4.1 million date palm trees from more than 15 Hassawi cultivars, with Khalas, Ruziz, and Shishi collectively contributing more than 70 % of the oasis's total date production (Almadini *et al*., 2021; MEWA, 2023). These cultivars are valued for their adaptability to extreme conditions such as drought and high temperatures, as well as their nutritional, economic, and cultural significance. Dates from these trees are rich in dietary fiber, minerals, and sugars beneficial for human health (Al-Saikhan, 2006).

The date palm (*Phoenix dactylifera* L.) plays a pivotal role in environmental sustainability and is integral to Saudi Arabia's Vision 2030, which emphasizes the preservation of genetic resources and the sustainable use of natural assets for future generations. Despite its long lifecycle and limited production of offshoots (20–30 over a lifetime), the palm is a significant source of antioxidants, primarily concentrated in its fruits during the ripening stage, which occurs 5–8 years after planting (Shehata *et al*., 2014). These antioxidants have been shown to support immune health, combat oxidative stress, and reduce the risks of chronic diseases, including cancer and neurodegenerative disorders (Al-Shwyeh, 2019).

Micronutrients, although required in small amounts, are vital for plant growth and development, contributing to processes such as cell division, elongation, and the synthesis of secondary metabolites like phenolic compounds and antioxidants (Rency *et al*., 2018; Sinkovič *et al*., 2023). Iron is critical as it facilitates enzymatic reactions in respiration and photosynthesis and aids in mitigating oxidative stress by reducing free radicals (Amente and Chimdessa, 2021).

Given the high antioxidant potential of date palms and the importance of phenolic compounds for plant and human health, this study investigates the role of chelated iron in enhancing the production of antioxidants during the callus formation stage. By utilizing somatic embryogenesis in tissue culture, the research aims to optimize the concentration of chelated iron in the Murashige and Skoog (MS) nutrient medium to maximize antioxidant and phenolic compound production in Khalas, Ruziz, and Shishi cultivars. This work complements prior studies by exploring the biochemical and physiological impacts of chelated iron, paving the way for advancements in date palm micropropagation.

MATERIALS AND METHODS

Callus initiation

This experiment aimed to induce callus formation through indirect somatic embryogenesis using explants from shoot tips, leaf primordia, and axillary buds, focusing on three key Hassawi date palm cultivars (Khalas, Ruziz, and Shishi) due to their agricultural importance and consumer preference. The study investigated the relationship between phenolic content and browning during callus development and morphogenesis. Young offshoots, aged 4–5 years, measuring 70–100 cm in length and weighing 5–7 kg, were carefully selected between 2021 and 2022 from mature trees at the King Faisal University farm and meticulously separated from the parent trees to ensure the integrity of the plant material.

Sterilization protocol

To minimize contamination, the explants underwent a stringent sterilization process. First, they were washed three times with sterile distilled water. Next, they were immersed in a 60 % Clorox solution (containing 5.25 % sodium hypochlorite) for 20 min, followed by a 2–3-min soak in 100 % ethyl alcohol. Subsequently, the explants were treated with a 1.5 g L^{-1} mercury chloride ($HgCl_2$) solution for 3–5 min. After each step, the explants were rinsed at least three times with sterile distilled water to ensure complete removal of sterilizing agents (Alturki *et al*., 2013; Aldaej *et al*., 2014; Shehata *et al*., 2014).

Nutrient medium preparation

The explants were cultured on a basal Murashige and Skoog (MS) nutrient medium (Murashige and Skoog, 1962), formulated with specific concentrations of inorganic salts (Table 1). The medium was prepared by mixing 20 mL each of stock solutions A and B and 5 mL each of stocks C, D, E, F, and G with approximately 1000 mL of distilled

Table 1. Impact factors of chelated iron (Stock F) and supplementary components used in the Murashige and Skoog (MS) medium for date palm (*Phoenix dactylifera* L.) callus formation.

Stock solution	Constituents	Concentration (g L^{-1})	Final concentration in MS medium (mg L^{-1})	To make up 1 L of MS medium (mL L^{-1})	Concentration difference	Code
A	NH_4NO_3	82.50	1650.00	20	Full	---
B	KNO_3	95.00	1900.00	20	Full	---
C	H_3BO_3	1.240	6.20	5	Full	---
	KH_2PO_4	34.00	170.00			
	KI	0.166	0.83			
	$Na_2MoO_4{\cdot}2H_2O$	0.050	0.25			
	$CoCl_2{\cdot}6H_2O$	0.005	0.025			
D	$CaCl_2{\cdot}2H_2O$	88.00	440.00	5	Full	---
E	$MgSO_4{\cdot}7H_2O$	74.00	370.00	5	Full	---
	$MnSO_4{\cdot}4H_2O$	4.460	22.30			
	$ZnSO_4{\cdot}7H_2O$	1.720	8.60			
	$CuSO_4{\cdot}5H_2O$	0.005	0.025			
F*	$Na_2{\cdot}EDTA$	7.450	37.25	5	Zero	F-1
					Half	F-2
	$FeSO_4{\cdot}7H_2O$	5.570	27.85		Full	F-3
					Double	F-4
G	Thiamine·HCl	0.200	0.10	5	Full	---
	Nicotinic acid	0.100	0.50			
	Pyrodoxine·HCl	0.100	0.50			
	Glycine	0.400	2.00			

*The standard Stock F levels (chelated iron F-1: zero; F-2: half; F-3: full; F-4: double).

water under continuous stirring. This medium provided a consistent foundation for the experimental procedures, ensuring successful callus initiation and enabling the investigation of phenolic compounds' role in browning and antioxidant production in date palm tissue cultures.

Experimental design and measurements

The experiment evaluated varying concentrations of Na_2·EDTA and $FeSO_4·7H_2O$ (Stock F solution) to improve the growth medium for *in vitro* date palm tissue culture. Key parameters, including explant survival rates, callus initiation, and browning, were systematically assessed after each subculture. Biochemical assays were used to quantify the total phenolics and antioxidant enzyme activities to assess the efficacy of the medium. The study aimed to determine the optimal balance of iron and chelating agents, enhancing plant growth and antioxidant production while avoiding toxicity or nutrient deficiencies. Since excessive iron can be detrimental, Na_2·EDTA was used carefully to prevent over-chelation and maintain a balanced nutrient profile (Table 1). This stock solution was prepared by dissolving each constituent in 200 mL of distilled water. The Na_2·EDTA·$2H_2O$ solution was heated, and the $FeSO_4·7H_2O$ solution was added with continuous stirring. After cooling, it was diluted to 1000 mL with distilled water. All stocks were stored in amber-colored bottles in refrigeration. Modified media used for cultures were supplemented with different concentrations of phytohormones, carbohydrates, vitamins, and other addenda (Murashige and Skoog, 1962).

Preparation of nutrient medium

The pH of the nutrient medium was adjusted to 5.7 using 1N KOH or 1N HCl. The medium was then autoclaved at 121 °C (1.2 kg cm^{-2} pressure) for 20 min before the addition of the gelling agent. To assess the impact of varying levels of Na_2·EDTA and $FeSO_4·7H_2O$ on synthetic antioxidant production, the medium was prepared with concentrations set at zero, half, full, and double the standard Stock F levels. It was further supplemented with specific compounds (mg L^{-1}): 170 $NaH_2PO_4·2H_2O$, 80 adenine sulfate, 100 myo-inositol, 30 000 sucrose, 2000 gerlite, 2000 activated charcoal, 2.5 thiamine-HCl, 2 biotin, 100 2,4-dichlorophenoxyacetic acid, and 3 6-benzylaminopurine (Sigma-Aldrich, USA). The final medium was dispensed into jars containing 25 ml each and sterilized again under the same autoclaving conditions (Alturki *et al*., 2013; Shehata *et al*., 2014; Aldaej *et al*., 2014).

Callus cultivation and incubation conditions

Sterilized explants were cultured on the prepared medium and incubated under dark conditions at 25 ± 2 °C. Cultures were refreshed with modified media every two months over an eight-month incubation period. Data were collected at the end of three subcultures (8, 16, and 24 weeks) for each date palm cultivar, recording the number of surviving explants, callus initiation, and the extent of browning. The visual scoring system used by Pottino (1981) was used to read callus data and brown discoloration on the explants of each variety under study, with five replicates for each treatment.

Methods of antioxidant analysis

After the callus formation stage for all explants from the three date palm cultivars, samples of the callus (3 g) from each treatment were collected for analysis to determine their total phenolic content (mg g^{-1}), expressed as gallic acid equivalents, and antioxidant activity using the 2,2′-azino-bis(3-ethylbenzothiazoline-6-sulfonic acid) (ABTS) method. The resulting data were analyzed and compared to identify significant differences between the treatments, using the least significant difference (LSD) test at the 5 % probability level.

Antioxidant analysis was conducted using 3 g of callus tissue, which was ground and homogenized for 10–12 min. The homogenized tissue was extracted with 100 mL of methanol at 20 °C for 5 h using an orbital shaker (LSI-LabTECH, Korea). After filtration, the mixture was centrifuged at 4000 rpm for 10 min under reduced pressure at 40 °C. The supernatant was concentrated using a rotary evaporator for 3 h, yielding the methanol crude extract, which was stored in dark glass bottles at freezer temperatures for three days prior to analysis.

Reagents for the analysis included catechin, sodium carbonate, gallic acid, ascorbic acid, sodium nitrate, trichloroacetic acid, methanol, aluminum chloride, and Folin-Ciocalteu's phenol reagent, which were sourced from Merck (Germany). Additional chemicals, such as 2,4,6-tripyridyl-S-triazine (TPTZ), ABTS, Trolox, $FeCl_3{\cdot}3H_2O$, potassium persulfate, sodium carbonate, and sodium acetate, were procured from Sigma-Aldrich (USA). Antioxidant activity was assessed using the enhanced ABTS method (Cai *et al*., 2004), with Trolox standard solutions (0–15 μM in 80 % ethanol) used to generate a standard curve. Sample absorbance was measured against the Trolox standard, and antioxidant activity was expressed in Trolox equivalents. Total phenolic content was determined using the Folin-Ciocalteu method (Singleton and Rossi, 1965), with results expressed as mg of gallic acid equivalents (GAE) per 100 g of sample, following the protocol by Shui and Leong (2006).

Data analysis

Data analysis was performed using analysis of variance (ANOVA) following a completely randomized design, as outlined by Gomez and Gomez (1984). Treatment means were compared using the least significant difference (LSD) test at a 5 % significance level to determine statistically significant differences. Statistical analyses were conducted using the SAS software (SAS Institute Inc., 2001). Additionally, multivariate analysis, including heat map visualization, was carried out using Orange Data Mining software (Demsar *et al*., 2013) to evaluate the correlation between antioxidant activity and total phenolic content in the explants.

RESULTS AND DISCUSSION

Effect of chelated iron (Stock F) on callus initiation of Hassawi date palm

Increasing the concentration of chelated iron positively influenced explant survival across all cultivars (Figure 1). Higher concentrations, particularly full and double, resulted in improved survival rates (3.67 and 3.33, respectively). Among the three cultivars, Shishi (Sh) exhibited the highest explant survival under increased iron concentrations (3.08), followed by Khalas (Kh) (2.34), while Ruziz (Ru) (2.25) demonstrated the lowest survival rates overall. These findings suggest that iron availability is a key factor in explant viability and callus initiation, likely due to its role in oxidative stress management (Briat *et al*., 2007; Xiao *et al*., 2021).

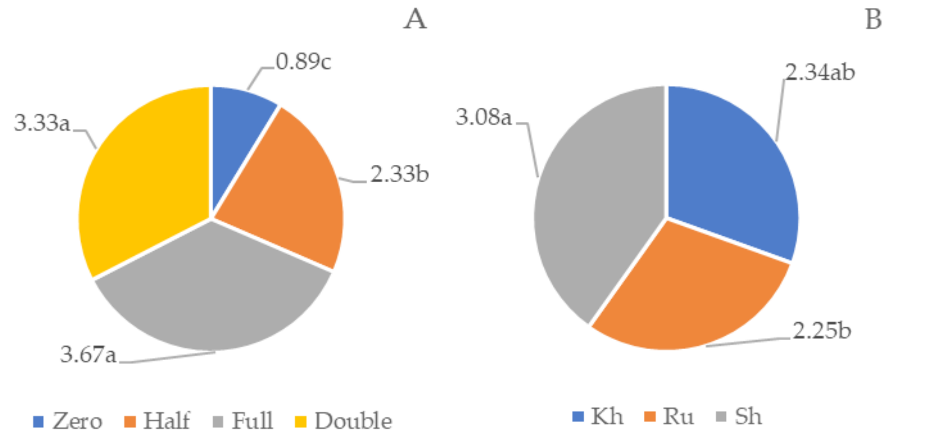

Figure 1. Effect of different concentrations of chelated iron (Stock F solution) (A) and three date palm cultivars (*Phoenix dactylifera* L.) (B) on the number of surviving explants during callus *in vitro* initiation. Kh: Khalas; Ru: Ruziz; Sh: Shishi. Values with different letters are statistically different ($p \leq 0.05$).

Data indicates that survival rates were significantly influenced by both iron concentration and cultivar type (Figure 2). Among the iron treatments, higher concentrations (full and double) resulted in greater explant survival across all cultivars, confirming the essential role of iron in promoting cell viability and reducing oxidative stress during early tissue culture stages. In contrast, explants treated with zero and half iron concentrations showed lower survival rates, indicating that insufficient iron availability affects cell division and metabolic activities (Al-Shwyeh, 2019). When comparing cultivars, Sh showed the highest survival rate at all iron concentrations, indicating a strong adaptive response to iron supplementation. Kh showed intermediate survival rates, while Ru had the lowest survival rates, even at high iron concentrations. This variation can be linked to the viability of the cultivar grown in iron absorption.

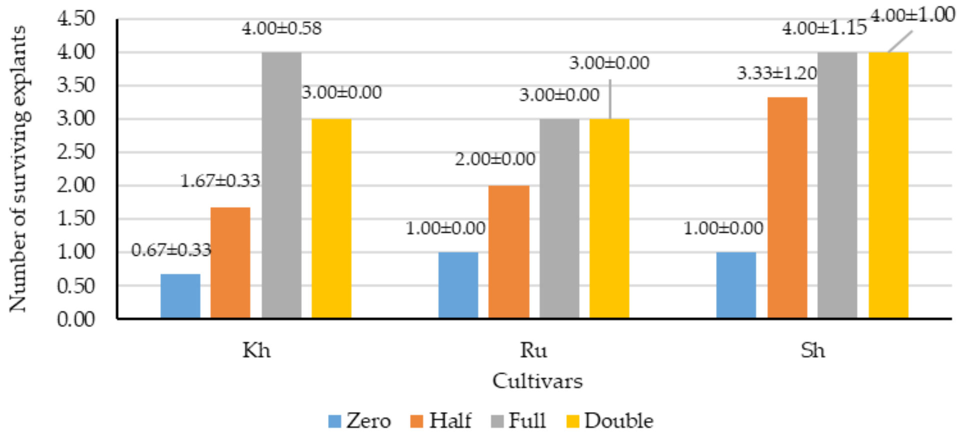

Figure 2. Interaction effects of different concentrations of chelated iron (Stock F solution) and date palm cultivars (*Phoenix dactylifera* L.) on the number of surviving explants during callus *in vitro* initiation. Kh: Khalas; Ru: Ruziz; Sh: Shishi. Significance level (S = 0.0001, T = not significant (NS), S × T = NS).

Increasing the concentration of chelated iron significantly enhanced callus initiation, with explants exposed to full and double iron levels exhibiting the highest callus formation at the same rates (1.56) (Figure 3A). In contrast, explants cultured with half and zero iron concentrations demonstrated slower and lower callus induction (1.11 and 1.00, respectively), suggesting that iron availability is a limiting factor in early-stage callus development. The positive effect of higher iron concentrations could be attributed to its role in cell division, enzyme activation, and oxidative stress reduction, all of which are critical for successful callus initiation (Rency *et al*., 2018).

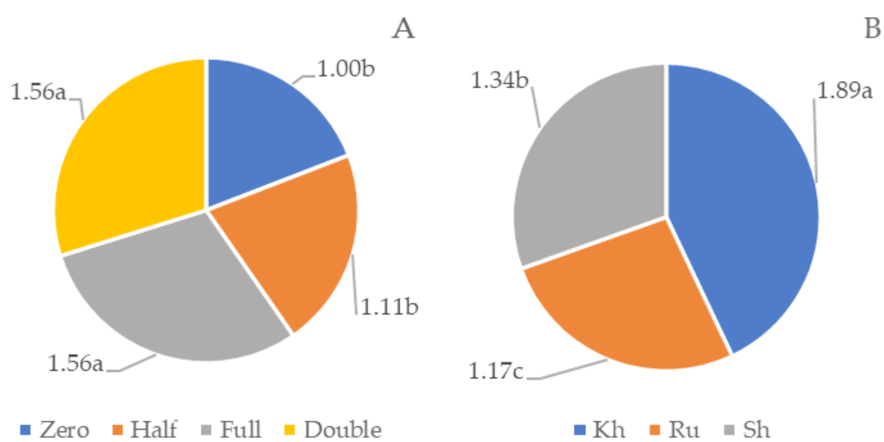

Figure 3. Effect of different concentrations of chelated iron (Stock F solution) (A) and three date palm cultivars (*Phoenix dactylifera* L.) (B) on callus initiation rates during *in vitro* culture. Kh: Khalas; Ru: Ruziz; Sh: Shishi. Values with different letters are statistically different ($p \leq 0.05$).

For the callus initiation responses among the three cultivars, Kh and Sh exhibited superior callus induction rates (1.89 and 1.34, respectively), particularly under full and double iron treatments, whereas Ru displayed relatively lower callus formation across all iron concentrations (1.17) (Figure 3B). This callus induction variation through different date palm rootstocks suggests that different cultivars may have distinct iron uptake mechanisms, influencing their responsiveness to iron supplementation in tissue culture (Al-Shwyeh, 2019).

The results indicated that higher iron concentrations (full and double) positively influenced callus initiation across all three cultivars (Figure 4). Notably, Kh and Sh achieved the highest callus induction rates under full and double iron treatments, with an average value of 1.67. In contrast, Ru showed a relatively lower response, particularly under zero and half iron concentrations, where callus initiation remained at 1.00.

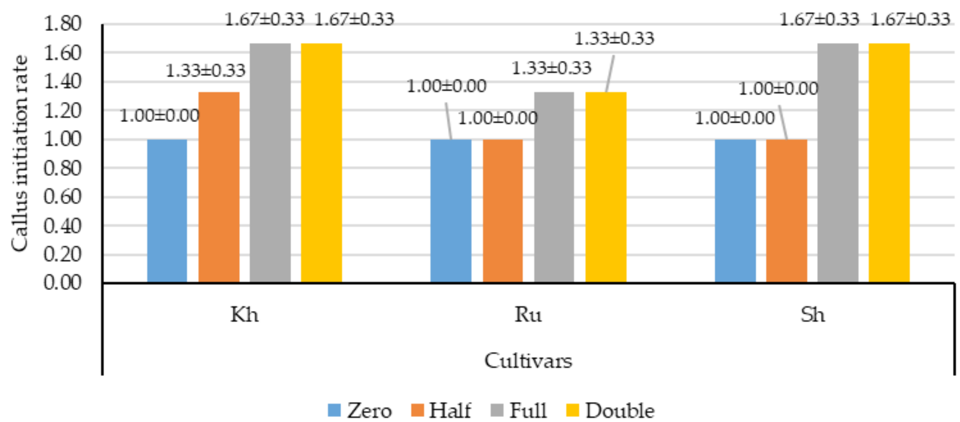

Figure 4. Interaction effect of different concentrations of chelated iron (Stock F solution) and three different date palm cultivars (*Phoenix dactylifera* L.) on callus initiation rate during *in vitro* culture. Kh: Khalas; Ru: Ruziz; Sh: Shishi. Significance level (S = not significant (NS), T = NS, S × T = NS).

These findings emphasize the importance of optimizing iron supplementation in tissue culture media to enhance callus induction, particularly for cultivars with lower inherent responsiveness, such as Ru. Future studies could further investigate the molecular mechanisms underlying cultivar-specific differences in iron metabolism to improve large-scale propagation strategies for elite date palm cultivars.

The varying iron concentrations on browning severity showed the highest browning observed at the double iron level (3.45), followed by the half (2.44) and full (1.78) treatments, while the lowest browning occurred under zero iron conditions (1.33) (Figure 5A). These results suggest that higher iron concentrations accelerate oxidative stress, leading to increased phenolic oxidation and tissue browning (Gill and Tuteja, 2010).

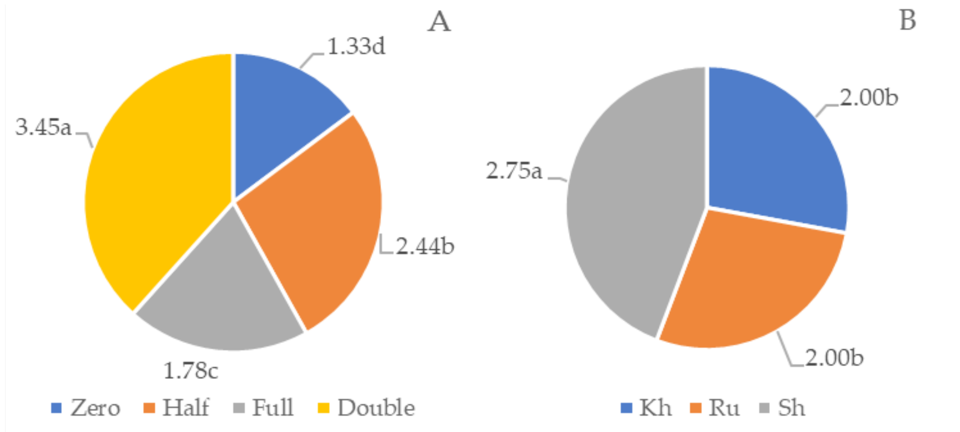

Figure 5. Specific effect of different concentrations of chelated iron (Stock F solution) (A) and three date palm cultivars (*Phoenix dactylifera* L.) (B) on the browning intensity during callus *in vitro* initiation. Kh: Khalas; Ru: Ruziz; Sh: Shishi. Values with different letters are statistically different ($p \leq 0.05$).

The cultivars showed an effect on the browning severity (Figure 5B). Sh exhibited the highest browning intensity (2.75), significantly greater than Kh and Ru, both of which showed similar browning levels (2.00). The higher browning observed in Sh may indicate a greater accumulation of phenolic compounds, which, upon oxidation, contribute to tissue browning. In contrast, the relatively lower browning in Kh and Ru suggests a better ability to regulate antioxidant enzyme activity, or potentially due to differences in iron uptake efficiency among cultivars, as previously indicated by Al-Saikhan (2006).

These results highlight the importance of cultivar selection when optimizing tissue culture conditions, as excessive browning can negatively affect explant viability and callus formation. Future studies should explore strategies to mitigate browning, such as the use of antioxidants, polyphenol oxidase inhibitors such as ascorbic acid, polyvinylpyrrolidone (PVP), and iron supplementation to minimize browning to enhance tissue culture success and elevate callus formation efficiency (Jones and Saxena, 2013; Amente and Chimdessa, 2021).

Both the iron concentration and cultivar significantly influenced browning intensity (Figure 6). Double-strength chelated iron resulted in the highest browning across all cultivars, with values of 3.67 in Kh and Sh and 3.00 in Ru, suggesting that excess iron may promote oxidative stress, leading to increased browning. The zero-iron treatment showed the lowest browning, with values of 1.00 in Kh and Ru and 2.00 in Sh, indicating that iron is involved in browning but excessive amounts accelerate the process. Meanwhile, the half- and full-strength iron treatments produced moderate browning levels, with cultivar-specific differences. For example, in Kh, half-strength (2.33) caused more browning than full-strength (1.00), while in Ru and Sh, full-strength iron led to slightly higher browning than half-strength.

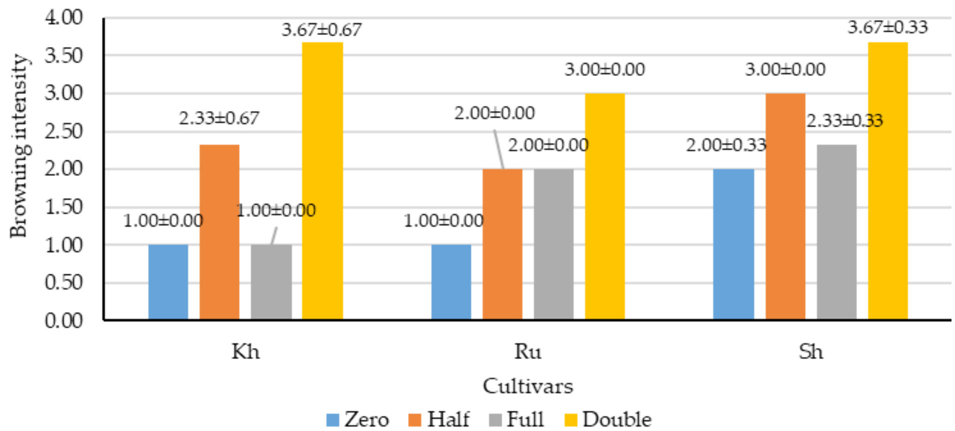

Figure 6. Interaction effect of different concentrations of chelated iron (Stock F solution) and three date palm cultivars (*Phoenix dactylifera* L.) on the browning intensity during callus *in vitro* initiation. Kh: Khalas; Ru: Ruziz; Sh: Shishi. Significance level (S = 0.001, T = 0.005, S × T = not significant).

These results suggest that the lack of chelated iron negatively affected cell growth and elongation, possibly due to insufficient enzyme formation required for respiration and photosynthesis, which are vital for cellular functions. Iron is involved in the synthesis of these enzymes and the reduction of free radicals, which helps mitigate oxidative stress (Gill and Tuteja, 2010; Amente and Chimdessa, 2021).

Effect of chelated iron on antioxidant activities of Hassawi date palm

After eight months of *in vitro* culture, increasing the iron concentration enhanced both phenolic accumulation and antioxidant activity, though the extent of this effect varies among cultivars (Table 2). In terms of total phenolic content, the data reveals a strong positive correlation between iron concentration and phenolic compound production. Sh exhibited the highest total phenolic content, reaching 2.987 mg g^{-1} under the double-strength iron treatment (F-4), followed by Kh, which showed a maximum phenolic content of 1.949 mg g^{-1} at the same iron level. In contrast, Ru exhibited the lowest phenolic accumulation, with its highest recorded value being 1.274 mg g^{-1} at F-4. These differences suggest that certain cultivars, particularly Sh and Kh, may have a stronger capacity for phenolic biosynthesis in response to iron supplementation, while Ru appears to be less responsive to increased iron availability.

Similarly, antioxidant activity, as measured by ABTS inhibition percentage and Trolox equivalent (µM Trolox), followed the same trend. Sh demonstrated the highest antioxidant activity, recording 96.75 % inhibition and 981.66 µM Trolox under the F-4 treatment, whereas Kh reached 74.95 % inhibition and 739.03 µM Trolox at the same iron concentration. Ru again exhibited the lowest antioxidant capacity, with its maximum values being 58.04 % inhibition and 554.81 µM Trolox at F-4. Explants cultured without chelated iron (F-1) had the lowest phenolic content and antioxidant activity, confirming the essential role of iron in secondary metabolite production.

Table 2. Impact of different concentrations of chelated iron and date palm cultivars (*Phoenix dactylifera* L.) on total phenolic content and antioxidant activity during eight months of *in vitro* culture.

Cultivar	Chelated iron	*Total phenolic content (mg g^{-1})	Antioxidant activity by ABTS Inhibation (%)	UMTrolox
Kh	F-1	0.843 ± 0.004[i]	37.650 ± 0.080[h]	333.568 ± 2.853[h]
	F-2	1.339 ± 0.003[d]	58.079 ± 0.201[d]	556.785 ± 3.742[d]
	F-3	0.998 ± 0.020[i]	42.853 ± 0.090[f]	391.654 ± 1.458[f]
	F-4	1.949 ± 0.007[c]	74.959 ± 0.279[c]	739.030 ± 2.873[c]
Ru	F-1	0.784 ± 0.004[k]	32.352 ± 0.214[i]	277.364 ± 4.720[i]
	F-2	1.257 ± 0.005[e,f]	51.167 ± 0.235[e]	482.674 ± 2.076[e]
	F-3	0.653 ± 0.002[l]	28.444 ± 0.130[k]	233.401 ± 3.001[j]
	F-4	1.274 ± 0.004[e]	58.048 ± 0.190[d]	554.812 ± 4.720[d]
Sh	F-1	0.955 ± 0.010[h]	39.324 ± 0.287[g]	359.867 ± 5.173[g]
	F-2	2.560 ± 0.003[b]	95.174 ± 0.060[b]	972.308 ± 0.449[b]
	F-3	0.837 ± 0.003[j]	28.945 ± 0.197[j]	234.278 ± 1.112[j]
	F-4	2.987 ± 0.010[a]	96.754 ± 0.211[a]	981.661 ± 3.704[a]
Least significant difference at $p \leq 0.05$		1.754	0.404	4.825

*Total phenolic concentration expressed as mg of gallic acid equivalents (GAE) per 100 g of sample. ABTS: 2,2’-azino-bis(3-ethylbenzothiazoline-6-sulfonic acid) method; Kh: Khalas; Ru: Ruziz; Sh: Shishi. Stock F (F-1: zero; F-2: half; F-3: full; F-4: double).

Additionally, cultivar differences were evident, as Sh consistently outperformed Kh and Ru in phenolic accumulation and antioxidant capacity across all iron treatments (Al-Saikhan, 2006). These findings highlight the importance of iron availability in tissue culture media, not only for promoting callus formation but also for enhancing the production of bioactive compounds, likely due to its role in activating antioxidant enzymes and promoting phenolic biosynthesis (Amente and Chimdessa, 2021).

The heat map (Figure 7) generated from the experimental data illustrates the significant effect of chelated iron on both total phenolic content and antioxidant activity across different date palm cultivars (Kh, Ru, and Sh). The data showed a clear increase in phenolic content and antioxidant activity (measured by inhibition percentage and μM Trolox) as the concentration of chelated iron rises. Specifically, Sh exhibited the highest levels of phenolic content (2.987 mg g^{-1}), inhibition (96.754 %), and μM Trolox (981.661) when exposed to the highest iron concentration (F-4). In contrast, Ru showed relatively lower phenolic content and antioxidant activity, indicating cultivar-specific responses to iron supplementation. Iron plays an important role in plant physiology, especially in enhancing secondary metabolite production and activating antioxidant defense mechanisms. Iron is crucial for the synthesis of antioxidant enzymes, such as catalase and peroxidase, which help mitigate oxidative stress by neutralizing reactive

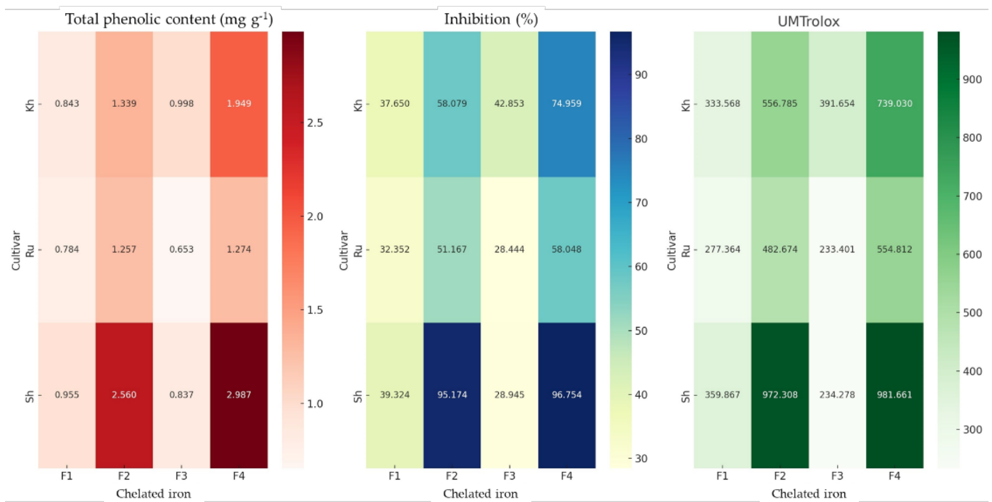

Figure 7. Heat map analysis of chelated iron effects on phenolic content, antioxidant activity, and Trolox equivalent levels (μM Trolox) in Khalas, Ruziz, and Shishi date palm cultivars (*Phoenix dactylifera* L.). Kh: Khalas; Ru: Ruziz; Sh: Shishi. Stock F (F-1: zero; F-2: half; F-3: full; F-4: double).

oxygen species (ROS) (Gopinathan *et al*., 2020). Furthermore, phenolic compounds, which contribute to a plant's antioxidant properties, are often produced in response to increased nutrient availability, including iron (Shui and Leong, 2006).

Iron is a vital component of chlorophyll, which is necessary for photosynthesis. Adequate iron levels, provided by $FeSO_4{\cdot}7H_2O$, can enhance photosynthetic efficiency in date palms. Increased photosynthesis can indirectly support the production of antioxidants. Additionally, iron acts as a cofactor for several enzymes involved in key metabolic processes, including antioxidant defense (Hell and Stephan, 2003). $FeSO_4{\cdot}7H_2O$ can activate enzymes such as catalase (CAT), superoxide dismutase (SOD), and peroxidase (POD), which help scavenge reactive oxygen species (ROS) and protect the plant from oxidative damage (Xiao *et al*., 2021). The availability of sufficient iron is crucial for the synthesis of antioxidants like vitamins C and E, which neutralize ROS and maintain cellular integrity (Abdellatif *et al*., 2022). By ensuring an adequate supply of iron, date palms may show enhanced tolerance to environmental stress, leading to a potential increase in antioxidant production (Sinha *et al*., 1997).

Iron is usually added to the MS nutrient medium in the form of $FeSO_4{\cdot}7H_2O$. It is prepared after dissolving it with the compound $Na_2{\cdot}$EDTA (sodium ethylenediaminetetraacetate) that has significant effects on plant growth, development, and antioxidant production. It plays a crucial role in plant metabolism by participating in univalent redox reactions, where it alternates between its oxidized form (ferric, Fe^{3+}) and its reduced form (ferrous, Fe^{2+}) (Gopinathan *et al*., 2020). These two oxidation states of iron can influence plant physiology, including the production of antioxidants, which are essential for protecting plants from oxidative stress (Xiao *et al*., 2021).

Iron is an integral component of chlorophyll, the molecule responsible for photosynthesis. Adequate levels of iron enhance photosynthetic efficiency, potentially boosting energy production and the synthesis of antioxidants (George *et al*., 2008). A deficiency in iron can result in chlorosis, a condition that hinders plant health and may disrupt antioxidant production (Krohling *et al*., 2016; Zhang *et al*., 2019). Ferric iron (Fe^{3+}), being the oxidized form, is generally less soluble in water compared to ferrous iron and is less accessible to plants, particularly in high pH environments (Marschner *et al*., 2011). As a result, plants may struggle to absorb ferric iron, leading to deficiencies that negatively impact growth and antioxidant formation (Briat *et al*., 2007 Al-Mayahi, 2021).

Ferrous iron (Fe^{2+}) is the reduced form of iron, meaning it has gained electrons. It is generally more soluble in water than ferric iron (Zhang *et al*., 2019). Ferrous iron is more readily absorbed by plantlet roots due to its higher solubility. However, under iron-deficient conditions, ferric iron is usually reduced to ferrous iron, transporting across cellular membranes (Jain *et al*., 2014). Adequate levels of ferrous iron support are essential for plant functions, including chlorophyll synthesis and various enzymatic activities. Sufficient ferrous iron availability can positively influence antioxidant formation in plants, since it is directly involved in the synthesis and activation of enzymes that contribute to antioxidant defense mechanisms (Al-Mayahi, 2021).

On the other hand, sodium ethylenediaminetetraacetate ($Na_2 \cdot EDTA$) is a chelating agent commonly used to improve the availability of essential micronutrients, particularly iron, in nutrient media by forming stable, water-soluble complexes with metal ions, enhancing their uptake by plants (Ramos *et al*., 2009). This process can influence antioxidant production in date palms by facilitating the absorption of key micronutrients like iron, zinc, copper, and manganese, which serve as cofactors for enzymes such as catalase (CAT), peroxidase (POD), and superoxide dismutase (SOD), all vital for combating oxidative stress (Abdellatif *et al*., 2022).

By improving micronutrient uptake, $Na_2 \cdot EDTA$ can also support the synthesis of photosynthetic pigments like chlorophyll, indirectly boosting antioxidant production and enhancing the plant's ability to respond to reactive oxygen species (ROS) (Al-Mayahi, 2021; Abdellatif *et al*., 2022). However, its use must be carefully managed, as environmental factors like light intensity and temperature can affect its efficiency (Aebi, 1983). Furthermore, while $Na_2 \cdot EDTA$ offers benefits in nutrient management, it poses potential environmental risks due to its ability to form stable complexes with heavy metals, which may become mobilized in the environment if improperly handled (Al-Mayahi, 2021). Therefore, $Na_2 \cdot EDTA$ should be applied cautiously, with careful consideration of its environmental impact and its influence on nutrient balance, especially in *in vitro* preparations where conditions such as light and temperature must be precisely controlled.

CONCLUSIONS

This study highlights the potential of date palm tissue culture as an efficient and sustainable method for producing antioxidants year-round, independent of fruit ripening or offshoot availability. The findings confirm that Murashige and Skoog medium supplemented with chelated iron supports optimal callus formation, even at low concentrations, while higher iron levels (double-strength) significantly enhance antioxidant production. Among the tested cultivars, Shishi, particularly under double-strength iron treatment, demonstrated superior potential for antioxidant biosynthesis, suggesting its suitability for nutritional and pharmaceutical applications. These results emphasize the role of optimized *in vitro* culture conditions in improving the production of secondary metabolites such as flavonoids and phenols, which enhance the antioxidant capacity of date palm explants.

ACKNOWLEDGEMENTS

I extend my thanks to the Deanship of Scientific Research, Vice Presidency for Graduate Studies and Scientific Research, King Faisal University, Saudi Arabia (Project No. KFU250516), for supporting this research work.

I also extend my sincere thanks to both Prof. Dr. Saleh Alturki and Prof. Dr. Muhammad Aldaej for participating in the previous work of this study, as well as Dr. Jamal Rayyan for his contribution in conducting the statistical analysis for this research.

FUNDING

This work was supported by the Deanship of Scientific Research, Vice Presidency for Graduate Studies and Scientific Research, King Faisal University, Saudi Arabia [Project No. KFU250516].

REFERENCES

Abdellatif YMR, Elsayed MS, Hassan MM, Ahmed IA, Ragab AH, Shams El-Din IM, Abdelaal WB, Abd El-Aal MS, Zein El Din AFM. 2022. Zinc oxide nanoparticles and Fe-modified activated carbon affecting the *in vitro* growth of date palm plantlets *cv*. Medjool. Horticulturae 8 (12): 1179. https://doi.org/10.3390/horticulturae8121179

Aebi H. 1983. Catalase. *In* Bergmeyer HU. (ed.), Methods of Enzymatic Analysis. Academic Press: New York, NY, USA, pp: 273–286.

Aldaej MI, Alturki SM, Shehata WF, Ghazzawy HS. 2014. Effect of potassium nitrate on antioxidants production of date palm (*Phoenix dactylifera* L.) *in vitro*. Pakistan Journal of Biological Sciences 17 (12): 1209–1218. https://doi.org/10.3923/pjbs.2014.1209.1218

Almadini AM, Ismail AIH, Ameen FA. 2021. Assessment of farmers practices to date palm soil fertilization and its impact on productivity at Al-Hassa oasis of KSA. Saudi Journal of Biological Sciences 28 (2): 1451–1458. https://doi.org/10.1016/-j.sjbs.2020.11.084

Al-Mayahi AMW. 2021. *In vitro* plant regeneration system for date palm (*Phoenix dactylifera* L.): Effect of chelated iron sources. Journal of Genetic Engineering and Biotechnology 19 (1): 83. https://doi.org/10.1186/s43141-021-00177-4

Al-Saikhan MS. 2006. Physical and chemical characteristics response of three date palm cultivars to source of pollen grains. The Journal of Agricultural Science, Mansoura University 31 (3): 1537–1546. https://doi.org/10.21608/jpp.2006.235752

Al-Shwyeh HA. 2019. Date palm (*Phoenix dactylifera* L.) fruit as potential antioxidant and antimicrobial agents. Journal of Pharmacy and Bioallied Sciences 11 (1): 1–11. https://doi.org/10.4103/jpbs.jpbs_168_18

Alturki SM, Shehata WF, Aldaej MI. 2013. Influence of nutrient medium on antioxidants production of date palm (*Phoenix dactylifera* L.) cultivars *in vitro*. Asian Journal of Plant Sciences 12 (3): 119–127. https://doi.org/10.3923/ajps.2013.119.127

Amente G, Chimdessa E. 2021. Control of browning in plant tissue culture: A review. Journal of Scientific Agriculture 5: 67–71. https://doi.org/10.25081/jsa.2021.v5.7266

Briat JF, Curie C, Gaymard F. 2007. Iron utilization and metabolism in plants. Current Opinion in Plant Biology 10 (3): 276–282. https://doi.org/10.1016/j.pbi.2007.04.003

Cai Y, Luo Q, Sun M, Corke H. 2004. Antioxidant activity and phenolic compounds of 112 traditional Chinese medicinal plants associated with anticancer. Life Sciences 74 (17): 2157–2184. https://doi.org/10.1016/j.lfs.2003.09.047

Demsar J, Curk T, Erjavec A, Gorup C, Hocevar T, Milutinovic M, Mozina M, Polajnar M, Toplak M, Staric A, *et al*. 2013. Orange: Data mining toolbox in Pytho. Journal of Machine Learning Research 14: 2349−2353.

George EF, Hall MA, Klerk GJ. 2008. Plant propagation by tissue culture (Third edition). Springer: Dordrecht, Netherlands. 107 p. https://doi.org/10.1007/978-1-4020-5005-3_8

Gill SS, Tuteja N. 2010. Reactive oxygen species and antioxidant machinery in abiotic stress tolerance in crop plants. Plant Physiology and Biochemistry 48 (12): 909–930. https://doi.org/10.1016/j.plaphy.2010.08.016

Gomez KA, Gomez AA. 1984. Statistical procedures for agricultural research (Second edition). John Wiley and Sons: New York, NY, USA. 680 p.

Gopinathan P, Parthiban S, Magendran T, Ayad M, Al-Quraishi F, Ashok SK, Singh PK. 2020. Mapping of ferric (Fe^{3+}) and ferrous (Fe^{2+}) iron oxides distribution using band ratio techniques with ASTER data and geochemistry of Kanjamalai and Godumalai, Tamil Nadu, South India. Remote Sensing Applications: Society and Environment 18: 100306. https://doi.org/10.1016/j.rsase.2020.100306

Hell R, Stephan UW. 2003. Iron uptake, trafficking and homeostasis in plants. Planta 216 (4): 541–551. https://doi.org/10.1007/s00425-002-0920-4

Jain A, Wilson GT, Connolly EL. 2014. The diverse roles of FRO family metalloreductases in iron and copper homeostasis. Frontiers in Plant Science 5: 100. https://doi.org/10.3389/fpls.2014.00100

Jones AMP, Saxena PK. 2013. Inhibition of phenylpropanoid biosynthesis in *Artemisia annua* L.: A novel approach to reduce oxidative browning in plant tissue culture. PLoS ONE 8 (10): e76802. https://doi.org/10.1371/journal.pone.0076802

Krohling CA, Eutrópio FJ, Bertolazi AA, Dobbss LB, Campostrini E, Dias T, Ramos AC. 2016. Ecophysiology of iron homeostasis in plants. Soil Science and Plant Nutrition 62 (1): 39–47. https://doi.org/10.1080/00380768.2015.1123116

Marschner P, Crowley D, Rengel Z. 2011. Rhizosphere interactions between microorganisms and plants govern iron and phosphorus acquisition along the root axis-model and research methods. Soil Biology and Biochemistry 43 (5): 883–894. https://doi.org/10.1016/j.soilbio.2011.01.005

MEWA (Ministry of Environment, Water and Agriculture, Water and Agriculture). 2023. MEWA Statistical Book 1444–1445. Department of General Information and Statistics. Deputyship of Economic and Investment Affairs. Ministry of Environment. Riyadh, Saudi Arabia. https://mewa.gov.sa/en/MediaCenter/Ads/Pages/Saudi-Agriculture-2023.aspx (Retrieved: February 2025).

Murashige T, Skoog FA. 1962. A revised medium for rapid growth and bioassays with tobacco tissue culture. Physiologia Plantarum 15 (3): 473–479. https://doi.org/10.1111/j.1399-3054.1962.tb08052.x

Pottino BG. 1981. Methods in plant tissue culture. Kemtec Educational Corporation: College Park, Maryland, USA. 72 p.

Ramos AC, Lima PT, Dias PN, Kasuya MCM, Feijó JA. 2009. A pH signaling mechanism involved in the spatial distribution of calcium and anion fluxes in ectomycorrhizal roots. New Phytologist 181 (2): 448–462. https://doi.org/10.1111/j.1469-8137.2008.02656.x

Rency AS, Pandian S, Ramesh M. 2018. Influence of adenine sulphate on multiple shoot induction in *Clitoria ternatea* L. and analysis of phyto-compounds in *in vitro* grown plants. Biocatalysis and Agricultural Biotechnology 16: 181–191. https://doi.org/10.1016/j.bcab.2018.07.034

SAS Institute Inc. 2001. SAS for windows, SAS user's guide: Statistics. Version 8.0 e. User's Guide. Cary, NC, USA. https://www.scirp.org/reference/ReferencesPapers?-ReferenceID-=1431657 (Retrieved: February 2025).

Shehata WF, Aldaej MI, Alturki SM, Ghazzawy HS. 2014. Effect of ammonium nitrate on antioxidants production of date palm (*Phoenix dactylifera* L.) *in vitro*. Biotechnology 13 (3): 116–125. https://doi.org/10.3923/biotech.2014.116.125

Shui G, Leong LP. 2006. Residue from star fruit as valuable source for functional food ingredients and antioxidant nutraceuticals. Food Chemistry 97 (2): 277–284. https://doi.org/10.1016/j.foodchem.2005.03.048

Singleton V, Rossi J. 1965. Colorimetry of total phenolic compounds with phosphomolybdic-phosphotungstic acid reagents. American Journal of Enology and Viticulture 16: 144–158.

Sinha S, Gupta M, Chandra P. 1997. Stress induced by iron in *Hydrella verticillata* (I.F.) Royele: Response of antioxidants. Ecotoxicology and Environmental Safety 38 (3): 286–291. https://doi.org/10.1006/eesa.1997.1598

Sinkovič L, Pipan B, Šibul F, Nemeš I, Horecki AT, Meglič V. 2023. Nutrients, phytic acid and bioactive compounds in marketable pulses. Plants 12 (1): 170. https://doi.org/10.3390/plants12010170

Xiao J, Park YG, Guo G, Jeong BR. 2021. Effect of iron source and medium pH on growth and development of *Sorbus commixta in vitro*. International Journal of Molecular Sciences 22 (1): 133. https://doi.org/10.3390/ijms22010133

Zhang X, Zhang D, Sun W, Wang T. 2019. The adaptive mechanism of plants to iron deficiency via iron uptake, transport, and homeostasis. International Journal of Molecular Sciences 20 (10): 2424. https://doi.org/10.3390/ijms20102424

Agrociencia

AGRONOMIC PERFORMANCE OF NATIVE AND HYBRID MAIZE (*Zea mays* L.) IN THE MUNICIPALITY OF ATENCO, STATE OF MEXICO

Alondra Jacqueline **Lira-Mendoza**[1], Amalio **Santacruz-Varela**[1*],
J. Jesús **García-Zavala**[1], Gilberto **Esquivel-Esquivel**[2]

[1]Colegio de Posgraduados Campus Montecillo. Carretera México-Texcoco km 36.5, Montecillo, Texcoco, State of Mexico, Mexico. C. P. 56264.
[2]Instituto Nacional de Investigaciones Forestales, Agrícolas y Pecuarias. Campo Experimental Valle de México. Carretera Texcoco-Los Reyes km 13.5, Coatlinchán, Texcoco, State of Mexico, Mexico. C. P. 56250.
* Author for correspondence: asvarela@colpos.mx

ABSTRACT

In the municipal area of Atenco, State of Mexico, Mexico, 20 % of maize (*Zea mays* L.) seeds planted are from hybrids and improved varieties, and the rest are from native varieties. However, the diversity of native maize is being noticeably lost, as the recent land conflict has pushed agricultural activities to the background, where they must be reinvigorated after the relocation of the Mexico City airport. To date, the investigations carried out in native maize races in the High Valleys are focused mainly in Puebla, Tlaxcala, and north of the State of Mexico, and little has been studied on the lake area of Texcoco. As a result, the aim was to determine the potential yield and agronomic characteristics of native varieties in relation to commercial varieties recommended for the area. Thirty-eight accessions from Atenco and surrounding municipal areas, along with 11 commercial hybrids recommended for the High Valleys, were evaluated. The evaluation was conducted in two locations: the ejido of San Salvador Atenco and the Valley of Mexico Experimental Field of the National Institute of Forestry, Agricultural, and Livestock Research (INIFAP) in Santa Lucía de Prías, Coatlinchán, Texcoco, State of Mexico, using a 7 × 7 lattice design with three replications. Information was recorded regarding days to female flowering (DFF) and male flowering (DMF), plant height (PH) and ear height (EH), ear diameter (ED), ear length (EL), number of rows per ear (RPE), and grain yield (GY). There were differences ($p \leq 0.01$) between genotypes for the variables; between locations, there were differences for the variables of flowering, plant morphology, and yield, and for the genotype × location interaction, there was no significance in two variables (EH and EL). The SAR-1 native genotype produced a similar grain yield to that of the best commercial hybrids, which can be used for further improvement.

Keywords: yield, agronomic performance.

Citation: Lira-Mendoza AJ, Santacruz-Varela A, García-Zavala JJ, Esquivel-Esquivel G. 2025. Agronomic performance of native and hybrid maize (*Zea mays* L.) in the municipality of Atenco, State of Mexico.
Agrociencia 59(3): 309-320.
https://doi.org/ 10.47163/agrociencia.v59i3.3105

Editor in Chief:
Dr. Fernando C. Gómez Merino

Received: November 07, 2023.
Approved: April 08, 2025.
Published in Agrociencia:
May 12, 2025.

INTRODUCTION

Maize (*Zea mays* L.) is the basis of the Mexican diet. Varieties and hybrids have been developed to cover the needs of the country's agroclimatic regions, with characteristics such as disease resistance, homogeneous phenotypes, and good yields (Espinosa *et al*., 2009). Nonetheless, for Mexico's seasonal small-scale agriculture, 59 maize races have been reported, with plants and ears that exhibit distinctive variability in size, color, and shape, indicating a wide genetic diversity.

The races from the High Valleys of central Mexico, whose distinguishing feature is the pyramidal shape of their ears, are distributed predominantly in regions with altitudes greater than 2000 m (Sánchez *et al*., 2000), and most of them are endemic to the High Valleys and mountain ranges of the center of the country (Wellhausen *et al*., 1951). In these regions, mainly native races are identified, including Cónico, Elotes Cónicos, Chalqueño, Arrocillo Amarillo, Palomero Toluqueño, and Cacahuacintle (Sierra-Macías *et al*., 2014). To date, the investigations carried out on maize native to the High Valleys have focused on Puebla, Tlaxcala, and the north of the State of Mexico, and little has been studied on the lake area of Texcoco.

The diversity of native maize in the area has been impacted, particularly in the municipal area of Atenco, where until 2019, 20 % of the maize seed planted was of commercial varieties and the rest of the native maize races (SIAP, 2019). A considerable loss is related to the long period of conflict lasting more than 15 years over land in the face of the construction of Mexico City's new airport, which led agriculture to a state of almost complete neglect. Due to this situation, there is a decline in the planting of native maize seeds, which lose their viability in a relatively short period, along with the lack of interest in youths to become farmers and the rapid demographic growth in recent years (Espinosa-Castillo, 2008).

The study of diversity in the highlands is essential. The diversity of native maize populations in the state of Puebla was investigated, with an evaluation of 41 native populations from the Serdán, Libres-Huamantla, and Puebla valleys, including 19 racial controls and two experimental varieties. The native populations were associated with the races Chalqueño, Cónico, Elotes Cónicos, and the sub-race Elotes Chalqueños, and variation was found in the resulting groups. Therefore, the environment and the dynamic process of selection of farmers favor a variation between and within groups (Flores-Pérez *et al*., 2015).

Alvarado *et al*. (2019) analyzed the morphologic variability of the native maize of the western Puebla and eastern Tlaxcala mountain ranges in order to define and relate races, commercial varieties, and the altitude of the collection sites, resulting in the morphologic variability of the populations being unrelated to the altitude of the sites. These samples had more relation to the Chalqueño race, little relation with the Cónico race, none with the Cónico Norteño and Palomero Toluqueño races, and almost none with the commercial varieties.

Likewise, in the southern State of Mexico, maize diversity was evaluated in 103 native maize samples of the Chalqueño race and eight hybrids from the High Valleys as controls in terms of morphology and grain yield. The creamy Chalqueño-type grain collections displayed similar yields to those of the best hybrids (Herrera-Cabrera *et al*., 2013). In addition, producers use empirical selection of seeds and prefer local varieties, which allows for the conservation of diversity and the improvement of productivity *in situ*.

Based on the above, the goal of this study was to compare the agronomic performance of native maize varieties to commercial maize varieties recommended for the Atenco area in the State of Mexico, with the hypothesis that there are native maize varieties that yield as much as commercial hybrid varieties.

MATERIALS AND METHODS

Genetic material

A total of 38 native varieties were collected, 21 of which were native to the municipal area of Atenco, nine from Texcoco, one from Ixtapaluca, four from Tepetlaoxtoc, and one from Otumba, in the State of Mexico, and two genotypes from San Juan Ixtenco, in the state of Tlaxcala, which were evaluated along with 11 hybrid maize varieties recommended for the High Valleys, including four from the company ASPROS, one from ASGROW, one from CERES, two from the Postgraduate College (COLPOS), and three from the National Forestry, Agricultural, and Livestock Research Institute (INIFAP).

Locations

The set of varieties was evaluated in the year 2022 in two locations: a) San Salvador Atenco, Atenco, State of Mexico (19° 33′ N, 98° 55′ W, at an altitude of 2250 m), with an annual average temperature of 15.1 °C and rainfall of 605 mm (García, 2004); and b) in the Valley of Mexico Experimental Field of the INIFAP in Santa Lucía de Prías, Coatlinchán, Texcoco, State of Mexico (19° 26′ N, 98° 53′ W, at an altitude of 2257 m), with an annual average temperature of 15.2 °C and rainfall of 637 mm (García, 2004), with hail 34 days after planting (the plant recovered because it was in a vegetative state).

Experimental design

A 7 × 7 lattice experimental design with three replications was used; the experimental plot consisted of two rows, each 5 m long and spaced 0.8 m apart. Two seeds were placed every 25 cm along the bottom of the row.

Agronomic management

In San Salvador Atenco, planting was carried out on May 28, and auxiliary irrigation was applied 16 days after planting (DAP), and in Santa Lucía, on June 13, with irrigations applied at 31 and 122 DAP. In each location, plants were fertilized 15 DAP with urea and triple superphosphate using an NPK formula of 140-40-00. For weed control, Primagram® (atrazine and smetolachlor, 2 kg ha^{-1}) was used 25 days after seedling emergence. In San Salvador Atenco, in order to control the fall armyworm (*Spodoptera frugiperda*), Karate Zeon® (lambda-cyhalothrin, dose 300 mL ha^{-1}) was applied 126 DAP. Grain harvest in San Salvador took place 189 DAP, and in Santa Lucía, 164 DAP.

Response variables

In each location, data were taken regarding days to male (DMF) and female flowering (DFF); the former, from planting until 50 % of the plants in the field released pollen; and the latter, until young ears were displayed, with exposed stigmata (SNICS, 2024). In order to record plant height (PH, cm) and ear height (EH, cm), five plants were chosen at random per plot and measured from the ground up to the knot of the flag leaf (cm) and up to the knot where the ear is inserted (cm), respectively (SNICS, 2024). In harvest, five representative ears were taken from each plot, whose lengths (EL, cm) were measured from the base to the tip, along with the diameter (ED, cm) in the middle section and the number of rows (RPE).

The ears dried outdoors, and the threshing factor (FCD, weight of grain without the cob divided by the weight of grain with the cob) was determined, along with the moisture content (%) and the weight of 100 g of seeds of each genotype. Later, using the Steinlite Electronic Tester, Model G (Chicago, IL, USA), the letter and number corresponding to the moisture content of the seed were determined. The temperature and grain yield (GY) were adjusted to 14 % moisture, extrapolating the weight of all the ears harvested from the experimental unit to kg per hectare using the formula:

$$Yield\left(\frac{kg}{ha}\right) = field\ weight \times shelling\ factor\left[1 - \frac{moisture\ percentage}{100}\right] + 0.14 \times 1250$$

Statistical analysis

A combined analysis was performed using the SAS statistical package (version 9.4, SAS Institute Inc., Cary, NC, USA) to determine the average performance of the genotypes associated with the variables. The means were compared using Tukey's test ($p \leq 0.05$).

RESULTS AND DISCUSSION

The varieties displayed differences ($p \leq 0.01$) for all variables, indicating the existence of genetic variability (Table 1). The diversity of native maize is not only found in the east of the State of Mexico but also in the Puebla Valley, where variations are found in ear shape and size. These traits are due to the selection practiced by farmers according to their needs, such as cob thickness and lodging of the plants (Hortelano-Santa Rosa *et al.*, 2008). Most variables (Table 1) showed significant differences ($p \leq 0.01$), with the exception of diameter and number of rows per ear, which were similar. This suggests that the crop's performance is primarily influenced by its environment (planting date and soil type).

Table 1. Mean squares and statistical significance for eight variables evaluated in 38 native maize (*Zea mays* L.) varieties and 11 commercial hybrids grown in two environments in the eastern State of Mexico, Mexico, during the spring-fall season of 2022.

FV	Genotypes	Locations	Gen × Loc	Error	CV (%)
DF	48	1	48	156	
DMF	3286 **	22 112 **	559	12	3.9
DFF	2179 **	22 466 **	445	11	3.9
PH	57 013 **	56 709 **	38 465	631	9.7
EH	88 609 **	12 129 **	64 471 **	785	17.4
EL	176 **	4 *	99 **	1	6.9
ED	11 **	0.02	2	0.05	5.4
RPE	533 **	10	201	3.18	12.2
GY	569 817 659 **	57 927 439 **	63 930 014	1 476 090	31.5

*, **Significance of 0.05 and 0.01, respectively. FV: Sources of variation; Gen: genotype; Loc: location; CV: coefficient of variation; DF: degrees of freedom; DMF: days to male flowering; DFF: days to female flowering; PH: plant height; EH: ear height; EL: ear length; ED: ear diameter; RPE: rows per ear; GY: grain yield.

In a study conducted in the State of Mexico that evaluated 11 hybrids in five locations (Ixtlahuaca, Jilotepec, Temascalcingo, Jocotitlán, and Cuendó), contrasting responses were presented for the environmental effect (Martínez-Gutiérrez *et al*., 2018). The performance of the germplasm evaluated was justified because the environments were contrasting, where the average temperature during the development of the cycle was the same, although rainfall displayed differences in both locations (Canales-Islas *et al*., 2017).

Tadeo-Robledo *et al*. (2015) evaluated the productivity of two native maize varieties (Ixtlahuaca and Atlacomulco) and two hybrids (H-50 and H-52) at the Faculty of Higher Studies Cuautitlán of the National Autonomous University of Mexico in Cuautitlán Izcalli, State of Mexico, on two planting dates. They obtained yields of 7185 kg ha^{-1} on the first planting date (May 17th) and 6082 kg ha^{-1} on the second (June 1st), where the yield was lower because the best time for planting for these genotypes is in May, which coincides with the greatest number of days between planting and harvest to achieve the best expression of yield.

The Gen × Loc interaction showed no significance for 6 out of 8 variables (Table 1), indicating that the expression is not influenced by changes in genotype across environments. These results contrast with a study conducted in Molcaxac, Puebla (Ángeles-Gaspar *et al*., 2010), where 52 native maize varieties from semi-warm and temperate environments and four hybrids recommended for the area under rainfed conditions were evaluated. In that study, a significant Gen × Loc interaction was found, indicating that the genotypes do not exhibit stable performance, and they respond differently in contrasting environments.

Varieties

The comparison of means shows 11 varieties that presented the statistically greater grain yields from the average of both locations (Table 2). Ten of these were commercial hybrid maize varieties, and one was native to the municipal area of Texcoco, which borders the municipal area of Atenco. Finding one outstanding native variety represents an important discovery since it opens up the possibility of incorporating it into a recurring selection program. Improving it would provide benefits to farmers, such as lower seed costs and less dependence on multinational corporations, fewer chemical inputs, preservation of the culinary quality of dishes derived from this maize, favorable forage use, and potential tolerance to adverse environmental factors in the face of climate change.

Table 2. Maize (*Zea mays* L.) grain yield of the statistically superior group planted in San Salvador Atenco and Santa Lucía de Prías, State of Mexico, Mexico, during the spring-fall season of 2022.

Genotype	Origin	Yield (kg ha^{-1})
H-52	National Institute of Forestry, Agricultural, and Livestock Research (INIFAP)	7755
XV1613	ASPROS	7299
Cherokee F1	ASPROS	7282
Cenzontle	ASGROW	6824
Aníbal	ASPROS	6665
HS-2	Postgraduate College (COLPOS)	6013
Niebla	CERES	5985
Caribú	INIFAP	5862
SAR-1	Texcoco, State of Mexico	5488
Promesa	COLPOS	5207
Cherokee F2	ASPROS	5084
Maximum value		7755
Minimum value		1164
Average		3855
HSD (α = 0.05)		2853

HSD: Honest significant difference.

The hybrid materials from commercial venues and institutions undergo a series of evaluations before being launched into the market, which provide information on the locations, potential yields, population density, and planting dates for the production of parents, lines, and simple crosses (Virgen-Vargas *et al*., 2015). On the other hand, farmers select native materials after harvesting, observing the physical characteristics of the ear, considering grain size, thin cobs, ear health (Magdaleno-Hernández *et al*., 2016), and ease of threshing. The performance shown by hybrids is due to their selection for greater stability in grain yield and development under favorable environmental conditions (Echarte *et al*., 2004); these characteristics are observed in the hybrids evaluated, which yielded over 5083 kg ha^{-1}.

Ángeles-Gaspar *et al*. (2010), in a similar study, identified the genetic diversity among the local maize populations in the municipal area of Molcaxac, Puebla, and noticed that some local varieties surpassed or matched the grain yield of commercial hybrids (used as controls) recommended for the region. This performance can also be observed in the native maize varieties of the municipal area of Atenco.

The 15 genotypes that had the statistically lowest yield in the evaluation were native maize varieties (Table 3). Grain yield is the primary feature that farmers look for, but it is not the only one. Five low-yield varieties outperformed others in terms of ear morphology. These varieties were C-1, from the municipal area of Ixtapaluca, State of Mexico, with an average length of 15.45 cm; N-1 from Atenco and T-3 from Tepetlaoxtoc, State of Mexico, with an average of 16 and 17 rows, respectively; and variety TQ-1 from Texcoco, State of Mexico, with an average diameter of 4.58 cm. These particularities can be used to perform stratified visual mass selection as an alternative for producers to obtain plants and seeds with desirable and outstanding characteristics in each production cycle.

Table 3. Grain yield of the statistically inferior group of maize (*Zea mays* L.) planted in San Salvador Atenco and Santa Lucía de Prías, State of Mexico, Mexico, during the spring-fall season of 2022.

Genotype	Origin	Yield (kg ha^{-1})
N-8	Atenco, State of Mexico	2710
C-1	Ixtapaluca, State of Mexico	2706
A-1	Atenco, State of Mexico	2690
SD-1	Texcoco, State of Mexico	2632
N-1	Atenco, State of Mexico	2588
TQ-1	Texcoco, State of Mexico	2554
N-3	Atenco, State of Mexico	2546
F-1	Atenco, State of Mexico	2477
SJI-2	San Juan Ixtenco, Tlaxcala	2375
A-9	Atenco, State of Mexico	2305
A-3	Atenco, State of Mexico	2288
T-3	Tepetlaoxtoc, State of Mexico	1617
SJI-2	San Juan Ixtenco, Tlaxcala	1369
T-2	Tepetlaoxtoc, State of Mexico	1296
T-1	Tepetlaoxtoc, State of Mexico	1164
Maximum value		7755
Minimum value		1164
Average		3855
DSH $\alpha=_{0.05}$		2853

Locations

In Santa Lucía, the time to male and female flowering observed was shorter than in San Salvador Atenco (Table 4). In both locations, the month of flowering was August (Figure 1). Planting dates are an important factor since the plant develops based on temperature; when it is hotter, the cycle shortens due to an acceleration in development. The cycle for Santa Lucía began in May and finished in November; therefore, the vegetative states were shorter, and germination and vegetative growth occurred in an average temperature of 25 °C. On the other hand, if it is cold during the reproductive

Table 4. Comparison of means of 49 varieties evaluated in two locations in the State of Mexico, Mexico, during the spring-fall season of 2022.

Locations	D (days)	DFF (days)	PH (cm)	EH (cm)	EL (cm)	ED (cm)	RPE	GY (kg ha^{-1})
San Salvador Atenco, Atenco	97 a	93 a	271 a	167 a	15 a	4 a	15 a	4297 a
Santa Lucía de Prías, Texcoco	80 b	76 b	243 b	154 b	14 b	4 a	14 a	3412 b

DMF: days to male flowering; DFF: days to female flowering; PH: plant height; EH: ear height; EL: ear length; ED: ear diameter; RPE: rows per ear; GY: grain yield. Different letters between columns indicate significant differences ($p \leq 0.05$).

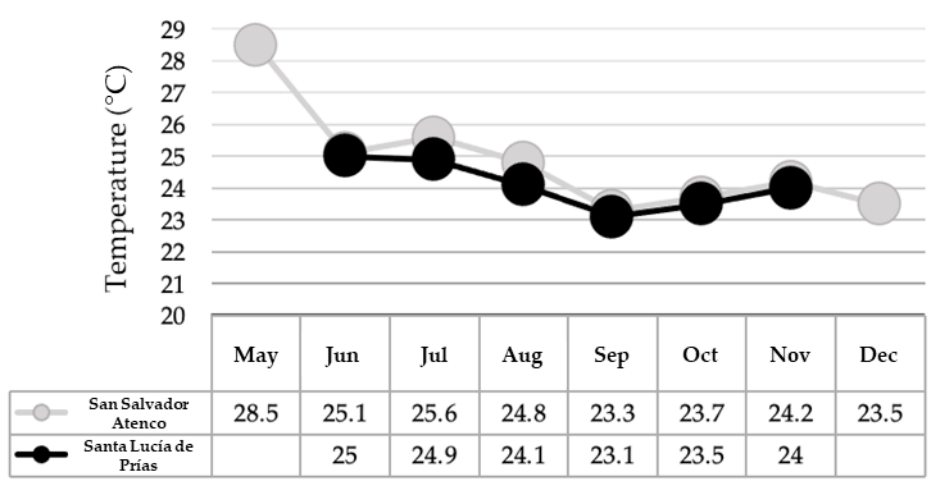

Figure 1. Average temperature during planting, germination, vegetative development, flowering, maturity, and harvest at the locations evaluated in the municipalities of Atenco and Texcoco, State of Mexico. Data were collected directly with maximum and minimum temperature thermometers in the center of the experiments, and the average was calculated as the median of the maximum and minimum temperatures.

stage, the crop cycle tends to elongate. In San Salvador Atenco, the temperature dropped during germination from 28.5 to 25.1 °C. During vegetative growth (June) and until flowering, the temperature dropped again (August) (Figure 1).

The ear morphology differed in both locations, with genotypes Niebla from CERES and Aníbal from ASPROS having the longest average of 16.6 and 16.2 cm, and yielding 6695.9 and 5984.5 kg ha^{-1}, respectively (Table 4). This response can be due to the inherent characteristics of the Chalqueño, Cónico, and Elotes Cónicos races (Wellhausen *et al*., 1951) as a result of the constant selection carried out by farmers who search for traits such as earliness, plant stature, and grain yield components (Muñoz-Orozco, 2003). Yields in both locations differed as genotypes responded to environmental variations in each location. This performance could be noticed in the evaluation of 29 hybrids in 15 environments of the tropical Americas carried out by Lozano-Ramírez *et al*. (2015), in which genotypes had to be obtained with greater yields and in stable environmental conditions.

Genotype × Location interaction

Both maize groups in both locations displayed similarities in DMF and DFF (Table 5). The earliest variety came from an unidentified farmer, with 80 DMF and 77 DFF, and the latest was also a native variety (from Cristian Zavala) with 96 DMF and 91 DFF, both from Tepetlaoxtoc. Quiroz-Mercado *et al.* (2017) mention that the average floral asynchrony interval for eight hybrid maize and two creole varieties of the region was four days. This evaluation was carried out in Cerrillo Piedras Blancas (Toluca), Mina México (Almoloya de Juárez), and Rancho Tiacaque (Jocotitlán), all of which are municipal areas in the State of Mexico.

Smith *et al*. (1969) mention that plant and ear height are characteristics that are affected to a certain degree by the environment. The Maximiliano Moran García variety from

Table 5. Comparison of means of the genotypes evaluated by group and by location in San Salvador Atenco and Santa Lucía de Prías, State of Mexico, Mexico, during the spring-fall season of 2022.

Varieties	DMF (days)	DFF (days)	PH (cm)	EH (cm)	EL (cm)	ED (cm)	RPE	GY (kg ha^{-1})
				San Salvador Atenco				
Natives	98 a	94 a	278 a	176 a	15 a	4 a	14 b	3722 b
Hybrids	96 b	93 b	250 b	136 b	15 a	4 a	16 a	6284 a
				Santa Lucía de Prías				
Natives	80 a	76 a	246 a	159 a	14 b	4 b	14 b	2636 b
Hybrids	78 b	75 b	233 b	135 b	16 a	5 a	16 a	6093 a

DMF: days to male flowering; DFF: days to female flowering; PH: plant height; EH: ear height; EL: ear length; ED: ear diameter; RPE: rows per ear; GY: grain yield. Different letters between columns indicate significant differences ($p \leq 0.05$).

Acuexcomac presented a height of 284 cm, making it statistically the tallest, with an ear height of 189.9 cm, which can be used for forage. According to Franco-Martínez *et al*. (2015), they evaluated 29 outstanding forage cultivars for the Toluca-Atlacomulco valley and identified landraces with contrasting plant heights in the range of 177 to 247 cm. Greater plant heights are considered a prerequisite to obtain a greater production of green and/or dry matter (Muñoz-Tlahuiz *et al*., 2013).

Among the characteristics observed, the hybrid varieties presented lower plant height in comparison with the native varieties, an average ear length of 15.5 cm, 16 rows per ear, and a higher average yield in both locations (Table 5). This is attributable to the hybrids being the result of a genetic improvement process for the species, and they express their productive potential (heterosis), generally under optimal fertilization, moisture, agronomic management, and pest and disease control conditions, whereas native varieties have better traits for adaptation to the environment due to their broad genetic variation (Gil-Muñoz *et al*., 2005).

CONCLUSIONS

In the Atenco municipality, a native maize population was identified as having a yield equal to the group of superior hybrids, which, due to its long-term adaptation to the soil and environment of the research locations, competes successfully with modern hybrids. This is attributable to its good agronomic performance and grain yield, making it a candidate for inclusion in a genetic improvement program through recurrent selection to further increase its potential in the short and medium term.

REFERENCES

Alvarado-Beltrán G, López-Sánchez H, Santacruz-Varela A, Muñoz-Orozco A, Valadez-Moctezuma E, Gutiérrez-Espinosa MA, López PA, Gil-Muñoz A, Guerrero-Rodríguez JD, Taboada-Gaytán OR. 2019. Variabilidad morfológica del maíz nativo (*Zea mays* L.) del altiplano poniente de Puebla y altiplano oriental de Tlaxcala, México. Revista de la Facultad de Ciencias Agrarias 51 (2): 217–234.

Ángeles-Gaspar E, Ortiz-Torres E, López PA, López-Romero G. 2010. Caracterización y rendimiento de poblaciones de maíz nativas de Molcaxac, Puebla. Revista Fitotecnia Mexicana 33 (4): 287–296.

Canales-Islas EI, Tadeo-Robledo M, Mejía-Contreras JA, García-Zavala JJ, Espinoza-Calderón A. 2017. Semilla fértil y androestéril de maíz bajo diferentes densidades de población. Ecosistemas y Recursos Agropecuarios 4 (12): 465–473. https://doi.org/10.19136/era.a4n12.997

Echarte L, Andrade FH, Vega CRC, Tollenaar M. 2004. Kernel number determination in Argentinean maize hybrids released between 1965 and 1993. Crop Science 44 (5): 1654–1661. https://doi.org/10.2135/cropsci2004.1654

Espinosa-Castillo M. 2008. Procesos y actores en la conformación del suelo urbano en el ex lago de Texcoco. Economía, Sociedad y Territorio 8 (27): 769–798.

Espinosa A, Tadeo M, Turrent A, Gómez N, Sierra M, Palafox A, Caballero F, Valdivia R, Rodríguez FA. 2009. El potencial de las variedades nativas y mejoradas de maíz. Ciencias 92: 118–125.

Flores-Pérez L, López PA, Gil-Muñoz A, Santacruz-Varela A, Chávez-Servía JL. 2015. Variación intra-racial de maíces nativos del altiplano de Puebla, México. Revista de la Facultad de Ciencias Agrarias 47 (1).

Franco-Martínez JRP, González-Huerta A, de Jesús Pérez-López, D, González-Ronquillo M. 2015. Caracterización fenotípica de híbridos y variedades de maíz forrajero en Valles Altos del Estado de México, México. Revista Mexicana de Ciencias Agrícolas 6 (8): 1915–1927.

García E. 2004. Modificaciones al sistema de clasificación climática de Köppen. Universidad Nacional Autónoma de México. Ciudad de México, México.

Gil-Muñoz A, López PA, Muñoz OA, López-Sánchez H. 2005. Variedades criollas de maíz (*Zea mays* L.) en el estado de Puebla, México: diversidad y utilización. *In* Chávez-Servia JL, Tuxill J, Jarvis DI. (eds.), Manejo de la Diversidad de los Cultivos en los Agroecosistemas Tradicionales. Instituto Internacional de Recursos Fitogenéticos: Cali, Colombia, pp: 18–25.

Herrera-Cabrera BE, Castillo-González F, Ortega-Pazkca RA, Delgado-Alvarado A. 2013. Poblaciones superiores de la diversidad de maíz en la región oriental del Estado de México. Revista Fitotecnia Mexicana 36 (1): 33–43.

Hortelano-Santa Rosa R, Gil-Muñoz A, Santacruz-Varela A, Miranda-Colín S, Córdova-Téllez L. 2008. Diversidad morfológica de maíces nativos del Valle de Puebla. Agricultura Técnica en México 34 (2): 189–200.

Lozano-Ramírez A, Santacruz-Varela A, San Vicente-García F, Crossa J, Burgueño J, Molina-Galán JD. 2015. Modelación de la interacción genotipo X ambiente en rendimiento de híbridos de maíz blanco en ambientes múltiples. Revista Fitotecnia Mexicana 38 (4): 347–357.

Magdaleno-Hernández E, Mejía-Contreras A, Martínez-Saldaña T, Jiménez-Velázquez MA, Sánchez-Escudero J, García-Cué JL. 2016. Selección tradicional de semilla de maíz criollo. Agricultura, Sociedad y Desarrollo 13 (3): 437–447.

Martínez-Gutiérrez A, Zamudio-González B, Tadeo-Robledo M, Espinosa-Calderón A, Cardoso-Galvão JC, Vázquez-Carrillo G, Turrent-Fernández A. 2018. Rendimiento de híbridos de maíz grano blanco en cinco localidades de Valles Altos de México. Revista Mexicana de Ciencias Agrícolas 9 (7): 1447–1458 https://doi.org/10.29312/remexca.v9i7.1357

Muñoz-Orozco A. 2003. Centli-maíz: prehistoria e historia, diversidad, potencial, origen genético y geográfico. Colegio de Postgraduados: Montecillo, México. 210 p.

Muñoz-Tlahuiz F, Guerrero-Rodríguez JD, López PA, Gil-Muñoz A, López-Sánchez H, Ortiz-Torres E, Hernández-Guzmán JA, Taboada-Gaytán O, Vargas-López S, Valadez-Ramírez M. 2013. Producción de rastrojo y grano de variedades locales de maíz en condiciones de temporal en los Valles Altos de Libres-Serdán, Puebla, México. Revista Mexicana de Ciencias Pecuarias 4 (4): 515–530.

Quiroz-Mercado J, Pérez-López DJ, González-Huerta A, Rubí-Arriaga M, Gutiérrez-Rodríguez F, Franco-Martínez JRP, Ramírez-Dávila JF. 2017. Respuesta de 10 cultivares de maíz a la densidad de población en tres localidades del centro mexiquense. Revista Mexicana de Ciencias Agrícolas 8 (7): 1521–1535.

Sánchez GJJ, Goodman MM, Stuber CW. 2000. Isozymatic and morphological diversity in the races of maize of Mexico. Botánica Económica 54 (1): 43–59. https://doi.org/10.1007/BF02866599

SIAP (Servicio de Información Agroalimentaria y Pesquera). 2019. Producción agrícola. Gobierno de México. Servicio de Información Agroalimentaria y Pesquera. Ciudad de México, México. https://www.gob.mx/siap/acciones-y-programas/produccion-agricola-33119 (Retrieved: May 2023).

Sierra-Macías M, Andrés-Meza P, Palafox-Caballero A, Meneses-Márquez I, Francisco-Nicolás N, Zambada-Martínez A, Rodríguez-Montalvo F, Espinosa-Calderón A, Tadeo-Robledo M. 2014. Variación morfológica de maíces nativos (*Zea mays* L.) en el Estado de Veracruz, México. Agro Productividad 7 (1): 58–65.

Smith H. 1969. The effect of selection upon certain physical characters in the corn plant. III Agricultural Experiment Station Bulletins: 132: 47–62.

SNICS (Servicio Nacional de Inspección y Certificación de Semillas). 2024. Guía para la descripción de variedades nativas Maíz (*Zea mays* L.). Secretaría de Agricultura y Desarrollo Rural. Servicio Nacional de Inspección y Certificación de Semillas. Ciudad de México, México. 41 p.

Tadeo-Robledo M, Zamudio-González B, Espinosa-Calderón A, Turrent-Fernández A, Cárdenas-Marcelo AL, López-López C, Arteaga-Escamilla I, Valdivia-Bernal R. 2015. Rendimiento de maíces nativos e híbridos en diferente fecha de siembra y sus unidades calor. Revista Mexicana de Ciencias Agrícolas 6 (1): 33–43.

Virgen-Vargas J, Zepeda-Bautista R, Ávila-Perches MA, Espinosa-Calderón A, Arellano-Vázquez JL, Gámez-Vázquez AJ. 2015. Producción y calidad de semilla de maíz en Valles Altos de México. Agronomía Mesoamericana 27 (1): 191–206. https://doi.org/10.15517/am.v27i1.21899

Wellhausen EJ, Roberts LM, Hernández XE. 1951. Razas de maíz en México, su origen, características y distribución. Secretaría de Agricultura y Ganadería de México. Fundación Rockefeller. Ciudad de México, México. 237 p.

Agrociencia

Agrociencia

OZONE AND AQUA REGIA SEED TREATMENTS ENHANCE GERMINATION IN TOMATO (*Solanum lycopersicum* L.) AND ROSELLE (*Hibiscus sabdariffa* L.)

Carlos Arturo **Guzmán-Nuñez**[1], Antonia **Macedo-Cruz**[1], Sergio Humberto **Chávez-Franco**[2], Guillermo **Carrillo-Castañeda**[3], Axel Eduardo **Rico-Sánchez**[1*]

[1]Colegio de Postgraduados Campus Montecillo. Posgrado de Hidrociencias. Carretera México-Texcoco km 36.5, Montecillo, Texcoco, State of Mexico, Mexico. C. P. 56264.
[2]Colegio de Postgraduados Campus Montecillo. Posgrado de Fruticultura. Carretera México-Texcoco km 36.5, Montecillo, Texcoco, State of Mexico, Mexico. C. P. 56264.
[3]Colegio de Postgraduados Campus Montecillo. Posgrado de Recursos Genéticos y Productividad-Genética. Carretera México-Texcoco km 36.5, Montecillo, Texcoco, State of Mexico, Mexico. C. P. 56264.
* Author for correspondence: rico.axel@colpos

Citation: Guzmán-Nuñez CA, Macedo-Cruz A, Chávez-Franco SH, Carrillo-Castañeda G, Rico-Sánchez AE. 2025. Ozone and aqua regia seed treatments enhance germination in tomato (*Solanum lycopersicum* L.) and roselle (*Hibiscus sabdariffa* L.). **Agrociencia** 59(3): 321-342. https://doi.org/ 10.47163/agrociencia.v59i3.3233

Editor in Chief:
Dr. Fernando C. Gómez Merino

Received: May 20, 2024.
Approved: April 01, 2025.
Published in Agrociencia: April 28, 2025.

ABSTRACT

Global food demand has surged, necessitating innovative agricultural practices to mitigate environmental impacts and ensure food security. This study investigates the effects of pre-sowing treatments, including ozonated water and aqua regia, on the germination of tomato (*Solanum lycopersicum* L.) and roselle (*Hibiscus sabdariffa* L.) seeds. A randomized complete block design was used, comparing treatments to a deionized water control. Seeds were subjected to one-minute exposures, and germination metrics were assessed over 10 days. Results indicated that the ozone treatment significantly enhanced tomato seed germination rates compared to the control and aqua regia (Kruskal-Wallis, $p \leq 0.01$). While statistical significance was not observed for all treatments in roselle, a trend towards improved germination with ozonated water and aqua regia was noted. Germination indices, including germination percentage, rate, and synchrony, were analyzed using principal component analysis (PCA), revealing distinct treatment effects. PCA highlighted that the ozone treatment promoted rapid and enhanced germination in tomato, correlating with metrics such as emergence rate and peak germination percentage. Aqua regia demonstrated efficacy in roselle, likely due to scarification of the seed coat. The study suggests that optimized ozone treatments can serve as a biostimulant, enhancing germination velocity, while aqua regia effectively improves germination in species with hard seed coats. These findings contribute to understanding the potential applications of pre-sowing treatments for improving crop production and sustainability.

Keywords: Solanceae, Malvaceae, crop yield, germination, priming, hormesis.

INTRODUCTION

Population growth in the past century has significantly increased global food demand, challenging the development of novel agricultural practices. This rapid has had profound consequences, including environmental pollution, the encroachment of agriculture onto natural lands, and the exacerbation of greenhouse emissions, among other unsustainable practices (Koop and van Leeuwen, 2017). In response to recent food crises, there has been a notable surge in the importation of food products, particularly in Mexico, primarily to address the region's escalating food demand (Valencia-Romero, 2019).

To mitigate the current set of food security challenges, a concerted effort is required to develop and implement new technologies and innovative agricultural methods. A critical aspect of this endeavor lies in a thorough understanding of plant development to optimize crop yields and enhance food production (Tester and Langridge, 2010; Tolhurst and Ker, 2015). Plant domestication has been instrumental in enhancing food crop production through selective breeding for desirable physiological and morphological traits. This process involves improving plant characteristics, such as seed number and size, while addressing issues like seed shattering, dormancy, flowering time, and stress tolerance. By optimizing these traits, crop yields can be significantly increased (Gross and Olsen, 2010; Meyer and Purugganan, 2013).

Seed germination is a critical stage in plant development, influencing subsequent growth and yield (Ashraf and Foolad, 2005). It involves three distinct phases: imbibition, metabolic activity, and radicle emergence (Bradford, 2017). Seed priming is a pre-sowing technique that can enhance germination and improve crop performance under various stress conditions, such as salinity, temperature extremes, and drought (Ashraf and Foolad, 2005; Draganić and Lekić, 2012; Kaya *et al*., 2006; Shahrokhi *et al*., 2011). Priming methods, including hydropriming, osmopriming, and chemical priming, can improve seed vigor and tolerance to environmental stresses. These techniques are cost-effective, low-risk, and readily applicable in various agricultural settings (Ashraf and Foolad, 2005).

Ozone (O_3), a triatomic allotrope of oxygen, while often associated with its detrimental effects in the lower atmosphere as a pollutant, plays a crucial and often overlooked role in plant physiology, particularly in seed germination and early seedling development (Kangasjärvi *et al*., 1994; Roshchina and Roshchina, 2003; Violleau *et al*., 2008; Patwardhan and Gandhare, 2013; Pandiselvam *et al*., 2020). While high concentrations of tropospheric ozone can induce oxidative stress and negatively impact plant growth (Pandiselvam *et al*., 2020), carefully controlled and optimized applications of ozone at lower concentrations have demonstrated significant beneficial effects across a range of plant species (Patwardhan and Gandhare, 2013; Tütüncü *et al*., 2024; Violleau *et al*., 2007).

The positive effects of ozone in plants include enhanced seed germination rates, improved seedling vigor, and increased tolerance to various environmental stresses (Kangasjärvi *et al*., 1994; Sudhakar *et al*., 2011; Pandiselvam and Thirupathi, 2015). The mechanisms underlying these beneficial effects are complex and involve a variety of physiological and biochemical processes, including the modulation of antioxidant systems, hormonal signaling pathways, and the activation of specific gene expression related to germination and growth (Godínez-Mendoza *et al*., 2023). Understanding these mechanisms is crucial for developing effective strategies for utilizing ozone in agriculture to improve crop production and sustainability.

This study focuses on the impact of ozone treatment on seed germination in two economically and nutritionally important species: tomato (*Solanum lycopersic*um L.) and roselle (*Hibiscus sabdariffa* L.). Tomato is a globally cultivated vegetable crop, valued for its nutritional content and versatility in culinary applications (Kumar *et al*., 2017; Casals *et al*., 2021; Canul-Ku *et al*., 2023). Roselle, on the other hand, is a valuable crop known for its edible calyces, used for making beverages and jams, as well as its potential medicinal properties (Herrera-Arellano *et al*., 2004; Montaño-Arango *et al*., 2024). While previous research has explored the effects of ozone on various plant species, including some crops (Pandiselvam and Thirupathi, 2015; Sudhakar *et al*., 2008; Violleau *et al*., 2007), a detailed investigation of the specific responses of tomato and roselle seeds to ozone treatment is still lacking.

This research aims to address this gap by investigating the effects of different ozone concentrations and exposure durations on the germination parameters of tomato and roselle seeds. It was hypothesized that optimized ozone treatments can significantly improve seed germination, germination rates, and seedling vigor in both species. The findings of this study will contribute to a better understanding of the potential applications of ozone in enhancing seed germination and promoting sustainable agriculture. This study aims to evaluate the impact of ozonated water (ozone) and aqua regia as pre-sowing treatments, compared to a control, on the germination of tomato and roselle seeds.

MATERIALS AND METHODS

Research facility

This research was conducted at the Molecular Genetics Laboratory at Postgraduate College Campus Montecillo, located in Texcoco municipality, State of Mexico, Mexico. The experiments were carried out during the final week of May and the first week of June 2023.

Experimental design

A randomized complete block design was used, with individual seeds serving as the experimental units. To investigate the effects of varying seed coat hardness treatments, tomato (*S. lycopersicum* var. Río Grande) and roselle (*H. sabdariffa*) seeds were selected. The treatments included ozonated water (ozone), aqua regia, and a deionized water control. Each treatment was replicated six times.

For each treatment, 150 seeds were utilized (α = 0.05). This was conducted in two independent experiments, one for each plant species. The seed treatments were as follows: a) Seeds were submerged in deionized water for 1 min as a control treatment;

b) seeds were imbibed in 200 mL of deionized water and then treated with an ozone-oxygen mixture (ozone concentration of 9.3 mg L^{-1}) generated by a Yuomo Aquapure APSO 0.5-D ozone generator for 1 min under constant stirring and bubbling at 21 °C; and c) seeds were imbibed in 200 mL of aqua regia for one minute under constant stirring, then rinsed thoroughly with deionized water.

The germination assay was conducted using primed seeds. Fifteen Petri dishes were prepared for each treatment, each containing 10 treated seeds placed equidistantly on a 90 mm Whatman filter paper. A total of 45 Petri dishes per plant species were randomly placed in a lidded box and incubated at 29 °C for 10 days. Seed germination was recorded daily for 10 days.

Data analysis

Germination rates data for each treatment and plant species were assessed for normality and homoscedasticity. Differences among control, aqua regia, and ozone treatments were then evaluated using a Kruskal-Wallis test, followed by Dunn's *post hoc* test. Numerous germination indices were calculated for each analyzed plant using the *germinationmetrics* R package (Aravind *et al*., 2019) and a germination matrix organized by day, replicate, and treatment (Table 1).

Table 1. Germination indices and their description for tomato (*Solanum lycopersicum* L.) and roselle (*Hibiscus sabdariffa* L.) seeds.

Index	Formula	Description	Reference
GerminationPercent (GP)	$GP = \frac{N_g}{N_t} \times 100$	N_g = Number of germinated seeds, N_t = Total number of seeds	(ISTA, 2023)
PeakGermPercent (PGP)	$PGP = \frac{N_{max}}{N_t} \times 100$	N_{max} = Maximum number of seeds germinated per interval	(Vallance, 1950; Roh *et al*., 2004)
FirstGermTime (t_0) LastGermTime (t_g) TimeSpreadGerm	$t_0 = min\{Ti : Ni \neq 0\}$ $t_g = \max\{Ti : Ni \neq 0\}$ $(t_g - t_0)$	Ti = Time from the start of the experiment to the *ith* interval, Ni = Number of seeds germinated in the *ith* time interval (not the accumulated number, but the number corresponding to the *ith* interval)	(Edwards, 1932; Czabator, 1962; Goloff and Bazzaz, 1975; Labouriau, 1983; Ranal, 1999; Quintanilla *et al*., 2000)
t50_Coolbear Median Germination Time (t50)	$t_{50} = T_i + \frac{(\frac{N+1}{2} - N_i)(T_j - T_i)}{N_j - N_i}$	N = Final number of germinated seeds, N_i and N_j = Cumulative germinated seed counts at times T_i and T_j where $N_i < (N+1)/2 < N_j$	(Coolbear *et al*., 1984)
t50_Farooq Germination time (t50)	$t_{50} = T_i + \frac{(\frac{N}{2} - N_i)(T_j - T_i)}{N_j - N_i}$	N = Final number of germinated seeds, N_i and N_j = Cumulative germinated seed counts at times T_i *and* T_j where $N_i < N/2 < N_j$	(Farooq *et al*., 2005)

Table 1. Continue

Index	Formula	Description	Reference
MeanGermTime ($\bar{T}$)	$\bar{T} = \frac{\sum_{i=1}^{k} N_i T_i}{\sum_{i=1}^{k} N_i}$	T_i = Time to *i*th interval, N_i = Seeds germinated in *i*th interval	(Edmond and Drapala, 1958; Czabator, 1962; Smith and Millet, 1964; Ellis and Roberts, 1980; Labouriau, 1983; Ranal, 1999)
VarGermTime (s_T^2)	$s_T^2 = \frac{\sum_{i=1}^{k} N_i (T_i - \bar{T})^2}{\sum_{i=1}^{k} N_i - 1}$	T_i = Time to *i*th interval, N_i = Seeds germinated in *i*th interval	(Labouriau, 1983; Ranal and de Santana, 2006)
SEGermTime (s_T)	$s_{\bar{T}} = \sqrt{\frac{s_T^2}{\sum_{i=1}^{k} N_i}}$	N_i = Seeds germinated in *i*th interval, *k* = Total number of intervals	
CVGermTime (CV_T)	$CV_T = \frac{\sqrt{s_T^2}}{\bar{T}}$		(Ranal and de Santana, 2006)
MeanGermRate ($\bar{V}$)	$\bar{V} = \frac{\sum_{i=1}^{k} N_i}{\sum_{i=1}^{k} N_i T_i}$	T_i = End time of *i*th interval, N_i = Seeds germinated in *i*th interval, *k* = Total intervals	(Labouriau and Bicalho-Valadares, 1976; Labouriau, 1983; Ranal and de Santana, 2006)
CVG Coefficient of velocity/Rate of germination	$CVG = \bar{V} \times 100$		(Kotowski, 1962; Nichols and Heydecker, 1968; Labouriau, 1983; Scott *et al*., 1984; Thompson *et al*., 1995)
GermRateRecip_Coolbear (v_{50})	$v_{50} = \frac{1}{t_{50}}$	*t50* = Median Germination Time (Coolbear)	(Coolbear *et al*., 1984)
GermRateRecip_Farooq		*t50* = Median Germination Time (Farooq)	(Farooq *et al*., 2005)
GermSpeed_Count (*S*)	$S = \frac{N_1}{T_1} + \frac{N_2}{T_2} + \frac{N_3}{T_3} + \cdots \frac{N_k}{T_k}$	N_i = Number or percent of germinated seeds at time T_i, *k* = Total intervals	
GermSpeed_Percent (*S*)			
GermSpeedAccumulated_ Count	$S_{accumulated} = \frac{N_1}{T_1} + \frac{N_1 + N_2}{T_2} + \frac{N_1 + N_2 + N_3}{T_3} + \dots \frac{N_1 + N_2 + \cdots N_k}{T_k}$	N_k = Number or percent of seeds germinated at times $T_{k,\,i,\,j}$ *k* = Number of intervals	
GermSpeedAccumulated_ Percent			(Throneberry and Smith, 1955)
GermSpeedAccumulated_ Normal	$S_{accumulated} = \sum_{i=1}^{k} \frac{\sum_{j=1}^{i} N_j}{T_i}$	T_i = Time from the start of the experiment to the *i*th interval, $\sum_{j=1}^{i} N_j$ = Cumulative number of seeds germinated up to the *i*th interval, *k* = Total number of time intervals	

Table 1. Continue

Index	Formula	Description	Reference
GermSpeedCorrected_ Normal GermSpeedCorrected_ Accumulated	$S_{corrected} = \frac{S}{FGP}$	S = Represents germination speed (calculated using germination percentage, either standard or accumulated, depending on the method argument: "normal" or "accumulated," respectively), FGP = Final germination percentage	(Evetts and Burnside, 1972)
WeightGermPercent	$WGP = \frac{\sum_{i=1}^{k}(k-i+1)N_i}{k \times N} \times 100$	N_i = Seeds germinated in interval i, N = Total seeds, k = Total intervals	
MeanGermPercent ($\overline{GP}$)	$\overline{GP} = \frac{GP}{T_k}$	GP = Final Germination Percentage, T_k = Time at final interval	(Czabator, 1962)
MeanGermNumber ($\bar{N}$)	$\bar{N} = \frac{N_g}{T_k}$	Ng = Final germinated seeds, T_k = Time at final interval	(Khamassi *et al*., 2013)
TimsonsIndex	$\Sigma k = \sum_{i=1}^{k} G_i$	G_i = Cumulative germination percentage at interval i, k = Total intervals	(Baskin and Baskin, 1998; Brown and Mayer, 1988; Grose and Zimmer, 1958)
TimsonsIndex_Labouriau (Σk_{mod})	$\Sigma k_{mod} = \frac{\Sigma k}{\sum_{i=1}^{k} g_i}$	g_i = Partial germination percentages	(Khan and Ungar, 1984; Ranal and de Santana, 2006)
Timsons Index_KhanUngar	$\Sigma k_{mod} = \frac{\Sigma k}{T_k}$	T_k = Total germination time	(Khan and Ungar, 1984)
GermRateGeorge (GR)	$GR = \sum_{i=1}^{k} N_i K_i$	N_i = Seeds germinated in interval i, K_i = Time until end of test from start of interval i, k = Total intervals	(Nichols and Heydecker, 1968; Tucker and Wright, 1965)
GermIndex (*GI*)	$GI = \sum_{i=1}^{k} \frac{\lvert(T_k - T_i)N_i\rvert}{N_t}$	T_i = Time to end of interval i, N_i = Seeds germinated in interval i, Nt = Total seeds, k = Total intervals	(Melville *et al*., 1980)
GermIndex_mod (*GI*)	$GI_{mod} = \sum_{i=1}^{k} \frac{\lvert(T_k - T_i)N_i\rvert}{N_g}$	T_i = Time to end of interval i, N_i = Seeds germinated in interval i, N_g = Total germinated seeds, k = Total intervals	(Ranal and de Santana, 2006)
EmergenceRateIndex_ SG (*ERI*)	$ERI = \sum_{i=1}^{k-1} N_i(k-i)$	N_i = Number of seeds germinated in the ith time interval (new germinations only), i = Index of the time interval, i_0 = Time interval at germination onset, k = Total number of time intervals	(Shmueli and Goldberg, 2022)
EmergenceRateIndex_ SG_mod (ERI_{mod})	$ERI_{mod} = \frac{\sum_{i=i_0}^{k-1} N_i(k-i)}{N_g}$	N_g = Total of germinated seeds at the end of assay	(Ranal and de Santana, 2006)

Table 1. Continue

Index	Formula	Description	Reference
EmergenceRateIndex_ BilbroWanjura (ERI_{bilb})	$ERI_{bilb} = \frac{\sum_{i=1}^{k} N_i}{\bar{T}}$	$\bar{T}$ = Mean germination time or mean emergence time	(Bilbro and Wanjura, 1982)
EmergenceRateIndex_ Fakorede (ERI_{fak})	$ERI_{fak} = \frac{\bar{T}}{FGP/100}$	FGP = Final germination time	(Fakorede and Agbana, 1983; Fakorede and Ayoola, 1980; Fakorede and Ojo, 1981)
PeakValue (PV)	$PV = max\left(\frac{G_1}{T_1}, \frac{G_2}{T_2}, \frac{G_3}{T_3}, \ldots \frac{G_k}{T_k}\right)$	T_n = Time from experiment start to the nth interval, G_n = Cumulative germination percentage at the nth interval, k = Total number of time intervals	(Czabator, 1962)
GermValue_Czabator (GV)	$GV = PV \times MDG$	MDG = Mean daily germination percentage from onset	
GermValue_DP (GV_{dp})	$GV_{dp} = \frac{\Sigma\, DGS}{N} \times GP \times c$	DGS = Speed of daily germination calculated by dividing the cumulative germination percentage by the number of days since germination began, N = Frequency of calculated DGS, c = Average daily germination speed	(Djavanshir and Pourbeik, 1976)
GermValue_Czabator_mod (GV_{mod}) GermValue_DP_mod (GV_{mod})	GV_{mod}	Germination Value (GV) calculations typically consider only the time from germination onset. However, a modified GV (GV_{mod}) incorporating the full test duration	(Brown and Mayer, 1988)
GermSynchrony (Z)	$Z = \frac{\sum_{i=1}^{k} C_{N_i,2}}{C_{\Sigma N_i,2}}$	$C_{Ni,2}$ = Number of two-seed combinations possible from the N_i = Seeds germinated in the ith interval (calculated as $C_{Ni,2} = N_i (N_i\text{-}1)/2$), $C_{\Sigma Ni,2}$ = Same calculation for the total number of germinated seeds, assuming simultaneous germination	(Primack, 1985; Ranal and de Santana, 2006)
GermUncertainty ($\bar{E}$)	$\bar{E} = -\sum_{i=1}^{k} f_i \log 2\, f_i$	f_i = Relative frequency of germination during the ith time interval, N_i = Number of seeds that germinated during the ith time interval, k = Total number of time intervals over which germination is observed	

A principal component analysis (PCA) was conducted on the seed germination data for each plant species. For this analysis, the data were structured into a matrix format suitable for use in R. Each row represented a biological replicate (n = 15 per treatment), and each column represented a calculated seed germination index derived from the three treatments (aqua regia, ozone, and control). Confidence ellipses were generated for each treatment. PCA computations were performed using the *prcomp* function, and visualizations were generated using the *fviz_pca_ind* function from the package *factoextra*. All statistical analyses were conducted in RStudio version 2024.04.0.

RESULTS AND DISCUSSION

A comparative analysis of various treatments on the germination of tomato and roselle seeds revealed varying degrees of efficacy. Germination rates were assessed relative to a control group. The analysis of germination rate data for tomato seeds exhibited a significant disparity between the control group and ozone treatment (Kruskal-Wallis test, $p \leq 0.01$) and between aqua regia and ozone treatment (Kruskal-Wallis test, $p \leq 0.01$). Ozone treatment demonstrated significantly higher germination rates compared to the control and aqua regia in tomato seeds (Table 2).

Table 2. Descriptive statistics of seed germination rates after 10 days for tomato (*Solanum lycopersicum* L.) and roselle (*Hibiscus sabdariffa* L.) under different treatments compared to a control group.

Treatment	Control		Aqua regia		Ozone	
Plant	Tomato	Roselle	Tomato	Roselle	Tomato	Roselle
Mean*	8A	4	8A	5	9B	4
Minimum	6	2	7	2	8	2
Maximun	10	6	10	9	10	7
Sum	124	64	122	73	140	58
Median	8	4	8	5	9	3
Standard error of the mean	0.4	0.4	0.2	0.55	0.2	0.44
Standard deviation	1.4	1.4	0.8	2.13	0.7	1.72
Coefficient variance	1.92	1.92	0.69	4.55	0.52	2.98

*Group means with different letters indicate statistically significant differences ($p \leq 0.01$) as determined by Kruskal-Wallis test.

No statistically significant differences were observed between the germination rates in seeds of the control group and either aqua regia or ozonated water treatments in roselle seeds (Kruskal-Wallis test, $p \geq 0.05$). Although not statistically significant in all cases, a discernible trend towards improved germination was observed across both plant species when utilizing ozonated water and aqua regia treatments (Table 2).

Previous research has extensively documented the capacity of pre-treatments to enhance plant growth by triggering a cascade of biochemical and physiological responses within the plant. Kangasjärvi *et al.* (1994) emphasized the potential of ozone to stimulate plant growth, suggesting that microdosing and short-term exposure can effectively enhance the growth and yield of various plant species. The findings of this study align with previous research that has highlighted the effectiveness of priming techniques, including the use of ozone and acids, in enhancing germination and crop yield in diverse plant species (Sudhakar *et al*., 2008, 2011; Varela and Arana, 2011; Condori Tarqui and Martinez Flores, 2020).

Seed germination varied both within and between treatments. A general trend of increasing germinated seeds was observed, although a proportion of seeds failed to germinate. In tomato, seed germination exhibited substantial inter-treatment variation (Figure 1A). Over the 10-day experimental period, tomato seed germination ranged from 0 to 100 seeds. The ozone treatment induced a rapid increase in germination between days 2 and 3, reaching a peak of approximately 100 germinated seeds. While both control and aqua regia treatments followed similar germination patterns, their peak germination counts were lower, reaching approximately 75 and 60 seeds, respectively, by day three. Following this peak, germination declined across all treatments, with the most pronounced decrease observed in the ozone treatment. Notably, the aqua regia treatment consistently resulted in the lowest germination rates in the tomato seed germination rate.

Roselle had a seed germination on a scale of 0 to 50 seeds. The ozone treatment stimulated rapid initial germination in roselle, peaking at approximately 50 seeds by day two. The control and aqua regia treatments exhibited similar germination

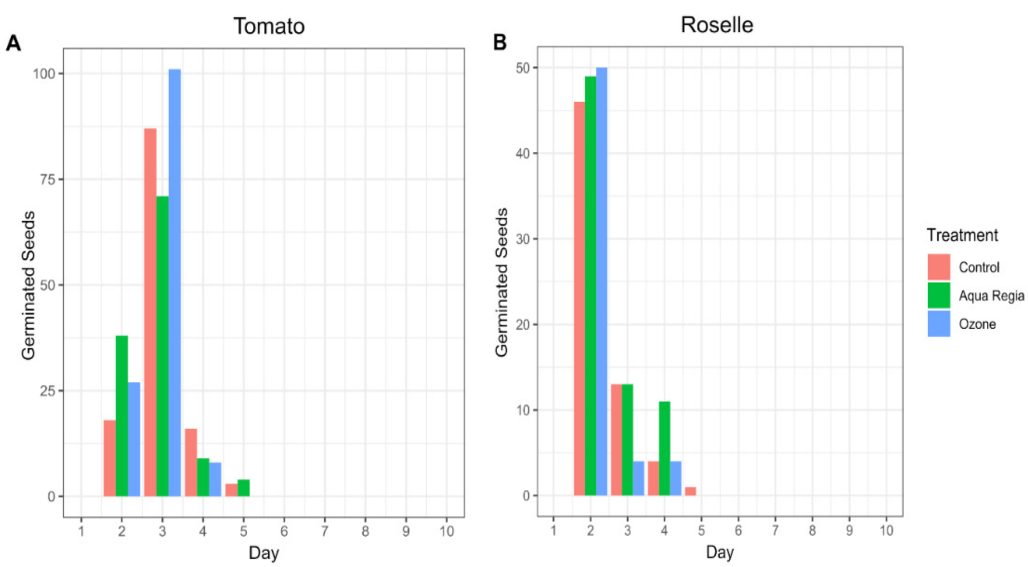

Figure 1. Histogram of seed germination frequency over 10 days in control and treated. seeds using ozonated water and aqua regia for two plant species. A: tomato (*Solanum lycopersicum* L.) seeds; B: roselle seeds (*Hibiscus sabdariffa* L.).

patterns, reaching approximately 48 and 45 seeds, respectively, also by day two. Following this peak, germination declined in both the control and ozone treatment. However, uniquely, the aqua regia treatment maintained a germination up of 10 seeds through day four.

The seeds of tomato and roselle possess distinct differences in their seed coats. Notably, tomato's seed coating is softer than roselle's due to the latter's thicker layer of irregular collapsed cells, contributing to increased hardness in the seed coating (Mabrouk *et al.*, 2016). The seed germination efficiency between both plant species is based on the effects of each treatment and the nature of the seed. On the one hand, ozone effects are well known to promote a trigger of biochemical and physiological responses after priming (Pandiselvam *et al*., 2020), which is mainly related to the high germination frequency by ozone in tomato seeds. On the other hand, treatment with aqua regia results in scarification of the roselle's coat, exposing the lumens of the macrosclereids cells. This process facilitates water imbibition and triggers seed germination (Nikoleave, 1977). Thus, the germination rate is influenced by the thickness of each type of seed when subjected to various treatments (Figure 1).

Ozone exhibited superior performance compared to control and aqua regia (Figure 2A). Seeds primed with ozone demonstrated a 95 % germination rate, surpassing the control group (83 %) and the aqua regia-primed seeds (83 %). Germination velocity also varied significantly. Ozone-primed seeds exhibited rapid

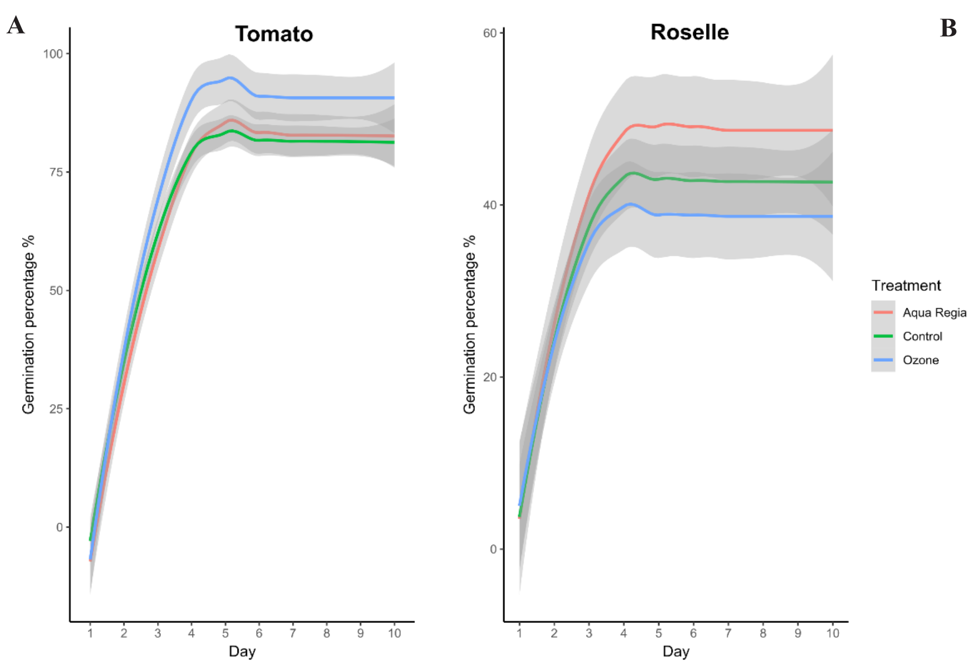

Figure 2. Germination percentages of the evaluated seeds over a 10-day period under three different treatments (control, aqua regia, and ozone). The shaded areas represent the variability or uncertainty associated with the measurements. A: tomato (*Solanum lycopersicum* L.) seeds; B: roselle seeds (*Hibiscus sabdariffa* L.).

germination, reaching maximum rates by the fourth day. In contrast, aqua regia-primed seeds displayed a delayed peak germination on the fifth day. These findings corroborate previous research by Kangasjärvi *et al.* (1994) and Pandiselvam *et al.* (2020), which demonstrated the potential of low-dose ozone to stimulate biochemical and physiological responses, enhancing germination and vigor in various plant species.

The observed increase in germination may be attributed to the stimulation of jasmonic acid production, a known promoter of root growth and seed germination in maize (*Zea mays* L.) and overall plants (Violleau *et al*., 2007). Several studies across various species have demonstrated significant differences in seed germination following ozone treatment (Dong *et al*., 2022; Tütüncü *et al*., 2024). These effects are likely mediated by the stimulation of biochemical cascades within the plant embryo and the release of volatile organic compounds (Dong *et al*., 2022). The observed enhancement of tomato seed germination is likely due to biostimulation rather than scarification of the seed coat. While these results align with those of Tütüncü *et al*. (2024) regarding the positive effects of ozone on seed germination, this study observed a more rapid response, achieved with only one minute of ozone exposure. The thin endosperm layer in tomato seeds may influence the efficacy of each priming treatment. It is possible that aqua regia treatment may have compromised the endosperm, leading to germination failure in some seeds (Madueño-Molina *et al*., 2006).

The germination of roselle seeds under ozonated water priming and aqua regia priming yielded distinct outcomes compared to those observed in tomato seeds (Figure 2B). The treatment using aqua regia priming demonstrated the most favorable germination rates for roselle seeds, reaching 48 % of the total germination. Conversely, ozonated water priming resulted in a maximum of 38 % germination (even lower than the control group, 43 %). The germination velocity exhibited a swift response when treated with aqua regia. The maximum germination was observed on the fifth day of incubation (Figure 2B). Despite the lower germination efficiency associated with ozonated water priming, this method demonstrates the quickest path to reaching maximum germination, typically observed by the fourth day.

While the use of aqua regia presents itself as the most beneficial method for seed germination under these conditions, it is noteworthy that ozonated water exhibits an interesting effect on germination velocity. Aqua regia is widely regarded as the most effective method for scarifying seeds with a hard coating and thicker endosperm, as demonstrated by its successful application in treating roselle seeds. Similar findings were documented in a study conducted by Babashpour *et al.* (2011), where enhanced germination rates were observed following imbibition in sulfuric acid of Fabaceae seeds. In the current study, seeds were subjected to a one-minute exposure to aqua regia, while other investigations have explored the effects of prolonged exposure to sulfuric acid. Youssef (2009) conducted studies that demonstrated promising outcomes in the germination of desert plant seeds following several days of exposure. However, additional research on the effects of exposure during varying time periods is required.

Subsequent to the application of ozone, there was a notable enhancement in germination velocity, which holds promising implications for agricultural productivity. As both species of seed plants demonstrated similar germination velocities, the present work suggests the utilization of ozone as a biostimulant for seed germination and plant growth. Substantial evidence supports the observed benefits resulting from ozone treatment (Kangasjärvi *et al.*, 1994; Violleau *et al.*, 2007; Sudhakar *et al.*, 2011; Pandiselvam and Thirupathi, 2015; Pandiselvam *et al.*, 2020); the current findings further support the recognition of this agent as a stimulant for enhancing germination velocity, irrespective of its impact on efficiency.

The PCA (Figure 3) was used to analyze inter-treatment variability in tomato seed germination indices. The first two principal components, Dim1 and Dim2, captured 74.2 % of the total variance, with Dim1 accounting for 55.5 % and Dim2 for 18.7 %. This ordination facilitated interpretation of the germination data based on biological relevance.

The first quadrant of the biplot (Figure 3) revealed a cluster of germination indices, including 'EmergenceRateIndex_SG_mod', 'TimsonsIndex_Labouriau', 'GermIndex_mod', 'MeanGermRate', 'GermValue_DP', 'GermRateRecip_Coolbear', 'PeakGermPercent', 'GermSpeedCorrected_Accumulated', 'CVG', 'GermValue_Czabator', 'GermValue_Czabator_mod', and 'GermSpeedCorrected_Normal', demonstrating strong positive correlations. This clustering suggests that the ozone and, to a lesser extent, aqua regia treatments within this quadrant are associated with elevated values across these germination metrics. Consequently, these treatments appear to promote rapid, coordinated, and enhanced germination, characterized by

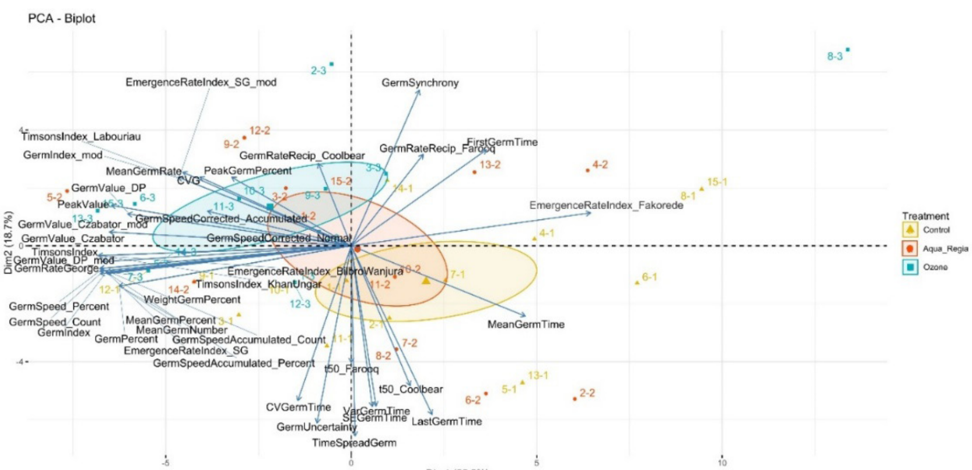

Figure 3. Principal Component Analysis (PCA) biplot of 42 tomato (*Solanum lycopersicum* L.) seed germination indices under different treatments and a control. The plot shows the relationships between germination indices (vectors) and treatments (points), with confidence ellipses representing treatment groups. Dim1 and Dim2 represent the first two principal components, explaining 55.5 and 18.7 % of the variance, respectively.

high emergence rates, peak germination percentages, and normalized germination speeds. The observed pattern indicates a synergistic effect of factors contributing to robust seed germination within this region of the PCA space.

The lower left quadrant of the PCA biplot (Figure 3) demonstrates a significant association among seed germination metrics and ozone treatment. Specifically, 'EmergenceRateIndex_SG' and 'GermSpeedAccumulated_Count/Percent' exhibit a strong positive correlation, indicating that accelerated emergence rates correspond to higher cumulative germination. Furthermore, 'MeanGermPercent,' 'MeanGermNumber,' 'GermPercent,' and 'GermIndex' cluster closely, suggesting redundancy in their measurement of overall germination success. Conversely, 't50_Farroq,' 'CVGermTime,' and 'TimeSpreadGerm' show a greater association with control and aqua regia treatments compared to ozone treatments.

In the lower right quadrant of the PCA biplot (Figure 3), control and aqua regia treatments exhibit a positive correlation with 'LastGermTime,' 'SEGermTime,' 't50_Coolbear,' 'VarGermTime,' and 'TimeSpreadGerm.' This indicates that these treatments are associated with increased variability and prolonged timing in seed germination, specifically influencing the time to reach 50 % germination (t50_Coolbear), the standard error of germination time (SEGermTime), the last germination time (LastGermTime), the variance of germination time (VarGermTime), and the spread of germination times (TimeSpreadGerm).

The upper right quadrant of the PCA biplot (Figure 3) reveals a strong association between ozone and aqua regia treatments and enhanced seed germination. This quadrant positively correlates with 'GermSynchrony,' 'GermRateRecip_Farooq,' and 'FirstGermTime,' indicating improved germination synchronicity, rate, and speed, respectively. The prominent projection of 'EmergenceRateIndex_Fakorede' along Dim1 confirms higher emergence rates for these treatments. Within this quadrant, the control and aqua regia treatments are differentiated, versus the control exhibiting the highest 'EmergenceRateIndex_Fakorede' and shortest 'FirstGermTime,' indicative of superior and faster emergence.

Variability in germination responses to seed treatments was observed in tomato seeds. This heterogeneity is attributable to a complex interplay of intrinsic and extrinsic factors, with particular emphasis on seed morphology and the specific nature of the applied stimulation. Therefore, analyzed indices on seed germination reflected a variation in their germination traits. PCA revealed distinct differentiation between control and treated seeds, particularly highlighting the divergence induced by ozone. Seed germination in control demonstrates that these seeds were delayed for seed germination because 'MeanGerminationTime' and 't50' indices reached the maximum scores for these seeds. The above reflects the baseline of the experiment and is very related to the natural dormancy of the seeds without treatment or stimulation. Gene expression plays a pivotal role in establishing phenotypic traits, encompassing size, morphology, and biochemical composition, during dormancy (Nonogaki, 2006). However, exogenous treatments can induce alterations in gene expression, primarily mediated through the modulation of hormone biosynthesis and catabolism.

The PCA (Figure 3) elucidated the integrated effects of the two treatments on seed germination, revealing a distinct separation of treatment effects characterized by increased germination quantity and rate. Aqua regia treatment induced a biphasic response in seed dormancy, characterized by the stimulation of germination initiation alongside a concomitant reduction in germination rate. This treatment effectively facilitated seed coat removal, yielding rapid results compared to prolonged acid treatments. Specifically, Sonkar *et al*. (2022) demonstrated the efficacy of hydrochloric acid (HCl) presowing treatments lasting four and six hours, underscoring the comparatively accelerated effect of aqua regia.

Results from PCA indicated that ozone treatment elicited the most significant and consistent improvement in seed germination parameters in tomato, suggesting a harmonized and accelerated germination process. Godínez-Mendoza *et al*. (2023) documented the biostimulant effects of various chemical treatments, characterizing a range of chemical stimuli. These authors emphasized the concept of hormesis, wherein a chemical stressor, when applied at an appropriate dose, elicits a beneficial response, termed "eustress." The observed hormetic effect, as demonstrated in the present study, exhibited similarities to those associated with gibberellic acid-mediated enhancement of seed germination, a crucial regulatory process (Finch-Savage and Leubner-Metzger, 2006).

Ozone priming appears to correlate with elevated gibberellic acid levels in treated plants (Kangasjärvi *et al*., 1994). Following ozone, a cascade of physiological and biochemical responses is initiated, potentially contributing to the enhanced efficiency, speed, and rate of germination in tomato seeds, as germination indices denote. Additionally, several studies have documented the beneficial effects of ozone on seed germination (Violleau *et al*., 2008; Patwardhan and Gandhare, 2013; Pandiselvam *et al*., 2020; Tütüncü *et al*., 2024), due to ozone treatment potentially activating ethylene and reactive oxygen species (ROS) signaling pathways, which contribute to the maintenance of "eustress" and the subsequent transition from dormancy in seeds (El-Maarouf-Bouteau and Bailly, 2008).

The PCA performed on roselle seeds was conducted to explore the relationships among various seed germination indices and to assess the influence of different seed treatments (control, aqua regia, and ozone). The biplot (Figure 4) revealed that the first two principal components (Dim1 and Dim2) accounted for 91.7 % of the total variance (Dim1: 52.1 %, Dim2: 39.6 %), indicating that these two components effectively captured the major patterns in the data.

The upper left quadrant of the PCA biplot (Figure 4) exhibits a strong correlation with variables including 'TimsonsIndex_Labouriau,' 'EmergenceRateIndex_SG_mod,' 'CVG,' 'GermIndex_mod,' 'MeanGermRate,' 'GermRateRecip_Coolbear,' 'GermSynchrony,' 'GermSpeedCorrected_Normal,' 'GermRateRecip_Farooq,' and 'GermSpeedCorrected_Accumulated.' This spatial distribution indicates that the ozone treatment significantly influenced germination kinetics, particularly enhancing the rate and synchrony of germination, thereby promoting a more consistent and accelerated

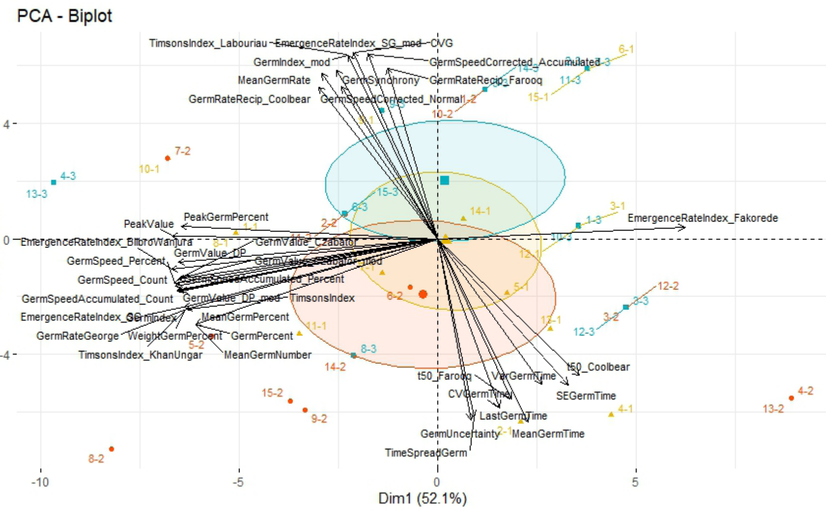

Figure 4. Principal Component Analysis (PCA) biplot of 42 roselle (*Hibiscus sabdariffa* L.) seed germination indices under different treatments and a control. The plot shows the relationships between germination indices (vectors) and treatments (points), with confidence ellipses representing treatment groups. Dim1 and Dim2 represent the first two principal components, explaining 52.1 and 39.6 % of the variance, respectively.

germination process. Furthermore, the observed correlation of 'GermPeakPercent' and 'PeakValue' with both the ozone treatment and control groups suggests that these treatments facilitated the attainment of maximum seed germination within a defined temporal window.

The lower left quadrant of the PCA biplot (Figure 4), characterized by vectors representing variables such as 'EmergenceRateIndex_BilbroWanjura,' 'GermValue_DP,' 'GermSpeed_Percent,' 'GermSpeed_Count,' 'GermValue_Czabator_mod,' 'GermSeedAccumulated_Percent,' 'GermRateRecip_Coolbear,' 'GermSpeedCorrected_Accumulated,' 'GermSeedAccumulated_Count,' 'TimsonsIndex,' 'EmergenceRateIndex_SG,' 'GermIndex,' 'MeanGermPercent,' 'GermRateGeorge,' 'WeightGermPercent,' 'GermPercent,' 'TimsonsIndex_KhanUngar,' and 'MeanGermNumber,' demonstrates a strong association with the aqua regia treatment. This spatial distribution suggests that seeds subjected to this treatment exhibited enhanced germination kinetics, characterized by elevated germination rates, increased percentages of germinated seeds, and a higher overall cumulative germination, as reflected by the aforementioned variables.

The lower right quadrant of the PCA biplot (Figure 4) revealed a clustering of variables including 'CVGermTime,' 'TimeSpreadGerm,' 'LastGermTime,' 'MeanGermTime,' 'SEGermTime,' 'VarGermTime,' 'GermUncertainty,' 't50_Farooq,' and 't50_Coolbear.' This spatial distribution reflects that both the control and aqua regia treatments were associated with a broader distribution of germination times and increased germination uncertainty. This pattern indicates a higher degree of heterogeneity in the germination process within these treatment groups. The upper right quadrant of the PCA biplot (Figure 4) revealed a strong correlation of the 'EmergenceRateIndex_Fakorede' index with both the ozone and control treatments. This spatial proximity relates that both treatments contributed to a more rapid and synchronized emergence of roselle seeds, as indicated by the enhanced values of this specific emergence index.

The PCA of roselle seed germination indices revealed distinct effects of the different treatments, highlighting their potential for enhancing germination in species with thicker seed coats, such as roselle. This study utilized a short seed imbibition time in aqua regia to enhance germination percentage and kinetics in roselle seeds. Aqua regia's scarification effect breaks down the hard seed coat, facilitating water imbibition and promoting germination (Youssef, 2009; Nasr *et al*., 2013). In contrast, Abdel Latef *et al*. (2020) reported negative effects on roselle seed germination with long-term aluminum oxide nanopriming. This discrepancy may stem from the differing treatment durations and mechanisms: short-term aqua regia exposure facilitates seed coat disruption, while extended nanopriming may hinder germination processes. The beneficial effects of acid imbibition for seed scarification have been acknowledged. Hence, it is imperative to conduct further studies in roselle to thoroughly evaluate extended time-lapses for imbibition in acids at overall, thus several assays have taken long period times on acid soaking for enhance seed germination (Habib, 2010; Aboelgoud, 2015; Nair *et al*., 2017). PCA showed that control reflects the baseline of delayed germination such as "baseline" response due to dormancy in seeds as was discussed previously in the case of tomato seeds.

Ozone treatment demonstrated the highest efficacy in promoting the speed and uniformity of germination in roselle seeds. However, evidence of hormesis was observed, characterized by the enhanced synchrony and rate of germination. While a reduction in overall germination rate was noted, the concurrent increase in several germination indices suggests the activation of a complex biochemical response cascade. Specifically, ozone-induced oxidative stress, leading to the production of ROS, particularly hydrogen peroxide (H_2O_2), is posited to play a critical role in dormancy release (Sudhakar *et al*., 2011). This mechanism likely contributes to the accelerated and more efficient germination process observed in ozone-treated roselle seeds. Furthermore, the observed reduction in abscisic acid (ABA) levels, a known germination inhibitor, likely contributed to the enhanced germination indices. Ozone may also stimulate the production of gibberellic acid and ethylene, both of which promote germination and antagonize ABA's inhibitory effects (El-Araby *et al*., 2006). This hormonal interplay likely underlies the observed improvements in germination synchrony and vigor. Additionally, ROS, particularly H_2O_2, are implicated in endosperm weakening, facilitating radicle protrusion (Leubner-Metzger, 2005). This mechanism elucidates how ozone priming can lead to faster and more uniform germination, as evidenced in both roselle and, as well, in tomato seeds.

CONCLUSIONS

The pre-sowing treatments applied to tomato and roselle seeds revealed species-specific effects on germination, underscoring their potential to enhance crop productivity and sustainability. Ozone treatment significantly improved germination rates and velocity in tomato seeds, outperforming both the control and aqua regia treatments, likely mediated by the triggering of biochemical and physiological mechanisms. Aqua regia effectively enhanced germination in roselle seeds by scarifying their thick seed coats, facilitating water absorption and improving germination percentages and kinetics. This presents a rapid alternative to prolonged acid treatments. These findings contribute to addressing global food security challenges and advancing sustainable agricultural development. Further research is warranted to optimize treatment protocols and evaluate their long-term effects on plant growth and yield under field conditions.

ACKNOWLEDGEMENTS

The first author wants to thank the Mexico's Secretariat of Science, Humanities, Technology, and Innovation (SECIHTI) for the given master's scholarship for developing the present study. The authors thank to the Postgraduate College Montecillo Campus for the monetary and in-kind resources provided for the development of the present research.

REFERENCES

Aboelgoud S. 2015. Pre-sowing treatments for breaking seed dormancy in relation to germination, seedling vigour and yield of teosinte. Journal of Plant Production 6 (12): 2177–2186. https://doi.org/10.21608/jpp.2015.52461

Aravind J, Vimala Devi S, Radhamani J, Jacob SR, Srinivasan K. 2019. germinationmetrics: Seed germination indices and curve fitting. ICAR-National Bureau of Plant Genetic Resources. New Delhi, India. https://github.com/aravind-j/germinationmetrics

Ashraf M, Foolad MR. 2005. Pre-sowing seed treatment—A shotgun approach to improve germination, plant growth, and crop yield under saline and non-saline conditions. Advances in Agronomy (88): 223–271. https://doi.org/10.1016/S0065-2113(05)88006-X

Babashpour AM, Sharivivash R, Rahbari A. 2011. Effect of different treatments on seed germination of honey locust (*Gleditschia triacanthos*). Modern Applied Science 5 (1): 200–204. https://doi.org/10.5539/mas.v5n1p200

Baskin CC, Baskin JM. 1998. Seeds: Ecology, biogeography, and evolution of dormancy and germination. Choice Reviews Online 36 (4): 2164. https://doi.org/10.5860/choice.36-2164

Bilbro JD, Wanjura DF. 1982. Soil crusts and cotton emergence relationships. Transactions of the ASAE 25 (6): 1484–1487. https://doi.org/10.13031/2013.33750

Bradford KJ. 2017. Water relations in seed germination. Seed Development and Germination: 351–396. https://doi.org/10.1201/9780203740071-13

Brown RF, Mayer DG. 1988. Representing cumulative germination. 1. A critical analysis of single-value germination indices. Annals of Botany 61 (2): 117–125. https://doi.org/10.1093/oxfordjournals.aob.a087534

Canul-Ku J, Morán-Girón D, Barrios-Gómez EJ, Hernández-Meneses E, Rangel-Estrada SE. 2023. Cruza manual en tomate nativo (*Solanum lycopersicum* L.) de México como base para su mejora genética. Brazilian Journal of Animal and Environmental Research 6 (3): 2261–2272. https://doi.org/10.34188/bjaerv6n3-024

Casals J, Martí M, Rull A, Pons C. 2021. Sustainable transfer of tomato landraces to modern cropping systems: The effects of environmental conditions and management practices on long-shelf-life tomatoes. Agronomy 11 (3): 533. https://doi.org/10.3390/agronomy11030533

Condori-Tarqui A, Martinez-Flores Z. 2020. Tratamientos físicos y químicos en la germinación de semillas de especies nativas del altiplano. Revista de Investigación Agropecuaria y de Recursos Naturales 7 (2): 46–57.

Coolbear P, Francis A, Grierson D. 1984. The effect of low temperature pre-sowing treatment on the germination performance and membrane integrity of artificially aged tomato seeds. Journal of Experimental Botany 35 (11): 1609–1617. https://doi.org/10.1093/jxb/35.11.1609

Czabator FJ. 1962. Germination value: An index combining speed and completeness of pine seed germination. Forest Science 8 (4): 386–396.

Djavanshir K, Pourbeik H. 1976. Germination value, a new formula. Silvae Genetica 25 (2): 79–83.

Dong X, Sun L, Maker G, Ren Y, Yu X. 2022. Ozone treatment increases the release of VOC from barley, which modifies seed germination. Journal of Agricultural and Food Chemistry 70 (10): 3127–3135. https://doi.org/10.1021/acs.jafc.1c06812

Draganić I, Lekić S. 2012. Seed priming with antioxidants improves sunflower seed germination and seedling growth under unfavorable germination conditions. Turkish Journal of Agriculture and Forestry 36 (4): 421–428. https://doi.org/10.3906/tar-1110-16

Edmond JB, Drapala WJ. 1958. The effects of temperature, sand and soil, and acetone on germination of okra seed. American Society for Horticultural Science 71: 428–434.

Edwards TI. 1932. Germination studies with the seeds of *Xanthium canadense*. American Journal of Botany 19 (8).

El-Araby MM, Moustafa SMA, Ismail AI, Hegazi AZA. 2006. Hormone and phenol levels during germination and osmopriming of tomato seeds, and associated variations in protein patterns and anatomical seed features. Acta Agronomica Hungarica 54 (4): 441–457. https://doi.org/10.1556/AAgr.54.2006.4.7

El-Maarouf-Bouteau H, Bailly C. 2008. Oxidative signaling in seed germination and dormancy. Plant Signaling and Behavior 3 (3): 175–182. https://doi.org/10.4161/psb.3.3.5539

Ellis RH, Roberts EH. 1980. Improved equations for the prediction of seed longevity. Annals of Botany 45 (1): 13–30. https://doi.org/10.1093/oxfordjournals.aob.a085797

Evetts LL, Burnside OC. 1972. Germination and seedling development of common milkweed and other species. Weed Science 20 (4): 371–378. https://doi.org/10.1017/s004317450003589x

Fakorede MAB, Agbana SB. 1983. Heterotic effects and association of seedling vigor with mature plant characteristics and grain yield in some tropical maize cultivars. Maydica 28 (4): 327–338.

Fakorede MAB, Ayoola AO. 1980. Relationship between seedling vigor and selection for yield improvement in maize. Maydica 25 (3): 135–147.

Fakorede MAB, Ojo DK. 1981. Variability for seedling vigour in maize. Experimental Agriculture 17 (2): 195–201. https://doi.org/10.1017/S0014479700011455

Farooq M, Basra SMA, Ahmad N, Hafeez K. 2005. Thermal hardening: A new seed vigor enhancement tool in rice. Journal of Integrative Plant Biology 47 (2): 187–193. https://doi.org/10.1111/j.1744-7909.2005.00031.x

Finch-Savage WE, Leubner-Metzger G. 2006. Seed dormancy and the control of germination. New Phytologist 171 (3): 501–523. https://doi.org/10.1111/j.1469-8137.2006.01787.x

Godínez-Mendoza PL, Rico-Chávez AK, Ferrusquía-Jimenez NI, Carbajal-Valenzuela IA, Villagómez-Aranda AL, Torres-Pacheco I, Guevara-González RG. 2023. Plant hormesis: Revising of the concepts of biostimulation, elicitation and their application in a sustainable agricultural production. Science of the Total Environment 894: 164883. https://doi.org/10.1016/j.scitotenv.2023.164883

Goloff A, Bazzaz FA. 1975. A life history analysis of the winter annual *Gnaphalium purpureum*. Oecologia 20 (2): 107–122.

Grose RJ, Zimmer WJ. 1958. Some laboratory germination responses of the seeds of river red gum, *Eucalyptus camaldulensis* Dehn. syn. *Eucalyptus rostrata* Schlecht. Australian Journal of Botany 6 (2): 129–153. https://doi.org/10.1071/BT9580129

Gross BL, Olsen KM. 2010. Genetic perspectives on crop domestication. Trends in Plant Science 15 (9): 529–537. https://doi.org/10.1016/j.tplants.2010.05.008

Habib M. 2010. Sugarbeet (*Beta vulgaris* L.) seed pre-treatment with water and HCl to improve germination. African Journal of Biotechnology 9 (9): 1338–1342. https://doi.org/10.5897/ajb10.1460

Herrera-Arellano A, Flores-Romero S, Chávez-Soto MA, Tortoriello J. 2004. Effectiveness and tolerability of a standardized extract from *Hibiscus sabdariffa* in patients with mild to moderate hypertension: A controlled and randomized clinical trial. Phytomedicine 11 (5): 375–382. https://doi.org/10.1016/j.phymed.2004.04.001

ISTA (International Seed Testing Association). 2023. International rules for seed testing. In Wallisellen, Switzerland.

Kangasjärvi J, Talvinen J, Utriainen M, Karjalainen R. 1994. Plant defence systems induced by ozone. Plant, Cell and Environment 17 (7): 783–794. https://doi.org/10.1111/j.1365-3040.1994.tb00173.x

Kaya MD, Okçu G, Atak M, Çıkılı Y, Kolsarıcı Ö. 2006. Seed treatments to overcome salt and drought stress during germination in sunflower (*Helianthus annuus* L.). European Journal of Agronomy 24 (4): 291–295. https://doi.org/10.1016/j.eja.2005.08.001

Khamassi K, Harbaoui K, Teixeira JA, Jeddi FB. 2013. Optimal germination temperature assessed by indices and models in field bean (*Vicia faba* L. var. minor). Agriculturae Conspectus Scientificus 78 (2): 131–136.

Khan MA, Ungar IA. 1984. The effect of salinity and temperature on the germination of polymorphic seeds and growth of *Atriplex triangularis* Willd. American Journal of Botany 71 (4): 481–489. https://doi.org/10.2307/2443323

Koop SHAA, van Leeuwen CJ. 2017. The challenges of water, waste and climate change in cities. Environment, Development and Sustainability 19 (2): 385–418. https://doi.org/10.1007/s10668-016-9760-4

Kotowski F. 1962. Temperature relations to germination of vegetable seed. Proceedings of the American Society for Horticultural Science 23: 176–184.

Kumar N, Bhardwaj ML, Sharma A, Kumar N. 2017. Assessment of genetic divergence in tomato (*Solanum lycopersicum* L.) through clustering and principal component analysis under mid hills conditions of Himachal Pradesh. International Journal of Current Microbiology and Applied Sciences 6 (5): 1811–1819. https://doi.org/10.20546/ijcmas.2017.605.197

Labouriau LG. 1983. A germinação das sementes. Secretaria Geral da OEA, Washington, DC, USA. 173 p.

Labouriau LG, Bicalho-Valadares M. 1976. On the germination of seeds of *Calotropis procera*. Anais da Academia Brasileira de Ciências 48 (2): 263–283.

Abdel Latef AAH, Zaid A, Abu Alhmad MF, Abdelfattah KE. 2020. The impact of priming with Al2O3 nanoparticles on growth, pigments, osmolytes, and antioxidant enzymes of Egyptian roselle (*Hibiscus sabdariffa* L.) cultivar. Agronomy 10 (5): 1–16. https://doi.org/10.3390/agronomy10050681

Leubner-Metzger G. 2005. Β-1,3-glucanase gene expression in low-hydrated seeds as a mechanism for dormancy release during tobacco after-ripening. Plant Journal 41 (1): 133–145. https://doi.org/10.1111/j.1365-313X.2004.02284.x

Mabrouk M, Youssef A, Amin W, Abou-Samaha R. 2016. Physical properties, microstructure and proximate chemical composition of roselle (*Hibiscus sabdariffa*) seeds and kernels. Alexandria Journal of Food Science and Technology 13 (2): 19–32. https://doi.org/10.12816/0038411

Madueño-Molina A, García-Paredes D, Martínez-Hernández J, Rubio-Torres C, Navarrete-Valencia A, Bojórquez-Serrano J. 2006. Germinación de semilla de frijolillo, *Rhynchosia minima* (L.) DC., luego de someterla a tratamientos pregerminativos. Bioagro 18 (2): 101–105.

Melville AH, Galletta GJ, Draper AD, Ng TJ. 1980. Seed germination and early seedling vigor in progenies of inbred strawberry selections. HortScience 15 (6): 749–750. https://doi.org/10.21273/hortsci.15.6.749

Meyer RS, Purugganan MD. 2013. Evolution of crop species: Genetics of domestication and diversification. Nature Reviews Genetics 14 (12): 840–852. https://doi.org/10.1038/nrg3605

Montaño-Arango O, Corona-Armenta JR, Ortega-Reyes AO, Garnica-González J. 2024. La flor de jamaica como producto estratégico para la salud humana en el contexto de México. Inter Disciplina 12 (33): 117–142. https://doi.org/10.22201/ceiich.24485705e.2024.33.88242

Nair AGH, Vidya P, Sreekumar J, Mohan C. 2017. Effect of seed pre-sowing treatment on germination of sweet potato. International Journal of Applied and Pure Science and Agriculture 3 (9): 69–75. https://doi.org/10.22623/ijapsa.2017.3101.fjzzz

Nasr SMH, Savadkoohi SK, Ahmadi E. 2013. Effect of different seed treatments on dormancy breaking and germination in three species in arid and semi-arid lands. Forest Science and Practice 15 (2): 130–136. https://doi.org/10.1007/s11632-013-0209-7

Nichols MA, Heydecker W. 1968. Two approaches to the study of mass media. Proceedings of the International Seed Testing Association 33 (3): 531–540.

Nikoleave MG. 1977. Factors controlling seed dormancy pattern. *In* Khan AA. (ed.), The Physiology and Biochemistry of Seed Dormancy and Germination. North Holland Publishing Company: Amsterdam, Netherlands, pp: 52–74

Nonogaki H. 2006. Seed germination. The biochemical and molecular mechanisms. Breeding Science 56 (2): 93–105. https://doi.org/10.1270/jsbbs.56.93

Pandiselvam R, Mayookha VP, Kothakota A, Sharmila L, Ramesh SV, Bharathi CP, Gomathy K, Srikanth V. 2020. Impact of ozone treatment on seed germination – A systematic review. Ozone: Science and Engineering 42 (4): 331–346. https://doi.org/10.1080/01919512.2019.1673697

Pandiselvam R, Thirupathi V. 2015. Reaction kinetics of ozone gas in green gram (*Vigna radiate*). Ozone: Science and Engineering 37 (4): 309–315. https://doi.org/10.1080/01919512.2014.984158

Patwardhan MS, Gandhare WZ. 2013. High voltage electric field effects on the germination rate of tomato seeds. Acta Agrophysica 20 (2): 403–413.

Primack RB. 1985. Longevity of individual flowers. Annual Review of Ecology and Systematics 16 (1): 15–37. https://doi.org/10.1146/annurev.es.16.110185.000311

Quintanilla LG, Pajarón S, Pangua E, Amigo J. 2000. Effect of temperature on germination in northernmost populations of *Culcita macrocarpa* and *Woodwardia radicans*. Plant Biology 2 (6): 612–617. https://doi.org/10.1055/s-2000-16638

Ranal MA. 1999. Seed germination. Brazilian Journal of Plant Physiology 11 (3): 153–161.

Ranal MA, de Santana DG. 2006. How and why to measure the germination process? Revista Brasileira de Botanica 29 (1): 1–11. https://doi.org/10.1590/S0100-84042006000100002

Roh MS, Bentz JA, Wang P, Ercheng LI, Koshioka M. 2004. Maturity and temperature stratification affect the germination of *Styrax japonicus* seeds. Journal of Horticultural Science and Biotechnology 79 (4): 645–651. https://doi.org/10.1080/14620316.2004.11511820

Roshchina VV, Roshchina VD. 2003. Ozone and plant cell. Springer: Dordrecht, Netherlands. 267 p. https://doi.org/10.1007/978-94-017-2523-1

Scott SJ, Jones RA, Williams WA. 1984. Review of data analysis methods for seed germination. Crop Science 24 (6): 1192–1199. https://doi.org/10.2135/cropsci1984.0011183x002400060043x

Shahrokhi M, Tehranifar A, Hadizadeh H, Selahvarzi Y. 2011. Effect of drought stress and paclobutrazol-treated seeds on physiological response of *Festuca arundinacea* L. Master and *Lolium perenne* L. Barrage. Journal Biology and Environment Science 5 (14): 77–85.

Shmueli M, Goldberg D. 2022. Emergence, early growth, and salinity of five vegetable crops germinated by sprinkle and trickle irrigation in an arid zone. Horticulture Science 6 (6): 563–565. https://doi.org/10.21273/hortsci.6.6.563

Smith PG, Millet AH. 1964. Germinating and sprouting responses of the tomato at low temperatures. Journal of the American Society for Horticultural Science 84: 480–484.

Sonkar A, Love SK, Sharma A, Pahwa C, Sharma I, Biju J, Amla S. 2022. Effect of HCl pretreatment on tomato (*Solanum lycopersicum* L.) seed germination. Zenodo 7 (10): 491–494. https://doi.org/10.5281/zenodo.7269311

Sudhakar N, Nagendra-Prasad D, Mohan N, Hill B, Gunasekaran M, Murugesan K. 2011. Assessing influence of ozone in tomato seed dormancy alleviation. American Journal of Plant Sciences 2 (3): 443–448. https://doi.org/10.4236/ajps.2011.23051

Sudhakar N, Nagendra-Prasad D, Mohan N, Murugesan K. 2008. A preliminary study on the effects of ozone exposure on growth of the tomato seedlings. Australian Journal of Crop Science 2 (1): 33–39.

Tester M, Langridge P. 2010. Breeding technologies to increase crop production in a changing world. Science 327 (5967): 818–822. https://doi.org/10.1126/science.1183700

Thompson K, Bewley JD, Black M. 1995. Seeds: Physiology of development and germination. The Journal of Ecology 83 (6): 1053. https://doi.org/10.2307/2261186

Throneberry GO, Smith FG. 1955. Relation of respiratory and enzymatic activity to corn seed viability. Plant Physiology 30 (4): 337–343. https://doi.org/10.1104/pp.30.4.337

Tolhurst TN, Ker AP. 2015. On Technological change in crop yields. American Journal of Agricultural Economics 97 (1): 137–158. https://doi.org/10.1093/ajae/aau082

Tucker H, Wright LN. 1965. Estimating rapidity of germination. Crop Science 5 (5): 398–399. https://doi.org/10.2135/cropsci1965.0011183x000500050006x

Tütüncü M, Andiç M, Kebeli F, Çelikel FG, Şimşek Ö. 2024. Effects of ozone treatments on *in vitro* seed germination of *Ruscus aculeatus*, *Ruscus hypoglossum* and *Danae racemosa*. Black Sea Journal of Agriculture 7 (5): 542–547. https://doi.org/10.47115/bsagriculture.1528904

Valencia-Romero R. 2019. Soberanía alimentaria de granos básicos en México: un enfoque de cointegración de Johansen a partir del TLCAN. Análisis Económico 34 (87): 223–248. https://doi.org/10.24275/uam/azc/dcsh/ae/2019v34n87/Valencia

Vallance KB. 1950. Studies on the germination of the seeds of *Striga hermonthica*. Annals of Botany 14 (3): 347–363. https://doi.org/10.1093/oxfordjournals.aob.a083251

Varela S, Arana V. 2011. Latencia y germinación de semillas. Instituto Nacional de Tecnología Agropecuaria, Estación Experimental Agropecuaria Paraná. Bariloche, Argentina. 10 p.

Violleau F, Hadjeba K, Albet J, Cazalis R, Surel O. 2007. Increase of corn seeds germination by oxygen and ozone treatment. IOA Conference and Exhibition. Valencia, Spain. 6 p.

Violleau F, Hadjeba K, Albet J, Cazalis R, Surel O. 2008. Effect of oxidative treatment on corn seed germination kinetics. Ozone: Science and Engineering 30 (6): 418–422. https://doi.org/10.1080/01919510802474631

Youssef AM. 2009. Seed germination of some desert plants from Egypt. Journal of Applied Sciences Research 5 (2): 144–150.

Agrociencia

UNLEASHING HALAL POTENTIAL: EXPLORING THE DYNAMICS OF HALAL LOGISTICS IN TANGERANG CITY, INDONESIA

Nurhayati **Nurhayati**[1,2*], Anis **Chelbi**[3,4], Amel Ben **Mabrouk**[4], Felina C. **Young**[2]

[1]Universitas Prasetiya Mulya. Food Business Technology. Edu Town Kavling Edu I No. 1, BSD City, Tangerang, Indonesia. C. P. 15339.
[2]Philippine Women's University. CBIBE School. 1743 Taft Avenue, Malate, Manila, Philippines. C. P. 1004.
[3]Université de Tunis. Higher School of Engineering of Tunis (ENSIT). Montfleury, Tunis, Tunisia. C. P. 1008.
[4]South Mediterranean University. Mediterranean School of Business (MSB). Les Jardins du Lac 2, Tunisia. C. P. 1053.
* Author for correspondence: nurhayati@pmbs.ac.id, nurhayati.anhar81@gmail.com

Citation: Nurhayati N, Chelbi A, Mabrouk AB, Young FC. 2025. Unleashing halal potential: exploring the dynamics of halal logistics in Tangerang City, Indonesia. **Agrociencia** 59(3): 343-355. https://doi.org/ 10.47163/agrociencia.v59i3.3272

Editor in Chief:
Dr. Fernando C. Gómez Merino

Received: July 16, 2024.
Approved: January 17, 2025.
Published in Agrociencia:
March 25, 2025.

ABSTRACT

The rapid expansion of the global halal market has increased the demand for efficient and standardized halal logistics. This study examines key challenges and enablers of halal logistics implementation in Tangerang City, Indonesia, a region experiencing significant growth in halal consumerism. Using a quantitative cross-sectional approach, data were collected from 170 consumers across diverse social backgrounds. The survey, distributed via Google Forms, was analyzed using structural equation modeling (SEM) with WrapPLS to identify key logistics barriers and improvement opportunities. The findings reveal three major challenges: 1) inconsistent halal certification processes, causing compliance confusion; 2) low consumer awareness, impacting purchasing confidence; and 3) weak stakeholder collaboration, leading to inefficiencies. The study also identifies four key enablers: 1) technology adoption, particularly tracking systems and digital platforms to enhance supply chain transparency and operational efficiency; 2) education and training programs to improve halal literacy among logistics professionals and consumers; 3) regulatory harmonization and stakeholder collaboration to ensure smoother implementation of halal logistics; and 4) optimized transportation solutions to maintain halal integrity and improve delivery efficiency.

Keywords: public awareness, information systems, information technology, regulations.

INTRODUCTION

The global market is increasing the demand for halal products that adhere to the teachings of the Islamic religion. Indonesia, as the country with the largest Muslim population in the world, has a big responsibility to ensure the production and distribution of quality halal products (Soesilowati and Yuliana, 2013). Challenges remain in ensuring the halal status of these products, especially in terms of logistics (Aziz and Zailani, 2016). Poorly managed logistics can lead to cross-contamination, violations of halal standards, and uncertainty in the halal supply chain (Zainuddin *et al*., 2020).

Halal logistics, according to Islamic principles, is a process that ensures that all aspects of the delivery of goods and services, including processing, production, storage, transportation, and distribution, do not contain haram or non-halal elements (Nafis, 2019; Gunardi, 2023). This requires the inspection and supervision of goods and their production processes in order to ensure the halal and cleanliness of products (Alfarizi, 2022), as well as meeting the requirements of Muslim consumers (Putra *et al*., 2023).

Companies must ensure that all activities carried out during the production process do not violate Islamic law, such as avoiding the use of non-halal materials and maintaining the cleanliness of the work environment (Mahmudah *et al*., 2022). Halal logistics must be carried out in accordance with Islamic law, which includes storage that is clean and free of contamination (Ahmad and Shariff, 2016). Transportation must be carried out using halal means of transportation while avoiding the use of non-halal means (Dewi and Trihardani, 2017). Distribution must ensure that the products are not contaminated during the handling, storage, and distribution processes (Kurniawati *et al*., 2022).

A well-integrated logistics system is an important aspect of ensuring halal production. (Mu'ti sazali and Ligte, 2019). This study investigates the factors that support the implementation of halal logistics and its strategies in Indonesia, with a focus on studies in Tangerang City, which raises a number of pertinent questions: 1) How does public awareness affect the implementation of halal logistics? 2) Is the information system influencing the implementation of halal logistics? 3) How do information technologies affect the implementation of halal logistics practices? 4) What role does transportation play in facilitating the implementation of halal logistics? And 5) How do regulations influence the implementation of halal logistics in Tangerang City?

The objectives of this study are to 1) examine the impact of public awareness on the implementation of halal logistics in Tangerang City, 2) examine the impact of information systems and technologies on the implementation of halal logistics, 3) investigate the impact of transportation in supporting the implementation of halal logistics, and 4) evaluate the role of regulations in the implementation of halal logistics in Tangerang City. By identifying the factors that play a role, this research aims to provide a better understanding of the implementation of the halal logistics system in Indonesia, particularly in Tangerang City, as well as recommendations to increase its effectiveness.

MATERIALS AND METHODS

This research used a quantitative approach (Creswell and Creswell, 2018) to obtain a comprehensive understanding of the implementation of halal logistics in Tangerang

City. A survey was designed to model the implementation of halal product logistics based on the consumer community's perception of the need for halal products.

Research sample size

The respondents to this study were members of the consumer community in Tangerang City, with 170 selected through a combination of purposive and convenience sampling. The sample was determined based on the requirements of partial least squares structural equation modeling (PLS-SEM), which suggests a minimum sample size of 10 times the number of research survey questions. Given that the survey consisted of 14 items, the required minimum sample size was 140 respondents.

To ensure diversity, respondents were selected randomly from various social and economic backgrounds. The survey was conducted at multiple shopping centers and traditional markets across Tangerang City, where consumers actively make purchasing decisions. These locations were chosen due to their high consumer footfall and relevance to the study's focus on consumer perceptions.

The inclusion criteria required participants to be aged 17 and above and to have a basic understanding of halal and non-halal food and beverages. Since the exact visitor numbers in these locations were unknown, a convenience sampling procedure was used, allowing researchers to approach and survey willing participants on-site. Data collection took place over a specified period, March to April 2024, to capture a representative consumer perspective.

Data collection

The survey was distributed to the consumer communities via Google Forms and WhatsApp to assess their awareness of halal products and perceptions of halal logistics implementation. In addition, secondary data from authoritative sources was used to document the regulatory framework and industry standards regulating halal practices. These sources included official government regulations, halal certification standards issued by the Indonesian Ulama Council (MUI), and guidelines from the Halal Product Assurance Agency (BPJPH). These references were crucial for analyzing how halal logistics principles are implemented and perceived in the market.

Researchers approached consumers directly. Following a brief introduction to potential participants, they were asked to complete the survey within 10 minutes. If the respondent was in a hurry, the researcher provided a survey link via phone/WhatsApp to allow respondents to complete the questionnaire via the Google Forms link provided. Relevant information from willing participants was recorded, including their responses to halal logistics.

Data analysis

Survey data was analyzed using structural equation modeling (SEM) with the warpPLS software (Purwanto *et al*., 2019) to test the relationship between variables and identify factors that impact the application of halal logistics by the consumer community (Wardhani *et al*., 2020).

RESULTS AND DISCUSSION

Participant characteristics

The participant population characteristics (Table 1) showed a balanced gender distribution, allowing for a nuanced analysis of how gender may influence perceptions and awareness of halal logistics. Understanding gender dynamics is essential, as it can impact consumer preferences and decision-making processes in the halal market. Participants are mostly male (53.53 %), with senior high school (52.94 %) being the most common education level and student (62.35 %) being the most frequent occupation.

The age distribution, educational background, and socioeconomic status of the respondents are critical factors that can affect awareness and understanding of halal logistics. For instance, younger consumers may exhibit different attitudes towards halal products compared to older generations, influenced by varying levels of education and exposure to halal standards. The educational background correlates with the level of awareness and understanding of halal logistics. Higher education levels may lead to greater awareness of halal certification processes and the importance of logistics in maintaining product integrity. Furthermore, socioeconomic status can influence purchasing power and access to halal products, thereby affecting consumer behavior in the halal market. By analyzing these demographic factors, the study aims to identify trends and patterns that can inform strategies for enhancing halal logistics practices and consumer engagement.

Consumer awareness is a critical factor influencing halal logistics adoption. This study finds that higher awareness levels significantly impact halal logistics implementation in Tangerang City ($p < 0.001$), highlighting the role of public knowledge in ensuring compliance. Rahman *et al.* (2021) similarly emphasize that consumers with greater

Table 1. Respondent characteristics from the consumer perception survey of halal logistics conducted in Tangerang City, Indonesia, in 2024.

Gender	Frequency	Percentage
Male	91	53.53
Female	79	46.47
Education		
Postgraduate	13	7.65
Under graduate	60	35.29
Senior high school	90	52.94
Junior high school	7	4.12
Occupation		
Teacher/Lecturer	4	2.35
Entrepreneurship	18	10.59
Employment	38	22.35
Students	106	62.35
Labor/Farmer	4	2.35

halal awareness demonstrate stronger trust and purchasing behavior toward halal-compliant businesses. The correlation between education and halal logistics awareness (Table 1) aligns with Rahman *et al*. (2021), who found that exposure to halal-related education enhances consumer preferences for halal-certified products. These findings reinforce the need for targeted educational programs and awareness campaigns to enhance consumer confidence, drive market competitiveness, and promote sustainable halal logistics practices.

The correlation between education and halal logistics awareness, as shown in Table 1, aligns with Rahman *et al*. (2021), who found that exposure to halal-related education enhances consumer preferences for halal-certified products. These findings reinforce the need for targeted educational programs and awareness campaigns to enhance consumer confidence, drive market competitiveness, and promote sustainable halal logistics practices.

Traceability is a crucial aspect of halal logistics, ensuring transparency and compliance throughout the supply chain. This study highlights the need for enhanced digital tracking and monitoring systems to maintain halal integrity. Sayogo (2018) emphasizes that online traceability systems significantly improve consumer trust by providing real-time access to halal product information, reducing uncertainty in the supply chain. Integrating digital traceability tools, such as blockchain and IoT-based tracking, can strengthen supply chain transparency, preventing cross-contamination risks and ensuring adherence to halal certification requirements. As the halal logistics sector evolves, technological advancements in traceability will be key to reinforcing compliance and consumer confidence.

Sustainability in halal logistics is increasingly vital, with the integration of green supply chain practices enhancing both compliance and environmental responsibility. This study highlights the importance of eco-friendly logistics solutions to maintain halal integrity while minimizing environmental impact. Firdiansyah *et al*. (2021) emphasize that green supply chain management (GSCM) can improve halal logistics efficiency by reducing waste, optimizing transportation, and ensuring sustainable resource utilization.

Effective stakeholder collaboration is essential for ensuring seamless halal logistics implementation. This study highlights the need for stronger partnerships between producers, distributors, certification bodies, and regulatory authorities to enhance compliance and efficiency. Haleem *et al*. (2021) emphasize that collaborative efforts among key stakeholders improve logistical coordination, reduce operational bottlenecks, and strengthen halal supply chain transparency. Enhancing communication channels, establishing standardized guidelines, and fostering cooperation between halal certification agencies and logistics providers can streamline halal compliance. As the halal logistics ecosystem expands, stakeholder collaboration will be instrumental in ensuring regulatory alignment, operational efficiency, and consumer trust.

The effectiveness of halal logistics services plays a crucial role in enhancing industry performance and market competitiveness. Well-integrated halal logistics frameworks contribute to operational efficiency, regulatory compliance, and consumer trust. Noorliza (2020) found that businesses that implemented structured halal logistics services had better supply chain resilience, higher customer satisfaction, and stronger brand positioning in the halal market. Optimizing logistics operations, such as streamlined warehousing, halal-certified transportation, and robust supply chain management, can enhance overall industry performance. As the demand for halal products grows, investment in high-quality halal logistics services will be a key differentiator for businesses looking to expand their market share and strengthen their competitive advantage.

Indonesia holds a dominant position in the global halal market, driven by its large Muslim population and increasing demand for halal-certified products. This study highlights the growing importance of halal logistics in supporting Indonesia's expanding halal industry. According to Bank Indonesia (2021), the halal sector has seen rapid development, particularly in food, pharmaceuticals, cosmetics, and logistics, as businesses and policymakers work to strengthen halal certification frameworks. As Indonesia strengthens its halal certification policies and logistics infrastructure, businesses must adapt to evolving regulations and consumer expectations to remain competitive in both domestic and international markets. A well-integrated halal logistics ecosystem will be essential in ensuring that Indonesia maintains its position as a global leader in the halal industry while supporting sustainable economic growth.

Digital transformation is reshaping both financial services and halal logistics, enabling greater efficiency, transparency, and compliance. This study highlights the importance of integrating digital financial solutions with halal logistics to optimize payment systems, enhance supply chain financing, and support traceability. Feyen *et al*. (2021) emphasize that fintech innovations, including blockchain-based smart contracts and digital payment systems, play a crucial role in modernizing halal logistics by improving transaction security and streamlining cross-border trade. Leveraging digital financial services, such as Islamic fintech platforms and real-time payment gateways, can enhance halal logistics operations by reducing delays, increasing financial accessibility for halal businesses, and ensuring seamless regulatory compliance. As halal supply chains become more globalized, digital transformation will be key to bridging gaps between logistics, financial systems, and halal certification authorities, fostering greater market integration and efficiency.

Measurement model analysis (outer model)

The construct variables, as well as their validity and reliability, were evaluated using the outer model of measurement analysis. Internal consistency analysis is used to determine a test's result consistency. This analysis makes use of a composite reliability value, where a variable is considered reliable if its value exceeds 0.7 (Budiastuti and Bandur, 2018; Sarstedt *et al*., 2021). The awareness variable is reliable, as evidenced by a composite reliability score of 0.826 (Table 2) (Utomo and Saragih, 2023). Similarly, the information system (0.798) and information technology (0.765) variables, as well as the regulation (0.805) and implementation (0.863), were found to be reliable.

Table 2. Internal consistency analysis of the halal logistics research survey conducted in Tangerang City, Indonesia, in 2024.

Variable	Cronbach's alpha	Composite reliability	Average variance extracted
Awareness (AW)	0.684	0.826	0.615
Information System (IS)	0.62	0.798	0.569
Information Technology (IT)	0.545	0.765	0.55
Transportation (TR)	0.636	0.873	0.579
Regulation (REG)	0.781	0.805	0.696
Implementation (PERFORM)	0.762	0.863	0.679

In PLS-SEM analysis, in addition to Cronbach's alpha, it is important to consider composite reliability (CR) and the average variance extracted (AVE) (Ahmed and Ishtiaq, 2021). CR is a frequently used alternative to Cronbach's alpha in the context of PLS-SEM. CR is usually considered more informative as it is not affected by the number of items in the construct and can provide a more accurate picture of the construct's reliability. CR values above 0.7 are generally considered adequate. Meanwhile, AVE is used to measure how much variance is explained by the construct compared to the variance caused by error. An AVE value above 0.5 indicates that the construct can explain more than half of the variance in the measured items (Hair *et al*., 2019). Because the CR and AVE values met the requirements, they can be used as a guideline that the reliability of the measurement model is sufficient (reliable).

There was an outer loading indicator value that is smaller than 0.5 (Table 3), so it was necessary to remove the IT_1 indicator from the model. After carrying out the second stage of analysis, it was obtained that the loading values for all indicators already had external loading values above 0.5 so that a structural analysis model could be carried out (Benitez *et al*., 2020).

Structural model (inner model) analysis

Structural model analysis was carried out to test research hypotheses. The coefficient of determination (R square) is used to test the hypothesis (Sarstedt *et al*., 2021). The collinearity test assesses the strength of the correlation between latent variables or constructs. A strong correlation indicates a methodological problem in the model, which could affect the estimate of statistical significance; this is referred to as collinearity. To analyze collinearity, the Variance Inflation Factor (VIF) value is used (Purwanto and Sudargini, 2021). A VIF value above 5.0 indicates a collinearity problem (Sarstedt *et al*., 2022).

All indicators had a VIF of less than 5.0 (Table 4). Thus, the structural model in this case does not contain collinearity problems. The collinearity analysis provides critical insights into the relationships among the latent variables influencing the implementation of halal logistics in Tangerang City. Collinearity refers to the degree of

Table 3. Convergent validity of the halal logistics research survey conducted in Tangerang City, Indonesia, in 2024.

Indicators	AW	IS	IT	REG	TR	PERFORM
AW1	0.837	0.036	0.021	-0.209	0.347	0.041
AW2	0.81	-0.142	-0.014	-0.186	0.107	-0.1
AW3	0.699	0.122	-0.009	0.466	-0.539	0.067
IS1	0.076	0.762	0.153	0.522	-0.692	-0.183
IS2	-0.182	0.778	-0.112	-0.101	0.462	-0.066
IS3	0.116	0.721	-0.04	-0.442	0.234	0.265
IT1	-0.28	0.477	0.345	0.286	-0.415	0.264
IT2	-0.032	-0.191	0.876	-0.066	-0.038	0.109
IT3	0.143	0.003	0.874	-0.047	0.201	-0.213
REG1	-0.166	0.172	0.089	0.792	-0.465	0.035
REG2	-0.006	-0.112	-0.019	0.726	0.15	0.024
REG3	0.178	-0.072	-0.074	0.763	0.34	-0.06
TR1	0.021	0.061	0.047	0.214	0.821	-0.013
TR2	-0.002	0.026	0.067	-0.137	0.803	0.029
PERFORM1	-0.025	0.049	-0.303	0.3	-0.245	0.768
PERFORM2	-0.016	-0.137	0.181	-0.237	0.15	0.844
PERFORM3	0.039	0.091	0.093	-0.035	0.071	0.856

AW: awareness; IS: information system; IT: information technology; REG: regulation; TR: transportation; PERFORM: implementation.

Table 4. Collinearity test results of halal logistics model evaluated in Tangerang City, Indonesia, in 2024.

AW	IS	IT	REG	TR	PERFORM
1.528	1.522	1.518	2.646	3.312	2.254

AW: awareness; IS: information system; IT: information technology; REG: regulation; TR: transportation; PERFORM: implementation.

correlation between independent variables in a regression model, and understanding this aspect is essential for ensuring the validity of the statistical analysis conducted in the study.

The absence of collinearity issues suggests that each independent variable contributes uniquely to the model, allowing to draw meaningful conclusions about the influence of each factor on the implementation of halal logistics. For example, the strong correlation between awareness and the adoption of halal logistics practices can be interpreted without the confounding effects of other variables, leading to clearer insights into how consumer awareness drives industry compliance.

Significance of the structural model path coefficients

The indirect influence hypothesis was evaluated. Testing the significance of the path coefficients of the structural model (Figure 1) is to assess the significance of the relationships or hypotheses in the structural model.

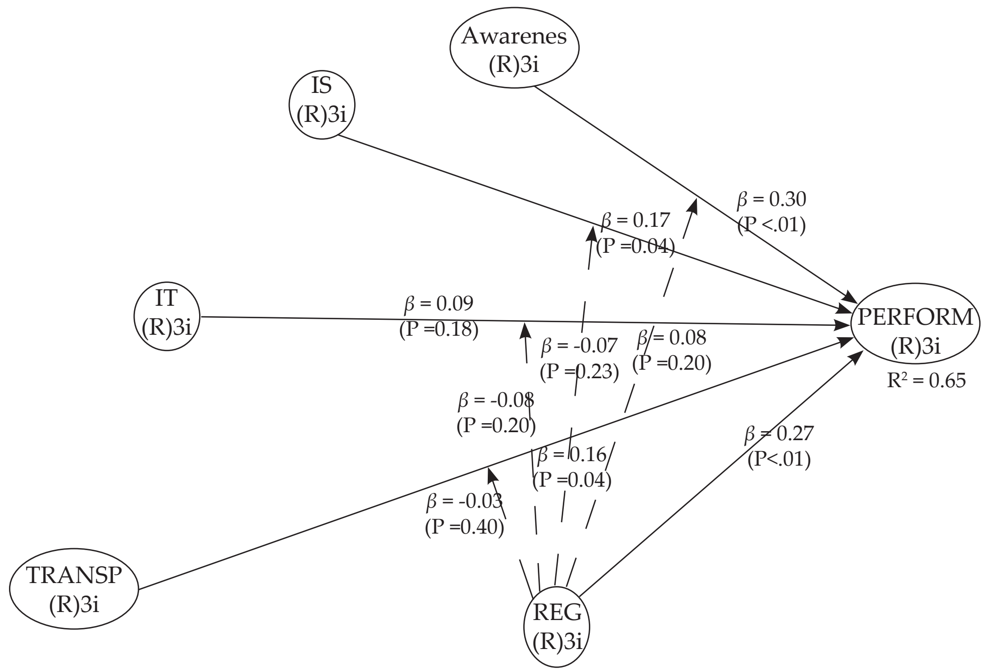

Figure 1. Path diagram of the structural model of halal logistics implementation in Tangerang City, Indonesia, in 2024**.**

The halal logistics implementation model output (Figure 1), which visually encapsulates the relationships and interactions among various factors influencing the implementation of halal logistics in Tangerang City, serves as a conceptual framework that illustrates how different variables contribute to the overall effectiveness of halal logistics practices. The model is structured to show the direct effects of independent variables, such as awareness, information systems, regulations, transportation, and information technology, on the dependent variable, which is the implementation of halal logistics.

Direct effect testing

The purpose of testing the direct influence hypothesis is to demonstrate how a variable directly affects other variables (Setyorini and Syahlani, 2019). A positive path coefficient indicates that when one variable increases, so do the others. Conversely, a negative path coefficient indicates that an increase in one variable results in a decrease in another. If the *p*-value is below the significance level (alpha) of 0.05, the null hypothesis (*Ho*) is rejected, indicating a significant influence of one variable on others. Conversely, if the *p*-value exceeds alpha (0.05), the null hypothesis (*Ho*) is not rejected, indicating that the influence of one variable on another is not significant (Purwanto and Sudargini, 2021).

The results show that the implementation of halal logistics in Tangerang City is significantly influenced by awareness, information systems, transportation, and government regulations, as evidenced by a *p*-value < 0.05 (Table 5). However, the implementation of halal logistics is not influenced by information technology, as evidenced by a *p*-value of 0.179.

Table 5. Path coefficient of the structural model of halal logistics implementation in Tangerang City, Indonesia, in 2024.

Relationship between Variable	Original sample	*p*-value
Awareness (AW) -> Implementation (PERFORM)	0.305	**< 0.001**
Information system (IS) -> Implementation (PERFORM)	0.172	**0.035**
Information Technology (IT) -> Implementation (PERFORM)	0.089	0.179
Transportation (TR) -> Implementation (PERFORM)	0.265	**0.002**
Regulation (REG)-> Implementation (PERFORM)	0.162	**0.044**

CONCLUSIONS

This study provides empirical insights into the key factors influencing the implementation of halal logistics in Tangerang City, Indonesia, with implications for both academic and industry stakeholders. The findings reveal that public awareness, regulatory frameworks, transportation systems, and integrated information systems significantly drive the successful adoption of halal logistics practices. Among these, consumer awareness emerged as the most influential, underscoring the need for targeted education and outreach initiatives to enhance halal literacy and market responsiveness.

While traditional information technology showed limited direct impact, integrated digital solutions that enhance traceability proved more critical. The limited influence of traditional information technology suggests that real-time monitoring and digital tracking systems offer greater value for ensuring halal integrity. Efficient transportation and strict adherence to regulatory standards are also essential for maintaining halal integrity, consumer trust, and ensuring timely deliveries throughout the supply chain. The findings also emphasize the importance of stakeholder collaboration and regulatory alignment in enhancing supply chain transparency and compliance. To meet the rising demand for halal-certified products and strengthen Indonesia's global position in the halal industry, investment in infrastructure, education, and strategic partnerships is essential. As Indonesia's halal industry continues to expand, fostering a cohesive logistics ecosystem will be crucial to maintaining global competitiveness and consumer trust.

ACKNOWLEDGEMENTS

The author would like to thank all parties who have helped carry out this research, especially respondents who have participated in this research, reviewers, and editors who provided input and suggestions so that this article was published.

REFERENCES

Ahmad N, Shariff SM. 2016. Supply chain management: Sertu cleansing for halal logistics integrity. Procedia Economics and Finance 37 (16): 418–425. https://doi.org/10.1016/s2212-5671(16)30146-0

Ahmed I, Ishtiaq S. 2021. Reliability and validity: Importance in medical research. Journal of the Pakistan Medical Association 71 (10): 2401–2406.

Alfarizi M, Ngatindriatun. 2022. Commitment to halal practices of Indonesian culinary MSMEs in the production chain: The impact of halal literacy and attitudes. Journal of Southeast Asian Islam and Society 1 (1).

Aziz AA, Zailani S. 2016. Halal logistics: The role of ports, issues and challenges. *In* Mutum DS, Butt MM, Rashid M. (eds.), Advances in Islamic Finance, Marketing, and Management. Emerald Group Publishing Limited: Leeds, UK, pp: 309–321. https://doi.org/10.1108/978-1-78635-899-820161015

Benitez J, Henseler J, Castillo A, Schuberth F. 2020. How to perform and report an impactful analysis using partial least squares: Guidelines for confirmatory and explanatory IS research. Information and Management 57 (2): 103168. https://doi.org/10.1016/j.im.2019.05.003

Budiastuti D, Bandur A. 2018. Validitas dan reliabilitas penelitian. Mitra Wacana Media: Jakarta, Indonesia.

Creswell JW, Creswell JD. 2018. Research design: Qualitative, quantitative, and mixed method approaches (Fifth edition). Sage Publications: Thousand Oaks, CA, USA. 275 p.

Dewi C, Trihardani L. 2017. How the halal transportation system impacts the location routing problem. Journal of Engineering and Management Industrial System 5 (1): 8–19.

Feyen E, Frost J, Gambacorta L, Natarajan H, Saal M. 2021. Fintech and the digital transformation of financial services: Implications for market structure and public policy. BIS Papers 117. Bank for International Settlements: Basel, Switzerland. 53 p.

Firdiansyah FA, Rosidi A, Nur Iman AK. 2021. Implementation of green supply chain management in halal supply chain management - A conceptual model. Islamiconomic: Jurnal Ekonomi Islam 12 (1). https://doi.org/10.32678/ijei.v12i1.257

Gunardi S. 2023. The role of Shari'ah principles in guaranteeing halal logistics: A review. Halalpshere 3 (1): 40–46. https://doi.org/10.31436/hs.v3i1.36

Hair JF, Risher JJ, Sarstedt M, Ringle CM. 2019. When to use and how to report the results of PLS-SEM. European Business Review 31 (1): 2–24. https://doi.org/10.1108/EBR-11-2018-0203

Haleem A, Khan MI, Khan S. 2021. Understanding the adoption of halal logistics through critical success factors and stakeholder objectives. Logistics 5 (2): 38. https://doi.org/10.3390/logistics5020038

Bank Indonesia. 2021. Indonesia halal markets report 2021/2022. Islamic economy. Bank Dinar Standard, Indonesia Halal Lifestyle Center, Bank Indonesia. Jakarta, Indonesia. 116 p.

Kurniawati DA, Handoko A, Piplani R, Rosdiahti R. 2022. Optimized distribution of halal products using tabu search. Journal of Islamic Marketing 14 (4): 1058–1083. https://doi.org/10.1108/JIMA-05-2020-0143

Mahmudah SN, Ridwan M, Ulya HN. 2022. Halal and haram in the clothing industry. Journal of Islamic Economics 2 (2): 164–84. https://doi.org/10.21154/joie.v2i2.5009

Mu'ti sazali A, Ligte JS. 2019. The Importance of halal logistics implementation in Indonesia in compliance with domestics and global halal market requirements. Jurnal Transportasi Multimoda 17 (2): 17–26. https://doi.org/10.25104/mtm.v17i2.1319

Nafis MC. 2019. The concept of halal and thayyib and its implementation in Indonesia. Journal of Halal Product and Research 2 (1). https://doi.org/10.20473/jhpr.vol.2-issue.1.1-5

Noorliza K. 2020. Resource-capability of halal logistics services, its extent and impact on performance. Journal of Islamic Marketing 12 (4): 813–829. https://doi.org/10.1108/jima-12-2019-0255

Purwanto A, Asbari M, Iman Santoso T, Grace Haque M. 2019. Marketing research quantitative analysis for large sample: Comparing of Lisrel, Tetrad, GSCA, Amos, SmartPLS, WarpPLS, and SPSS. Jurnal Ilmiah Imu Administrasi Publik: Jurnal Pemikiran dan Penelitian Administrasi Publik 9 (2): 355–372.

Purwanto A, Sudargini Y. 2021. Partial least squares structural equation modeling (PLS-SEM) analysis for social and management research: A literature review. Journal of Industrial Engineering and Management Research 2 (4): 114–123.

Putra AB, Wulandari WR, Nur M, Khasan K. 2023. International dynamics of halal industry development: A literature review. Review of Islamic Economics and Finance 6 (1): 75–90.

Rahman RA, Zahari MSM, Hanafiah MH, Mamat MN. 2021. Effect of halal food knowledge and trust on Muslim consumer purchase behavior of syubhah semi-processed food products. Journal of Food Products Marketing 27 (6): 319–330. https://doi.org/10.1080/10454446.2021.1994079

Sarstedt M, Hair JF, Pick M, Liengaard BD, Radomir L, Ringle CM. 2022. Progress in partial least squares structural equation modeling use in marketing research in the last decade. Psychology and Marketing 39 (5): 1035–1064. https://doi.org/10.1002/mar.21640

Sarstedt M, Ringle CM, Hair JF. 2021. Partial least square structural equation modeling. *In* Homburg C, Klarmann M, Vomberg A. (eds.), Handbook of Market Research. Springer: Cham, Switzerland. https://doi.org/10.1007/978-3-319-05542-8

Sayogo DS. 2018. Online traceability for halal product information: Perceptions of Muslim consumers in Indonesia. Journal of Islamic Marketing 9 (1): 99–116. https://doi.org/10.1108/jima-07-2016-0057

Setyorini D, Syahlani A. 2019. Analisis jalur (path analysis) pengaruh kondisi sosial ekonomi dan motivasi belajar terhadap prestasi belajar mahasiswa. Jurnal Akuntansi dan Manajemen 16 (2): 177–193. https://doi.org/10.36406/jam.v16i02.241

Soesilowati E, Yuliana C. 2013. Komparasi perilaku konsumen produk halal di area mayoritas dan minoritas muslim. Jurnal Ekonomi Pembangunan LIPI 21 (2): 49–60.

Utomo S, Saragih A. 2023. The effect of brand awareness and service quality on customer satisfaction and its implications for container terminal customer loyalty. International Journal of Advanced Multidisciplinary 2 (2): 551–561. https://doi.org/10.38035/ijam.v2i2.336

Wardhani NWS, Nugroho WH, Fernandes AAR, Solimun S. 2020. Structural equation modeling (SEM) analysis with Warp-PLS approach based on the theory of planned behavior (TPB). Mathematics and Statistics 8 (3): 311–322. https://doi.org/10.13189/ms.2020.080310

Zainuddin N, Saifudin AM, Deraman N, Osman AA. 2020. The effect of halal traceability system on halal supply chain performance. International Journal of Supply Chain Management 9 (1): 490–498.

Agrociencia

SAMPLE SIZE CALCULATOR FOR PHYTOSANITARY SAMPLING PLANS BASED ON CONSUMER RISK

Luis Gabriel **Otero-Prevost**[1,2], Pedro **Macías-Canales**[2], Gustavo **Ramírez-Valverde**[3*], Juan A. **Villanueva-Jiménez**[1], Jorge Luis **Leyva-Vázquez**[2]

[1]Colegio de Postgraduados Campus Veracruz. Carretera Xalapa-Veracruz km 88.5, Manlio F. Altamirano, Veracruz, Mexico. C. P. 91963.
[2]Servicio Nacional de Sanidad, Inocuidad y Calidad Agroalimentaria. Dirección General de Inspección Fitozoosanitaria. Insurgentes Sur 489, Hipódromo, Mexico City, Mexico. C. P. 06100.
[3]Colegio de Postgraduados Campus Montecillo. Carretera México-Texcoco km 36.5, Montecillo, Texcoco, State of Mexico, Mexico. C. P. 56264.
* Author for correspondence: gramirez@colpos.mx

Citation: Otero-Prevost LG, Macías-Canales P, Ramírez-Valverde G, Villanueva-Jiménez JA, Leyva-Vázquez JL. 2025. Sample size calculator for phytosanitary sampling plans based on consumer risk. **Agrociencia** 59(3): 356-368. https://doi.org/ 10.47163/agrociencia.v59i3.3239

Editor in Chief:
Dr. Fernando C. Gómez Merino

Received: May 25, 2024.
Approved: January 09, 2025.
Published in Agrociencia:
April 04, 2025.

ABSTRACT

The international flow of agricultural products is a key factor in the spread of potentially harmful species. Pests and non-native organisms that spread between countries in commercial transport can establish themselves and significantly alter biodiversity, the functioning of agroecosystem services, human health, and the economy. Between 1970 and 2017, the economic cost of biological invasions and control methods represented an estimated global investment of USD 1.288 trillion; in Mexico alone, the cost on the agricultural sector represented an estimated investment of USD 1.01 billion. Because of the volume and diversity of imported products, as well as the economic and environmental damage caused by pest species, sanitary inspection must explicitly incorporate the concepts of producer risk (rejecting a lot with an acceptable sanitary level) and consumer risk (accepting a lot with a minimum sanitary level) to decide whether to accept or reject a lot. This paper introduces the main features of risk-based sampling, defines the acceptable and minimum sanitation levels, discusses how changes in parameters affect the behavior of the characteristic operating curve, and presents the user interface of an interactive web calculator that was programmed in R to automate the development of sampling plans and calculate the risk-based sample size. The estimates obtained compared to other sources indicate that the computation performed with the calculator is accurate and determines sample sizes and acceptance numbers. The inspection should explore sampling methods that explicitly include risk and coin its own concepts that fit its information needs and objectives.

Key words: inspection, R programming, quarantine pests.

INTRODUCTION

The international exchange of food and raw materials of animal and plant origin has increased in recent decades, and with this, the risk of introduction of pests, diseases, and non-native organisms of quarantine importance (NAPPO, 2020; Diagne *et al.*, 2021; SENASICA, 2024). The economic-environmental impact of invasive species on a product system and the impact derived from the cost of applying targeted measures for their control (Villanueva-Jiménez *et al*., 2017) represent annual investments estimated in billions of dollars (Pimentel *et al*., 2000; Jáquez-Mata *et al*., 2022). Hoffmann and Broadhurst (2016) estimated a multinational investment (USA, UK, India, South Africa, Australia, and Brazil) of USD 306 billion in damages, plus USD 30 billion in management and handling costs; Warziniack *et al*. (2021) reported an approximate annual global cost of half a trillion dollars between 1999 and 2000. Diagne *et al*. (2021) estimated that the global economic losses associated with border biosecurity programs between 1970 and 2017 totaled approximately USD 1.288 trillion. In Mexico, the estimated cost was USD 5.33 billion between 1992 and 2019; during this time, the agricultural sector generated the highest costs with USD 1.01 billion; the second place was occupied by fisheries with USD 517.24 million, while the rest was invested in unspecified sectors (Rico-Sánchez *et al*., 2021).

To safeguard the health of agricultural resources and reduce the economic-environmental cost, each country developed and implemented protection systems or border biosecurity programs that inspect products to determine if they meet the sanitary standard (Lane *et al*., 2019; Trouvé and Robinson, 2024). These programs change depending on the country, its geographical position, socio-economic condition, commercial needs, and the stages associated with control actions. Regardless of the particular conditions, Warziniack *et al*. (2021) classified the general strategies common to all protection systems or border biosecurity programs into stages. The first stage corresponds to actions that prevent the introduction of pests, diseases, and non-native organisms. This stage includes the rules and procedures for the review of goods at the point of origin, the set of documentary and legal obligations to carry out the purchase and sale of the product, and the inspection at the point of entry. The second category is surveillance and eradication programs, which are activated when the first records of the organism's presence within the national territory are identified; these practices include monitoring programs for free zones and national mobilization. Finally, the third category is what authors call optimal control to stop the spread, consisting of quarantine programs and integrated control methods.

Inspection is the measure most used by national agencies to prevent the entry of a pest, disease, or non-native organism; therefore, regardless of the country where it is carried out, operational and regulatory responsibilities guarantee the standards that ensure the sanitation of products. These responsibilities are closely related, since the documentary and physical review or inspection and the set of laboratory tests that provide empirical, technical, and scientific support for the sanitary status of a product (NAPPO, 2020; IPPC, 2005, 2008) are supported and delimited to the guidelines defined by international standards and treaties, for example, the Agreement on the Application of Sanitary and Phytosanitary Measures of the World Trade Organization (WTO), for free, fair, and safe trade between countries.

In addition to being important, inspection is complex and faces multiple challenges. Due to the volume, it is impractical to completely review the products, so the inspection and determination of the sanitary status of a lot is done from the study of a sample; the diversity of the commodities requires that different probability functions be used to study it (SIICEX, 2024). Due to the complex nature of the biology of the species, some pests cannot be detected without special diagnostic procedures, while others have different levels of detection (NAPPO, 2020). Inspections, on the other hand, are carried out in places with their own infrastructure, which do not always have the best lighting, equipment, and spaces, and are carried out by officers with particular needs, behaviors, and attachments (NAPPO, 2022); that is, the particular differences of each inspection point and the methods used in each of them promote that the unit of effort, cost, and time invested are heterogeneous (Follett and Hennessey, 2007; Decrouez and Robinson, 2013).

As a rule, each country is free to define the sampling plan, the development of inspection guidelines (IPPC, 2005), and methodologies for sampling consignments (IPPC, 2008); however, different inspection designs and methods produce different results. To standardize phytosanitary inspection sampling plans, it is necessary to investigate sampling methods that explicitly incorporate the concept of risk and estimate sample sizes based on parameter relationships, as opposed to other inspection sampling design methods such as fixed proportion and acceptance sampling. The most common sanitary inspection sampling designs are fixed proportion sampling and acceptance sampling. In the former, the sample size is estimated as a percentage; however, with the increase in the flow of goods, the larger the volume, the larger the sample size.

Acceptance sampling depends on the definition of the consumer risk. The probability function is estimated from the producer risk, the consumer risk, and the definition of the acceptance number and volume; this type of sampling allows the inclusion of the risk concept but depends on volume and, in particular, on the acceptance number (C): the lower the acceptance number, the larger the sample size. The problem with this type of sampling is the effect of the acceptance number, which determines very rigorous programs when $C = 0$, as occurs with quarantine pests. The definition of the acceptance number does not reflect the sanitation level of a lot, and the goal is to determine the quality of a product rather than its health.

Risk-based sampling includes risk levels but differs from acceptance sampling in that the sample size and acceptance number are determined by the definition of an acceptable or desired sanitation level and a minimum or limit sanitation level. The sample size and acceptance number depend on the definition of risk and sanitation levels, rather than the tolerance or acceptance limit, with the goal to estimate sampling units as small as possible in order to reduce inspection time, costs, unit of effort, handling of goods, and the introduction of products that do not meet sanitary standards.

This paper presents consumer risk-based sampling derived from simple attribute acceptance sampling schemes (McWilliams *et al*., 2001; Chen *et al*., 2017). The objectives are to present the elements that define risk-based sampling, the advantages of its implementation, the definition of the acceptable sanitation level, and the minimum sanitation level. A free open-source calculation was developed in R and Shiny to create an interactive web application that computes sampling plans with a minimum sample size and a given acceptance number based on two types of risk (consumer risk and producer risk). Based on the review, unlike the dynamic tables of the North American Plant Protection Organization (NAPPO) and the National Service for Health, Safety, and Food Quality (SENASICA), which are programmed in commercial software for the estimation of sample size through acceptance sampling or fixed proportion, the calculator presented in this work is the first record with technical-scientific support of a free interactive web application, open-source and with internet access, which aims to estimate sampling plans based on the risk of introduction of pests and diseases of agricultural products.

MATERIALS AND METHODS

The proposed risk-based sampling model is derived from a simple attribute acceptance sampling scheme, which consists of defining a sample size and an acceptance value such that the following conditional probability relationships are met (McWilliams *et al*., 2001):

$$P\ (x \leq C \mid n, ASL) = 1 - \alpha$$

$$P\ (x \leq C \mid n, MSL) = \beta$$

where $P(x)$ is the probability of acceptance under two risk criteria: 1-α is the producer risk and α (type I error) represents the probability of not accepting a lot that has a satisfactory sanitation level; β is the consumer risk and represents the probability of accepting a lot that has a minimum sanitation level (Gutiérrez-Pulido and de la Vara-Salazar, 2009; Schilling and Neubauer, 2009). x is the attribute representing the number of defective items in the sample, where a defective item is one that evidences the presence of a pest or disease. C is the acceptance number or the number of items not meeting the sanitary standard in the sample. A lot will be rejected if, under certain levels of consumer and producer risk, the number of units not meeting the standard exceeds C. n is the sample size, ASL is the acceptable sanitation level, and MSL is the minimum sanitation level.

For many years, phytosanitary inspection sampling and risk-based sampling programs adopted two concepts from industrial activities: the acceptable quality level (AQL) and the tolerable lot defective ratio (LTPD) (Chen *et al*., 2017; NAPPO, 2020). Although both represent the upper and lower limits of the quality of a lot, multiple names for these concepts were found in the literature. For example, McWilliams *et al*. (2001) defined them as p_1 and p_2, two probabilities related to an acceptance sampling program, while Kiermeier (2008) refers to them as the producer risk point (PRP) and consumer risk point (CRP). The differences in the use of concepts and the lack of terms applied in healthcare lead us to assume that risk-based sampling is in a moment of expansion, where disciplines other than industry have identified the advantages of using this type of sampling. The AQL and LTPD concepts present clear conceptual limitations in the sanitary field, since what an inspector evaluates is not the quality of the product but the sanitary status.

Therefore, the terms of acceptable sanitation level (ASL) are proposed, which is calculated equal to p_1 (AQL or PRP) and refers to the sanitation level where the lot presents such a low infestation that the probability of acceptance will be high; and minimum sanitation level term (MSL), which is estimated equal to p_2 (LTPD or CRP), which refers to the sanitation level associated with the lowest level of the probability of acceptance, i.e., a lot that does not comply with the standard and will be rejected (Gutiérrez-Pulido and de la Vara-Salazar, 2009).

Because one or more probability functions are used based on the characteristics of a lot, the calculator included a variety of these functions. Small, isolated lots, as well as shipments transported by air or in small boxes, can be modeled with the hypergeometric distribution (type A plan) because they are size dependent. Using the binomial distribution (type B plan), large batches of continuous supply can be modeled (McWilliams *et al*., 2001; Gutiérrez-Pulido and de la Vara-Salazar, 2009), such as cargo vans or ships. The Poisson distribution was included, which allows modeling situations with low infestation probabilities in very large lot sizes (Thomson, 2012) and can be used in records with low infestation proportions. The differences between the probability functions or the type of plan (A and B) depend on the sample size; if the sample size is approximately 5 to 10 % of the lot, the differences of the curves are small and statistically significant, and the lot size can be considered negligible (Gutiérrez-Pulido and de la Vara-Salazar, 2009).

The calculator was programmed using the R language (R Core Team, 2023) with the objective of programming an interactive web application with remote access via mobile devices and personal computers. The R package Shiny was used to create a user interface that allows for quick capture of the producer risk level, consumer risk level, ASL, and MSL through editable fields. Using the *AcceptanceSampling* package (Kiermeier, 2008), the calculations can be performed to obtain the sampling plans by defining the sanitation and risk levels, plotting the characteristic operating curve, and estimating the sample size and acceptance number based on the conditional probabilities. Therefore, by entering values for 1-α, β, ASL, and MSL, the calculator provides the minimum sample size that complies with $P(x \leq C \mid n, ASL) = 1 - \alpha$ and $P(x \leq C \mid n, MSL) = \beta$ (McWilliams *et al*., 2001).

When the program is run, the graphical interface (Figure 1) is displayed with its input components: A) Title of the calculator; B) selection of the probability function, depending on the nature and type of batch; C) data entry section: 1-α (producer risk), β (consumer risk), ASL (acceptable sanitation level), and MSL (minimum tolerable sanitation level); and D) three tabs with the program results: the first (Figure 1) shows the sampling plan with acceptance probabilities for different product infestation proportions, sample size (n), and acceptance number (C); the second (Figure 2) presents the characteristic operating curve; and the third (Figure 3) presents the main characteristics of the sampling plan.

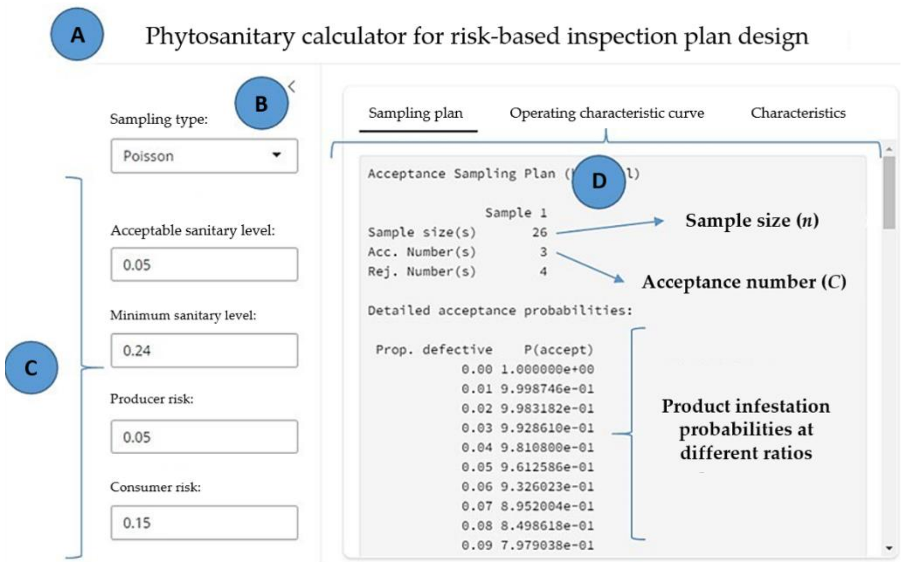

Figure 1. Risk-based sample size calculator user interface for phytosanitary sampling. A: Calculator title; B: probability function selection; C: data entry section; D: program results.

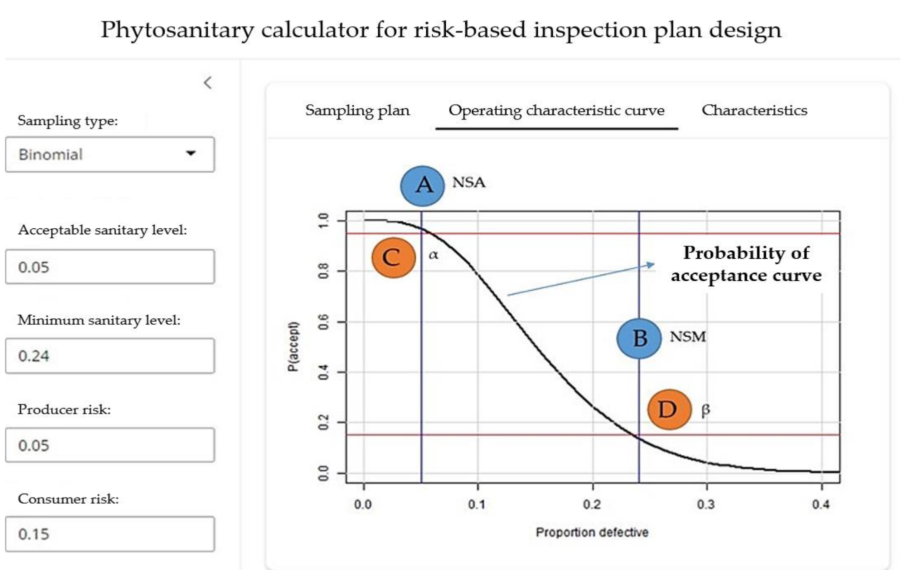

Figure 2. Characteristic operating curve estimated by the calculator. A: acceptable sanitation level; B: minimum sanitation level; C: producer risk; D: consumer risk.

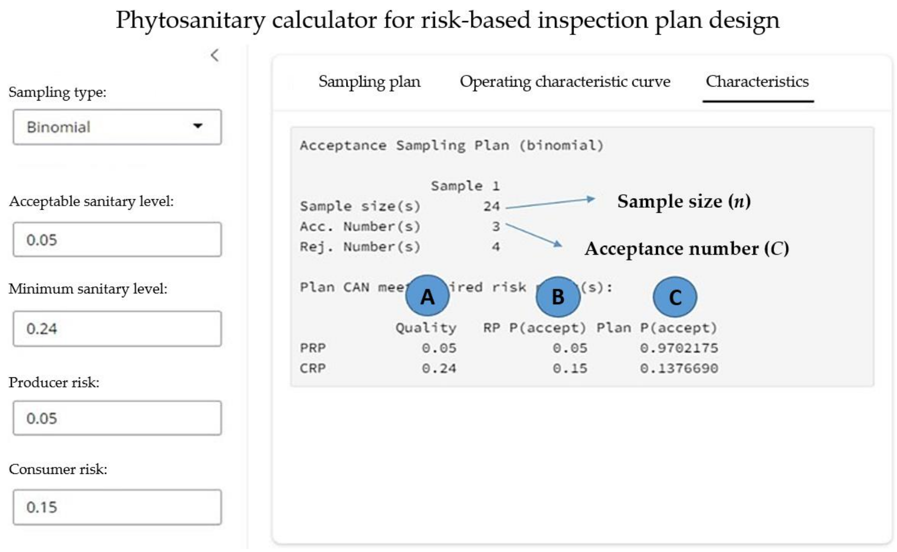

Figure 3. Characteristics proposed by the calculator for the sampling plan for phytosanitary inspection. **A:** Quality values according to the sanitation levels related to the producer risk point (PRP) and the consumer risk point (CRP); B: acceptance probability values of producer risk (1-α) and consumer risk (β); C: acceptance probabilities estimated using an optimization function included in the *AcceptanceSampling* R library.

The interface is intuitive and easy to use (Figure 1), as the user only has to enter four numerical values in the editable fields to define the ASL, MSL, producer risk, and consumer risk. For the type of sampling, the user must only decide on one of the selection fields with the options Poisson, hypergeometric, and binomial. The system automatically calculates the acceptance number and sample size. The tabbed arrangement of options allows the user to quickly select between sampling plan, characteristics, and operating curve.

The characteristic operating curve (Figure 2) shows a pair of blue and red lines; the blue lines represent the acceptance probability levels associated with the user-defined ASL and MSL, while the red lines represent the producer risk (1-α) and the consumer risk (β). These lines make the graph easier to read. The plan can be considered to meet the user conditions if the characteristic operating curve (black line) passes exactly at the intersection of the red and blue lines at the top left of the graph, as well as the intersection of the red and blue lines at the bottom right of the graph.

The calculator determines the smallest sampling plan that meets the specifications given for the producer and consumer risks. Increasing the producer risk increases the probability that lots that meet the sanitary standard will be rejected, while increasing the consumer risk increases the likelihood that lots that do not meet the standard will be introduced into the country. It is important to keep both levels of risk low, so the inspection plan is a compromise that maintains a balance between the two types of risk with a minimum sample size so that the operational part of the inspection can be carried out quickly. For this reason, it is common for the characteristic operating curve to pass above the A-B intersection or below C-D (Figure 2) because the calculator is conservative towards the consumer risk. It is important to emphasize that the sampling plans generated, as evidenced by the characteristic operating curve or the plan characteristics, always reduce both producer and consumer risks for the stipulated ASL and MSL.

The characteristics of the sampling provide information on the proposed plan. The first column labeled "Quality" (Figure 3) reads the values related to the sanitation of the lot, the acceptable sanitation level in the PRP column, and the minimum sanitation level in the CRP column. In the next column, "RP P(accept)," the values of producer risk (1-α) in the PRP column and consumer risk (β) in the CRP column are read. In the "Plan P(accept)" column, the acceptance probabilities are estimated using an optimization function included in the *AcceptanceSampling* library (Kiermeier, 2008); for example, the data-driven probability of acceptance yields a probability of 0.9702 for producer acceptance and 0.137 for consumer acceptance.

To determine the degree of precision of the calculator, the results obtained with this tool were compared with those presented by McWilliams *et al*. (2001), who compared the sample size and acceptance number of some simple attribute acceptance sampling plans with the approximate and exact estimation methods programmed in FORTRAN. The approximate estimation method is used once there are multiple results that comply with $P(X \leq C \mid n, p)$, so the acceptance probability of the hypergeometric distribution (p_h) was calculated with the following expression:

$$P(X \leq C \mid n, p_h) = \sum_{d=0}^{c} \frac{\frac{D!}{d!\,(D-d)!}\frac{(N-D)!}{(n-d)!\,(N-D-n+d)!}}{\frac{N!}{n!\,(N-n)!}}$$

where N is the lot size, d is the number of infested units in the sample, and $D = Np$ is the number of infested units in the lot. Meanwhile, the estimation of the probability of acceptance of the binomial distribution (p_b) was estimated as:

$$P(X \leq C \mid n, p_b) = \sum_{d=0}^{c} \frac{n!}{d!\,(n-d)!} p^d (1-p)^{n-d}$$

RESULTS AND DISCUSSION

Fixed ratio sampling and acceptance sampling are methods commonly used in phytosanitary inspection; however, increasing lot flow and volumes pose challenges to these methods. With fixed proportion, the larger the lot volume, the larger the sample size; however, with acceptance sampling, the limitations of the acceptance number to determine the level of sanitation, as well as the lack of concepts specific to sanitary activities, independent of the concept of quality, require research into other sampling methods used in inspection. Risk-based sampling is an alternative that has gained importance in inspection in recent years (NAPPO, 2020, 2024) due to the conceptual and operational benefits implied by the explicit inclusion of the concept of risk, as well as the change in the relationship between parameters for the estimation of sample size and the acceptance number based on risk and sanitation levels.

The calculator for risk-based sample size estimation in phytosanitary inspection sampling programs is versatile and allows to quickly obtain the number of units to be taken and the acceptance number of a lot with user-defined producer risk (1-α), consumer risk (β), acceptable sanitation level (ASL), and minimum sanitation level (MSL). The instrument can be tailored to the characteristics of the lot, as it includes three functions for risk-based probability of acceptance estimation. Therefore, it can be used for sampling designs of lots with small volumes (hypergeometric, type A plan), large volumes (binomial, type B plan) (Gutiérrez-Pulido and de la Vara-Salazar, 2009; Schilling and Neubauer, 2009), and lots with low probability of finding a pest (Poisson) (Thomson, 2012). The behavior of the curves and sample sizes estimated by the calculator are consistent with those reported in the literature (Gutiérrez-Pulido and de la Vara-Salazar, 2009; Schilling and Neubauer, 2009). As ASL increases, the sample size increases; as MSL increases, the sample size decreases; in both cases, the characteristic operating curve shifts to the right.

To check the veracity of the computation and results obtained by the calculator, they were compared with the sample size and acceptance number presented by McWilliams *et al*. (2001). The check (Tables 1 and 2) indicates that using fixed values of 1-α = 0.05 and β = 0.1 results in higher decay of the acceptance probability and stiffer sampling design, while lower values produce smaller sample sizes. With fixed levels of ASL and MSL, the same results for sample size (n) and acceptance number (C) were obtained as those estimated by McWilliams *et al*. (2001), both by the exact method (Table 1) and the approximate method (Table 2).

Although the acceptance number and sample size were the same in both tables, the α and β values captured in the calculator tended to be equivalent or very close to those obtained by the exact method. The approximate method produced cases with varying β values, while the others had consistent results. The calculator produced the same results as McWilliams *et al*. (2001), who used the exact method programmed in FORTRAN, while differences in the value of the consumer risk were identified. The differences are minimal and could be attributed to rounding of the calculations.

The calculator could be improved by incorporating a diagram into the code that identifies the units in the lots to be sampled based on any inspection sampling plan generated and displaying the information as a written or printed report. Finally, there is a lack of research on machine learning as an aid in determining the level of risk for a particular sampling program from historical grower data. However, it is worth noting that there are scenarios where the plan is not practical, as may occur on very small lots; in such cases, an installment-based inspection plan may be used.

Table 1. Sample size and acceptance number results comparison to the exact method presented by McWilliams *et al*. (2001), taking into account producer and consumer risks with fixed values of acceptable sanitation level (ASL) and minimum sanitation level (MSLT).

Example	Type	ASL	MSL	α_e	α_c	β_e	β_c	C	*n*
1	A/10000	0.01	0.025	0.0450	0.046	0.0863	0.0864	10	620
2	A/5000	0.01	0.035	0.0442	0.0443	0.0974	0.0975	5	261
3	A/1000	0.01	0.04	0.0546	0.0547	0.1085	01086	3	155
4	A/500	0.01	0.06	0.0332	0.0334	0.1023	0.1024	2	82
5	A/500	0.01	0.10	0.0463	0.0464	0.0949	0.095	1	37
6	B	0.01	0.028	0.0499	0.05	0.0884	0.0089	8	471
7	B	0.01	0.02	0.0491	0.05	0.0936	0.0937	18	1244
8	B	0.01	0.03	0.0445	0.045	0.0999	0.10	7	390
9	B	0.01	0.05	0.0443	0.044	0.0992	0.0993	3	132
10	B	0.01	0.07	0.0424	0.0425	0.087	0.0876	2	77

Type: probability function/N (lot size); A: hypergeometric function; B: binomial function; α_e: producer risk by exact method in FORTRAN; α_c: producer risk by calculator; β_e: consumer risk by exact method in FORTRAN; β_c: consumer risk by calculator; C: acceptance number; *n*: sample size.

Table 2. Sample size and acceptance number results comparison to the approximate method presented by McWilliams *et al*. (2001), taking into account producer and consumer risks with fixed values of acceptable sanitation level (ASL) and minimum sanitation level (MSLT).

Example	Type	ASL	MSL	α_e	α_c	β_e	β_c	C	*n*
1	A/10000	0.01	0.025	0.0445	0.0449	0.1211	0.122	9	543
2	A/5000	0.01	0.035	0.0442	0.04	0.0974	0.073	5	261
3	A/1000	0.01	0.04	0.0302	0.0302	0.0783	0.08	4	197
4	A/500	0.01	0.06	0.0332	0.034	0.1023	0.1023	2	82
5	A/500	0.01	0.10	0.0439	0.0439	0.1038	0.114	1	36
6	B	0.01	0.028	0.0491	0.0499	0.1305	0.132	7	398
7	B	0.01	0.02	0.049	0.049	0.1102	0.111	17	1163
8	B	0.01	0.03	0.0494	0.0445	0.1347	0.154	6	329
9	B	0.01	0.05	0.0495	0.0495	0.2164	0.223	2	82
10	B	0.01	0.07	0.0503	0.042	0.2721	0.2228	1	36

Type: probability function/N (lot size); A: hypergeometric function; B: binomial function; α_e: producer risk by exact method in FORTRAN; α_c: producer risk by calculator; β_e: consumer risk by exact method in FORTRAN; β_c: consumer risk by calculator; C: acceptance number; *n*: sample size.

CONCLUSIONS

The sanitary inspection should explore other sampling methods that explicitly include risk and coin concepts of their own that fit the information needs and objectives of sanitary inspection. Risk-based sampling is advantageous because it allows obtaining a sample size and acceptance number from the definition of the producer and consumer risks and the acceptable and minimum sanitation levels. Using the R software, a remote access interactive web calculator was designed to provide the user with a quick way to develop and design risk-based import product acceptance sampling plans, plot the characteristic operating curve, and provide information that can be used to make product inspection easier and more efficient.

ACKNOWLEDGMENTS

We gratefully acknowledge the invaluable collaboration of the General Directorate of Phytosanitary Inspection team, as well as the valuable participation of inspectors from the Agricultural Health Inspection Offices of the Cargo Airport in Mexico City, Nuevo Laredo, Tamaulipas, and the port area of Veracruz, Mexico.

REFERENCES

Chen C, Epanchin-Niell RS, Haight RG. 2017. Optimal inspection of imports to prevent invasive pest introduction. Risk Analysis 38 (3): 603–619. https://doi.org/10.1111/risa.12880

IPPC (International Plant Protection Convention). 2005. International Standard for Phytosanitary Measures 23. Guidelines for inspection. Food and Agriculture Organization of the United Nations. International Plant Protection Convention. Rome, Italy. https://www.ippc.int/static/media/files/publication/en/2016/01/ISPM_23_2005_En_2015-12-22_PostCPM10_InkAmReformatted.pdf (Retrieved: April 2024).

IPPC (International Plant Protection Convention). 2008. International Standards for Phytosanitary Measures 31. Methodologies for sampling of consignments. Food and Agriculture Organization of the United Nations. International Plant Protection Convention. Rome, Italy. https://www.ippc.int/static/media/files/publication/en/2016/11/ISPM_31_2008_Sampling_of_consignments_EN.pdf (Retrieved: April 2024).

Decrouez G, Robinson A. 2013. Time-series models for border inspection data. Risk Analysis 33 (12): 2142–2153. https://doi.org/10.1111/risa.12058

Diagne C, Leroy B, Vaissière AC, Gozlan RE, Roiz D, Jaric I, Salles JM, Bradshaw CJA, Courchamp F. 2021. High and rising economic cost of biological invasions worldwide. Nature 592 (7855): 571–576. https://doi.org/10.1038/s41586-021-03405-6

Follett PA, Hennessey MK. 2007. Confidence limits and sample size for determining nonhost status of fruits and vegetables to tephritid fruit flies as a quarantine measure. Journal of Economic Entomology 100 (2): 251–257. https://doi.org/10.1093/jee/100.2.251

Gutiérrez-Pulido H, de la Vara-Salazar R. 2009. Control estadístico de calidad y Seis Sigma (Segunda edición). McGraw-Hill/Interamericana Editores S.A. de C.V.: Ciudad de México, México. 482 p.

Hoffmann BD, Broadhurst LM. 2016. The economic cost of managing invasive species in Australia. NeoBiota 31: 1–18. https://doi.org/10.3897/neobiota.31.6960

Jáquez-Mata SV, Pérez-Santiago G, Márquez-Linares MA, Pérez-Verdín G. 2022. Impactos económicos y ambientales de los plaguicidas en cultivos de maíz, alfalfa y nogal en Durango, México. Revista Internacional de Contaminación Ambiental 38: 219–233. https://doi.org/10.20937/rica.54169

Kiermeier A. 2008. Visualizing and assessing acceptance sampling plans: The R package AcceptanceSampling. Journal of Statistical Software 26 (6): 1–20. https://doi.org/10.18637/jss.v026.i06

Lane SE, Cannon RM, Arthur AD, Robinson AP. 2019. Sample size for inspection intended to manage risk with mixed consignments. Neobiota 42: 59–69. https://doi.org/10.3897/neobiota.42.29757

McWilliams TP, Saniga EM, Davis, DJ. 2001. On the design of simple acceptance sampling plans. Economic Quality Control 16 (2): 193–198. https://doi.org/10.1515/eqc.2001.193

NAPPO (North America Plant Protection Organization). 2020. Manual de muestreo fundamentado en el riesgo (MFR) – parte I. Raleigh, NC, USA. 156 p.

NAPPO (North America Plant Protection Organization). 2022. Manual de muestreo fundamentado en el riesgo (MFR)– parte II. Raleigh, NC, USA. 134 p.

Pimentel D, Larch L, Zuniga R, Morrison D. 2000. Environmental and economic costs of nonindigenous species in the United States. BioScience 50 (1): 53–65. https://doi.org/10.1641/0006-3568(2000)050[0053:eaecon]2.3.co;2

R Core Team. 2023. R: A language and environment for statistical computing. R Foundation for Statistical Computing. Vienna, Australia. https://www.R-project.org (Retrieved: April 2024).

Rico-Sánchez AE, Haubrock PJ, Cuthbert RN, Angulo E, Ballesteros-Mejia L, López-López E, Duboscq-Carra VG, Númez MA, Diagne C, Courchamp F. 2021. Economic costs of invasive species in Mexico. NeoBiota 67: 459–483. https://doi.org/10.3897/neobiota.67.63846

Schilling EG, Neubauer DV. 2009. Acceptance sampling in quality control (Second edition). Chapman and Hall: New York, NY, USA. https://doi.org/10.1201/9781584889533

SENASICA (Servicio Nacional de Sanidad e Inocuidad Agroalimentaria). 2024. Programa de sanidad e inocuidad agroalimentaria. Gobierno de México. Servicio Nacional de Sanidad e Inocuidad Agroalimentaria. Ciudad de México, México. https://www.gob.mx/senasica/acciones-y-programas/programa-de-sanidad-e-inocuidad-agroalimentaria-194083 (Retrieved: April 2024).

SIICEX (Sistema Integral de Información de Comercio Exterior). 2024. Tarifa de la ley de los impuestos generales de importación y exportación. Gobierno de México. Secretaría de Economía. Ciudad de México, México. http://www.siicex-caaarem.org.mx (Retrieved: April 2024).

Thomson SK. 2012. Sampling (Third edition). John Wiley and Sons: Hoboken, NJ, USA. https://doi.org/10.1002/9781118162934

Trouvé R, Robinson AR. 2024. Efficient border biosecurity inspection leverages superspreading to reduce biological invasion risk. Risk Analysis 44 (8): 1839–1849. https://doi.org/10.1111/risa.14277

Villanueva-Jiménez JA, Reyes-Pérez N, Abato-Zárate M. 2017. Manejo integrado de plagas y sostenibilidad. *In* Jarquín GR, Huerta PA. (coords.), Agricultura Sostenible como Base para los Agronegocios. Universidad Autónoma de San Luis Potosí: San Luis Potosí, México, pp: 32–42.

Warziniack T, Haight RG, Yemshanov D, Apriesnig JL, Holmes P, Countryman AM, Rothlisberger JD, Haberland C. 2021. Economics of invasive species. *In* Poland TM, Patel-Weynard T, Finch DM, Miniat CF, Hayes DC, López VM. (eds.), Invasive Species in Forest and Rangelands of the United States. Springer: Cham, Switzerland, pp: 305–320. https://www.doi.org/10.1007/978-3-030-45367-1_14

Agrociencia

In vitro EFFECT OF *Trichoderma asperellum* METABOLITES ON *Fusarium oxysporum* AND *Fusarium equiseti*

César **Chacón**[1], Emanuel **Bojórquez-Quintal**[2], Goretty **Caamal-Chan**[3], Jairo **Cristobal-Alejo**[4], Nancy **Ruiz-Lau**[5*]

[1]Tecnológico Nacional de México. Instituto Tecnológico de Tuxtla Gutiérrez. Carretera Panamericana km 1080, Tuxtla Gutiérrez, Chiapas, Mexico. Z. C. 29050.
[2]Secretaría de Ciencia, Humanidades, Tecnología e Innovación. Laboratorio de Análisis y Diagnóstico del Patrimonio. El Colegio de Michoacán A. C. Cerro de Nahuatzen 85, Fracc. Jardines del Cerro Grande. La Piedad, Michoacán, Mexico. Z. C. 59370.
[3]Secretaría de Ciencia, Humanidades, Tecnología e Innovación. Centro de Investigaciones Biológicas del Noroeste S. C. Instituto Politécnico Nacional 195, Playa Palo de Santa Rita Sur, La Paz, Baja California Sur, Mexico. Z. C. 23096.
[4]Tecnológico Nacional de México. Instituto Tecnológico de Conkal. Avenida Tecnológico s/n, Conkal, Conkal, Yucatán, Mexico. Z. C. 97345.
[5]Secretaría de Ciencia, Humanidades, Tecnología e Innovación. Tecnológico Nacional de México. Instituto Tecnológico de Tuxtla Gutiérrez. Carretera Panamericana km 1080, Tuxtla Gutiérrez, Chiapas, Mexico. Z. C. 29050.
* Author for correspondence: nruizla@secihti.mx; nancy.rl@tuxtla.tecnm.mx

Citation: Chacón C, Bojórquez-Quintal E, Caamal-Chan G, Cristobal-Alejo J, Ruiz-Lau N. 2025. *In vitro* effect of *Trichoderma asperellum* metabolites on *Fusarium oxysporum* and *Fusarium equiseti*. **Agrociencia** 59(3): 369-382. https://doi.org/ 10.47163/agrociencia.v59i2.3255

Editor in Chief: Dr. Fernando C. Gómez Merino

Received: June 24, 2024.
Approved: February 21, 2025.
Published in Agrociencia: March 24, 2025.

ABSTRACT

The control of phytopathogenic fungi in agricultural crops requires the use of synthetic chemical fungicides, which have damaged the environment for decades. Biocontrol with microorganisms is one option to reduce their use, with the fungi of the *Trichoderma* genus standing out for their ability to interact with soil pathogens through different control mechanisms through antibiosis or production of substances harmful to other microorganisms. The objective of this work was to evaluate the biological control mechanism using *Trichoderma asperellum* antibiotics on the growth of *Fusarium oxysporum* and *F. equiseti*. Antibiosis bioassays were performed using the cellophane test (diffusible metabolite assay), the reverse plate technique (volatility assay), and poisoned foods (*T. asperellum* mycelium extracts and extracellular metabolite assays). The diffusible metabolites of *T. asperellum* presented the greatest inhibition of growth. The highest percentage of inhibition was observed on *F. oxysporum* in plates where *T. asperellum* developed for 72 h (>25 %), while *F. equiseti* inhibition was more effective in plates with 48 h (>40 %). In both species, no significant inhibitory effect was observed in volatility tests (>10 %), while extracellular metabolites showed no inhibition. In contrast, metabolites extracted from *T. asperellum* mycelium with ethyl acetate inhibited *Fusarium* between 18 and 40 %; with hexane, between 9 and 20 %; and with methanol, no inhibition was observed. The direct analysis in real-time mass spectrometry (DART-MS) analysis showed the presence of pyrones, fatty acids, alcohols, and carbohydrates in extracts and liquid culture of *T. asperellum*, which suggests that the control mechanism through antibiotics on *F. oxysporum* and *F. equiseti* is fungistatic.

Keywords: biocontrol, fungistatic, inhibition, mechanism, metabolite, phytopathogen.

INTRODUCTION

Soil-borne pathogens are a problem in agriculture worldwide, causing yield and quality losses in many crops (Madbouly and Abdelbacki, 2017). Among the pathogens that contribute the most to yield losses, the *Fusarium* genus stands out (Rivera-Jiménez *et al*., 2018). *Fusarium oxysporum* causes wilting and subsequent death due to colonization of the roots and vascular bundles (Zheng *et al*., 2022), while *F. equiseti* is associated with leaf spot, crown, and root rot, which causes seed deterioration and seedling infection (Gilardi *et al*., 2017).

Capsicum is a crop generally associated with infection by phytopathogenic fungi of the *Fusarium* genus (Hami *et al*., 2021), affecting its yield and commercial value. Currently, pathogenic fungi are effectively controlled with synthetic fungicides, but these are harmful to the environment (Shafique *et al*., 2018) and toxic to farmers, communities, and consumers; in addition, the indiscriminate use of these fungicides results in residual toxicity due to accumulation (Pathak *et al*., 2022). Therefore, there is a motivation to find fungicides that are safe, effective, and do not cause environmental damage (Wu *et al*., 2023).

Biological control with antagonistic microorganisms has increased and is successful as a green, low-cost, and agroecological alternative to synthetic fungicides since they colonize the rhizosphere without leaving toxic residues, unlike chemical fungicides used in conventional agriculture to control soilborne pathogens (Palmieri *et al*., 2022). Several microorganisms are used as biocontrol agents, including *Trichoderma*, a genus of avirulent hyperparasitic fungal species symbionts of plants that act against phytopathogenic fungi through several antagonistic mechanisms, including antibiosis, induction of plant defense, mycoparasitism, and competition for nutrients in the rhizosphere (Marques *et al*., 2018).

The antibiosis process of *Trichoderma* spp. is based on the production of antibiotic chemical compounds associated with competition for nutrients in the rhizosphere (Contreras-Cornejo *et al*., 2016). These fungi use antibiosis as a generalized strategy used for defense (Tyskiewicz *et al*., 2022) and produce a spectrum of antifungal secondary metabolites that inhibit microbial growth without physical contact (Dawidziuk *et al*., 2016), such as polyketides, gliotoxin, anthraquinones, pyrones, and peptaibols. Other metabolites associated with *Trichoderma* are enzymes that degrade the cell wall, siderophores, iron chelators, and volatile and non-volatile metabolites (Tyskiewicz *et al*., 2022).

Trichoderma spp. inhibit phytopathogenic fungi *in vitro* by producing diffusible, volatile, and non-volatile secondary metabolites. Although most *Trichoderma* species produce toxic volatile metabolites that affect the growth and development of phytopathogens (Stracquadanio *et al*., 2020), Sánchez-García *et al*. (2017) reported inhibition percentages of over 70 % of diffusible metabolites in two isolates of *T. asperellum* (Tri-3 and Tri-5) on three root phytopathogenic fungi in *Phaseolus vulgaris* L. (*F. oxysporum*, *F. verticillioides*, and *F. solani*). Likewise, Mishra *et al*. (2018) evaluated the ability of *T. asperellum* to produce volatile and non-volatile metabolites against *F. oxysporum* f. sp. *capsici* and found that volatile metabolites are less effective in reducing mycelial growth (22 %) of the pathogen than non-volatile compounds, with inhibition percentages higher than 25 %.

There is evidence that metabolites produced by *T. asperellum* have an inhibitory effect on the development of phytopathogens in relation to their mode of action. *In vitro* studies could be a useful tool for identifying sources of antifungal compounds. Therefore, the objective of this work was to evaluate the biological control mechanism by antibiosis of *T. asperellum* metabolites on two pathogenic strains (*F. oxysporum* and *F. equiseti*).

MATERIALS AND METHODS

The biological control agent *Trichoderma asperellum* ITC17 Ta13-17 (GenBank number: MH015346) and the pathogen strains *Fusarium oxysporum* FCHJ-T6, *F. oxysporum* FCHA-T7, and *F. equiseti* FCHE-T8 (GenBank numbers MG020428, MG020429, and MG020433, respectively) were provided by Dr. Jairo Cristóbal Alejo and belong to the microbial collection of the Technological Institute of Conkal, Mexico. The *T. asperellum* strain was isolated from the root and stem crown of sweet pepper (*Capsicum annuum* L.), and *F. oxysporum* and *F. equiseti* were isolated from habanero pepper root (*C. chinense* Jacq.).

Diffusible metabolites assay

The assay was carried out in two stages using the cellophane test as described by Sánchez-García *et al*. (2017). Cellophane circles were placed on plates with potato dextrose agar medium (PDA, BD Bioxon, México), one per plate; then, a 6 mm diameter mycelial disc of *T. asperellum* (three-day culture) was centrally inoculated for growth on the cellophane and removed after 24, 48, and 72 h. To assess metabolite diffusion, the plates were incubated at 30±2 °C in the dark. A sterile filter paper disk (6 mm diameter) (Whatman™, Grade 1) was used as a control.

In the second stage, a 6 mm diameter mycelial disc with *F. oxysporum* FCHJ-T6, *F. oxysporum* FCHA-T7, and *F. equiseti* FCHE-T8 (seven-day culture in PDA medium) was placed on the central position where the antagonist was inoculated. The plates were incubated at 30±2 °C in the dark, and radial growth (mm) was recorded every 24 h until the control reached the edge of the plate. Three repetitions were established for each treatment and a control. The diameter was measured with a ruler, and the percentage inhibition of radial growth (PIRG) of the pathogen was calculated according to the following formula:

$$PIRG = \frac{(D1 - D2)}{D1} \times 100$$

where $D1$ is the diameter of the pathogen on the control plate and $D2$ is the diameter of the pathogen on the plate with *T. asperellum*.

Volatility assay

The effect of volatile metabolites of *T. asperellum* was evaluated by the inverted plate technique as reported by Toghueo *et al*. (2016). In different Petri dishes, 6-mm mycelial discs (one per plate) of *T. asperellum* or *Fusarium* sp. were inoculated, taken from cultures of two and seven days in PDA medium, respectively; three replicates were established for each *Trichoderma-Fusarium* interaction and a control. Subsequently, the bases of both plates were placed opposite, sealed with adhesive tape and plastic film, and incubated at 30±2 °C in the dark. As a control, the base of the Petri dish inoculated with the pathogen was placed opposite another with a sterile filter paper disc. The pathogen was placed on top to avoid interference by *T. asperellum* spores. The diameters of the *Fusarium* colonies were measured every 24 h for five days (all measurements were taken in the same box) (Chen *et al*., 2016). The inhibition percentage was calculated using the following equation:

$$I = \frac{C - T}{C} \times 100$$

where C is the mycelial growth of the pathogen in the control plate, T is the mycelial growth in the tests with *Trichoderma*, and I represents the percentage of mycelial growth that has been inhibited.

Trichoderma asperellum mycelium extracts assay

Mycelium extracts were obtained as reported by Ibrahim *et al*. (2017), with some modifications. *Trichoderma asperellum* was cultivated in potato dextrose broth (PDB) at 30±2 °C for 30 days in the dark. Under sterile conditions, the culture medium with five days of growth was filtered with sterile gauze to recover the mycelium, which was then dried in an incubator at room temperature for eight days. Dried mycelial mats were ground, extracted with 200 mL hexane with shaking for 24 h at room temperature, and filtered through Whatman no. 1 paper. The solid residue was extracted again with hexane as described above. The filtrates were combined and evaporated to obtain the hexane extract. The solid residue was extracted with ethyl acetate and methanol, respectively, as described for the hexane extract.

For the test, 55 mm Petri dishes were used with PDA medium added with 1000 μg mL^{-1} of the extracts. The plates were inoculated by placing a *Fusarium* sp. mycelial disk from a seven-day culture in PDA medium in the center. Petri dishes without organic extract and with sterile distilled water (negative control) and dimethyl sulfoxide (DMSO ACS reagent, Sigma-Aldrich, France) (solvent test) were used as controls. Three replicates were used for each treatment. The plates were incubated at 30±2 °C and the colony diameter was measured with a ruler every 24 h until the control treatment reached the edge of the plate. The percentage of growth inhibition was calculated as described in the previous assay.

Extracellular metabolites assay

Flasks of 250 mL volume containing 100 mL of sterile PDB were inoculated with mycelial plugs taken from the edge of a seven-day culture of *T. asperellum* in PDA medium. Each flask was inoculated with three discs (6 mm) and incubated without shaking at 30±2 °C in the dark for seven days (Anees *et al*., 2018). For the elimination of spores, the liquid medium was filtered through a cloth, sterile gauze, and Whatman paper, and centrifuged twice at 4500 rpm for 25 min (Hermle Labortechnik™, Germany). A syringe filter (LINKTOR™ syringe filter, 25 mm diameter, 0.22 µm pore size) to obtain sterile culture liquid (Marques *et al*., 2018).

For the assay with extracellular metabolites, the culture filtrate was added to the sterile PDA medium in concentrations of 0, 5, 10, 15, 20, and 25 % (v/v) (Mishra *et al*., 2016; Petrisor *et al*., 2017; Anees *et al*., 2018; Mishra *et al*., 2018) using PDA plates. These were inoculated in the center with a 6 mm diameter mycelial disc of the pathogen and incubated at 30±2 °C until the fungus reached the edge of the plate in the control treatment. The trial treatments were completely randomized with three replicates. The radial growth of the phytopathogens was measured every 24 h with a ruler. The percentage inhibition of mycelial growth in relation to the growth of the controls was calculated as previously described.

Analysis of *T. asperellum* mycelium extract and sterile culture liquid

Two samples obtained from the culture of *T. asperellum* were analyzed and identified. The extract of dry mycelium was obtained with hexane and ethyl acetate. Samples were analyzed in the form of crude extract and diluted to a concentration of 1 mg mL^{-1} from the crude-dry extract in their corresponding extraction solvent (HPLC grade). The 1 mg mL^{-1} aliquots were kept refrigerated until analysis.

Direct analysis in real-time mass spectrometry (DART-MS) was carried out on a JMS-T100LP AccuTOF LC-PLUS spectrometer (JEOL, Tokyo, Japan) with a DART SVP100 ion source (Ionsense, Saugus, MA, USA). The DART ion source was operated with helium for analysis and nitrogen for standard mode; gas temperature was 300 °C, inlet pressure was 0.55 MPa, and voltage was ±600 V for positive and negative ion modes. The acquisition of the mass spectra was recorded with the Mass Center System Version 1.5.0k software in a mass range of m/z 50–1000 Da. Each sample was detected at least three to five times over 1–4 min. The analysis of the *T. asperellum* extracts at 1 mg mL^{-1} was carried out by placing 10 µL of volume in a capillary tube; subsequently, the capillary tube was placed between the helium stream from the DART ionization source and the vacuum interface to obtain DART mass spectra. Crude extracts were directly analyzed on DART-MS; the extract was taken with a capillary tube, and the sample adhered to the walls of the glass tube was analyzed (Procacci *et al*., 2021).

Statistical analysis

The data was analyzed using a completely randomized design of experiments with an analysis of variance (ANOVA) and Tukey's test at 95 % confidence using the Centurion XVII software (Statgraphics Technologies, VA, USA).

RESULTS AND DISCUSSION

In vitro antagonism of *T. asperellum* against *Fusarium* spp. by antibiosis

In the assay with diffusible metabolites, it was observed that the effect on the mycelial growth of the *Fusarium* strains was different in each treatment (Ta-24, Ta-48, and Ta-72). Inhibition was greater compared to the control at 192 h for *F. oxysporum* and at 216 h for *F. equiseti*, with Ta72 and Ta48 being the best treatments, respectively (Table 1). In an antibiosis assay, Sánchez-García *et al*. (2017) reported that *T. asperellum* inhibited radial growth (>75 %) of five *Fusarium* strains (two of *F. solani*, two of *F. oxysporum*, and one of *F. verticilloides*). In this work, growth inhibition was >25 % (192 h) in *F. oxysporum* and >40 % (216 h) in *F. equiseti*; this growth inhibition in the assay varied over time between strains, at days 8 and 9, respectively.

Trichoderma spp. have antagonistic activity against phytopathogens through multiple mechanisms that include mycoparasitism, competition for space and nutrients, induction of systemic resistance in plants, and antibiosis (Li *et al*., 2018). Regarding antibiosis, *Trichoderma* spp. produce secondary metabolites in the culture medium with potential antimicrobial activity. The identification and *in vitro* evaluation of these molecules against pathogens is important to identify strains with biocontrol potential. Different species of the *Trichoderma* genus can produce similar molecules (Morais *et al*., 2022) and different isolates of the same species can produce different secondary metabolites at various concentrations, which leads to the individuality of the species (Mesa-Vanegas *et al*., 2019).

The growth inhibition of *F. equiseti* depended on the development time of the biological control agent on the plate prior to culturing the pathogen, since the Ta48 treatment was more efficient with this strain than Ta72. The inhibition effect is due to the excretion of metabolites by *T. asperellum*, causing antibiosis (production of harmful substances for another organism) and inhibiting the growth of the pathogen. Metabolites excreted by antagonist agents may be volatile or non-volatile. In this case, *Trichoderma* spp. can produce both (Olmedo and Casas-Flores, 2014). The results demonstrated a fungistatic effect (that which prevents their growth) in the *Fusarium* strains caused by antibiosis (Table 1) through the synthesis and diffusion of *Trichoderma* metabolites in the plates with PDA medium.

The inhibitory effect of volatile metabolites produced by *T. asperellum* using the inverted plate technique has previously been reported (Morales-Rodríguez *et al*., 2018). However, in the volatility test, the results did not show statistical differences in the interactions between *T. asperellum* and *F. oxysporum* FCHA-T7 (<7 %) and *T. asperellum* and *F. equiseti* FCHE-T8 (<8 %) compared to the control.

For the poisoned food test, fungal extracts were obtained from *T. asperellum* mycelium using hexane (Hx-Ta), ethyl acetate (AcEt-Ta), and methanol (Me-Ta); these were tested at 1000 μg mL^{-1} (ppm) to evaluate their effect on the growth of *F. oxysporum* and *F. equiseti*, observing inhibition values less than 50 %. The AcEt-Ta extract presented the greatest growth inhibition on *F. oxysporum* (30.7 % for FCHJ-T6 and 18.1 % for FCHA-T7) and *F. equiseti* (38.1 %) at 120 and 168 h, respectively, followed by the Hx-

Table 1. Radial growth inhibition of *Fusarium oxysporum* FCHJ-T6, *F. oxysporum* FCHA-T7, and *F. equiseti* FCHE-T8 by *Trichoderma asperellum* in the diffusible metabolites† assay.

Treatment	*F. oxysporum* FCHJ-T6 (192 h)	*F. oxysporum* FCHA-T7 (192 h)	*F. equiseti* FCHE-T8 (216 h)
TST	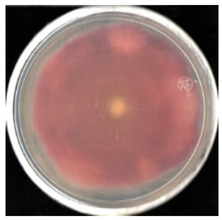 0.0±0.0 b	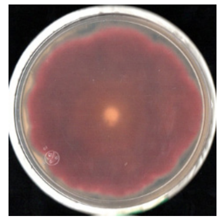 0.0±0.0 b	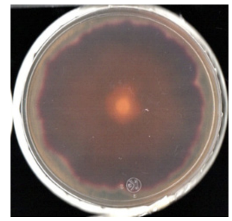 0.0±0.0 d
Ta-24	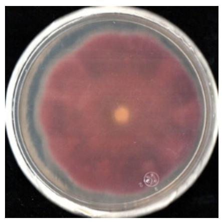 0.7±2.0 b	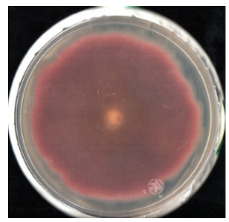 1.2±0.5 b	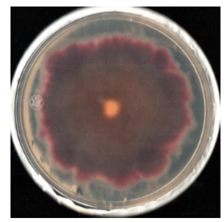 5.9±0.5 c
Ta-48	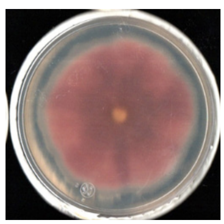 12.9±1.7 ab	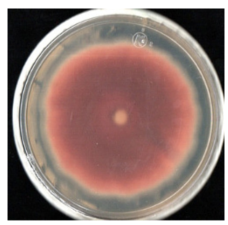 12.8±1.5 ab	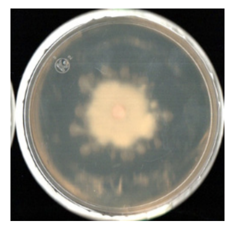 41.1±1.8 a
Ta-72	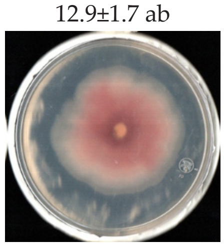 25.4±7.3 a	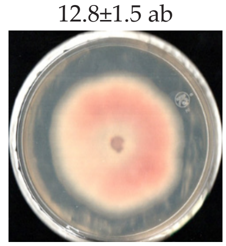 26.2±5.8 a	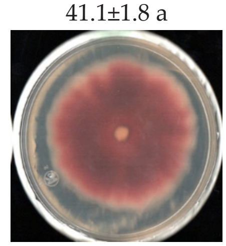 15.2±0.2 b

†The values are presented as percentages of inhibition of radial growth and correspond to the average of three repetitions ± standard error. Values with different letters in the same column are statistically different ($p \leq 0.05$). TST: control; Ta-24, Ta-48, and Ta-72: treatments in which *T. asperellum* grew on cellophane for 24, 48, and 72 h, respectively.

Ta extract (9.3–18.6 %), while Me-Ta did not show a significant inhibitory effect in any strain compared to the control. The effect of Hx-Ta and AcEt-Ta on *F. oxysporum* was fungistatic; in contrast, Me-Ta promoted the mycelial growth of the phytopathogen while the inhibitory effect of the solvent could be dismissed (Table 2).

Table 2. Inhibition of radial growth of *Fusarium oxysporum* FCHJ-T6, *F. oxysporum* FCHA-T7, and *F. equiseti* FCHE-T8 by *Trichoderma asperellum* in the fungal mycelium extracts test†.

Treatment	*F. oxysporum* FCHJ-T6 (120 h)	*F. oxysporum* FCHA-T7 (120 h)	*F. equiseti* FCHE-T8 (168 h)
H_2O (-)	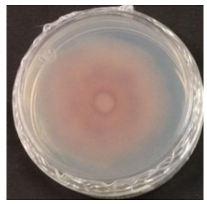 0.0±0.0 c	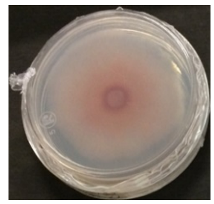 0.0±0.0 b	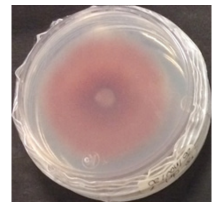 0.0±0.0 cd
DMSO	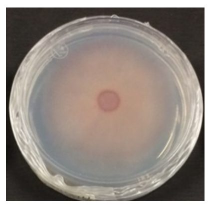 -2.7±0.0 d	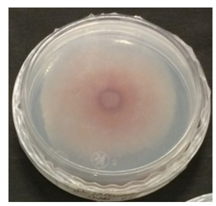 3.0±1.3 b	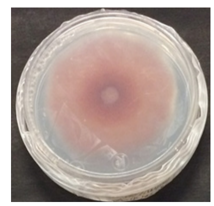 0.9±0.4 c
Hx-Ta	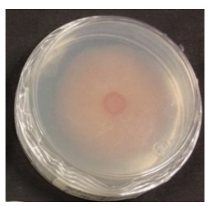 9.3±0.0 b	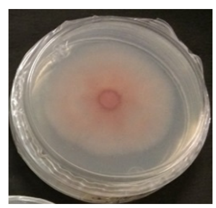 15.5±0.4 a	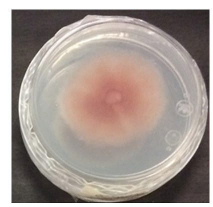 18.6±0.9 b
AcEt-Ta	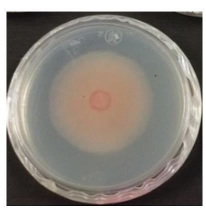 30.7±0.0 a	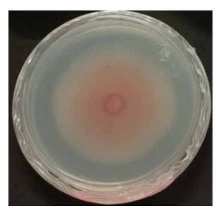 18.1±0.4 a	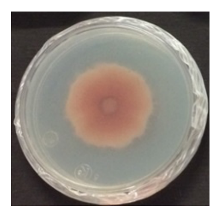 38.1±1.2 a
Me-Ta	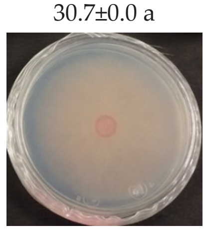 -7.1±0.4 e	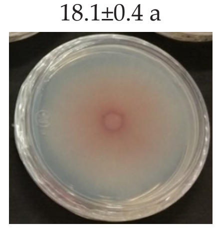 -5.2±0.9 c	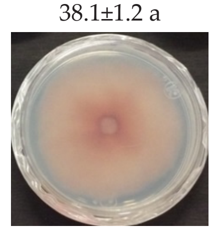 -3.1±0.4 d

†The values are presented as percentages of inhibition of radial growth, correspond to the average of three repetitions ± standard error. Values with different letters in the same column are statistically different ($p \leq 0.05$). H_2O (-): sterile distilled water (negative control); DMSO: dimethyl sulfoxide (solvent test): Hx-Ta: hexane extract; AcEt-Ta: ethyl acetate extract and Me-Ta: methanolic extract.

Ibrahim *et al*. (2017), when evaluating the antifungal activity of crude extracts of ethyl acetate (AcET) of two isolates of *T. longibrachiatum* (MF1 and MF5) and two fractions of these extracts partitioned with 90 % hexane and methanol and applied at 1000 μg mL^{-1}, observed that the crude extract of ethyl acetate and the methanolic fraction of both isolates had less than 50 % inhibition on the growth of *F. oxysporum*. In contrast, the hexane fraction of *T. longibrachiatum* MF1 was slightly active against *F. oxysporum*, while the hexane fraction of *T. longibrachiatum* MF5 was inactive against the pathogen. Therefore, this study and other reports suggest that the inhibitory effect of *Trichoderma* metabolites contained in the organic extracts may vary from one microorganism to another.

In the test with extracellular metabolites of the *T. asperellum* growth medium, none of the treatments with 0, 5, 10, 15, 20, and 25 % (v/v) of the filtrate in PDA medium inhibited the mycelial growth of the three *Fusarium* strains evaluated.

DART-MS analysis of mycelium extracts and sterile liquid culture of *T. asperellum*

The DART-MS analysis of the organic extracts allowed the identification of possible constituent compounds of diverse chemical nature. The hexane extract (Hx-Ta) produced signals associated with pyrans (1), pyrones (2 and 3), carboxylic acids (4), alcohols (5), fatty acids (6), and terpenes (7 and 8) (Table 3). The peaks associated with pyrones and fatty acids had the highest intensity and corresponded to the adducts $[M+O+H]^+$ and $[M+OH]^-$ and to the anion $[M-H]^-$.

The ethyl acetate (AcEt-Ta) extract contained 12 chemical groups, including furans (1), pyrans (2), pyrones (3, 4, and 5), carboxylic acids (6), alcohols (7), fatty acids (8 and 9), terpenes (10), polycyclic heteroarenes (11), and α-amino acid derivatives (12). The signals associated with fatty acids, pyrones, and alcohols presented the highest intensity and corresponded to the anion $[M-H]^-$ and the adducts $[M+O+H]^+$ and $[M+OH]^-$, respectively (Table 4).

In this study, the secondary metabolites extracted from *T. asperellum* mycelium with hexane and ethyl acetate caused inhibition of *Fusarium* spp. The signals with the highest intensity detected by DART-MS in both extracts corresponded to pyrone and fatty acid metabolites (Tables 3 and 4), while, in the ethyl acetate extract, a high-intensity peak attributed to a long-chain alcohol was detected (Table 4), which could explain the greater inhibitory activity of the AcEt extract on *Fusarium* spp. compared to the hexane extract. Sakpetch *et al*. (2018) had reported the presence of (2) 6-pentyl-2H-pyran-2-one (Table 3) in the hexane extract of the filtered liquid medium of *T. asperellum* and (1) 5-hydroxymethyl, 2-furancarboxaldehyde, (2) 4H-pyran-4-one, 2,3-dihydro-3,5-dihydroxy-6-methyl, and (9) 9,12-octadecenoic acid (Table 4) in the ethyl acetate extract. These compounds were associated with antimicrobial and antifungal activity. The abundance and variety of secondary metabolites identified in the mycelium fungal extracts indicate that the *T. asperellum* strain is capable of producing metabolites with biological activity. Among the three extracts evaluated, the presence of pyrones and fatty acids was represented with greater intensity in the hexane and ethyl acetate

Table 3. Ions and adducts detected in the hexane extract of *Trichoderma asperellum* mycelium analyzed in mode (+) and (-) by direct analysis in real time mass spectrometry (DART-MS).

Suggested metabolite	Crude and dry extract [Ion]/(m/z)		Diluted extract (1 mg mL^{-1}) [Ion]/(m/z)	
	Mode (+)	Mode (-)	Mode (+)	Mode (-)
(1) 4H-pyran-4-one, 2,3-dihydro-3,5-dihydroxy-6-methyl-	-----	$[M+Cl]^-$/ (179.068)	-----	-----
(2) 6-pentyl-2H-pyran-2-one	†$[M+O+H]^+$/ (183.127)	-----	†$[M+O+H]^+$/ (183.133)	-----
(3) 6-pent-1-enylpyran-2-one	-----	†$[M+OH]^-$/ (181.086)	$[M+H]^+$/ (165.117)	$[M+OH]^-$/ (181.083) $[2M-H]^-$/ (327.262)
(4) Benzeneacetic acid	-----	$[2M-H]^-$/ (271.121)	-----	-----
(5) 1-hydroxyheptadecane	-----	$[M-H]^-$/ (255.249)	-----	$[M-H]^-$/ (255.248)
(6) 9,12-octadecenoic acid	-----	-----	-----	†$[M-H]^-$/ (279.250)
(7) (3aR,4R,7R)-1,4-dimethyl-7-prop-1-en-2-yl-1,2,3,3a,4,5,6,7-octahydroazulene	$[M+O+H]^+$/ (221.240)	-----	-----	-----
(8) 2,6,10,15,19,23-hexamethyl-2,6,10,14,18,22-tetracosahexaene	-----	$[M-H]^-$/ (409.234)	-----	-----

†Most abundant ions in the DART-MS spectrum. The sample was detected at least three times. The metabolites were observed in the majority of the DART-MS spectra. m/z: mass to charge ratio; the letter M indicates the molecular weight of the metabolite.

extracts (Tables 3 and 4), as was the case of 6-pentyl-2H-pyran-2-one, which has been reported to have antimicrobial activity (Morais *et al*., 2022). According to the results, there is variability in the antimicrobial activity of this compound, since the fungal strains showed different degrees of sensitivity, which is dependent on the concentration of pyrone (Ismaiel and Ali, 2017). Given this evidence, and based on the inhibition results observed in the present study, it is suggested that the different secondary metabolites present in each extract and their concentrations exhibit various levels of antibiotic activity.

Table 4. Ions and adducts detected in the ethyl acetate extract of *Trichoderma asperellum* mycelium analyzed in mode (+) and (-) by direct analysis in real time mass spectrometry (DART-MS).

Suggested metabolite	Crude and dry extract [Ion]/(m/z)		Diluted extract (1 mg mL^{-1}) [Ion]/(m/z)	
	Mode (+)	Mode (-)	Mode (+)	Mode (-)
(1) 5-hydroxymethyl, 2-furancarboxaldehyde-	-----	-----	$[M+H]^+$/ (127.069)	-----
(2) 4H-pyran-4-one, 2,3-dihydro-3,5-dihydroxy-6-methyl-	-----	$[M+OH]^-$/ (161.055)	$[M+H]^+$/ (145.087)	$[M+OH]^-$/ (161.055)
(3) 6-pent-1-enylpyran-2-one	-----	-----	$[M+H]^+$/ (165.121, 165.124)	-----
(4) 6-amyl-alpha-pyrone	-----	-----	†$[M+O+H]^+$/ (183.137, 183.140)	$[M-H+O_2]^-$/ (197.043)
(5) 2H-pyran-2-one, tetrahydro-4-hydroxy -4-methyl-	-----	$[M-H+O_2]^-$/ (161.055)	$[M+O+H]^+$/ (147.104)	$[M-H+O_2]^-$/ (161.055) $[2M-H]^-$/ (259.071)
(6) 2-furancarboxylic acid	-----	-----	$[M+O+H]^+$/ (129.087)	$[M+OH]^-$/ (129.026) $[2M-H]^-$/ (223.094)
(7) 1-hydroxyheptadecane	-----	-----	-----	†$[M+OH]^-$/ (273.092)
(8) n-octadecanoic acid	-----	$[M-H]^-$/ (283.279)	-----	-----
(9) 9,12-octadecenoic acid	-----	†$[M-H]^-$/ (279.251)	-----	-----
(10) (3R,3aS,7aR)-1,4-dimethyl-7-prop-1-en-2-yl-1,2,3,3a,4,5,6,7-octahydroazulene	-----	$[M+O_2]^-$/ (312.249)	$[M+H]^+$/ (205.130)	-----
(11) 1H-indole	-----	-----	-----	-----
(12) Pyrrolo[1,2-a] pyrazine-1,4-dione, hexahydro-	-----	M^-/ (117.027)	-----	$[2M-H]^-$/ (307.205)

†Most abundant ions in the DART-MS spectrum. The sample was detected at least three times. The metabolites were observed in the majority of the DART-MS spectra. m/z: mass to charge ratio; the letter M indicates the molecular weight of the metabolite.

CONCLUSIONS

Diffusible metabolites extracted with hexane and ethyl acetate from *Trichoderma asperellum* mycelium showed a fungistatic effect on the growth of *Fusarium oxysporum* and *F. equiseti*. On the contrary, the volatile, extracellular, and methanol-extracted metabolites of *Trichoderma* mycelium did not show a significant inhibitory effect on growth. This suggests that these compounds play a role as a signal or stimulus during pathogen-biological control agent confrontation and that the antibiosis mechanism. Inhibition values lower than 50 % could be synergistically associated with other antagonistic mechanisms of *T. asperellum,* such as competition for space and nutrients.

ACKNOWLEDGEMENTS

To the Secretariat of Science, Humanities, Technology, and Innovation (SECIHTI) for the scholarship awarded to César Chacón (support number 715167). To Luis M. Rojas-Abarca for the technical support for the analysis of the extracts in DART-MS (Laboratory for the Analysis and Diagnosis of Heritage, El Colegio de Michoacán A. C.).

REFERENCES

Anees M, Azim R, Ur Rehman S, Jamil M, El Hendawy SE, Al-Suhaiban NA. 2018. Antifungal potential of *Trichoderma* strains originated from north western regions of Pakistan against the plant pathogens. Pakistan Journal of Botany 50 (5): 2031–2040.

Chen JL, Liu K, Miao CP, Sun SZ, Chen YW, Xu LH, Guan HL, Zhao LX. 2016. Salt tolerance of endophytic *Trichoderma koningiopsis* YIM PH30002 and its volatile organic compounds (VOCs) allelopathic activity against phytopathogens associated with *Panax notoginseng*. Annals of Microbiology 66 (3): 981–990. https://doi.org/10.1007/s13213-015-1171-5

Contreras-Cornejo HA, Macías-Rodríguez L, del-Val E, Larsen J. 2016. Ecological functions of *Trichoderma* spp. and their secondary metabolites in the rhizosphere: Interactions with plants. FEMS Microbiology Ecology 92 (4): fiw036. https://doi.org/10.1093/femsec/fiw036

Dawidziuk A, Popiel D, Kaczmarek J, Strakowska J, Jedryczka M. 2016. Optimal *Trichoderma* strains for control of stem canker of brassicas: Molecular basis of biocontrol properties and azole resistance. BioControl 61 (6): 755–768. https://doi.org/10.1007/s10526-016-9743-2

Gilardi G, Pintore I, Gullino ML, Garibaldi A. 2017. Occurence of *Fusarium equiseti* as a contaminant of *Diplotaxis tenuifolia* seeds. Journal of Plant Pathology 99 (1): 245–248. https://doi.org/10.4454/jpp.v99i1.3830

Hami A, Rasool RS, Khan NA, Mansoor S, Mir MA, Ahmed N, Masoodi KZ. 2021. Morpho-molecular identification and first report of *Fusarium equiseti* in causing chilli wilt from Kashmir (Northern Himalayas). Scientifc Reports 11 (1): 3610. https://doi.org/10.1038/s41598-021-82854-5

Ibrahim M, Kaushik N, Sowemimo A, Chhipa H, Koekemoer T, van de Venter M, Odukoya OA. 2017. Antifungal and antiproliferative activities of endophytic fungi isolated from the leaves of *Markhamia tomentosa*. Pharmaceutical Biology 55 (1): 590–595. https://doi.org/10.1080/13880209.2016.1263671

Ismaiel AA, Ali DMI. 2017. Antimicrobial properties of 6-pentyl-α-pyrone produced by endophytic strains of *Trichoderma koningii* and its effect on aflatoxin B1 production. Biologia 72 (12): 1403–1415. https://doi.org/10.1515/biolog-2017-0173

Li YT, Hwang SG, Huang YM, Huang CH. 2018. Effects of *Trichoderma asperellum* on nutrient uptake and *Fusarium* wilt of tomato. Crop Protection 110: 275–282. https://doi.org/10.1016/j.cropro.2017.03.021

Madbouly AK, Abdelbacki AMM. 2017. Biocontrol of certain soilborne diseases and promotion of growth of *Capsicum annuum* using biofungicides. Pakistan Journal of Botany 49 (1): 371–378.

Marques E, Martins I, de Mello SCM. 2018. Antifungal potential of crude extracts of *Trichoderma* spp. Biota Neotropica 18 (1): e20170418. https://doi.org/10.1590/1676-0611-BN-2017-0418

Mesa-Vanegas AM, Marín A, Calle-Osorno J. 2019. Secondary metabolites in *Trichoderma* spp. and its agricultural biotechnological applications. Actualidades Biológicas 41 (111): 32–44. https://doi.org/10.17533/udea.acbi.v41n111a02

Mishra A, Dixit S, Ratan V, Srivastava M, Trivedi S, Srivastava YK. 2018. Identification and *in silico* screening of biologically active secondary metabolites isolated from *Trichoderma harzianum*. Annals of Phytomedicine 7 (1): 78–86. https://doi.org/10.21276/ap.2018.7.1.9

Mishra N, Khan SS, Krishna Sundari S. 2016. Native isolate of *Trichoderma*: a biocontrol agent with unique stress tolerance properties. World Journal of Microbiology and Biotechnology 32: 130. https://doi.org/10.1007/s11274-016-2086-4

Morais EM, Silva AAR, de Sousa FWA, de Azevedo IMB, Silva HF, Santos AMG, Júnior JEAB, de Carvalho CP, Eberlin MN, Porcari AM, Araújo FD da S. 2022. Endophytic *Trichoderma* strains isolated from forest species of the Cerrado-Caatinga ecotone are potential biocontrol agents against crop pathogenic fungi. PLOS ONE 17 (4): e0265824. https://doi.org/10.1371/journal.pone.0265824

Morales-Rodríguez C, Bastianelli G, Aleandri MP, Chilosi G, Vannini A. 2018. Application of *Trichoderma* spp. complex and biofumigation to control damping-off of *Pinus radiata* D. Don caused by *Fusarium circinatum* Nirenberg and O'Donnell. Forests 9 (7): 421. https://doi.org/10.3390/f9070421

Olmedo VM, Casas-Flores S. 2014. Molecular mechanisms of biocontrol in *Trichoderma* spp. and their applications in agriculture. *In* Gupta V, Schmoll M, Herrera-Estrella A, Upadhyay R, Druzhinina I, Tuohy M. (eds.), Biotechnology and Biology of *Trichoderma*. Elsevier: Amsterdam, Netherlands, pp: 429–453. https://doi.org/10.1016/B978-0-444-59576-8.00032-1

Palmieri D, Ianiri G, del Grosso C, Barone G, de Curtis F, Castoria R, Lima G. 2022. Advances and perspectives in the use of biocontrol agents against fungal plant diseases. Horticulturae 8: 577. https://doi.org/10.3390/horticulturae8070577

Pathak VM, Verma VK, Rawat BS, Kaur B, Babu N, Sharma A, Dewali S, Yadav M, Kumari R, Singh S, *et al*. 2022. Current status of pesticide effects on environment, human health and its eco-friendly management as bioremediation: A comprehensive review. Frontiers in Microbiology 13: 962619. https://doi.org/10.3389/fmicb.2022.962619

Petrisor C, Paica A, Constantinescu F. 2017. Effect of secondary metabolites produced by different *Trichoderma* spp. isolates against *Fusarium oxysporum* f. sp. *radicis-lycopersici* and *Fusarium solani*. Scientific Papers Series B Horticulture 61: 407–411.

Procacci S, Bojórquez-Quintal E, Platamone G, Maccioni O, Vecchio VL, Morreale V, Alisi C, Balducchi R, Bacchetta L. 2021. *Opuntia ficus-indica* pruning waste recycling: Recovery and characterization of mucilage from cladodes. Natural Resources 12 (4): 91–107. https://doi.org/10.4236/nr.2021.124008

Rivera-Jiménez MN, Zavaleta-Mancera HA, Rebollar-Alviter A, Aguilar-Rincón VH, García-de los Santos G, Vaquera-Huerta H, Silva-Rojas HV. 2018. Phylogenetics and histology provide insight into damping-off infections of 'Poblano' pepper seedlings caused by *Fusarium* wilt in greenhouses. Mycological Progress 17 (11): 1237–1249. https://doi.org/10.1007/s11557-018-1441-2

Sakpetch P, H-Kittikun A, Kuwahara Y, Komeda H, Asano Y. 2018. Isolation of indigenous antagonistic microorganism to inhibit *Rigidoporus microporus* and other plant pathogens and analysis of the bioactive compounds. Biological Control 124: 53–60. https://doi.org/10.1016/j.biocontrol.2018.01.007

Sánchez-García BM, Espinosa-Huerta E, Villordo-Pineda E, Rodríguez-Guerra R, Mora-Avilés MA. 2017. *Trichoderma* spp. native strains molecular identification and *in vitro* antagonistic evaluation of root phitopathogenic fungus of the common bean (*Phaseolus vulgaris* L.) cv. Montcalm. Agrociencia 51 (1): 63–79.

Shafique S, Shafique S, Ahmad A. 2018. Biochemical and molecular screening of varieties of chili plants that are resistant against *Fusarium* wilt infection. European Journal of Microbiology and Immunology 8 (1): 12–19. https://doi.org/10.1556/1886.2017.00031

Stracquadanio C, Quiles JM, Meca G, Cacciola SO. 2020. Antifungal activity of bioactive metabolites produced by *Trichoderma asperellum* and *Trichoderma atroviride* in liquid medium. Journal of Fungi 6 (4): 263. https://doi.org/10.3390/jof6040263

Toghueo RMK, Eke P, Zabalgogeazcoa Í, de Aldana BRV, Nana LW, Boyom FF. 2016. Biocontrol and growth enhancement potential of two endophytic *Trichoderma* spp. from *Terminalia catappa* against the causative agent of common bean root rot (*Fusarium solani*). Biological Control 96: 8–20. https://doi.org/10.1016/j.biocontrol.2016.01.008

Tyskiewicz R, Nowak A, Ozimek E, Jaroszuk-Sciseł J. 2022. *Trichoderma*: The current status of its application in agriculture for the biocontrol of fungal phytopathogens and stimulation of plant growth. International Journal of Molecular Sciences 23 (4): 2329. https://doi.org/10.3390/ijms23042329

Wu PH, Chang HX, Shen YM. 2023. Effects of synthetic and environmentally friendly fungicides on powdery mildew management and the phyllosphere microbiome of cucumber. PLOS ONE 18 (3): e0282809. https://doi.org/10.1371/journal.pone.0282809

Zheng J, Wang L, Hou W, Han Y. 2022. *Fusarium oxysporum* associated with *Fusarium* wilt on *Pennisetum sinese* in China. Pathogens 11 (9): 999. https://doi.org/10.3390/pathogens11090999

Agrociencia

VULNERABILITY OF THE CHICKEN MEAT MARKET TO CHANGES IN THE PRICE OF FEED GRAINS

Alvaro **Nochebuena-Molina**[1], José Alberto **García-Salazar**[1*]

[1]Colegio de Postgraduados Campus Montecillo. Posgrado en Socioeconomía, Estadística e Informática-Economía. Carretera México-Texcoco km 36.5, Montecillo, Texcoco, State of Mexico, Mexico. C. P. 56264.
* Author for correspondence: jsalazar@colpos.mx

ABSTRACT

In the past three decades, the chicken (*Gallus gallus domesticus* L.) meat market has been favored by the commercial liberation established in the Free Trade Agreement, since the growth in production of this product was largely due to the supply of inputs used to feed cattle, such as maize and soybeans, based on imports at low costs from the USA. This situation could be reversed in the future, since the dependence on grains determines if the cattle markets are vulnerable to international exogenous changes. The aim of this investigation was to determine the effects of an increase in the price of feed grains on the chicken meat market in Mexico using a spatial equilibrium model for 2021. Results indicate that, in the year of analysis, chicken meat production, imports, and consumption were 3669 and 4419 thousand Mg, respectively. A 60 % increase in the price of feed grains would have considerable effects on the chicken meat market, since production would decrease by 390 thousand Mg and imports would increase by 363 thousand Mg. Due to these changes, consumption would only decrease by 27 thousand Mg, an expected result in a market open to international trade such as chicken meat. Due to the negative effects on the production and increase in imports, it is recommended for the government to take all necessary measures to reduce the dependence on feed grains demanded by the livestock sector, since an increase in the international price would make it difficult to guarantee the supply of such inputs.

Keywords: Free Trade Agreement, food dependence, production, imports, spatial equilibrium model.

INTRODUCTION

Ever since the North American Free Trade Agreement (NAFTA, now known as the T-MEC), the livestock sector dedicated to the production of meats has been one of the most dynamic sectors in Mexico's economy. Between 1994 and 2021, the production of chicken, beef, and pork grew by 225.8, 56.1, and 93.9 %, respectively. In the same period, chicken meat production increased from 1126 to 3669 thousand Mg, beef from 1365 to 2131 thousand Mg, and pork from 873 to 1693 thousand Mg (SIAP, 2023).

Citation: Nochebuena-Molina Á, García-Salazar JA. 2025. Vulnerability of the chicken meat market to changes in the price of feed grains. **Agrociencia** 59(3): 383-396. https://doi.org/ 10.47163/ agrociencia.v59i3.3078

Editor in Chief:
Dr. Fernando C. Gómez Merino

Received: October 05, 2023.
Approved: January 21, 2025.
Published in Agrociencia:
April 08, 2025.

Despite the increase in production, meat imports carried out by Mexico presented a similar behavior, influenced by the commercial liberation established in the agreement. From 1994 to 2021, chicken meat imports increased from 124 to 813 thousand Mg, beef imports from 122 to 173 thousand Mg, and pork imports from 251 to 1275 thousand Mg (ABPA, 2022; COMECARNE, 2022; FAO, 2023a; National Customs Directorate of Chile, 2023; USITC, 2023). As in the case of production, the above data indicate a strong growth in external purchases of 554.9, 41.9, and 407.9 % for chicken, beef, and pork, respectively.

As a result of the growth in production and imports, the demand for all three types of meats grew. From 1994 to 2021, the growth experienced by the National Apparent Consumption (NAC) was 258.7 % for chicken meat, 33.9 % for beef, and 142.9 % for pork. In this period, chicken meat consumption went from 1248 to 4475 thousand Mg, beef consumption from 1485 to 1989 thousand Mg, and pork from 1118 to 2716 thousand Mg (ABPA, 2022; COMECARNE, 2022; FAO, 2023a; National Customs Directorate of Chile, 2023; USITC, 2023). The highest growth was found in chicken meat, which was positioned as the most important in terms of the preferences of meat consumers.

These trends show the positive effects of NAFTA on meat producers and consumers, since the strong production growth during the 1994–2021 period was a consequence of low international prices in maize and soybean, the main inputs used in the production of chicken feed, which allowed prices to be reduced. The increase in production allowed for a greater consumption of meat. Feed costs are the main expense in meat production: for chicken meat, they represent up to 62 % of total costs (UNA, 2022); for pork, between 63.6 and 86.6 % (Hernández-Cruz *et al*., 2019); and for beef, between 75 and 80 % (Castro-Samano *et al*., 2019). The balanced feed used in the production of chicken meat is a mixture of maize (or sorghum), which provides energy, and soybean, which provides protein. Fats, oils, vitamins, and supplements are also used. Maize and sorghum are substitute goods in the production of balanced feed (OECD, 2018).

In 2021, 38.7 million Mg of raw material were used for the production of balanced feed in Mexico, out of which 17.6, 8.6, and 4.2 million Mg correspond to maize, soybean, and sorghum, respectively (CONAFAB, 2022). The greatest use of these crops was a consequence of the dynamic observed in the market variables, influenced by the commercial liberalization. From 1994 to 2021, maize production increased from 18 236 to 27 503 thousand Mg; sorghum production from 3701 to 4370 thousand Mg, and soybean production decreased from 523 to 288 thousand Mg (SIAP, 2023). These data represent a growth rate of 50.8, 18.1, and -44.9 % for these crops, respectively.

The real international prices (in 2010 USD Mg^{-1}) of these products in 1994 were 128.49, 124.09, and 300.88 for maize, sorghum, and soybean, whereas in 2021, their real prices were USD 237.24, 198.41, and 533.20 per Mg, respectively (World Bank, 2023). In this period, maize imports increased significantly from 2747 to 17 396 thousand Mg, representing a growth of 533.4 %. The same trend was observed with soybean imports, which grew 84.1 %, from 2497 to 4597 thousand Mg. In regard to sorghum, imports fell from 3475 to 66 thousand Mg, representing a decrease of almost 100 % (FAO, 2023a). In the period, maize consumption increased 113.9 %, from 20 946 to 44 802 thousand Mg, and soybean consumption grew 61.8 %, from 3019 to 4885 thousand Mg. Due to the greatest use of maize in diets as a source of energy, the consumption of sorghum decreased by 38.2 %, from 7176 to 4436 thousand Mg.

The production and import behavior of feed grains determined a change in the structure of the demand exerted by livestock farming. During the 2010–2020 period, the amount of maize used as feed for cattle increased from 11.78 to 20.07 million Mg, displaying an increase of 8.3 million Mg and a growth of 70.4 %. Sorghum presented an opposite behavior, since in 2010, the amount of this product used in the balanced food industry was 8.8 million Mg, whereas for 2020, 4.8 million Mg were used, representing 3.9 million Mg less than in 2010 (FAO, 2023b).

The above change was a consequence of several factors. The first was the reduction in the price of maize in relation to the price of sorghum. Although at the beginning of NAFTA the maize/sorghum price ratio was 1.04, by 2021 this ratio was 0.96, indicating that the price of maize decreased faster than the price of sorghum (World Bank, 2023). The second factor that determined the change in the structure of feed grain demand was the removal of the prohibition on the use of maize for cattle consumption. According to data from the US Department of Agriculture (USDA, 2022), prices are expected to resume their downward tendency shown until before the COVID-19 pandemic and the armed conflict between Russia and Ukraine. By 2024, maize, sorghum, and soybean prices were expected to be USD 169.33, 167.37, and 372.49 per Mg, respectively. Due to this, the maize/sorghum ratio for 2022 was expected to be 1.02, and by 2023 and 2024, 1.01, which implies that the price of maize is expected to rise faster than that of sorghum, implying that the price of the balanced feed for fattening chicken will increase its price, affecting this industry.

In the last three decades, Mexican feed grain food policies have taken advantage of international prices in the world market, allowing an increased percentage of the consumption to be supplied with imports. In the case of maize, in 1994, the food dependence index was 13.1 %, whereas by 2021, it had increased to 38.8 %. In the case of soybean, the dependency index changed from 82.7 to 94.1 %. In the case of maize, the data on the food dependency index is aggregated and takes into account human, industrial, and livestock consumption; if only livestock consumption alone were considered, the issue of food dependency would be greater.

The evolution of the dependency index reflects the policy followed since 1994 to ensure the consumption of forage grains. In order to take advantage of low international prices, the country has preferred to supply consumption with imports. From an economic point of view, this could be justified in an international environment of low international prices, as was the case since 1994; however, should the international market change and international prices rise in the future, the country must make an effort to increase production and depend less on imports. Should there be an increase in the international price of maize and soybean, the cost of the balanced feed would rise, resulting in an increase in retail price and a decrease in chicken meat production, requiring the import of more of this product to meet national demand.

Given that chicken meat is widely consumed by Mexicans, the most produced in the country, and its production cost depends on the price of the grains used in the feed (maize and soybean), the aim of this investigation was to determine the effects of an increase in the price of feed grains on the chicken meat market in Mexico using a spatial equilibrium model for 2021. The main hypothesis considers that, should the prices of maize and soybean increase, chicken meat production costs would increase, resulting in a reduction in national production of chicken meat and an increase in imports to meet internal demand.

MATERIALS AND METHODS

Chicken producing and consuming regions

Twelve chicken-producing and consuming regions were considered, based on their geographic location and production importance: 1) Northwest (Nayarit, Sinaloa, and Sonora), 2) Baja California Peninsula (Baja California and Baja California Sur), 3) North (Chihuahua, Coahuila, and Durango), 4) Northeast and Center North (Nuevo León, San Luis Potosí, Tamaulipas, and Zacatecas), 5) Aguascalientes, 6) West (Jalisco and Colima), 7) Bajío (Michoacán and Guanajuato), 8) Querétaro, 9) Center (Mexico City, Hidalgo, State of Mexico, Morelos, Puebla, and Tlaxcala), 10) Gulf (Tabasco and Veracruz), 11) South (Chiapas, Guerrero, and Oaxaca), and 12) Yucatán Peninsula (Campeche, Quintana Roo, and Yucatán).

The cities taken as references to calculate the transportation costs were Culiacán, Tijuana, Torreón, Monterrey, Guadalajara, Guanajuato, Querétaro, Mexico City, Veracruz, Tuxtla Gutiérrez, and Mérida. The seven points of entry of the imports (m) were defined based on information from USITC (2023), and they are Ciudad Juárez, Nuevo Laredo, Port of Veracruz, Progreso, Nogales, Tijuana, and Manzanillo.

A spatial equilibrium model was formulated, which included variables of the chicken meat market. Considering d consumer regions and s production regions, the functions of supply and demand are:

$$P_d = \lambda_d + \omega_d Y_d$$

$$P_s = \upsilon_s + \kappa_s PRAB_s + \eta_s X_s$$

where P_d is the retail price of chicken meat in d, λ_d is the intercept of the demand function in d, w_d is the slope of the demand function in d, Y_d is the amount of chicken meat consumed in d, Ps is the chicken meat producer price in s, υ_s is the intercept of the supply function in s, η_s is the slope of the supply function in s, X_s is the amount of chicken meat produced in s, κ_s is the coefficient that relates the price of feed and the chicken meat producer price in s, and $PRABs$ is the real price of feed in s.

$$MaxNSP = \sum_{d=1}^{12}\left[\lambda_d Y_d + \frac{1}{2} w_d Y_d^2\right] - \sum_{s=1}^{12}\left[v_s + k_s PRAB_s + \frac{1}{2}\eta_s X_s^2\right] - \sum_{m=1}^{7}[P_m X_m] - \sum_{s=1}^{12}\sum_{d=1}^{12}[t_{sd} X_{sd}] - \sum_{m=1}^{7}\sum_{d=1}^{7}[t_{md} X_{md}]$$

The empirical formulation of the model was based on Takayama and Judge (1971). The target function of the model maximizes the Net Social Payoff (NSP), which is the area under the demand curve minus the area under the supply curve minus the value of imports and minus transportation costs. Considering s (s=1, 2, …, 12) chicken meat producing regions, d (d=1, 2, …, 12) consumer regions, and m (m=1, 2, …, 7) points of entry of the imports, the objective function is:

The target function is subject to the following restrictions:

$$\sum_{s=1}^{12}[X_{sd}] + \sum_{m=1}^{7} X_{md} \geq Y_d \tag{1}$$

$$\sum_{s=1}^{12} X_{sd} \leq X_s \tag{2}$$

$$\sum_{m=1}^{7} X_{md} \leq X_m \tag{3}$$

$$\sum_{s=1}^{12} X_s + \sum_{m=1}^{7} X_m = \sum_{j=1}^{12} Y_j \tag{4}$$

$$Y_d, X_s, X_{sd}, X_{md} \geq 0 \tag{5}$$

where P_m is the international price of chicken meat imported by m, X_m is the amount of chicken meat imported by m, t_{sd} is the cost of transporting one Mg of chicken meat from s to d, X_{sd} is the amount of chicken meat sent from s to d, t_{md} is the cost of transporting from m to d, and X_{md} is the amount of chicken meat sent from m to d.

Equation 1 establishes that the amount of chicken meat sent from the producing regions *s* to the consumer region *d* plus the amount of chicken meat sent from entry points *m* to consumer region *d* must be greater than or equal to the consumption in region *d*. Equation 2 establishes that the amount of chicken meat sent from producing region *s* to consumer regions *d* must be less than, or equal, to the amount of chicken meat produced in region *s*. Equation 3 establishes that the amount of chicken meat sent from entry points *m* to consumer regions *d* must be lower than, or equal, to the total amount of imported chicken meat. Equation 4 indicates the balance in the chicken meat market. Finally, Equation 5 establishes the conditions of non-negativity of the model.

The model was validated by comparing the base model estimates to observed data on production, consumption, imports, and retail prices. The base model must estimate values for the mentioned variables that are 10 % lower or higher than those observed in 2021. After obtaining the base model, three scenarios were tested, which included price increases of 20, 40, and 60 % for the balanced feed. Hypothetical increases in PRAB between 20 and 60% were used since, according to the OECD-FAO (2022), the international price of maize in 2021 was 50 % of the price expected in 2020. This increase was caused by a decrease in grain supply, an increase in demand, uncertainty caused by global trade policy, weather-related maize production in South America, an increase in production costs, and China's large volume of imports. Likewise, the nominal price of soybean increased by 40 % due to an increase in demand (mainly in China) and a slight reduction in the supply as a consequence of adverse weather conditions in South America that impacted their yield.

Information sources and analysis

The information used in the model corresponds to the period from January to December 2021. The functions of supply and demand were obtained using information on production, consumption, prices for the producer, retail price for the consumer, and demand price elasticities. The elasticities that relate chicken meat with the price of balanced feed were obtained from Nochebuena-Molina *et al*. (2023), and the price elasticity of the demand was obtained from Vázquez-Alvarado and Martínez-Damián (2015).

Chicken meat production data was obtained from the SIAP (2023), whereas the price of the balanced feed was obtained from the National Market Information and Integration System (SNIIM, 2023). The regional chicken meat consumption was obtained as follows: a) The national production of meat was added to the imports to obtain the National Apparent Consumption (NAC), without considering exports since they are very low; b) The NAC of chicken meat was used by the National Population Council (CONAPO, 2023) to obtain the national per capita consumption of chicken meat for 2021; c) The regional consumption of chicken meat was obtained by multiplying the national per capita consumption by the consumption of each state (CONAPO, 2023). The costs of transportation from producing regions and points of entry to the consumer regions were calculated using the software GlobalMap (2023), using the cities of reference mentioned earlier and the customs entry points for imports as origins and destinations.

The retail price to the consumers of the different regions was calculated using the price per Mg of chicken meat in the nearest entry point to the consumer region. Because the largest amount of imported chicken meat comes from the USA (83.86 %), the unit value of this product (USD per Mg) was used to obtain the price of a Mg of chicken meat at the different points of entry (USITC, 2023). The international price in USD was multiplied by the average 2021 exchange rate. The previous cost was added to the 2.7 % entry expenses if the chicken was brought into the country by land or 3.4 % if it entered by sea (García-Salazar and Williams, 2004), and the financial cost of importing the chicken using the average six-month LIBOR rate reported for 2021 by the Bank of Mexico (BANXICO, 2023).

The price for producers was calculated using the following procedure: a) The retail price for the consumer calculated earlier was taken; b) Using data on the retail price of chicken meat reported by the National Statistics and Geography Institute (INEGI, 2023) and the mean rural price paid to the chicken meat producer reported by the SIAP (2023), a margin was calculated between the price for the consumer and the price for the farmer; c) The retail price obtained for the consumer was discounted the previously mentioned percentage to obtain the estimated price to the producer. Given that the analysis carried out is for a specific year (2021), it was not necessary to calculate real prices; therefore, the prices for the consumer and the producer used in the model were nominal.

Chicken meat imports were obtained from official sources of the countries that exported this product to Mexico in 2021 (USITC, 2023; National Customs Directorate of Chile, 2023; ABPA, 2022). The solution of the model was obtained using the General Algebraic Modeling Systems programming language (GAMS Development Corporation, 2023).

RESULTS AND DISCUSSION

The observed values of the main variables of the chicken meat market in Mexico (Table 1) show that, in 2021, production, consumption, and imports were 3.7, 4.5, and 0.8 million Mg, respectively. The average retail price for the consumer was MXN 44 637 per Mg. Production was concentrated in six regions, representing 69 % of the country's production. In the case of consumption, three regions demand 52.3 % of chicken meat in Mexico. The results of the model validation (Table 1) showed that the difference between the data observed and the data estimated by the model is lower than ±10 %, so it is assumed that the base model can be used to generate scenarios.

Nationwide, the model overestimates consumption and production by 0.8 and 1.2 %, and underestimates imports and the retail price for the consumer by 0.8 and 4.7 %, respectively. The base model overestimates the consumption in the North, Center, and South regions by 0.7, 1.2, and 1.4 %. In production, the model underestimates

Table 1. Validation of the spatial equilibrium model of the gutted chicken meat market in Mexico for year 2021.

Region	Situation observed	Base model	Change	%
	Regional consumption (Mg)			
Northwest	264 047	266 511	2464	0.9
Baja California Peninsula	156 757	156 370	-387	-0.2
North	312 122	314 420	2298	0.7
Northeast and Center North	484 013	485 471	1458	0.3
Aguascalientes	50 505	51 007	502	1
West	322 744	326 435	3691	1.1
Bajío	387 041	389 896	2855	0.7
Querétaro	80 600	81 883	1283	1.6
Center	1 384 857	1 401 296	16 439	1.2
Gulf	388 768	386 304	-2464	-0.6
South	474 209	480 799	6590	1.4
Yucatan Peninsula	175 908	176 965	1057	0.6
National	4 481 573	4 517 357	35 784	0.8
	Regional production (Mg)			
Northwest	218 486	220 553	2067	0.9
Baja California Peninsula	1902	2052	150	7.9
North	370 984	355 909	-15 075	-4.1
Norheast and Center North	184 616	178 300	-6316	-3.4
Aguascalientes	405 465	434 736	29 271	7.2
West	431 779	436 209	4430	1.0
Bajío	289 376	301 511	12 135	4.2
Querétaro	371 332	405 268	33 936	9.1
Center	468 236	450 333	-17 903	-3.8
Gulf	481 954	472 422	-9532	-2.0
South	247 334	264 380	17 046	6.9
Yucatán Peninsula	197 087	189 381	-7706	-3.9
National	3 668 551	3 711 054	42 503	1.2
	Imports (Mg)			
National	813 022	806 305	-6717	-0.8
	Retail price (MXN per Mg)			
Northwest	58 291	55 959	-2332	-4.0
Baja California Peninsula	46 648	46 648	0	0.0
North	47 977	45 099	-2879	-6.0
Northeast and Center North	45 258	45 258	0	0.0
Aguascalientes	36 854	34 274	-2580	-7.0
West	45 707	41 136	-4571	-10.0
Bajío	42 465	39 493	-2972	-7.0
Querétaro	48 860	43 974	-4886	-10.0
Center	51 838	49 246	-2592	-5.0
Gulf	43 894	43 894	0	0.0
South	53 371	50 702	-2669	-5.0
Yucatán Peninsula	41 195	39 959	-1236	-3.0
Average	46 863	44 637	-2226	-4.8

the amount of this meat produced in the North and Center regions (4.1 and 3.8 %, respectively), whereas it overestimates it in the South (6.9 %). Regarding the retail price, the model underestimates it by 6, 5, and 5 %, respectively.

The scenario for a rise in the price of feed grains (maize and soybean) showed that a 20 % increase in the price of balanced feed would lead to a reduction in the production of chicken meat by 117 thousand Mg, which would represent a decrease of 3.2 % compared to the production of the base model, and the reduction would take place in all regions. Due to the commercial opening considered in the model, imports would experience a rise of 103 thousand Mg, which represents an increase of 12.8 % compared to the value estimated by the base model (Table 2).

Changes in production and imports would have an effect on consumption. Due to the increase in imports, which would compensate part of the decrease in production, the consumption of chicken meat would only decrease by 14 thousand Mg, distributed in 8 out of 12 regions considered, which represents a 0.3 % reduction in regard to the consumption estimated by the base model.

Increases of over 20 % in the price of feed grain would have greater effects on the chicken meat market. If the price of balanced feed were to increase by 60 %, the production of the meat in question would fall by 390 thousand Mg, which would represent a 10.5 % decrease in regard to the production of the base model. Imports, on the one hand, would increase by 363 thousand Mg. As a consequence of these changes, consumption would decrease by 27 thousand Mg, only 0.6 % less than the consumption estimated by the base model.

The results indicate a considerable effect on the production of chicken meat and a low effect on the consumption. This situation is a result of commercial liberalization established in trade agreements, which allows for the supply of consumption with imports when domestic production is declining. In fact, the change in price of balanced feed would have an effect on the retail price for consumers. In the first scenario, the retail price would display an increase of MXN 908.6 per Mg, which represents an increase in the retail price of 2 % compared to the price observed in the base model.

In light of an increase of the *PRAB* by 60 %, the amount of chicken meat produced nationwide would decrease by 10.5 %. This means that, should the *PRAB* increase, there would be a reduction in the production of chicken meat less than proportional to the increase in the *PRAB*. This result is consistent with those obtained by other authors (Rebollar-Rebollar *et al*., 2019a, 2019b; Ramírez-González *et al*., 2003). The strong dependence of livestock consumption on the inputs used in animal feed could pose significant risks for the future. As imports of forage grains account for a larger share of consumption, the market for these products becomes more vulnerable to exogenous changes taking place in the global market (Valencia-Romero *et al*., 2019; Moreno-Sáenz *et al*., 2016).

There are arguments to justify a probable increase in the international price of feed grains. The prices of cereals have displayed a volatile behavior due to the effects of the world supply chain caused by Covid-19, the Russia-Ukraine conflict, constant

Table 2. Effects of a rise in the price of feed grains on the chicken meat market in Mexico for year 2021 according to the spatial equilibrium model.

Region	Base model	Increase in price by:			Change by:		
		20 %	40 %	60 %	20 %	40 %	60 %
			Consumption (Mg)				
Northwest	266 511	265 501	264 808	264 628	-0.4	-0.6	-0.7
Baja California Peninsula	156 370	156 370	156 370	156 370	0.0	0.0	0.0
North	314 420	314 420	314 420	314 420	0.0	0.0	0.0
Northeast and Center North	485 471	485 471	485 471	485 471	0.0	0.0	0.0
Aguascalientes	51 007	50 703	50 494	50 406	-0.6	-1.0	-1.2
West	326 435	324 871	323 798	323 347	-0.5	-0.8	-0.9
Bajío	389 896	387 876	386 489	385 905	-0.5	-0.9	-1.0
Querétaro	81 883	81 517	81 265	81 159	-0.4	-0.8	-0.9
Center	1 401 296	1 395 328	1 391 229	1 389 506	-0.4	-0.7	-0.8
Gulf	386 304	386 304	386 304	386 304	0.0	0.0	0.0
South	480 799	478 809	477 443	476 868	-0.4	-0.7	-0.8
Yucatán Peninsula	176 965	176 014	176 014	176 014	-0.5	-0.5	-0.5
National	4 517 357	4 503 184	4 494 105	4 490 398	-0.3	-0.5	-0.6
			Production (Mg)				
Northwest	220 553	213 098	205 105	196 235	-3.4	-7.0	-11.0
Baja California Peninsula	2052	1972	1892	1812	-3.9	-7.8	-11.7
North	355 909	340 330	324 750	309 171	-4.4	-8.8	-13.1
Northeast and Center North	178 300	170 546	162 792	155 038	-4.3	-8.7	-13.0
Aguascalientes	434 736	424 928	412 858	397 913	-2.3	-5.0	-8.5
West	436 209	424 273	410 395	394 048	-2.7	-5.9	-9.7
Bajío	301 511	292 488	282 484	271 233	-2.9	-6.3	-10.0
Querétaro	405 268	394 661	382 493	368 337	-2.6	-5.6	-9.1
Center	450 333	434 819	418 005	399 540	-3.4	-7.2	-11.3
Gulf	472 422	457 228	440 454	421 671	-3.2	-6.8	-10.7
South	264 380	256 121	247 195	237 421	-3.1	-6.5	-10.2
Yucatán Peninsula	189 381	183 301	176 534	168 891	-3.2	-6.8	-10.8
National	3 711 054	3 593 765	3 464 957	3 321 310	-3.2	-6.6	-10.5
			Imports (Mg)				
National	806 305	909 420	1 029 145	1 169 087	12.8	27.6	45
			Retail price (MXN per Mg)				
Northwest	55 960	57 040	57 942	58 176	1.9	3.5	4.0
Baja California Peninsula	46 648	46 648	46 648	46 648	0.0	0.0	0.0
North	45 099	44 908	44 908	44 908	-0.4	-0.4	-0.4
Northeast and Center North	45 258	45 258	45 258	45 258	0.0	0.0	0.0
Aguascalientes	34 275	35 755	36 657	37 036	4.3	7.0	8.1
West	41 136	42 471	43 373	43 752	3.2	5.4	6.4
Bajío	39 493	40 879	41 781	42 160	3.5	5.8	6.8
Querétaro	43 974	45 290	46 192	46 571	3.0	5.0	5.9
Center	49 247	50 698	51 600	51 979	2.9	4.8	5.5
Gulf	43 894	44 035	44 035	44 035	0.3	0.3	0.3
South	50 703	52 230	53 132	53 511	3.0	4.8	5.5
Yucatán Peninsula	39 959	41 336	41 336	41 336	3.4	3.4	3.4
Average	44 637	45 546	46 072	46 281	2.0	3.2	3.7

change in yield, the increase in the costs of fertilizers and transportation, as well as a macroeconomic environment of high inflation (OECD-FAO, 2022). Due to uncertainty in South America in terms of maize production, the rise in production costs, and the large amount of maize imported by China, the OECD-FAO (2022) indicate that, in 2021, the international price of grain was 50 % higher than the previous year. These factors and the growing exposure to extreme weather phenomena, such as droughts and floods in producing countries, have caused a reduction in the price of maize, leading to volatility in international prices.

In the case of soybean, the OECD-FAO (2022) mention that, in 2021, there was an increase of over 40 % in the nominal price of this product, going from USD 406.64 per Mg in 2020 to USD 583.32 per Mg in 2021. The following factors may cause an increase in the international price of soybean for the following years: a) Extreme weather phenomena that affect the yield, a scenario already seen in 2021; b) Ukraine is an important soybean exporter; therefore, the conflict would reduce world supply, leading to a rise in the price of this legume.

There are arguments in favor of reducing the dependency on feed grain imports. The results of the programming model indicate that an increase in the price of balanced feed would have a negative effect on the chicken meat market, even in a scenario of trade liberalization. On the one hand, the production of chicken meat would decrease, which would have undesirable effects on its use in the agricultural industry, and, on the other hand, imports would increase, leading to an increase in the amount of foreign currency spent on purchases abroad.

Regarding the feed grain markets, there is a risk of a possible increase in the international price of maize. If this situation were to arise, a large amount of foreign currency would be spent to ensure the availability of maize in order to achieve food security (García-Salazar *et al*., 2023). The United Nations (UN, 2022) mentions that, if the world price of food imports was to increase, importing countries could face difficulties affording such a rise, which could lead to importing countries with fewer economic resources not being able to deal with the rise in international prices and seeing their access to imported food jeopardized.

The OECD-FAO (2022) and USDA (2022) forecast that maize and soybean prices will pick up the downward trend they had been presenting before the Covid-19 pandemic. Unpredictable events, such as the pandemic, the Russia-Ukraine conflict, and adverse weather phenomena that affect countries that produce these crops, would cause a reduction in their supply, which, combined with a growing demand, would generate a rise in international prices, as in 2021. According to data from the World Bank (2023), from 2020 to 2021, the international price of maize went from USD 169.02 to 237.24 per Mg in 2020, experiencing an increase of 40.4 %. Soybean went from an international price of USD 415.36 to 533.20 per Mg, which represented an increase of 28.4 %.

CONCLUSIONS

Since the implementation of the North American Free Trade Agreement (NAFTA), chicken meat has become a popular choice among Mexicans. The increase in production was due to a decrease in production costs, which was only made possible by the commercial liberalization agreed upon in NAFTA, which allowed the use of cheaper inputs in balanced feed mixes. The balanced feed has maize and soybean as its main inputs, which the country must import in large quantities to meet the demands of the livestock sector. Import growth has increased food dependency on maize and soybeans, making these markets more vulnerable to exogenous international changes.

In the time in which NAFTA has been effective, the supply of the consumption of feed grains used has been based on food dependence and has taken advantage of low international grain prices in the world market. However, this situation could be reverted in the future. The results of the programming model used in this investigation indicate that an increase of 60 % in the price of feed grain would have a considerable effect on production and imports. In a liberalized economy like the chicken meat market, the effect on consumption and retail prices would be less pronounced.

It is recommended that public policies be developed and implemented to encourage domestic maize and soybean production in order to reduce reliance on imports, thereby reducing the risk of exogenous changes in these crops, which could lead to an increase in the cost of chicken meat production. It is also recommended that public policies be designed and implemented to encourage more chicken meat production, such as those aimed at researching and developing genetic chicken varieties with better feed conversion.

REFERENCES

ABPA (Brazilian Association of Animal Protein). 2022. Annual report 2022. Sao Paulo, Brazil. 139 p.

BANXICO (Banco de México). 2023. Tasas de interés en los mercados internacionales (CI40). Ciudad de México, México. https://www.banxico.org.mx/SieInternet/consultarDirectorioInternetAction.do?accion=consultarCuadro&idCuadro=CI40&locale=es (Retrieved: March 2025).

Castro-Samano MA, García-Mata R, Parra-Insunza F, Portillo-Vásquez M, Márquez-Sánchez I, García-Sánchez RC. 2019. El mercado de la carne de bovino en México, considerados los factores externos. Agricultura, Sociedad y Desarrollo 16 (1): 85–103.

COMECARNE (Consejo Mexicano de la Carne). 2022. Compendio estadístico 2022. Ciudad de México, México. 106 p.

CONAFAB (Consejo Nacional de Fabricantes de Alimentos Balanceados y de la Nutrición Animal). 2022. La industria alimentaria animal de México 2022. Ciudad de México, México. https://www.conafab.org/informativos/anuario-estadistico (Retrieved: March 2025).

CONAPO (Consejo Nacional de Población). 2023. Proyecciones de la población de México y de las entidades federativas, 2016-2050. Gobierno de México. Consejo Nacional de Población. Ciudad de México, México. https://datos.gob.mx/busca/dataset/proyecciones-de-la-poblacion-de-mexico-y-de-las-entidades-federativas-2016-2050 (Retrieved: March 2025).

FAO (Food and Agriculture Organization). 2023a. FAOSTAT. Crops and livestock products. Food and Agriculture Organization. Rome, Italy. https://www.fao.org/faostat/es/#home (Retrieved: March 2025).

FAO (Food and Agriculture Organization). 2023b. FAOSTAT. Food balance sheets and trade indices. Food and Agriculture Organization. Rome, Italy. http://www.fao.org/faostat/en/#data (Retrieved: March 2025).

García-Salazar JA, Ramírez-Jaspeado R, Ávila-Soler E, Ramírez-Barraza BA. 2023. ¿Es posible disminuir la dependencia alimentaria de maíz en México? Revista Fitotecnia Mexicana 46 (3): 299–307.

García-Salazar JA, Willliams GW. 2004. Evaluación de la política comercial de México respecto al mercado de maíz. El Trimestre Económico 71 (281): 169–213.

GAMS Development Corporation. 2023. General Algebraic Modeling System (GAMS) Release 36.1.0. Fairfax, VA, USA.

GlobalMap. 2023. Rutas de autotransporter. Carreteras de México (versión gratuita). Ciudad de México, México. http://www.globalmap.mx/9.html (Retrieved: March 2025).

Hernández-Cruz R, García-Mata R, García-Salazar JA, Sagarnaga-Villegas LM, Mora-Flores JS. 2019. Rentabilidad de diez granjas porcícolas en 2018 de Tarimoro, Guanajuato, México. Agro Productividad 12 (6): 3–8. https://doi.org/ 10.32854/agrop.v0i0.1118

INEGI (Instituto Nacional de Estadística y Geografía). 2023. Sistema de cuentas nacionales de México. Consulta de precios promedio. Ciudad de México, México. https://www.inegi.org.mx/app/preciospromedio/?bs=18 (Retrieved: March 2025).

Moreno-Sáenz LI, González-Andrade S, Matus-Gardea JA. 2016. Dependencia de México a las importaciones de maíz en la era del TLCAN. Revista Mexicana de Ciencias Agrícolas 7 (1): 115–126.

National Customs Directorate of Chile. 2023. Exportación por país y código arancelario. Valparaíso, Chile. https://www.aduana.cl/exportacion-por-pais-y-codigo-arancelario/aduana/2018-12-14/101258.html (Retrieved: March 2025).

Nochebuena-Molina A, García-Salazar JA, González-Estrada E, López-Reyna MC. 2023. Determinantes de la oferta de carne de pollo en México de 1994 a 2021: Importancia del desarrollo tecnológico y el precio de los granos forrajeros. Acta Universitaria (33): 1–15. https://doi.org/10.15174/au.2023.3901

OECD (Organization for Economic Cooperation and Development). 2018. Exámenes de mercado en México. Estudio de caso del mercado de la carne de pollo. 141 p.

OECD-FAO (Organization for Economic Cooperation and Development - Food and Agriculture Organization). 2022. Perspectivas Agrícolas 2022-2031. OECD Publishing: Paris, France. https://doi.org/10.1787/820ef1bb-es

Ramírez-González A, García-Mata R, García-Delgado G, Matus-Gardea JA. 2003. Un modelo de ecuaciones simultáneas para el mercado de la carne de pollo en México, 1970-1998. Agrociencia 37 (1): 73–84.

Rebollar-Rebollar E, Rebollar-Rebollar A, Mondragón-Ancelmo J, Gómez-Tenorio G. 2019a. Oferta y demanda regional de carne de pollo en México, 1996-2016. Revista Mexicana de Ciencias Pecuarias 10 (4): 917–932. https://doi.org/10.22319/rmcp.v10i4.4839

Rebollar-Rebollar E, Rebollar Rebollar S, Guzmán Soria E. 2019b. Determinantes de la oferta de carne de pollo en México. Panorama Económico 27 (2): 336–348.

SIAP (Servicio de Información Agroalimentaria y Pesquera). 2023. Sistema de información agroalimentaria de consulta. Base de datos 2023. Gobierno de México, Servicio de

Información Agroalimentaria y Pesquera. Ciudad de México, México. https://www.gob.mx/siap/documentos/siacon-ng-161430 (Retrieved: March 2025).

SNIIM (Sistema Nacional de Información e Integración de Mercados). 2023. Mercados nacionales pecuarios, alimentos balanceados. Ciudad de México, México. http://www.economia-sniim.gob.mx/nuevo/Home.aspx?opcion=/SNIIM-Pecuarios-Nacionales/SelAli.asp (Retrieved: March 2025).

Takayama T, Judge GG. 1971. Spatial and temporal price and allocation models. North-Holland Publishing Company: Amsterdam, Netherlands. https://doi.org/10.1016/0038-0121(84)90002-8

UNA (Unión Nacional de Avicultores). 2022. Compendio de indicadores económicos del sector avícola. Ciudad de México, México. https://una.org.mx/indicadores-economicos/ (Retrieved: March 2025).

UN (United Nations). 2022. La inflación provocará que el coste de las importaciones de alimentos supere un récord mundial. November 11, 2022. https://news.un.org/es/story/2022/11/1516812 (Retrieved: March 2025).

USDA (United States Department of Agriculture). 2022. USDA agricultural projections to 2031. Washington, DC, USA. 106 pp.

USITC (United States International Trade Commission). 2023. Data web. U.S. trade and tariff. Washington, DC, USA. https://dataweb.usitc.gov/ (Retrieved: March 2025).

Valencia-Romero R, Sánchez-Bárcenas H, Robles-Ortiz D. 2019. Soberanía alimentaria de granos básicos en México: un enfoque de cointegración de Johansen a partir del TLCAN. Revista Análisis Económico 34 (87): 223–248.

Vázquez-Alvarado JMP, Martínez-Damián MA. 2015. Estimación empírica de elasticidades de oferta y demanda. Revista Mexicana de Ciencias Agrícolas 6 (5): 955–965.

World Bank. 2023. World commodity price data. Washington, DC, USA. https://www.worldbank.org/en/research/commodity-markets (Retrieved: March 2025).

Agrociencia

RISK FACTORS AND PROTECTION STRATEGIES IN SMALL AGRICULTURAL PRODUCTION UNITS IN THE STATES OF TABASCO, GUERRERO, AND CHIAPAS, MEXICO

Carlos A. **Quintero-Nieto**[1], J. Reyes **Altamirano-Cárdenas**[1*],
Enrique G. **Martínez-González**[1], Humberto **Vaquera-Huerta**[2]

[1]Universidad Autónoma Chapingo. Centro de Investigaciones Económicas, Sociales y Tecnológicas de la Agroindustria y la Agricultura Mundial. Carretera México-Texcoco km 38.5, Chapingo. State of Mexico, Mexico. Z. C. 56227.
[2]Colegio de Postgraduados Campus Montecillo. Postgrado en Estadística y Ciencia de Datos. Carretera México-Texcoco km 36.5, Montecillo, Texcoco, State of Mexico, Mexico. Z. C. 56264.
* Author for correspondence: jreyesa@ciestaam.edu.mx

ABSTRACT

There are currently multiple risks in Mexico's agricultural sector, so it is critical to have concise and accurate information on the main mitigating factors faced by producers in order to contribute to the creation of risk management instruments that meet their needs. In this work, the unit of analysis was established on the basis of a census of 6852 small farmers (those with less than five hectares of sown area). Using a stratified sampling of 317 producers in the states of Tabasco, Guerrero, and Chiapas, risk management was analyzed in their production units. The sampling, with a precision level of 5 % and a reliability of 95 %, allowed obtaining representative results for the target population. Through a descriptive analysis, the profile of the producers was identified, detecting the main risks they face and the strategies they use to mitigate them. Frequency graphs were used to visualize the distribution of the variables analyzed. To evaluate the relationship between risk management and risk perception, chi-square and Cramér's V contingency tests were applied. This study revealed a statistically significant relationship among 9 out of 13 risks analyzed and the risk management. In only six cases, the strength of association is moderate. This suggests that different tools exist to mitigate various hazards (natural disasters, pests and diseases, input prices, etc.), but their effectiveness varies by type. In the face of an adverse situation, producers often resort to strategies such as reducing food at home, using savings, and relying on government support. This study provides specific data on the specific conditions and challenges of these regions, enriching the general knowledge on family farming in Mexico.

Keywords: management, risk, perception, farmers.

Citation: Quintero-Nieto CA, Altamirano-Cárdenas JR, Martínez-González EG, Vaquera-Huerta H. 2025. Risk factors and protection strategies in small agricultural production units in the states of Tabasco, Guerrero, and Chiapas, Mexico. **Agrociencia** 59(3): 397-409. https://doi.org/ 10.47163/agrociencia.v59i3.3323

Editor in Chief:
Dr. Fernando C. Gómez Merino

Received: October 11, 2024.
Approved: January 15, 2025.
Published in Agrociencia:
March 27, 2025.

INTRODUCTION

Agriculture is a business with a high level of risk since all activities related to the production of any type of crop involve a high degree of uncertainty. Structural adjustments in economic matters, trade changes, and climatic anomalies, among other factors, affect producers directly or indirectly (Calatayud and Ketterer, 2016; Spiegel *et al*., 2021). In order to cope with all these risks, reduce vulnerability, and increase resilience, farmers tend to implement two risk management strategies: the ex-ante strategies that are used to reduce risk and mitigate any potential loss caused by any adverse factor to the production unit, and the ex-post coping strategies that are applied after suffering a loss as a result of a specific risk (Musyoki *et al.*, 2022).

Currently, policy makers have a strong interest in ensuring investments that encourage the implementation of actions capable of contributing to the generation of resilience, with the goal of making them more effective and targeted, particularly to the sectors that require them the most. Robust resilience measurement can make valuable contributions by identifying hotspots, understanding drivers, and inferring impact (Jones and d'Errico, 2019).

Producers' adaptation measures from the short to the long term are not limited to the resources available for agricultural production but also to how they understand and perceive the various risks, such as systemic risks (changes in government, product price, farm support, labor availability, and the presence of hydrometeorological phenomena), operational (soil fertility, bank credits or loans, and presence of diseases or pests), market (requirements for the sale of products, availability, and price of agricultural inputs), and the risk related to the life of the producers, such as health (Goodwin and Ker, 2002; Hardaker *et al*., 2015; Spiegel *et al*., 2021; Tapia-Díaz, 2006).

The uncertainty associated with these aspects can influence decision-making (Etongo *et al*., 2022) and, consequently, the risk management strategies that producers apply. The identification and perception of these risks are a key step for the development of effective and innovative management strategies. These strategies can range from the creation of public policies that generate certainty in agricultural activity to the modification of existing policies with a focus on protection, support, and consolidation of the various existing production units.

In the Mexican context, the problem of agricultural risks is more acute in the case of small producers, who represent a significant percentage of the sector and face specific conditions of vulnerability. Specifically, in the study area comprising the states of Guerrero, Chiapas, and Tabasco, these risks are intensified due to the prevalence of subsistence agriculture, the high dependence on staple crops such as corn (*Zea mays* L.) and beans (*Phaseolus vulgaris* L.), the limited productive infrastructure, and the presence of recurrent meteorological phenomena (CENAPRED, 2022; SIAP, 2023).

The situation is aggravated by the high degree of land fractionation in the region. According to the National Agricultural Census (INEGI, 2023), there are 4 629 134 active agricultural production units in Mexico. The states of Guerrero, Chiapas, and Tabasco account for 19.8 % of these units, but only 12.1 % of the planted area, resulting in a smaller scale of production (2.9 ha) compared to the national average (4.7 ha). In addition, these states present high poverty rates, exceeding 50 % of the population in each of them (CONEVAL, 2020a).

This study seeks to analyze the risk factors and protection strategies implemented by small producers in the aforementioned states in order to generate knowledge that may contribute to the design of public policies that promote their resilience and improve their living conditions. This study provides theoretical information on risk, resilience, aversion, types of risks and their sources, as well as the forms of risk management in small agricultural production units, in order to better understand the conditions and ways in which producers face the difficulties that may arise within their units.

MATERIALS AND METHODS

A survey was designed to analyze the different types of risk that a small farmer may suffer in the states of Tabasco, Guerrero, and Chiapas, Mexico. The approach is of mixed type, which implies a set of processes for collecting, analyzing, and linking quantitative and qualitative data in the same study, with the goal of solving the research problem (Sampieri *et al*., 2014).

Delimitation of the analysis unit

The unit of analysis was established based on the census of 6852 small producers registered in the ProBienestar program in the states of Tabasco (municipalities of Centla and Tenosique), Guerrero (municipalities of Cuajinicuilapa and Zapotitlán Tablas), and Chiapas (municipalities of Chiapilla and Nicolás Ruíz). According to the National Council for the Evaluation of Social Development Policy (CONEVAL, 2020b), the rural population of the selected municipalities presents high percentages of poverty. The municipality of Zapotitlán Tablas in the state of Guerrero has the highest poverty rate and is classified as very highly marginalized, according to the National Population Council (CONAPO, 2020). The main existent crop is rainfed corn (Table 1).

Table 1. Characteristics of the analysis unit by state and municipality (CONAPO, 2020; CONEVAL, 2020b).

State	Municipality	Rural population*	Rural population in poverty (%)*	Farmers**	Degree of marginalization*
Chiapas	Chiapilla	3128	83.13	282	High
	Nicolás Ruíz	n.d.	n.d.	503	High
Guerrero	Cuajinicuilapa	13 073	53.37	665	High
	Zapotitlán Tablas	12 414	91.37	3256	Very high
Tabasco	Centla	95 916	80.77	1025	Medium
	Tenosique	26 384	66.81	1121	Low

*Year 2020 information; **year 2021 information. n.a.: not available.

Sample determination and data collection

The sample size was determined using stratified sampling methodology with a precision of 5 % and reliability of 95 %. The producers' planting area was used as a stratification variable. This produced a base of 317 small producers distributed in three states and six municipalities: Chiapas: Chiapilla (n = 13) and Nicolás Ruíz (n = 23); Guerrero: Cuajinicuilapa (n = 31) and Zapotitlán Tablas (n = 151); and Tabasco: Centla (n = 47) and Tenosique (n = 52).

The information was collected through face-to-face surveys with randomly selected farmers from April 11 to June 30, 2022. The surveys were conducted after the pilot test information sessions at the Parametric Insurance Program for Small Corn Producers, implemented by AXA Climate, Guy Carpenter, Munich Re, Raincoat, and Swiss, in collaboration with the Ministry of Agriculture and Rural Development and AGROASEMEX. Producers who attended the different sessions were identified, randomly selected, and asked whether or not they could answer a simple questionnaire related to risk management in their production unit (translated in a more understandable way to producers as a questionnaire of problems that may affect them in their plot). The questionnaire consisted of four sections.

The first section of the survey analyzed the producer's profile (age, gender, and schooling); the second focused on characterizing the production unit (seniority within the activity, main crop, area planted, and number of members employed in the production unit); the third analyzed the main risk management strategies in their production unit (sale of animals, land, crop change, adjustment of planting dates, government support, etc.); and finally, the fourth section consisted of the different sources of risk and their perception of them (price of agricultural inputs, credit or bank loans, soil fertility, insecurity, etc.).

The first two sections included "open-ended" questions, and the third section presented dichotomous (yes and no) responses. The items comprising the risk perception section consisted of a series of Likert-type questions ("not at all challenging," "not very challenging," "slightly challenging," "neutral," "moderately challenging," "very challenging," and "extremely challenging").

Information analysis

The data on the producer's profile and the characteristics of the production unit were analyzed to obtain descriptive statistics (mean, standard deviation, maximum, minimum). The risk factors were analyzed by summing the individual values of the responses according to each item (absolute value on the Likert scale) and finally expressing them in percentages. The risk management strategies mentioned by the producers were coded using a binary system (Yes = 1, No = 0). Then, the frequency of each strategy was calculated, i.e., the number of producers who mentioned at least one or more options.

For the study of the association between risk perception and risk mitigation strategies, the chi-square test of independence was used, which compares the sample results with the expected results if the null hypothesis is true. The conclusion of the hypothesis test is based on how "close" the sample results are to the expected results (Anderson *et al*., 2008). The null and alternative hypotheses required to be tested were:

Null hypothesis (H_0) = Producers' perception of risk sources is not related to the risk management strategies they adopt.
Alternative hypothesis (H_1) = Producers' perception of sources of risk is related to the risk management strategies they adopt.
The following formula for chi-square was used:

$$x^2 = \sum_{i=1}^{R} \sum_{j=1}^{C} \frac{(O_{ij} - E_{ij})^2}{E_{ij}}$$

where x^2 is the chi-square statistic and O_{ij} is the frequency of the observed value of k number of categories. In order to simplify the analysis and obtain clearer conclusions, the number of risk perception categories was reduced from seven to three. For this purpose, the values obtained in each of the seven original categories were summed, and the results were reclassified into the following groups: a) the producer sees the different types of risks as challenging, b) the producer recognizes that challenging risk conditions exist, and c) the producer sees the different types of risks as very challenging. For the frequency of the expected value, $E_{ij} = \frac{R_i C_j}{n}$, R_j is the total number of rows, C_j is the total number of columns, and n is the total sample size.

Under the critical value method, the significance level was 5 %, $x^2 = x^2_{0.05}$ with (i - 1) (j - 1) degrees of freedom. Therefore, the null hypothesis is rejected when:

$$x^2 \geq x^2_{0.05}$$

If the chi-square results determine that there is an association between risk perception and the strategies implemented by producers, the index of association between variables will be measured. For this, the V of Cramér coefficient was used, which takes the value of one when there is a perfect association between attributes (risk perception and strategies), whatever the number of rows and columns in the contingency table analyzed (Shah and Alharthi, 2022). The strength of the association varies according to the value of V: it is weak if V < 0.2, moderate if 0.2 < V < 0.6, and strong if V > 0.6. The V of Cramér formula is:

$$V = \sqrt{\frac{x^2}{N(k-1)}}$$

where V is Cramér's V statistic, x^2 is the chi-square statistic, N is the total number of observations, and k is the minimum between the number of rows and columns.

Data were analyzed using the SPSS 24.0 software (IBM Statistics, Chicago, IL, USA).

RESULTS AND DISCUSSION

Socioeconomic profile

The survey covered 317 producers, of whom 32 % (111 producers) are women and 68 % (232 producers) are men. This composition reflects the participation of women in agriculture, which is significant in this sector, although there are still gender gaps. Regarding age and farming experience, the descriptive statistical analysis revealed a remarkable variability. Producers present different ages and therefore different degrees of experience within the agricultural activity. This diversity is an important aspect to consider when designing and evaluating public policies and support programs aimed at this sector. In contrast, the characteristics of the production units did not show significant variation (Table 2). This suggests that, in general, producers share similar conditions in terms of the size of their plots, the crops they produce, and the resources available.

Table 2. Characteristics of the small-producer population analyzed in the states of Tabasco, Guerrero, and Chiapas, Mexico.

Variables	Mean	SD	Minimum	Maximum
Age	49.52	15.35	18	95
Last degree of study	6.73	3.93	0	18
Agricultural experience	24.66	15.53	1	70
Area planted (hectares)	2.71	1.29	1	9
Family members	4.65	1.99	1	12

Risk factors

Agricultural activities are exposed to a wide variety of risk factors (Figure 1), which may or may not generate negative impacts on producers. Understanding these risks and the degree of challenge they pose for producers is essential to develop tools that provide certainty at all stages of agricultural production.

According to the data, hydrometeorological phenomena are the primary risks that producers face in their production units (Shah and Alharthi, 2022). According to the National Agricultural Survey (INEGI, 2017, 2019), a high percentage of producers reported crop or animal losses due to climatic events such as droughts (74.7 % in 2017 and 85.3 % in 2019), excess humidity, floods, and frost, among others, which coincides with what was reported by Tapia-Díaz (2006). This climate variability can trigger the development and spread of weeds, pests, and diseases, altering the balance in agroecosystems (FAO, 2024).

Therefore, understanding climate risks and vulnerabilities is fundamental to implementing more resilient production practices (Etongo *et al*., 2022). Failure to do so increases the risk of relying on the intensive use of agrochemicals, which can generate negative impacts on the environment and raise production costs.

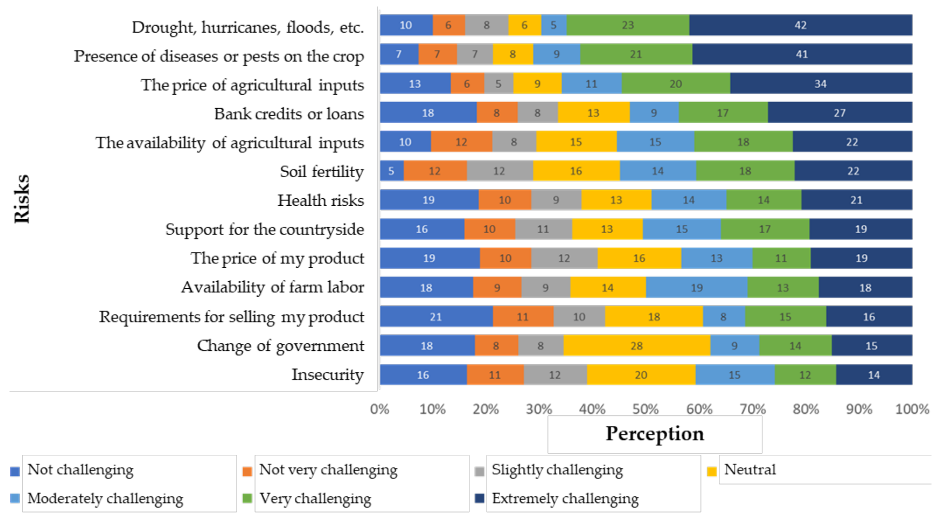

Figure 1. Perception of the different types of risk faced by producers in their production units in the states of Tabasco, Guerrero, and Chiapas, Mexico, using a Likert-type scale.

Strategies for risk

Facing any type of risk entails the implementation of various strategies and approaches, ranging from seeking or receiving direct support from government institutions to considering options such as selling assets or applying for credit. In order to better interpret the results, the different strategies were classified into four main groups: a) support strategies contracted by the producer, b) support strategies external to the producer, c) support strategies not foreseen by the producer, and d) support strategies involving the management of the production unit.

Ex-post strategies, such as those not foreseen by the producer, have a greater weight compared to the other strategies (Figure 2). This would indicate that the producer,

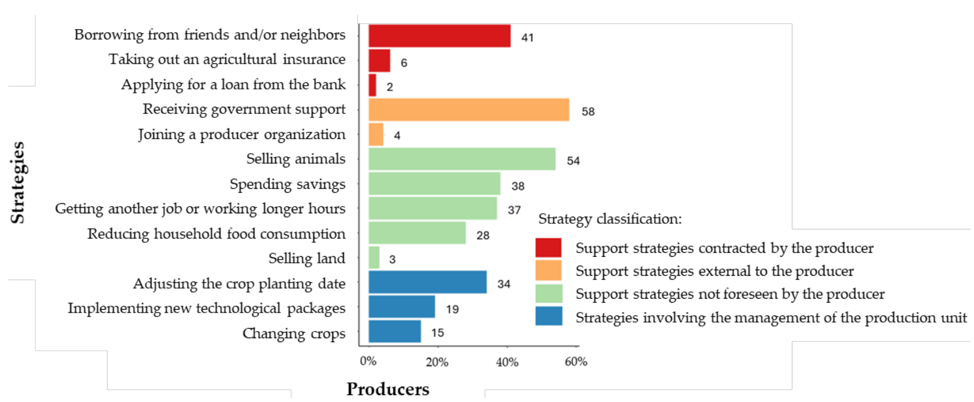

Figure 2. Strategies adopted by producers in the face of different types of risk in the states of Tabasco, Guerrero, and Chiapas, Mexico.

faced with a risk situation in his production unit, prefers, for example, to dispose of his current fixed assets or use his savings, which in the short term would mean the decapitalization of the producer. Support strategies not contracted by producers tend to be the least attractive options.

A crucial aspect that emerged from the survey was the direct opinion of the producers on government support. Although they pointed out that this support was of great help, they also stated that it was insufficient since it allowed them to return to their productive activities, but they could not recover all the investment generated in the management of the crop at the time of the loss. This is why they are considered in this research as secondary management options for external support to the producer.

Association between risk perception and risk mitigation strategies

Humans perceive risk and act upon it in two ways. The first is based on emotions, reflecting the instinctive and intuitive reactions of individuals to danger such as fear or anxiety that drive them to seek refuge (Slovic and Peters, 2006). The second is based on logical and reasoned analysis for the management of different types of risk. In their study, Wachinger *et al*. (2013) suggest that high risk perception may motivate producers to take personal protective measures. However, this possibility depends on various factors.

First, memory of past events and the ability to imagine the potential effects of a natural disaster are crucial to risk perception. If producers have not directly experienced a disaster or cannot visualize its consequences, they are less likely to take preventive measures. In addition, confidence in the receipt of government support can create a dynamic in which farmers are disincentivized to take precautions in the face of impending risks. If they perceive that the government will cover their losses, the need to invest in protective measures or modify their farming practices to minimize risk becomes less pressing (González-Estrada and Orrantia-Bustos, 2006). This situation can result in lower productivity and competitiveness for the sector. Furthermore, not all of the strategies that producers can take coincide with their perception of them (Table 3).

Since the X^2 calculated for the variables of contracting agricultural insurance, receiving government support, selling animals, spending savings, getting another job or working more hours, reducing household food consumption, adjusting planting dates, implementing new technological packages, and changing crops is greater or equal in at least one of the four risk categories with a significance of $X^2_{0.05} = 5.99$, it is inferred that there is a significant difference between the expected values under the null hypothesis and the observed values. Consequently, producers' perception of the different types of risk related to their production unit is associated with their choice to adopt any of the nine risk management strategies (Osiemo *et al*., 2021). The use of strategies such as applying for loans, accessing credit, joining organizations, or selling their land was not considered by producers as a viable management option. However, despite this perception, these alternatives should not be less important.

Table 3. Chi-square tests for the relationship between strategies against risks and different types of risk perceived by small producers in the states of Tabasco, Guerrero, and Chiapas, Mexico.

Strategy	Risks			
	Systemic	Market	Operatives	Producer
Borrowing from friends and/or neighbors	4.88	3.62	3.32	4.52
Taking out agricultural insurance	10.80*	8.62*	3.78	12.57*
Applying for a loan from the bank	1.14	1.61	1.88	3.49
Receiving government support	13.96*	19.17*	14.60*	0.22
Joining a producer organization	2.45	1.83	4.15	4.38
Selling animals	6.30*	8.28*	6.59*	2.65
Spending savings	24.78*	20.92*	6.97*	6.50*
Getting another job or working longer hours	5.13	21.39*	10.42*	1.85
Reducing food consumption at home	22.85*	35.53*	23.95*	23.44*
Selling land	2.20	1.12	0.79	1.04
Adjusting the crop planting date	2.26	6.36*	2.53	14.93*
Implementing new technological packages	10.61*	13.44*	10.87*	19.35*
Changing crops	0.01	6.35*	2.91	1.54

*$x^2 \geq x^2_{0.05}$ significant.

The association index between the perception of different types of risk and their decisions to opt for a risk management strategy (Table 4) is moderate ($0.2 < V < 0.6$) for six of the nine risk management strategies. The absence of a strong association may be due to the socioeconomic characteristics of the farmers analyzed and the alternatives

Table 4. Association between risk perception and mitigation strategies in the states of Tabasco, Guerrero, and Chiapas, Mexico, with Cramér's V.

Strategy	Risks			
	Sistemic	Market	Operatives	Farmer
Borrowing from friends and/or neighbors	0.122	0.105	0.100	0.117
Taking out agricultural insurance	0.181	0.162	0.107	0.195
Applying for a loan from the bank	0.059	0.070	0.075	0.103
Receiving government support	0.206	0.241	0.210	0.026
Joining a producer organization	0.086	0.074	0.112	0.115
Selling animals	0.138	0.158	0.141	0.090
Spending savings	0.274	0.252	0.145	0.140
Getting another job or working longer hours	0.125	0.255	0.178	0.075
Reducing food consumption at home	0.263	0.328	0.269	0.267
Selling land	0.082	0.058	0.049	0.056
Adjusting the crop planting date	0.083	0.139	0.088	0.213
Implementing new technological packages	0.179	0.202	0.182	0.242
Changing crops	0.007	0.139	0.094	0.068

they may or may not apply in their production unit (Shah and Alharthi, 2022b). Smallholders choose various alternatives to cope with the risks and challenges they face in their farming activity. These decisions are influenced by their risk aversion, their perception of uncertainty, and their search for strategies to ensure the economic and food security of their families.

Austerity measures such as reducing household food consumption to conserve resources and face the financial crisis, together with the use of previously accumulated savings, which can serve as a financial cushion in times of scarcity or production losses, as well as the search for employment outside the production unit to supplement monthly income, are risk management strategies not foreseen by the producer. Government programs such as subsidies, technical assistance, or subsidized agricultural insurance can be a source of support for small producers in times of difficulty. These public policies are aligned with the National Development Plan (PND), published in the Official Gazette of the Federation on July 12, 2019 (DOF, 2019), which establishes that the main objective is to achieve the well-being of the population. Likewise, it establishes three general axes: I. policy and government, II. social policy, and III. economy. The final axis mentions a strategy of food self-sufficiency and countryside rescue in order to achieve this in basic foods consumed by the population, as well as most of the inputs, machinery, equipment, and fuel for agriculture with the consideration for sustainability, equity, welfare, and respect for the rights of *ejidatarios*, commoners, small landowners, and indigenous peoples.

A notable example is the Production for Well-Being program, whose objective is to channel productive support per hectare prior to planting. This program promotes the adoption of agroecological and sustainable practices, soil, water, and agrodiversity conservation. Another important initiative is the Fertilizers for Well-being program, whose objective is to contribute to the production of priority crops through the delivery of fertilizers to producers throughout the country. This program seeks to ensure the availability of essential inputs for agricultural production, especially for small producers who face difficulties in accessing these inputs on the market.

In addition to programs focused on production and sustainability, the Mexican government has also implemented specific programs to address natural disasters. A historical example was the Agricultural Disaster Assistance Component of the Ministry of Agriculture, Livestock, Fisheries, and Food (SAGARPA), which aimed to support small producers who did not have insurance to protect themselves in case of catastrophic natural events through the delivery of ex-post financial support (Cabestany-Noriega *et al*., 2013). The second program was the Agricultural Insurance Premium Subsidy program granted by the Ministry of Finance and Public Credit (SHCP) and operated by AGROASEMEX, which supported agricultural insurance funds with a percentage of the payment of the insurance premium contracted by producers. Both programs, implemented until 2019 and 2020, respectively, were two of the best-executed producer support strategies by the Mexican government and have even been replicated by other countries.

Finally, the strategies that producers opt for directly within their production unit include the change in crop planting date and the implementation of new technological packages. These have been some of the options that go hand in hand with the implementation of programs and public policies that help generate greater certainty for producers.

CONCLUSIONS

The risk perception of small-scale producers directly influences the selection of adaptation strategies. The results indicate that, in the face of risk, producers especially value government support. Likewise, the importance given to savings strategies and the search for additional income is evidence of the precariousness of their economic conditions and the need to diversify their sources of income. In addition, it became evident that the reduction of household food consumption plays a crucial role in adapting to adverse conditions. Similarly, adjustments in agricultural practices, such as changing planting dates and adopting new technologies, demonstrate a willingness to innovate and adapt to the new climatic conditions.

These findings highlight the importance of designing interventions that address both the immediate needs of producers (such as economic support services, although necessary, should promote producers' independence and avoid creating dependency) and their long-term adaptive capacities (encouraging the adoption of new technologies). These short- and long-term interventions identified in this study seek to strengthen the resilience of producers in the face of adverse conditions.

ACKNOWLEDGEMENTS

The authors are grateful for the support provided by the Chapingo Autonomous University, AGROASEMEX, S. A. and Guy Carpenter México Intermediario de Reaseguro S.A. de C.V. under project 3147 UACH-GP- AGROASEMEX/22 with agreement number 037-2022.

REFERENCES

Anderson DR, Sweeney DJ, Williams TA. 2008. Estadística para administración y economía (10a. edición). Cengage Learning: Ciudad de México, México. 1056 p.

Cabestany-Noriega J, Hernández-Hernández E, Celaya-del Toro V. 2013. La gestión de riesgos climáticos catastróficos para el sector agropecuario en México: caso del componente para la atención a desastres naturales para el sector agropecuario. Organización de las Naciones Unidas para la Alimentación y la Agricultura Secretaría de Agricultura, Ganadería, Desarrollo Rural, Pesca y Alimentación. Ciudad de México, México. 81 p.

Calatayud A, Ketterer JA. 2016. Gestión integral de riesgos para cadenas de valor. IDB: Washington, DC, USA. http://www.iadb.org (Retrieved: February 2025).

CENAPRED (Centro Nacional de Prevención de Desastres). 2022. Atlas nacional de riesgos. Gobierno de México. Centro Nacional de Prevención de Desastres. Ciudad de México,

México. http://www.atlasnacionalderiesgos.gob.mx/archivo/visualizacion-datos.html (Retrieved: February 2025).

CONAPO (Consejo Nacional de Población). 2020. Índices de marginación 2020. Gobierno de México. Consejo Nacional de Población. Ciudad de México, México. https://www.gob.mx/conapo/documentos/indices-de-marginacion-2020-284372 (Retrieved: February 2025).

CONEVAL (Consejo Nacional de Evaluación de la Política de Desarrollo Social). 2020a. Pobreza a nivel municipio 2010-2020. Medición de la pobreza. Ciudad de México, México. https://www.coneval.org.mx/Medicion/Paginas/Pobreza-municipio-2010-2020.aspx (Retrieved: February 2025).

CONEVAL (Consejo Nacional de Evaluación de la Política de Desarrollo Social). 2020b. Pobreza a nivel municipio 2010-2020. Medición de la pobreza. Ciudad de México, México. https://www.coneval.org.mx/Medicion/Paginas/Pobreza-municipio-2010-2020.aspx (Retrieved: February 2025).

DOF (Diario Oficial de la Nación). 2019. Plan nacional de desarrollo 2019-2024. Gobierno de México. Presidencia de la República. Ciudad de México, México. http://www.dof.gob.mx/nota_detalle.php?codigo=5565599&fecha=12/07/2019 (Retrieved: February 2025).

Etongo D, Bandara A, Murugaiyan A, Bristol U, Nancy K, Petrousse B, Sinon S. 2022. Risk perceptions, vulnerability and adaptation to climate change at farm level across four agricultural zones in Seychelles. World Development Sustainability 1: 100025. https://doi.org/10.1016/J.WDS.2022.100025

FAO (Food and Agriculture Organization of the United Nations). 2024. El cambio climático, las plagas y las enfermedades transfronterizas. Rome, Italy. 2 p.

González-Estrada A, Orrantia-Bustos M. 2006. Los subsidios agrícolas de México. Agricultura Técnica en México 32 (3): 323–331.

Goodwin BK, Ker AP. 2002. Modeling price and yield risk. *In* Just RE, Pope RD. (eds.), A Comprehensive Assessment of the Role of Risk in U.S. Agriculture. Springer: Boston, MA, USA, pp: 289–325. https://doi.org/10.1007/978-1-4757-3583-3_14

Hardaker JB, Lien G, Anderson JR, Huirne BMR. 2015. Coping with risk in agriculture: Applied decision analysis (Third edition). CABI: Wallingford, UK. https://doi.org/10.1079/9780851998312.0000

INEGI (Instituto Nacional de Estadística y Geografía). 2017. Encuesta nacional agropecuaria (ENA) 2017. Ciudad de México, México. https://www.inegi.org.mx/programas/ena/2017/ (Retrieved: February 2025).

INEGI (Instituto Nacional de Estadística y Geografía). 2019. Encuesta nacional agropecuaria (ENA) 2019. Ciudad de México, México. https://www.inegi.org.mx/programas/ena/2019/ (Retrieved: February 2025).

INEGI (Instituto Nacional de Estadística y Geografía). 2023. Censo agropecuario (CA) 2022. Ciudad de México, México. https://www.inegi.org.mx/programas/cagf/2022/#Documentacion (Retrieved: February 2025).

Jones L, d'Errico M. 2019. Whose resilience matters? Like-for-like comparison of objective and subjective evaluations of resilience. World Development 124: 104632. https://doi.org/10.1016/j.worlddev.2019.104632

Musyoki ME, Busienei JR, Gathiaka JK, Karuku GN. 2022. Linking farmers' risk attitudes, livelihood diversification and adoption of climate smart agriculture technologies in the Nyando basin, South-Western Kenya. Heliyon 8 (4): e09305. https://doi.org/10.1016/j.heliyon.2022.e09305

Osiemo J, Ruben R, Girvetz E. 2021. Farmer perceptions of agricultural risks; which risk attributes matter most for men and women. Sustainability 13 (23): 12978. https://doi.org/10.3390/su132312978

Sampieri R, Collado C, Lucio M. 2014. Metodología de la investigación (Sexta edición). McGrawHill: Ciudad de México, México. 600 p.

Shah J, Alharthi M. 2022a. The association between farmers' psychological factors and their choice to adopt risk management strategies: The case of Pakistan. Agriculture 12 (3): 412. https://doi.org/10.3390/agriculture12030412

SIAP (Servicio de Información Agroalimentaria y Pesquera). 2023. Estadística de producción agrícola. Gobierno de México. Secretaría de Agricultura y Desarrollo Rural. Servicio de Información Agroalimentaria y Pesquera. Ciudad de México, México. https://www.gob.mx/siap/acciones-y-programas/produccion-agricola-33119 (Retrieved: February 2025).

Slovic P, Peters E. 2006. Risk perception and affect. Current Directions in Psychological Science 15 (6): 322–325. https://doi.org/10.1111/j.1467-8721.2006.00461.x

Spiegel A, Slijper T, de Mey Y, Meuwissen MPM, Poortvliet PM, Rommel J, Hansson H, Vigani M, Soriano B, Wauters E, *et al*. 2021. Resilience capacities as perceived by European farmers. Agricultural Systems 193: 103224. https://doi.org/10.1016/j.agsy.2021.103224

Tapia-Díaz E. 2006. El seguro agropecuario en México: experiencias recientes. Comisión Económica para América Latina y el Caribe. Ciudad de México, México. https://repositorio.cepal.org/handle/11362/4985 (Retrieved: February 2025).

Wachinger G, Renn O, Begg C, Kuhlicke C. 2013. The risk perception paradox—implications for governance and communication of natural hazards. Risk Analysis 33 (6): 1049–1065. https://doi.org/10.1111/j.1539-6924.2012.01942.x

Agrociencia

CHARACTERISTICS, RISKS, AND REVALUATION OF THE VALUE NETWORKS OF AN AGRICULTURAL LAND

Zaira Sarahi **Sánchez-Sánchez**[1], Jorge **Cadena-Iñiguez**[1*], Victor Manuel **Ruiz-Vera**[1], Victor Manuel **Cisneros-Solano**[2], Francisco Javier **Morales-Flores**[2], Ernesto **Peredo-Rivera**[1], Brenda I. **Trejo-Téllez**[1]

[1]Colegio de Posgraduados Campus San Luis Potosí. Posgrado en Innovación en Manejo de Recursos Naturales. Iturbide 73, Salinas de Hidalgo, S.L.P., México. C.P. 78600.
[2]Universidad Autónoma Chapingo. Centro Regional Universitario Oriente. Carretera Federal Huatusco-Xalapa Km. 6.5, Huatusco, Veracruz, México. C.P. 94100.
* Author for correspondence: jocadena@gmail.com

ABSTRACT

Several crops generate local employment and drive the economy in the High Mountain Region (RAM: Región Altas Montañas) of Veracruz. However, changes in sale price, oversupply, natural disasters, new pests, and scarce or lack of training regarding agricultural activities can lead producers to the abandonment of crops, unemployment, and migration. Consequently, identifying the type of value networks and risks and developing revaluation proposals is fundamental to foster the consolidation and permanence of products, both in domestic and international markets. Surveys —based on socioeconomic, environmental, commercial, and technological variables, as well as on the integration of links from internal logistics— were applied to crop (n=15) producers (n=131). The RStudio v. 4.3.3 software was used for the analysis. Six types of value networks were identified; none of them fell into a single classification type (primary, emergent, or potential). The percentage of the distinctive features indicated that the networks were dynamic and that their common features establish them as mixed and evolving. To facilitate their study, risks were classified per social segments. The products of the network have an accumulated dependency on the domestic, local, regional, and Mexico City (CDMX) markets (86%). Only chayote and banana leaves are exported. Chayote is included in the six value networks and has the highest consolidation level as primary network. The explained cumulative variance (73.95%) is divided into four main components. It frequently includes technical support, unauthorized agrochemicals, and raw manure. In order to consolidate the networks, risky activities that limit the dynamics and evolution of crops should be taken into account.

Keywords: raw materials, self-consumption, agroindustry, sustainability, agriculture.

INTRODUCCIÓN

Agriculture is an activity that gathers rural producers (INEGI, 2023), who grow crops, provide raw material to the agroindustry, and generate local and self-employment

Citation: Sánchez-Sánchez ZS, Cadena-Iñiguez J, Ruiz-Vera VM, Cisneros-Solano VM, Morales-Flores FJ, Peredo-Rivera E, Trejo-Téllez BI. 2025. Characteristics, risks, and revaluation of the value networks of an agricultural land.
Agrociencia 59(3): 410-427.
https://doi.org/ 10.47163/agrociencia.v59i3.3336

Editor in Chief:
Dr. Fernando C. Gómez Merino

Received: October 29, 2024.
Approved: April 10, 2025.
Published in Agrociencia:
May 06, 2025.

(SIAP, 2022). In Mexico, Veracruz is an agricultural region with annual and perennial crops (Almaraz-Vidal, 2016; INEGI, 2023; SIAP, 2022) and is divided into ten strategic regions. One of these regions is the High Mountain Region (RAM), 48% of whose area is used for agricultural activities (INEGI, 2023; Rivera-Hernández, 2018; SIAP, 2022). In RAM, exportations generate income to producers. Crops such as chayote (Sechium edule (Jacq.) Sw.), coffee (Coffea arabica L.), and sugarcane (Saccharum spp.) provide raw materials to the agroindustry (Bada Carbajal *et al*., 2010). Other regional producers grow crops as food for the rural population and their produce is sold locally (Beltrán-Morales, 2022). Their activities are not structured and their operations are not consolidated (Gómez-Núñez *et al*., 2019; INEGI, 2024b; SIAP, 2022). The value networks of agricultural activities include the following characteristics: field production, packaging (Sánchez-Galván *et al*., 2020), and technical support in areas such as phytosanitary control, nutrition, waste management, shelf life, food safety, transfer of business, marketing, and sales (Rosa and de Paredes, 2017). However, the structure and operation of some crops have not reached the same maturity level (Vargas-Canales *et al*., 2020) and, consequently, not all of them can be classified as primary or consolidated value networks. Although value networks in agricultural areas are not highly consolidated, they play a major role in food security (Urquía-Fernández, 2014), trade, input supply, and local employment (Sánchez-Sánchez *et al*., 2023).

In order to produce or promote additional economic development poles in the region, the emergent or potential value networks should be revaluated or reorientated through the improvement of technology aimed to guarantee their socio-economic consolidation, competitiveness, and permanence (Torre, 2020). These proposals would help certain local or ancestral products to reach domestic and international markets (Cañarte *et al*., 2021). This objective can be reached through the identification of limitations, the level of adoption of local practices, and the compliance with the quality and safety regulations and standards demanded by international markets (Carenzo, 2007).

Consequently, the types of value networks, their structural and operational levels, and their socio-economic, environmental, technological, trade, and public health risks, as well as their integration of internal logistics must be identified (Singh *et al*., 2018).

Therefore, primary, emergent, and potential value networks of crops in the High Mountain Region of Veracruz were identified and characterized. The objective was to determine the limitations and advantages in order to propose a revaluation and consolidation. These findings will help to predict or avoid failures in the region, caused by unemployment, migration, and oversupply. In addition, they would help producers to achieve long-term sustainability for their crops.

MATERIALS AND METHODS

Study Area

The following municipalities of Veracruz were included as agricultural areas: Alpatláhuac, Calcahualco, Coscomatepec, Fortín, Huatusco, and Ixhuatlán del Café

(Figure 1) They are located from 19° 07″ to 18° 58′ 39″ N and from 97° 06″ to 96° 57′ 25″ W, at 987-1,860 m.a.s.l. The weather of the area is mainly humid, semi-warm, and temperate (INEGI, 2000, 2024a).

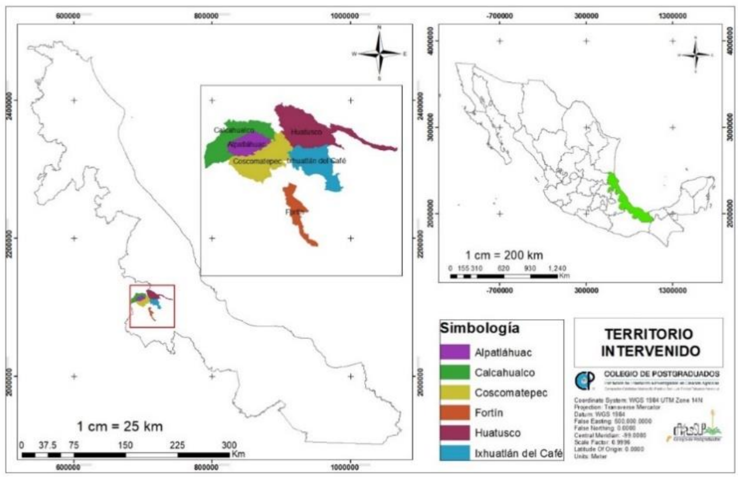

Figure 1. Location of the municipalities included in the study area of the High Mountain Region, Veracruz. Figure developed by Mayra Aragón Magadán, based on the layers of CONABIO (2024).

The crops identified in the study area included: avocado (*Persea americana*), coffee (*Coffea arabica*), zucchini (*Cucurbita pepo* L.), sugarcane (*Saccharum* spp.), chayote (*Sechium edule*), chilacayote (*Cucurbita ficifolia*), manzano pepper (*Capsicum pubescens*), prune plum (*Prunus domestica*), peach (*Prunus persica* L.), tomato (*Solanum lycopersicum L.),* prickly pear *(Opuntia ficus-indica),* potato *(Solanum tuberosum* L.*), pear (Pyrus communis*), tomatillo (*Physalis philadelphica*), and banana leaf (*Musa acuminata*).

Research Method

The study was conducted through a structured survey, that included questions about social, economic, technical, environmental, biosafety, trade, and risk issues. In order to determine the size of the sample, producers from the RAM were identified, based on the data available for 2019, 2021, and 2022, from the Programa para el Bienestar "Corte a junio 2022, beneficiarios del Programa Producción para el Bienestar 2022" (SADER, 2022) and the *Anuario Estadístico de la Producción Agrícola* (SIAP, 2022). The Brenlla-Martínez (1997) formula was applied to the universe of producers (N= 1,131). This author suggested that a >107 >145 sample size provides a 97% confidence level.

The operation and structure of value networks poses several risks. Meanwhile, their impact can be related to factors such as public health (authorized agrochemicals, use of manure), environment (agrochemical application, water, soil), socio-economic (job offer/lack of) and technological (lack of training) issues. These factors also include trade (oversupply/missing products), maintenance —as a consequence of the displacement of local genetic resources by other highly-successful commercial resources—, and, finally, generational change for each crop and network (Table 1). Table 2 and 3 shows the activities that set primary (consolidated), emergent, and potential value networks apart (Sánchez-Sánchez *et al*., 2023; Porter, 1985).

In order to identify the consolidation level of the regional value networks, acceptance criteria and acceptable ranges, based on the percentage value, were adopted from Porter (1985) and Sánchez-Sánchez *et al.* (2023). Since a consolidated primary network must have evolved from a potential and emergent value network (3), the percentage of primary, emergent, and potential characteristics was codified to determine the status and level of the features that are mixed in or define a network.

In order to understand the acceptance criteria and the acceptable ranges of the characteristics that define agricultural value networks, a location triangle was developed. The percentages of the networks are drawn with different colors: orange for the emergent-potential-mixed value network, purple for the primary-mixed value network, and green for the primary value network (Figure 2).

A breakdown of the answers was structured to confirm the level of each network, based on their activities (Table 4).

Table 1. Study variables included in the survey to identify the value networks of crops.

Variable	Description
Social	Land ownership, cultivation, surface area, irrigation, rainfed, technical assistance. Rural stakeholders: age, gender, education, economic activity.
Economic	Local employment (number and gender, week, month, year). New crop pests.
Environmental	Type of agrochemicals, fertilizers, organic and biological inputs, biosecurity: use of raw or composted manure.
Commercial	Markets (local, regional, national, and export). Direct sales, local or national intermediary, central supply center, or self-service stores. Product presentation (fruit, packaging: box, with or without refrigeration). Product destination: local, regional, national, or export. National or international certification (field and packaging).
Technological	Agronomic, nutritional, and sanitary management, harvesting, and post-harvest. Monoculture, associated, extensive (≥1.0 ha), backyard.
Integration of links in the internal logistics of the value chain	Producers, suppliers in general, collectors, distribution (local, regional, national, and export), consumers, processors.

Table 2. Activities that distinguish the value networks adapted from Porter (1985) and Sánchez-Sánchez *et al.* (2023).

Value network	Criterios de definición	Rango de aceptación
Primary mixed	40%Prim-33%Emer-27%Pote	45%-35-%Prim-38%-28%Emer-32%-22%Pote
Emerging mixed	28%Prim-39%Emer-33%Pote	28-26% Prim-39%Emer-33%Pote
Potentially emerging mixed	21%Prim-45%Emer-34%Pote	25%-16%Prim-50%-40%Emer-39%-19%Pote
Primary prevalence	50%Prim-30%Emer-20%Pote	55%-45% Prim-35%-24%Emer-25%-15%Pote
Transition to primary	65%Prim-25%Emer-10Pote	69%-59%Prim-26%-23%Emer-15%-12%Pote
Primary	75%Prim-18%Emer-7%Pote	80%-70%Prim-22%-13%Emer-11%-1%Pote

Table 3. Agricultural value networks, acceptable ranges, and acceptance criteria.

Activities	Primary network	Emerging network	Potential network
Operations Product Presentation	Product packaged under refrigeration	Bulk product	Packaged and unrefrigerated product
Marketing and Sales Sales requirements	The producer has a certificate that guarantees good food safety practices	The producer does not have a certificate that endorses good practices and does not deliver product selected and packaged according to quality.	The producer delivers product selected and packaged according to quality

Source: Table developed by the authors.

Statistical Analysis

The data obtained from the surveys were systematized and codified using Google Forms and Excel, respectively. The codification integrated dichotomous, polytomous, ordinal, and continuous qualitative variables. Subsequently, the RStudio v.4.3.3 software, with a similarity matrix based on Gower's distance (Palacio *et al*., 2020), was used for the cluster analysis. The fviz_nbclust function of the factoextra package was used to determine the optimal number of the cluster. Once the number of clusters was determined, Ward's method was used to develop a scatter plot and to determine the cluster groups. Afterwards, Excel was used to identify the networks, taking into account the acceptable ranges and the acceptance criteria (Table 3). The risks of the networks were established using the distinctive features of each network (Table 2) and Statistics. Finally, the revaluation proposal was developed through an analysis of their main elements.

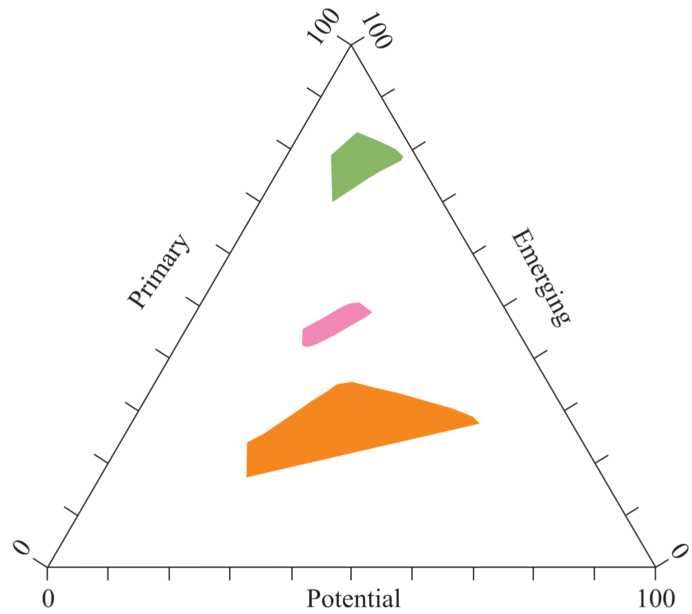

Figure 2. Location triangle of an agricultural value network, based on the percentage obtained from the acceptable ranges and acceptance criteria.

Table 4. Breakdown of the answers based on the characteristics of the crop value networks.

Feature Name	Value network	Feature component
Activity	Primary	Grow, Sell, and Store
	Emerging	Grow and Buy
	Potential	Grow, Sell, and Distribute
Crops	Primary	Coffee, sugarcane, and chayote
	Emerging	Zucchini, wax pepper, plum, tomato, peach, potato, pear, chilacayote, and nopal (vegetables)
	Potential	Tomato, avocado, banana leaf, or velillo
	Primary Potential	No crops grown during dry weather
JanEmp, FebEmp, MarEmp, AprEmp, MayEmp, JunEmp, JulEmp, AugEmp, SeptEmp, OctEmp, NovEmp, DecEmp	Emerging	Year-round employment generation
	Potential	Job creation for 3 to 6 months of the year
	Potential	Year-round employment generation
Leave Someone	Primary	I've already solved it
	Emerging	I haven't thought about it
	Potential	I haven't solved it
ATReceives	Primary	I frequently receive technical support
	Emerging	I rarely receive technical assistance
	Potential	I rarely receive technical assistance
New Plague	Primary	There are many new pests
	Emerging	New pests are present
	Potential	There are no pests

Table 4. Continued.

Feature Name	Value network	Feature component
I apply	Primary Emerging Potential	Permitted agrochemicals or composted manure; Unregulated agrochemicals or Raw manure
Use equipment	Primary Emerging Potential	No application I use it every time I rarely use it
DeliveryWho	Primary Emerging Potential	I don't use it I sell it to a distributor I sell it on the lot
Post-Practice	Primary Emerging Potential	Extending shelf life and managing product volumes Product volume management I don't do this
Destination	Primary Emerging Potential	Export (US, Canada, UK) Local market (Coscomatepec-Huatusco) or domestic market Metropolitan area supply center (CDMX, Guadalajara, Jalisco, Monterrey, NL)
Delivery Requirements	Primary Emerging Potential	Regional market (Córdoba-Orizaba-Puebla) He doesn't ask me for anything Deliver my product selected and packaged according to quality
ReasonReturn	Primary Emerging Potential	Presence of pesticides My product is not inspected Inert objects

RESULTS AND DISCUSSION

Six types of agricultural value networks were identified (Table 5) based on the typical activities of each type of network (Table 2) and the acceptable ranges and acceptance criteria (Table 3). Sánchez-Sánchez *et al*. (2023) mentioned that networks with different consolidation levels can be found within a region and that they can generate a combination of distinctive features.

Table 5. Consolidation level of agricultural value networks, based on the integration (%) of the characteristics of primary, emergent, and potential networks.

Value Network (acronym)	Description	Valuation (%)	Level of consolidation
MixtEmer	Emerging mixed	Prim (33), Emer (43), and Pote (23)	Emerging
MixtPoteEmer	Potentially emerging mixed	Prim (21), Eme (45), and Pote (34)	Emerging
PrevPrim	Primary prevalence	Prim (52), Emer (29), and Pote (19)	Primary
MixtPrim	Primary mixed	Prim (36), Emer (33), and Pote (30)	Primary
TPrim	Transition to primary	Prim (62), Emer (23), and Pote (15)	Primary
Prim	Primary	Prim (75), Emer (14), and Pote (11)	Primary

The dynamics of value networks depend on the supply, demand, and importance of the input supply link; consequently, they have multi-level features. For example, the emergent mixed network (EmerMix) recorded 33% of the features of a primary network, 43% of an emergent network, and 23% of a potential network. These percentages showed that the dynamics of the structural and operational levels of the agricultural networks depend on the requirements of the markets.

Singh *et al*. (2018) pointed out that, as a result of globalization, agricultural networks made up of small producers have modified their operations and structures, in order to achieve competitiveness in international markets. Likewise, the highest percentage determines the consolidation level of other networks. Therefore, the emergent-potential-mixed network (EmerPotMix) would be classified as an emergent network (45%), while the transition consolidated primary network (TConsPrim) and the primary consolidated network (ConsPrim) are transition (62%) and primary (75%) networks.

A mixed primary (MixPrim) network is integrated with 36, 33, and 30% features; these percentages indicate that their activities, operations, and structures are balanced. However, the small difference between these percentages suggests which characteristics require assistance or support in areas such as product packaging, additional markets, life shelf, etc.

Figure 3 shows a low statistical weight of the features of the value network. Dimensions 1 and 2 recorded 10.4 and 8%, respectively, in a wide range of groups, suggesting that neither network is completely consolidated and that they share primary, emergent, and potential features.

The characteristics of some value networks (e.g., emergent mixed and emergent potential mixed) can overlap (Figure 4). The diverse crops that make up each network suggest the existence of a sustainable rural employment, local commerce, external commerce (regional, domestic, and exportation), diversification of activities,

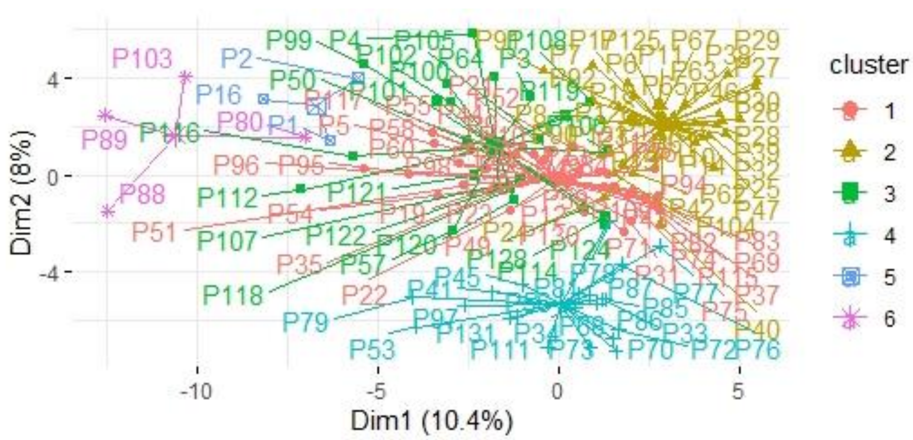

Figure 3. Scatter plot of value networks of crops, based on the features of primary, emergent, and potential networks.

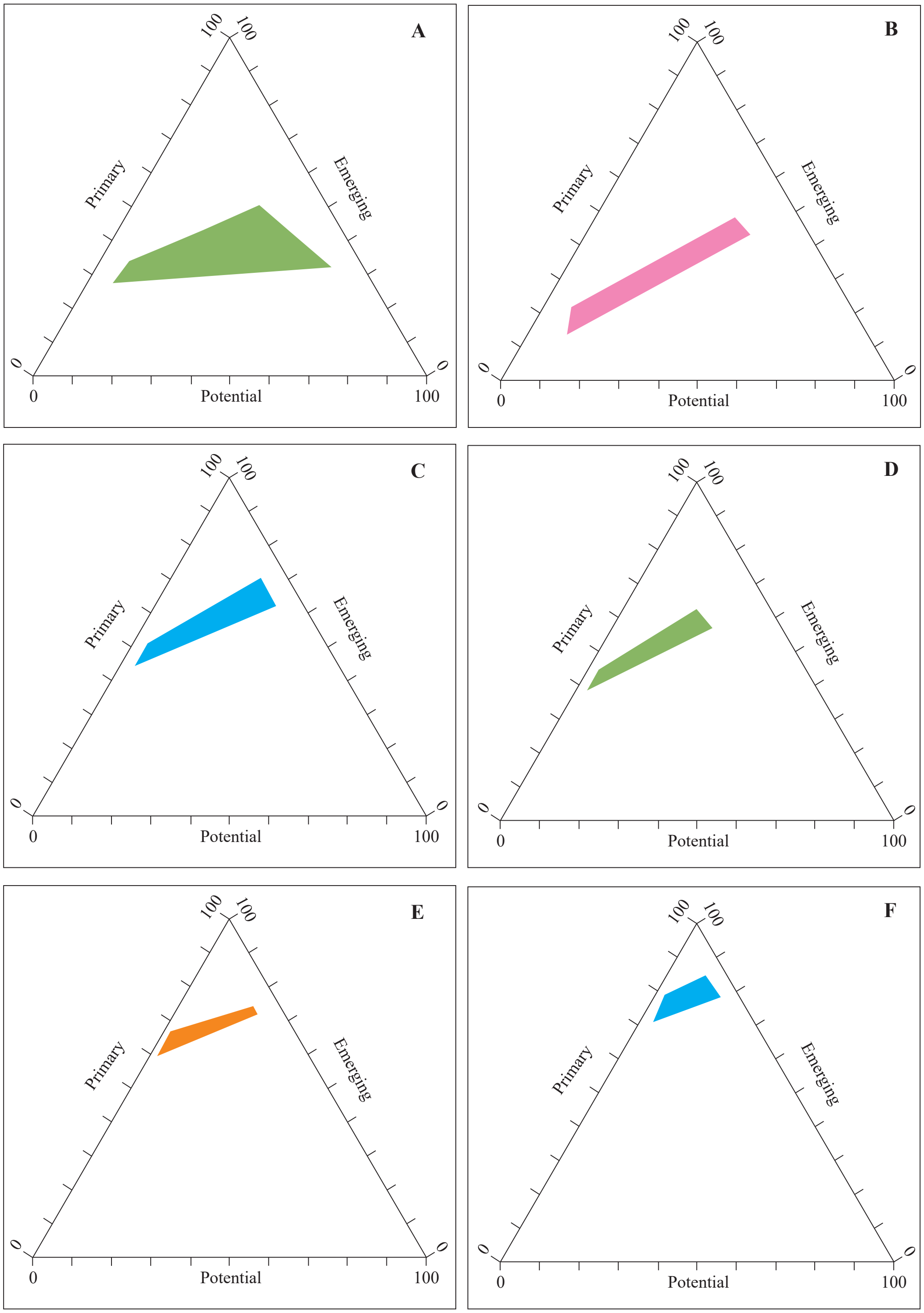

Figure 4. Value networks identified in the High Mountains Region (RAM) of Veracruz: A) EmerMix; B) EmerPotMix; C) PrimPrev; D) PrimMix; E) TPrim; and F) Prim.

differences in offer throughout the year, and the number of exploited local genetic resources (Table 6).

The diversified agricultural activities reported in the territory suggest that producers that participate in the value networks do not depend on a single activity (Waha et al., 2018). These results match the findings of Rojas and Saavedra-Mera (2022), who reported that having several crops guarantees the sustainability of the producers. Being able to distribute their economic dependency between multiple sources of income allows them to overcome the risks involved by changes in market prices, the effects of climate change, or the impact of new pests.

Productive and economic diversity can help to reduce the risks posed to certain crops by employment loss and climate change displacement, particularly those crops involved in primary networks, such as chayote in TConsPrim (100%) and ConsPrim (75%). Chayote is included in the six networks, followed by avocado, tomato, peaches, manzano pepper, and coffee. Sugarcane has a restricted surface and depends on the capacity of the sugar mill. Meanwhile, price instability and new pests have caused a loss of interest in coffee, which has been substituted by chayote. Regardless of their consolidation level, value networks may face diverse threats (Figure 4).

Public health risks were detected, particularly as a result of the application of raw chicken manure in crops from the emerged mixed, emergent potential mixed, and consolidated primary networks, exposing the product and the consumer to *Escherichia colli* (Luna-Guevara *et al*., 2019) and *Salmonella sp*. These findings match the reports of Rosas-Martínez and Aguilar-Rivera (2022), who identified *E. colli* and *Salmonella sp*. (Natarén Velázquez *et al*., 2020) in chicken manure (Table 7), a situation that is penalized in international audits.

The socioeconomical risks reported show the presence of new pests that impact crops (Rojas and Saavedra-Mera, 2022; Skendžić *et al*., 2021). The application of agrochemicals impacts the financial costs involved in the emergent mixed, emergent-potential-mixed,

Table 6. Percentage value that each crop contributes to the value network.

Value network	Crops
MixtEmer	Chayote (30%), avocado (21%), plantain veil (21%), peach (14%), tomato (7%), wax pepper (5%), and plum (2%)
MixtPoteEmer	Avocado (22%), coffee (14%), potato (11%), nopal (11%), tomato (8%), zucchini (5%), plum (5%), peach (5%), pear (5%), tomato (5%), chayote (3%), wax pepper (3%), and chilacayote (3%)
PrevPrim	Coffee (61%), sugarcane (9%), plum (9%), chayote (5%), tomato (4%), zucchini (4%), peach (4%), and avocado (4%)
MixtPrim	Chayote (19%), plum (14%), peach (14%), wax pepper (9%), potato (9%), avocado (10%), tomato (10%), plantain veil (10%), and chilacayote (5%)
TPrimCons	Chayote (100%)
PrimCons	Chayote (75%) and avocado (25%)

Table 7. Risks associated with the activities of the crop value networks.

Variable	Risk and related network
Public Health	Application of raw manure exposes crops and people to microorganisms (Escherichia coli and Salmonella sp.) representing a high risk to marketing and health (MixtEmer), (MixtPoteEmer) and (PrimCons).
Socioeconomic	The business transfer to the next generation (MixtPoteEmer) and (MixtPrim) has not been completed.
	The value chains are experiencing new pest organisms, leading to increased application of agrochemicals (MixtEmer), (MixtPoteEmer), (MixtPrim), (TPrimCons), and (PrimCons).
	Worker shortages occur in the months of January, February, March (PrevPrim), (MixtPrim), July, August (TPrimCons), (PrimCons), September, October, and December (PrimCons).
	Worker shortages due to migration (MixedPrim), (TPrimCons), (PrimCons), high demand, or other agricultural activity (PrimCons).
	Presence of fungi in crops affecting leaves (PrevPrim), stems (MixedPrim) (PrimCons), and fruits (PrimCons).
Environmental	Unregulated agrochemicals are used, putting personnel at risk and negatively impacting the environment (MixtEmer). The network is vulnerable to natural disasters (frost, hail and drought) that affect crops and reduce supply to the market (MixtEmer), (MixtPoteEmer), (PrevPrim) and (PrimCons).
Technological	It does not have technical assistance in health, nutritional, biosecurity and post-harvest management (MixtPoteEmer) and (MixtPrim).
	They do not receive technical assistance after natural disasters (MixtEmer). By delivering their produce to a buyer (intermediary), they earn less during peak supply periods (MixtEmer).
Comercial	There is no certification for field and post-harvest activities (MixtPoteEmer).
Conservation	Coffee monoculture, producers have been cultivating the crop for a long time (PrevPrim).
	The price of avocado fruit has influenced the establishment and substitution of potatoes, chayote and coffee (PrimCons)
Integration of links in internal logistics	Producers cultivate without expanding purchasing, selling and distribution activities of their product along the agri-food chain to be more competitive (MixtEmer), (MixtPoteEmer), (PrevPrim) and (MixtPrim).

primary mixed, in transition to a consolidated primary, and consolidated primary networks (Tudi *et al*., 2021). According to Shrestha (2019), this situation diminishes production and impacts the quality of the product in the destination market. Likewise, it impacts producers who lack economic solvency to support an increase in the long-term production costs (Acevedo-Suárez *et al*., 2012; Natarén Velázquez *et al*., 2020; Skendžić *et al*., 2021).

Rana *et al*. (2022), Rojas and Saavedra-Mera (2022) and Raza *et al*. (2019) pointed out that the vulnerability of emergent, potential emergent, and primary value networks to frost, hail, and droughts poses a third environmental risk, affecting income and the creation of employment (Erokhin *et al*., 2020).

The lack of training in the health, nutritional, biosafety, and postharvest handling poses a technological risk (Njoroge *et al*., 2019). Fonseca-Carreño *et al*. (2020) and other authors report that good agricultural practices should be applied in the management of a specialized agricultural production (Leong *et al*., 2020).

The low consolidation of chain links poses a risk to commercialization. Those risks include middlemen and the lack of integration of producers into the purchase, sale, and commercialization links. This situation puts the producers at a disadvantage in markets that require processed or added-value products. Producers who do not put into practice entrepreneurial measures will not have a greater participation in specialized markets with high quality and competitiveness standards (Durham and Mizik, 2021). The displacement of chayote by avocado endangers the conservation of local genetic resources, as a consequence of the price increase in the market. A distinctive feature of the type of value network is its activity, which can suggest the consolidation level of its structure and operation. Table 8 shows the main activity of the identified network, highlighting that the raw material (RM) supply is a priority for the first four networks, whose classification includes emergent, potential, and primary features. Meanwhile, the last two integrate the raw material (RM) supply links: the purchase and sale of agricultural products (PAP and SAP). This situation suggests that the inner logistics in the network have a higher level of consolidation.

Table 8. Value networks and their integration into the supply chain.

Value Network	Activity (%)	Description of the priority activity
MixtEmer	SM (98)	SM: Supply of raw materials
MixtPoteEmer	SM (100)	SM: Supply of raw materials
PrevPrim	SM (96)	SM: Supply of raw materials
MixtPrim	SM (100)	SM: Supply of raw materials
TPrimCons	SM (100), PAP (100) and SAP (67)	SM: Supply of raw materials, PAP: Purchase of agricultural products, SAP: Sale of agricultural products
PrimCons	SM (100), PAP (75) and SAP (75)	SM: Supply of raw materials, PAP: Purchase of agricultural products, SAP: Sale of agricultural products

MixtEmer (EmerMix): emergent mixed network. MixtPoteEmer (EmerPotMix): emergent potential mixed network. PrevPrim (PrimPrev): primary prevalence network. MixtPrim (PrimMix): primary mixed network. TPrimCons (TConsPrim): transition to consolidated primary network. PrimCons (ConsPrim): consolidated primary network.

Revaluation proposals for local or endogenous products are established to strengthen territorial development, seeking to overcome several limits, including scale and adaptation to the quality standards established in international commercialization regulations. Figure 5 shows the destination market of the by-products of each network that has been identified in the territory.

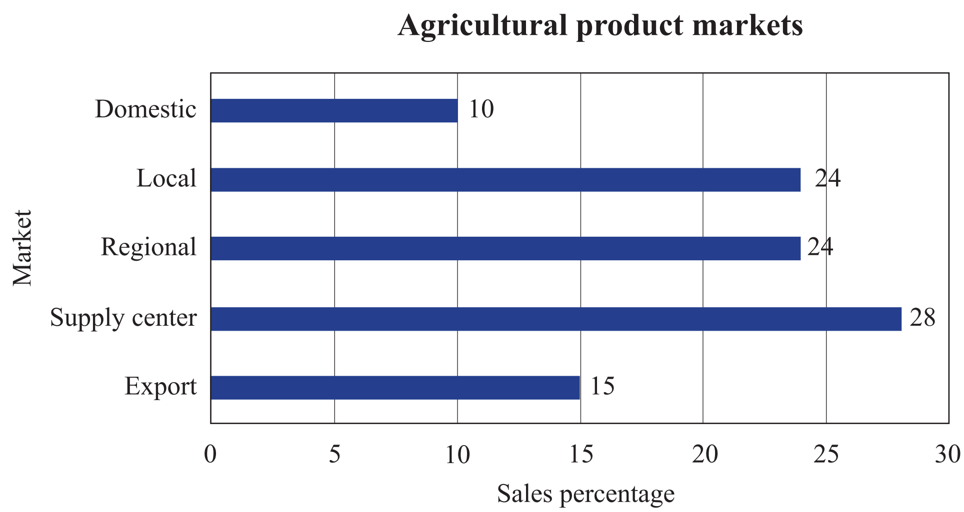

Figure 5. Destination markets for the agricultural products from the High Mountains Region of Veracruz. Figure developed by the authors based on producer surveys.

The Central de Abasto of Mexico City has the highest value, followed by regional and local destinations, suggesting the involvement of middlemen in commercialization. This is also the case of informal and traditional sale points that operate two or more days per week, in Coscomatepec, Orizaba, and Iztaczoquitlán, Veracruz, as well as the Central de Abasto of the city of Puebla, Puebla. Only chayote and banana leaf are exported and 15% of their production is sold to the United States and Canada.
The surveyed socioeconomic sector does not generally export coffee. Producers only sell their production to middlemen who specialize in coffee cherry (direct from the field), In their turn, middlemen sell coffee cherries to processing and exporting companies. Since the territory does not have a North American pest free area certificate, producers only sell their avocados in their hometowns and in the region. Some of the limitations to the exportation of manzano pepper (*Capiscum pubescens*) is the presence of the Mexican fruit fly (*Anastrepha* spp.). The remaining crops, including tomatillo (*Physalis* sp.) and tomato (*S. lycopersicum*), are commercialized in the local and regional markets. Risk characteristics were selected to identify the activities of the revaluation proposal (Carenzo, 2007). A principal component analysis revealed that nine characteristics of the networks are key for the said proposal (Tables 9 and 10).

Table 9. Activities required to revaluate the value networks of crops.

Value Network Characteristics	Description	Activity in the value chain
AT Frequency	Frequency of technical assistance	Purchasing
ApplyAgroPermitted	Applies permitted agrochemicals	Logistics
ApplyCompost	Applies organic compost	Logistics
ApplyAgroNotRegulated	Applies prohibited agrochemicals	Logistics
ApplyRawManure	Applies manure without composting	Logistics
UseEquipment	Uses used equipment	Purchasing
PostPractice	Applies post-harvest techniques	Operations
DeliveryRequirements	Proper product delivery	Marketing and sales
ReturnReasonNotReviewed	Applies product traceability	Marketing and sales

Table 10. Integrated variables of the principal components (PC) that account for the cumulative variance for the revaluation of crops.

Component Structure	Variables (number)	Cumulative explained variance (%)
CP1 = -0.75 Equipment Use -0.73 Post-Practice -0.68 ATFrequency. Technical Assistance and Post-Harvest Handling Asistencia técnica y manejo postcosecha	2.9	32.57
CP2 = 0.63 ApplyAgroPermit -0.63 ApplyAgroNoRegulate + 0.47 DeliveryRequirements + 0.32 ReturnNoReview Requirements for Product Sale	4.4	49.81
CP3 = 0.78 ApplyCompost -0.54 ApplyRawManure +0.15 Equipment Use +0.10 ATFrequency +0.07 Post-Practice Field Training	5.6	63.23
CP4 = -0.86 ReturnNoReview +0.29 ATFrequency -0.22 ApplyRawManure -0.18 ApplyAgroNoRegulate +0.05 ApplyAgroPermit -0.01 DeliveryRequirements	6.7	73.95

After grouping the activities according to their statistical weight, a 73.95% cumulative variance was recorded in four principal components (PC) which determine the priority of the activities (Table 10).

To boost network consolidation and bring producers into the supply chain, purchase activities must be improved (Dias *et al*., 2019), along with logistics, operations, marketing, and sales. This approach matches the proposal of Bada Carbajal *et al*. (2010) and Carenzo (2007), who reported that the problems must be identified before local products are revaluated; likewise, quality standards must be adapted to international regulations to facilitate the participation of producers in domestic and foreign markets.

Likewise, Singh *et al.* (2018) point out that globalization has changed the structure and operation of agricultural networks; therefore, they suggest improving competitiveness to comply with the standards of the international market. In summary, value networks are characterized by their activities, structure, and operation. The type of value network and its consolidation depend on structural differences and the ratio between its economic, logistical, social, technological, and risk values. Improvements for the consolidation of value networks can be suggested, as well as action strategies aimed at the less structured activities of each network.

Value networks harbor local genetic resources of great importance. These resources preserve agrobiodiversity, as well as productive and economic diversity. Likewise, they boost and support the local economy, mitigating migration and promoting local employment.

CONCLUSIONS

Six types of value networks with different consolidation levels were identified in the territory in question. None of them had a single classification type (e.g., primary, emergent, and potential). The percentage value of distinctive characteristics pointed out that these dynamic networks share features that classify them as mixed and evolving. Different risks were identified and classified per social group to facilitate their study. The network by-products recorded a cumulative dependency (≤85%) on the domestic, local, regional, and Mexico City markets. Only chayote and banana leaf are exported. Chayote is the most widespread crop in the six networks and it has the highest consolidation level as a primary network. Both crops and risks that can limit their dynamics and evolution should be revaluated and reorientated to strengthen the networks. The most frequent factors were technical support and the application of banned agrochemicals and raw manure.

ACKNOWLEDGMENTS

To CONAHCyT, for the economic support provided for the education of the MSc candidate. To COLPOS, particularly the SLP campus, for the education opportunities and their advice for this research. To the agricultural producers of the High Mountains Region of Veracruz, Mexico, for their information and trust.

REFERENCES

Acevedo-Suárez, J. A., Gómez-Acosta, M. I., & López-Joy, T. (2012). Análisis de la cadena de valor hortofrutícola del municipio Marianao en La Habana, Cuba. XXXIII (2), 200–2013.

Almaraz-Vidal, D. (2016). Las serpientes venenosas de importancia médica de la región de Las Grandes Montañas de Veracruz, México: Aspectos ecológicos y accidentes ofídicos. Revista mundo de investigación, 2(1). https://web.archive.org/web/20210716165525id_/https://mundoinvestigacion.es/wp-content/uploads/2017/03/5-SERPIENTES-VENENOSAS_Almaraz.pdf

Bada Carbajal, L. M., Rivas Tovar, L. A., Bada Carbajal, L. M., & Rivas Tovar, L. A. (2010). Los clusters agroindustriales en el estado de Veracruz. Investigación administrativa, 39(105), 73–100.

Beltran-Morales, N. N. (2022). La etnografía en los estudios turísticos, el caso del tianguis tradicional de Coscomatepec de Bravo, Veracruz; México [Colegio de Postgraduados]. http://colposdigital.colpos.mx:8080/xmlui/bitstream/handle/10521/4998/Beltran_Morales_NN_MP_PTR_2022.pdf?sequence=1&isAllowed=y

Brenlla-Martínez, M. (1997). Calculo tamaño de muestra. Universidad de Granada, España. https://www.ugr.es/~ecordon/master/docus/calculotama%C3%B1omuestra.xls

Cañarte, J. S. R., García, J. G. M., Intriago, M. A. L., & Moreira, J. A. F. (2021). El desarrollo territorial y el pensamiento económico. Sociedad & Tecnología, 4(3), Article 3. https://doi.org/10.51247/st.v4i3.145

Carenzo, S. (2007). Territorio, identidades y consumo: Reflexiones en torno a la construcción de nuevos paradigmas en el desarrollo.

Dias, C. S. L., Rodrigues, R. G., & Ferreira, J. J. (2019). What's new in the research on agricultural entrepreneurship? Journal of Rural Studies, 65, 99–115. https://doi.org/10.1016/j.jrurstud.2018.11.003

Durham, T. C., & Mizik, T. (2021). Comparative Economics of Conventional, Organic, and Alternative Agricultural Production Systems. Economies, 9(2), Article 2. https://doi.org/10.3390/economies9020064

Erokhin, V., Diao, L., & Du, P. (2020). Sustainability-Related Implications of Competitive Advantages in Agricultural Value Chains: Evidence from Central Asia—China Trade and Investment. Sustainability, 12(3), Article 3. https://doi.org/10.3390/su12031117

Fonseca-Carreño, N. E., González Moreno, M. R., & Narváez Benavides, C. A. (2020). Asociatividad para la administración los sistemas de producción campesina. Revista Estrategia Organizacional, 9(1). https://doi.org/10.22490/25392786.3644

Gómez-Núñez, J., Gómez-Martínez, E., Morales, H., González-Santiago, M. V., & Aiterwegmair, K. (2019). Construcción social de la soberanía alimentaria por la organización campesina OCEZ-CNPA en Chiapas, México. Estudios Sociales. Revista de Alimentación Contemporánea y Desarrollo Regional, 29(54). https://doi.org/10.24836/es.v29i54.799

INEGI (Instituto Nacional de Estadística y Geografía). (2000). Espacio y datos de México. Instituto Nacional de Estadística y Geografía. INEGI. https://www.inegi.org.mx/app/mapa/espacioydatos/default.aspx

INEGI (Instituto Nacional de Estadística y Geografía). (2024a). Climatología. https://www.inegi.org.mx/temas/climatologia/#mapas

INEGI (Instituto Nacional de Estadística y Geografía). (2024b). Directorio Nacional de Unidades Económicas. DENUE. Censos Económicos 2014; Instituto Nacional de Estadística y Geografía. INEGI. https://www.inegi.org.mx/app/mapa/denue/default.aspx

INEGI, I. N. de E. y. (2023). Censo Agropecuario (CA) 2022. https://www.inegi.org.mx/programas/ca/2022/

Leong, W.-H., Teh, S.-Y., Hossain, M. M., Nadarajaw, T., Zabidi-Hussin, Z., Chin, S.-Y., Lai, K.-S., & Lim, S.-H. E. (2020). Application, monitoring and adverse effects in pesticide use: The importance of reinforcement of Good Agricultural Practices (GAPs). Journal of Environmental Management, 260, 109987. https://doi.org/10.1016/j.jenvman.2019.109987

Luna-Guevara, J. J., Arenas-Hernandez, M. M. P., Martínez de la Peña, C., Silva, J. L., & Luna-Guevara, M. L. (2019). The Role of Pathogenic E. coli in Fresh Vegetables: Behavior, Contamination Factors, and Preventive Measures. International Journal of Microbiology, 2019(1), 2894328. https://doi.org/10.1155/2019/2894328

Nataren Velazquez, J., Del Ángel Pérez, A. L., Megchún-García, J. V., Ramírez Herrera, E., & Meneses Márquez, I. (2020). Caracterización productiva del aguacate (Persea americana Mill.) en la zona de alta montaña Veracruz, México. Rev. iberoam. bioecon. cambio clim., 6(12), 1406–1423. https://doi.org/10.5377/ribcc.v6i12.9941

Njoroge, A. W., Baoua, I., & Baributsa, D. (2019). Postharvest Management Practices of Grains in the Eastern Region of Kenya. Journal of Agricultural Science (Toronto, Ont.), 11(3), 10.5539/jas.v11n3p33. https://doi.org/10.5539/jas.v11n3p33

Palacio, F. X., Apodaca, M. J., & Crisci, J. V. (2020). Análisis multivariado para datos biológicos: Teoría y su aplicación utilizando el lenguaje R (1a ed .). Fundación de Historia Natural Félix de Azara. https://fundacionazara.org.ar/img/libros/analisis-multivariado-para-datos-biologicos/analisis-multivariado-para-datos-biologicos.pdf

Porter, M. E. (1985). Competitive Advantage: Creating and Sustaining Superior Performance.

Rana, V. S., Sharma, S., Rana, N., Sharma, U., Patiyal, V., Banita, & Prasad, H. (2022). Management of hailstorms under a changing climate in agriculture: A review. Environmental Chemistry Letters, 20(6), 3971–3991. https://doi.org/10.1007/s10311-022-01502-0

Raza, A., Razzaq, A., Mehmood, S. S., Zou, X., Zhang, X., Lv, Y., & Xu, J. (2019). Impact of Climate Change on Crops Adaptation and Strategies to Tackle Its Outcome: A Review. Plants, 8(2), Article 2. https://doi.org/10.3390/plants8020034

Rivera-Hernández, J. E. (2018). El ecoturismo y el turismo rural en la región de las altas montañas de veracruz, méxico: Potencial, retos y realidades. Agro Productividad, 11(8), Article 8. https://doi.org/10.32854/agrop.v11i8.1108

Rojas, F. E., & Saavedra-Mera, K. A. (2022). Diversificación de Cultivos y su Impacto Económico en las Fincas Ecuatorianas. Revista Científica Zambos, 1(1), 51–68. https://doi.org/10.69484/rcz/v1/n1/21

Rosa, O., & de Paredes, M. (2017). Rentabilidad de la producción agrícola desde la perspectiva de los costos reales: Municipios Pueblo Llano y Rangel del estado Mérida, Venezuela.

Rosas-Martínez, V., & Aguilar-Rivera, N. (2022). Compostaje para la reducción de excretas de aves (Gallus gallus domesticus)1. Agronomía Mesoamericana, 33(1), 1–19.

SADER (Secretaría de Agricultura y Desarrollo Rural). (2022). Corte a junio 2022. Beneficiarios del Programa Producción para el Bienestar 2022. - Corte a junio 2022. Beneficiarios del Programa Producción para el Bienestar 2022 en Veracruz de Ignacio de la llave. - Datos.gob.mx/busca. https://datos.gob.mx/busca/dataset/corte-a-junio-2022-beneficiarios-del-programa-produccion-para-el-bienestar-2022/resource/efe4c7cd-9891-4568-a5bf-d70bfdc4cdcd?inner_span=True

Sánchez-Galván, F., Bautista-Santos, H., Martínez-Flores, J. L., Ireta-Paredes, A. del R., & Sánchez-Partida, D. (2020). Cadena de suministro de productos agrícolas de traspatio. Agro Productividad, 13(8), Article 8. https://doi.org/10.32854/agrop.vi.1705

Sánchez-Sánchez, Z. S., Cadena-Íñiguez, J., Morales-Flores, F. J., Cisneros-Solano, V. M., & Ruíz-Vera, V. M. (2023). Método para identificar redes de valor en un territorio con vocación agrícola. XXVI Congreso Internacional de Dirección e Ingeniería de Proyectos. Donostia, España, 2023.

Scheiterle, L., Ulmer, A., Birner, R., & Pyka, A. (2018). From commodity-based value chains to biomass-based value webs: The case of sugarcane in Brazil's bioeconomy. Journal of Cleaner Production, 172, 3851–3863. https://doi.org/10.1016/j.jclepro.2017.05.150

Shrestha, S. (2019). Effects of Climate Change in Agricultural Insect Pest. Acta Scientific Agriculture, 3(12), 74–80. https://doi.org/10.31080/ASAG.2019.03.0727

SIAP (Servicio de Información Agroalimentaria y Pesquera). (2022). Anuario Estadístico de la Producción Agrícola. https://nube.siap.gob.mx/cierreagricola/

Singh, G., Budhiraja, P., & Vatta, K. (2018). Sustainability of Farmer Producer Organisations under Agricultural Value Networks in India: A Case of Punjab and Gujarat. Indian Journal of Agricultural Economics, 73, 70–85.

Skendžić, S., Zovko, M., Živković, I. P., Lešić, V., & Lemić, D. (2021). The Impact of Climate Change on Agricultural Insect Pests. Insects, 12(5), Article 5. https://doi.org/10.3390/insects12050440

Torre, A. (2020). Nuevas propuestas para analizar el desarrollo territorial. Eutopía. Revista de Desarrollo Económico Territorial, 17. https://doi.org/10.17141/eutopia.17.2020.4549

Tudi, M., Daniel Ruan, H., Wang, L., Lyu, J., Sadler, R., Connell, D., Chu, C., & Phung, D. T. (2021). Agriculture Development, Pesticide Application and Its Impact on the Environment. International Journal of Environmental Research and Public Health, 18(3), Article 3. https://doi.org/10.3390/ijerph18031112

Urquía-Fernández, N. (2014). La seguridad alimentaria en México. Salud pública de méxico, 56, 92–98.

Vargas-Canales, J. M., Guido-López, D. L., Rodríguez-Haros, B., Bustamante-Lara, T. I., Camacho-Vera, J. H., & Orozco-Cirilo, S. (2020). Evolución de la especialización y competitividad de la producción de limón en México. Revista Mexicana de Ciencias Agrícolas, 11(5), 1043–1056. https://doi.org/10.29312/remexca.v11i5.2218

Waha, K., van Wijk, M. T., Fritz, S., See, L., Thornton, P. K., Wichern, J., & Herrero, M. (2018). Agricultural diversification as an important strategy for achieving food security in Africa. Global Change Biology, 24(8), 3390–3400. https://doi.org/10.1111/gcb.14158

Agrociencia

USE OF TRAIL CAMERAS TO ESTIMATE THE ABUNDANCE AND POPULATION STRUCTURE OF BIGHORN SHEEP IN BAJA CALIFORNIA, MEXICO

Enrique de Jesús **Ruiz-Mondragón**[1], Fernando Isaac **Gastelum-Mendoza**[1], Guillermo **Romero-Figueroa**[1*], Crystian Sadiel **Venegas-Barrera**[2], María Evarista **Arrellano-García**[1], Israel **Guerrero-Cárdenas**[3], Eloy Alejandro **Lozano-Cavazos**[4], Raul **Valdez**[5]

[1]Universidad Autónoma de Baja California. Facultad de Ciencias. Carretera Ensenada-Tijuana 3917, Pedregal Playitas, Ensenada, Baja California, Mexico. C. P. 22860.
[2]Instituto Tecnológico de Ciudad Victoria. División de Estudios de Posgrado e Investigación. Emilio Portes Gil 1301, José López Portillo, Ciudad Victoria, Tamaulipas, Mexico. C. P. 87010.
[3]Centro de Investigaciones Biológicas del Noroeste. Instituto Politécnico Nacional 195, Playa Palo de Santa Rita Sur, La Paz, Baja California Sur, Mexico. C. P. 23096.
[4]Universidad Autónoma Agraria Antonio Narro, Departamento de Recursos Naturales Renovables. Antonio Narro 1923, Buenavista, Saltillo, Coahuila, Mexico. C. P. 25315.
[5]New Mexico State University. Department of Fish, Wildlife, and Conservation Ecology. University Avenue 1780, Las Cruces, New Mexico, USA. C. P. 88003.
* Author for correspondence: isaacgastelum@uabc.edu.mx

Citation: Ruiz-Mondragón EJ, Gastelum-Mendoza FI, Romero-Figueroa G, Venegas-Barrera CS, Arrellano-García ME, Guerrero-Cárdenas I, Lozano-Cavazos EA, Valdez R. 2025. Use of trail cameras to estimate abundance and population structure of bighorn sheep in Baja California, Mexico. **Agrociencia** 59(3): 428-442. https://doi.org/ 10.47163/agrociencia.v59i3.3202

Editor in Chief: Dr. Fernando C. Gómez Merino

Received: April 17, 2024.
Approved: January 15, 2025.
Published in Agrociencia: April 08, 2025.

ABSTRACT

Monitoring abundance and population structure is essential to guide the management of wild species. Few population studies of bighorn sheep (*Ovis canadensis* Shaw) have been conducted in Baja California, Mexico, due to the complicated and costly nature of monitoring these animals. The objective of the study was to determine the abundance and structure of a bighorn sheep population using trail cameras. The study was conducted in the coastal region of the Sierra Santa Isabel from April to July 2022. Trail cameras were deployed at four natural watering holes and on a trail that is frequently used by bighorn sheep. The Lincoln-Petersen method was used to estimate abundance with four criteria to define independent records: separated by one hour, by one hour without taking into account samples with only one record, by at least one day, and by one week. The estimates generated with this method were compared with those reported in the aerial monitoring conducted in the study area in 2021. The abundance calculated from independent sampling periods separated by one week was found to be within the range of that estimated from aerial monitoring. The abundance of bighorn sheep in the coastal region of the Sierra Santa Isabel was 129 ± 9 animals, and the ratio of rams, ewes, yearlings, and lambs was 8:10:1:2. The results suggest that the population of the species at this site is in a good state of conservation. In addition, the use of trail cameras proved to be a viable alternative to traditional monitoring methods for bighorn sheep population assessments.

Key words: wild sheep, big game species, population status, Lincoln-Petersen, *Ovis canadensis* Shaw, Sierra Santa Isabel.

INTRODUCTION

Population monitoring is the fundamental mechanism for collecting biological information and systematic data needed to determine the conservation status and demographic trends of wildlife populations (Bolen and Robinson, 2003). In addition, it allows the evaluation of the impact of the factors that exert pressure on these populations, as well as the effectiveness of the conservation actions applied for their protection (Kuvlensky *et al*., 2022). Among the essential attributes to guide the management of wild species, the abundance (expressed in the number of individuals) and demographic structure (encompassing sex ratio and age classes) of these populations stand out (Gallina-Tessaro, 2015).

Bighorn sheep (*Ovis canadensis* Shaw) play an ecological role in the desert scrublands of northwestern Mexico, as they are directly involved in the nutrient cycling of the ecosystem (Monson and Sumner, 1980), influencing vegetation dynamics (Gastelum-Mendoza *et al*., 2024), and being a source of nourishment for some predators (Rosas-Rosas *et al*., 2003). They also possess cultural (Sandoval *et al*., 2019) and economic importance (Lee, 2011). In Mexico, it is classified as a species subject to special protection (SEMARNAT, 2019), which implies that its exploitation must be based on accurate information on the status of its populations to avoid jeopardizing its viability. Therefore, it is imperative to have efficient monitoring methods that provide useful data on the abundance and structure of these populations (Ruiz-Mondragón *et al*., 2023).

This species inhabits arid mountain systems with steep slopes and difficult access (Conroy *et al*., 2018), where monitoring its populations demands a considerable investment of time, money, and technical personnel. Among the methods used to determine their abundance and population structure are aerial monitoring (Romero-Figueroa *et al*., 2024), ground monitoring (López *et al*., 1995), and trail camera monitoring, the latter being a lower-cost and less intrusive methodology that allows for periodic and standardized population estimates (Perry *et al*., 2010; Harris *et al*., 2020).

In this regard, several methods based on the use of trail cameras have been developed to estimate the abundance of wild species, both for populations with marked specimens (Alonso *et al*., 2015) and populations with no marked specimens (Palencia *et al*., 2021). For bighorn sheep, accurate estimates of population size have been obtained using trail cameras under captive conditions (Perry *et al*., 2010; Harris *et al*., 2020). However, for free-living sheep populations, the most viable alternative for estimating abundance is the Lincoln-Petersen mark-recapture method (Jaeger *et al*., 1991; Douglass and Longshore, 1995). Methods developed for unmarked populations require cameras to be randomly placed in the delimited study area (Palencia *et al*., 2021), which increases sampling costs due to the inaccessible and rugged habitat of this species.

When using the Lincoln-Petersen method for population estimation, the assumption is to work with a closed population where all animals have the same probability of being captured, remain tagged throughout the sampling period, and observers may detect all tags (Pollock *et al*., 1990; Perry *et al*., 2010). Therefore, a catch period is set to fit the limitations of the method; in addition, to mitigate the risk of violating the assumptions of the method, a cumulative estimate should be made from a sufficient number of individual catch periods (Jaeger *et al*., 1991; Douglass and Longshore, 1995; Perry *et al*., 2010).

In the state of Baja California, Mexico, the evaluation of the size and structure of bighorn sheep populations has been scarcely addressed, which is reflected in the existence of only five aerial monitoring studies (Romero-Figueroa *et al*., 2024) and one terrestrial monitoring study (López *et al*., 1995). This limitation in research is attributed to the lack of financial resources and trained personnel to sustain a continuous monitoring program for bighorn sheep populations, aggravated by the ban on sport hunting in Baja California since 1990 (Ruiz-Mondragón *et al*., 2023). The lack of data has hindered the formulation of management plans that promote the conservation of both the species and its habitats in the Baja California region (Romero-Figueroa *et al*., 2024).

In this context, it is important to have a method for monitoring bighorn sheep populations that is inexpensive and simple to implement, accessible to landowners, authorities, technical personnel, and researchers with a basic level of training and technological equipment. Therefore, this study aims to resolve the following questions: 1) What independent sampling interval produces a bighorn sheep population estimate comparable to that obtained from aerial monitoring? and 2) What level of sampling effort is required with trail cameras to achieve an estimate of bighorn sheep population abundance comparable to that from aerial monitoring? Therefore, the main objective of this research was to determine the abundance and structure of a bighorn sheep population in the wild using trail cameras as a monitoring method.

MATERIALS AND METHODS

Description of the study area

The study was conducted in the coastal region of the Sierra Santa Isabel, located in the central portion of the state of Baja California, Mexico (30.1544° N, 114.8464° W and 29.7933° N, 114.5209° W) (Figure 1). This area comprises a low mountain range with plateaus and covers an area of 43 888 ha, with altitudes ranging from 5 to 876 m. The climate is very arid and semi-warm, with an average annual temperature that varies between 18 and 22 °C. Rainfall is distributed throughout the year, with a percentage of winter rainfall greater than 18 % of the annual total (BWh(x'); García, 2004). Average annual precipitation ranges from 0 to 125 mm (Vidal, 1990). In terms of vegetation, microphyllous desert scrub predominates, with species such as the gobernadora (*Larrea tridentata*), ocotillo (*Fouquieria splendens*), and flor de rocío (*Encelia farinose*) (Miranda and Hernández, 1963).

Figure 1. Location of trail camera monitoring sites (red dots) in the coastal region of Sierra Santa Isabel, Baja California, Mexico.

The natural waterholes used by bighorn sheep are known locally as Tinaja del Miramar, Cinco Islas, La O, and Las Palmitas (Ruiz-Mondragón *et al.*, 2023). The longest distance between waterholes is 9 km and corresponds to the stretch between Tinaja del Miramar and Las Palmitas; the shortest distance between these water sources is 1 km and corresponds to the separation between Cinco Islas and La O. The Tinaja del Miramar is a waterhole that is 7 m wide, 4 m long, and 1 m deep. Cinco Islas is a body of water that springs in the bed of a stream; it is 1 m wide, 0.7 m long, and 0.3 m deep. The O is a cavern in the mountains; the body of water at this site is 1 m wide, 1.5 m long, and 0.3 m deep. Las Palmitas is an oasis immersed in the mountain range; the body of water at this site is 1.5 m wide, 2.5 m long, and 0.4 m deep (Figure 2).

The study was conducted from April 15 to July 31, 2022, which corresponds to the hottest season of the year in the region (García, 2004). However, the research was interrupted in July due to the passage of Hurricane Kay, which resulted in the loss of all cameras used in the study. Bushnell Core Low Glow 24 MP cameras were used to carry out the population monitoring. These cameras were installed at four natural waterholes and on a trail that is frequently used by wild sheep (Figure 1). A camera was installed at each site and mounted on a wooden stake at a height of 0.5 m from the ground and programmed to capture three photographs at 3 s intervals for each detection of motion. Monthly maintenance was performed to change memory cards and batteries.

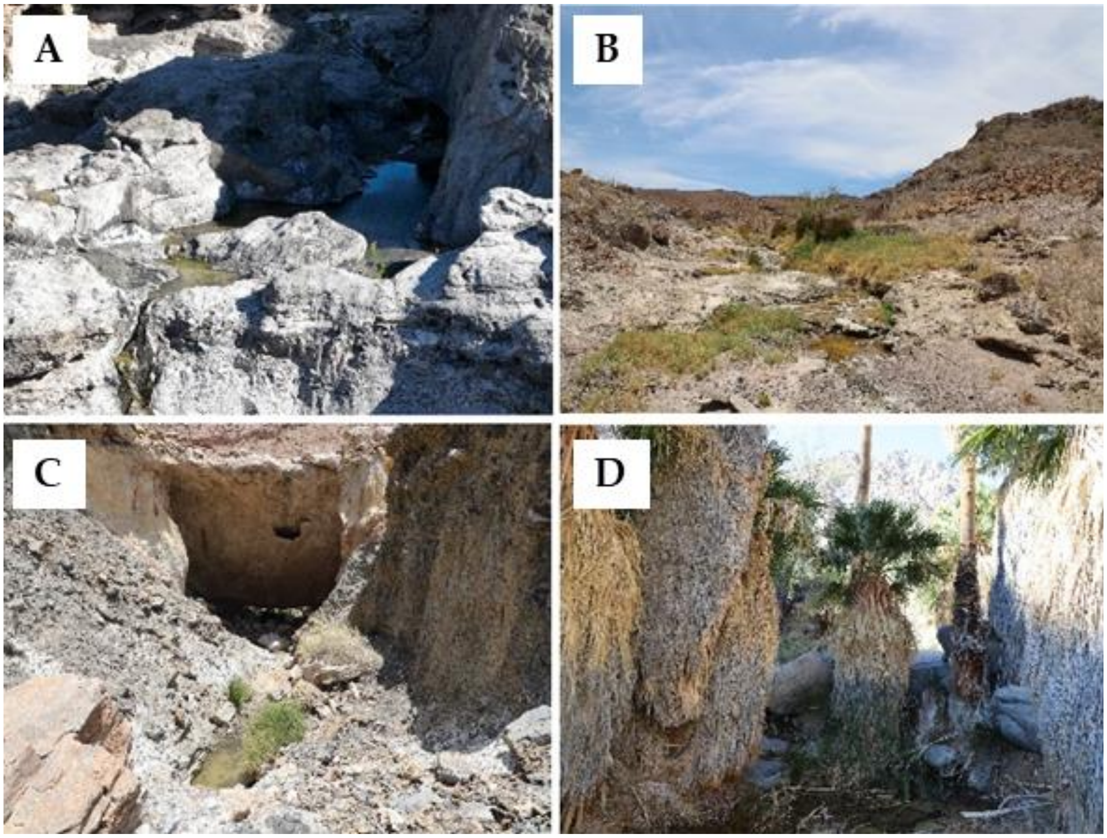

Figure 2. Natural waterholes used by bighorn sheep (*Ovis canadensis* Shaw) in the coastal region of the Sierra Santa Isabel, Baja California, Mexico. A: Tinaja del Miramar; B: Cinco Islas; C: La O; D: Las Palmitas.

For individual identification of the sheep, the natural characteristics of the animals were used, including the size and shape of the horns, body size, and condition, as well as scars, deformities, and other notable marks on the horns and body. Only records that could be fully identified were considered in the estimation of population size. All photographs of animals that could not be observed in sufficient detail due to poor lighting conditions, distance, or the speed at which they moved through the camera's field of view were excluded.

The use of natural characteristics to differentiate individuals in a population is not recommended in mark-recapture studies, as these characteristics may change over time, which could affect the accuracy of the estimate of population abundance. However, Perry *et al*. (2010) carried out a comparison of the estimation of the size of a bighorn sheep population considering different types of tags and found similar results.

The population size was estimated with the Lincoln-Petersen method (Chapman, 1951) modified by Pollock *et al*. (1990) according to the following formula:

$$N = \left[\frac{(n_1 + 1)(n_2 + 1)}{m + 1}\right] - 1$$

where N is the population size, n_1 is the number of individuals recorded (captured) and identified (marked) in the first sampling period, n_2 is the number of individuals recorded in the subsequent sampling period, and m is the number of individuals recorded in the first sampling period and recorded again in the subsequent sampling period (recaptured). The population size estimate was the average of all individual estimates. The 95 % confidence interval (CI) of the estimate was calculated as 1.96 times the standard error of the mean:

$$SE = \sqrt{\left[\left(\frac{1}{(k)(k-1)}\right)\left(\sum (N_i - N_m)^2\right)\right]}$$

where K is the number of individual estimates of the population size, N_i is each individual estimate and N_m is the average estimate.

Four estimates of population abundance were made, each based on a different time period for independent sampling. To carry out these estimates, series of photographs separated by more than one hour, by at least one day, and by one week were considered as independent samples. Furthermore, an additional estimation was performed with independent samples separated by more than one hour, excluding those samples with only one record ($n_i = 1$) (Perry *et al*., 2010).

In the case of independent samples separated by more than one hour, each set of photographs was considered as an individual sample. For example, if in the first photograph, two rams and one ewe were recorded, and in the second photograph, taken 45 minutes later, two ewes and one lamb were recorded, neither would equal six individuals: two rams, three ewes, and one lamb. For independent samples separated by at least one day, animals were recorded on the first day (n_1) and the following day on which the camera was activated (n_2). For example, if two sheep were recorded on April 15 and five on April 17, n_1 would equal two and n_2 would equal five. In the case of samples separated by one week, n_1 would be equal to the number of sheep recorded during the first seven days, and n_2 would be equal to the number of sheep recorded during the following seven days.

The cumulative average of the individual estimates of the population size (from K= 2) was calculated. The precision of these estimates was evaluated by comparing them with the estimate reported for the study area in the 2021 aerial monitoring (Romero-Figueroa *et al.*, 2024). The success of trail camera sampling was estimated for each month and installation site, defining success as the number of independent samples obtained divided by the number of days/cameras used (one day/camera = one camera in operation per 24 h) (Perry *et al*., 2010).

The bighorn sheep recorded were classified according to the age and sex class criteria defined by Geist (1968), labeling the sheep into eight categories according to the shape and size of their horns, as well as their body size (Figure 3). From this classification, the ram:ewe:yearling:lamb ratio of each individual estimate was determined. The age and sex class ratio for the estimated population was obtained as the average of all individual estimates. The Kruskal-Wallis nonparametric statistical test was used to compare the ratio of age and sex classes obtained from the different sampling periods. This statistical analysis was performed using the Past4 software (Hammer *et al*., 2001). Likewise, the photographic records of the species were classified based on the social configurations observed: solitary, in pairs, or in herds.

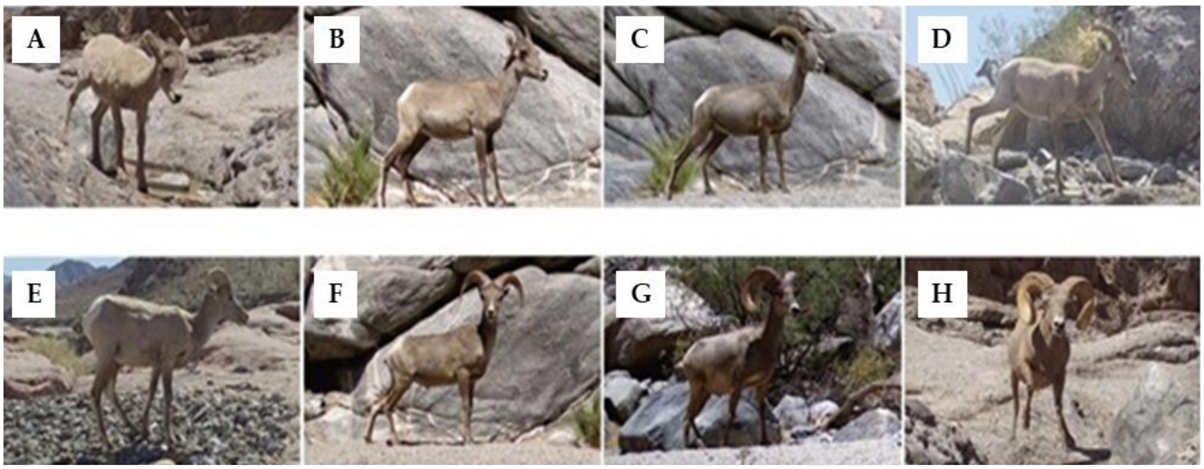

Figure 3. Age and sex classes of bighorn sheep (*Ovis canadensis* Shaw) according to Geist (1968). A: lamb; B: yearling ewe; C: ewe; D: yearling ram; E: class I ram; F: class II ram; G: class III ram; H: class IV ram.

RESULTS AND DISCUSSION

In 535 days/cameras, 6062 photographs of bighorn sheep were obtained. In 41 % (2468) of these images, the specimens could be fully identified. These records were organized into 255 independent samples, which consisted of series of photographs separated by more than one hour. In addition, 166 independent samples separated by more than one hour were obtained, each with more than one sheep per record, 99 independent samples separated by at least one day, and 14 independent samples separated by one week.

At each location where a trail camera was installed, photographs of the sheep were captured throughout each month during the study period (Figure 4). The number of images taken per day gradually increased over time, and there was no difference between the number of photographs taken at the different sites in April and May; however, in June and July, the number of images captured both on the trail and at Cinco Islas was lower than those obtained at La Tinaja del Miramar, Las Palmitas, and La O.

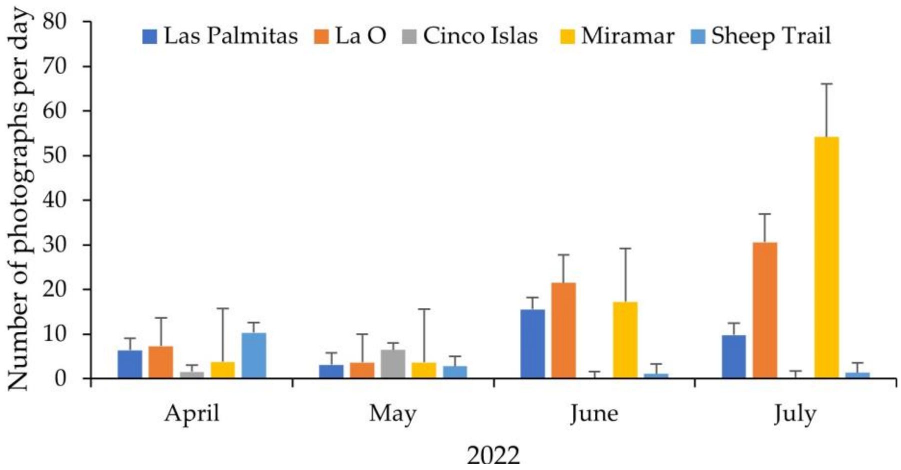

Figure 4. Trail camera photography rate according to month and monitoring site in Sierra Santa Isabel, Baja California, Mexico (vertical lines above bars indicate standard error).

With independent samples separated by more than one hour, 127 individual estimates of bighorn sheep population abundance were made. Likewise, 83 individual estimations were carried out with the independent samples separated by more than one hour and with more than one sheep per record, 49 individual estimations with the independent samples separated by at least one day, and 7 individual estimations with the independent samples separated by one week (Figure 5).

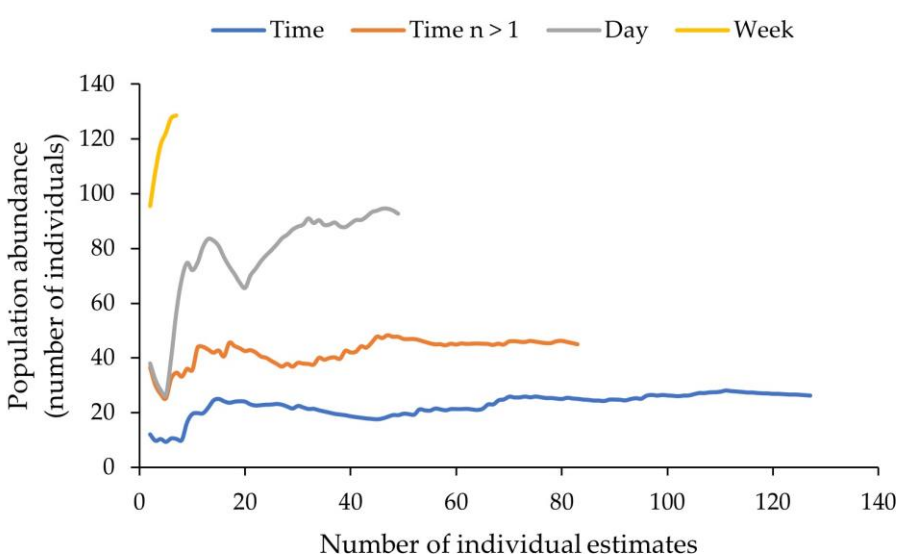

Figure 5. Average cumulative estimate of bighorn sheep (*Ovis canadensis* Shaw) population abundance for the coastal region of the Sierra Santa Isabel in Baja California, Mexico, based on different independent sampling intervals.

The maximum number of bighorn sheep recorded in a period of independent sampling separated by more than one hour, as well as in a period of independent sampling separated by more than one hour and with more than one sheep per record, was 56 different individuals; in a period of independent sampling separated by at least one day, it was 58 different individuals; and in a period of independent sampling separated by one week, it was 128 different individuals. The mean abundance of the species, together with its 95 % confidence interval, calculated from independent samples separated by more than one hour, was 26 ± 4 ($K = 127$); while from independent samples separated by more than one hour and with more than one sheep per record, it was 45 ± 4 ($K = 83$); 93 ± 7 ($K = 49$) with independent samples separated by at least one day; and 129 ± 9 ($K = 7$) with independent samples separated by one week (Figure 6).

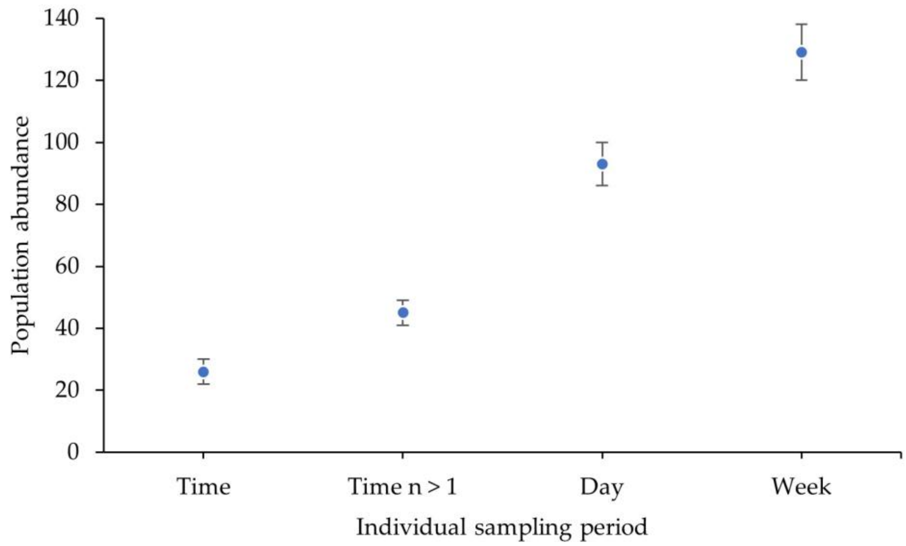

Figure 6. Average abundance ± 95 % confidence interval of the bighorn sheep (*Ovis canadensis* Shaw) population in the coastal region of the Sierra Santa Isabel in Baja California, Mexico, obtained from different sampling periods.

In terms of population structure, a similar age and sex class ratio was observed in the one-hour, one-hour capture periods with more than one sheep per record and one-day capture periods. It was found that the number of rams was double that of ewes, and that for every 10 ewes, there was one yearling and two lambs (Table 1). The age and sex class ratio obtained from the weekly samples collected indicated that the proportion of rams in the population was lower than that of ewes. However, as in the other sampling periods, it was observed that for every 10 ewes, there was one yearling and two lambs. Statistical comparison of the age-sex class ratio revealed that there was no difference between the proportion of males obtained from the different sampling periods (Kruskal-Wallis, $p \geq 0.05$). However, a difference was observed in the

Table 1. Population abundance of bighorn sheep (Ovis canadensis Shaw) according to sex and age in the Sierra Santa Isabel, Baja California, Mexico, for different s ampling periods.

Sex and age classification	Sampling period											
	Time			Time n > 1			Day			Week		
	x̄	σ	Me.	x̄	σ	Me.	x̄	σ	Me.	x̄	σ	Me.
Ram	21	20	17	23	25	15	22	30	12	8	1	8
Ewe	10			10			10			10		
Yearling	1	2		1	3		1	1	1	1	1	1
Lamb	2	3		2	3	1	2	2	2	2	1	2

x̄ : mean; σ: standard deviation; Me.: median.

proportion of yearlings (Kruskal-Wallis, $p \leq 0.05$) and lambs (Kruskal-Wallis, $p \leq 0.05$), being higher in the one-day and one-week trapping periods than in the one-hour and one-hour trapping periods with more than one sheep per record.

In the coastal region of the Sierra Santa Isabel, sheep were recorded in different social configurations: solitary, in pairs, and in herds that could be composed of up to 17 animals (Figure 7). The most commonly observed herds consisted of three to five sheep, while groups of six or more animals represented an observation rate of 1 to 2 % each. In terms of sex composition, 35 % of the records were of solitary rams, 17 % of groups of rams, and 13 % of solitary ewes. The other herd types and solitary sheep were observed with a frequency of less than 10 %.

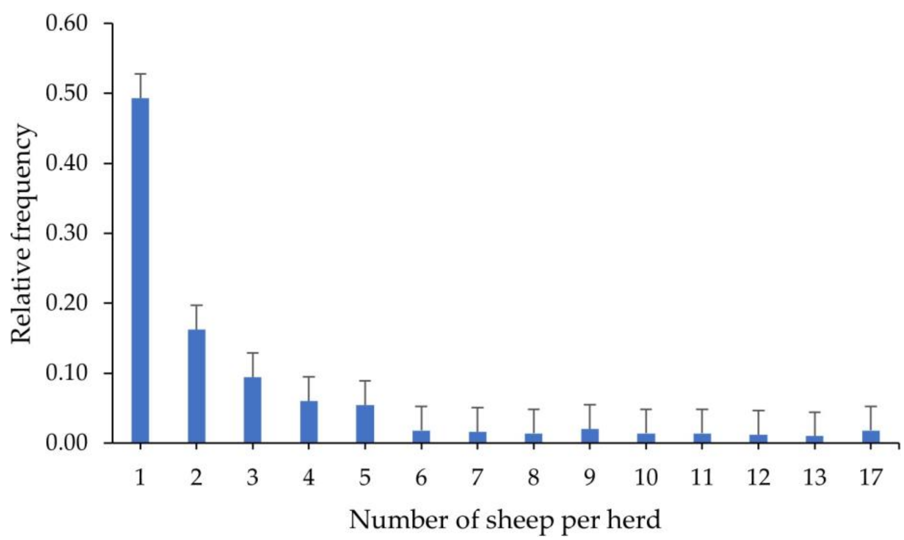

Figure 7. Relative frequency of the number of sheep (*Ovis canadensis* Shaw) that made up the herds recorded in the coastal region of Sierra Santa Isabel, Baja California, Mexico.

Romero-Figueroa *et al*. (2024) conducted an aerial count in the Sierra Santa Isabel, during which they observed 81 sheep and estimated a population abundance of 135 animals using a detectability rate of 60 %. This estimate is within the range of that obtained using trail cameras from independent samples separated by one week taken during the summer (129 ± 9). In the Black Mountains of Death Valley National Park and the Old Dad Mountain of the Mojave Desert, USA, accurate estimates of free-living bighorn sheep population size were also obtained by the Lincoln-Petersen method using camera traps deployed at waterholes during the summer and independently sampled one week apart (Jaeger *et al.*, 1991; Douglass and Longshore, 1995). In this sense, Perry *et al.* (2010) point out that summer is the season in which sampling should be carried out to estimate the bighorn sheep population using trail cameras because arid conditions serve to concentrate most, or all, of the individuals of a population in a few water sources.

Short periods of independent sampling, such as those separated by an hour or a day, tend to underestimate the population of the species because most of the records obtained of bighorn sheep through trail cameras correspond to solitary specimens (Perry *et al*., 2010; Escobar-Flores *et al*., 2016). Perry *et al*. (2010), who worked with a confined population at a site with artificial waterholes, corrected this bias by eliminating independent samples composed of a single specimen from the analysis. However, in the present study, a positive adjustment in the population estimate was not observed, which is attributed to the fact that in this area, most of the records corresponded to small groups (< 5 sheep), in contrast to the aforementioned study, where the record of large groups (> 5 sheep) was more frequent.

Bighorn sheep sighted in the coastal region of the Sierra Santa Isabel during aerial monitoring in 2021 were recorded at a distance between 12 and 45 km from the waterholes where trail cameras were deployed in 2022 (Romero-Figueroa *et al*., 2024). This distance between waterholes and animals observed in 2021 is within the home range of desert bighorn sheep in the fall (Longshore and Douglas, 1995; Hoglander *et al*., 2015), the season in which aerial monitoring was conducted. This suggests that the population monitored in the 2021 flight is the same as that monitored in 2022 in this study.

The ram:ewe:yearling:lamb ratio obtained from independent sampling periods separated by one week (8:10:1:2) is consistent with that reported on the western slope of the Sierra Santa Isabel (5:10:4; Escobar-Flores *et al*., 2016), on the Sierra de Las Pintas (7:10:1; López *et al*., 1995), and generally for the states of Baja California (6:10:1:1:1; Romero-Figueroa *et al*., 2024) and Arizona (5:10:4; Murphy, 2021). In the rest of the independent sampling periods, the ram:ewe ratio was 20:10. The high proportion of rams obtained from these periods is due to the fact that most of the photographic records were of solitary rams and groups of rams. In this sense, the ram:ewe:lamb:yearling ratio obtained from the short independent sampling periods did not reflect the population structure of the species but rather the intensity with which the different age classes and sexes made use of the areas in which the cameras were deployed.

The structure of bighorn sheep populations responds to their natural dynamics and the intensity of the extractive use to which they are subjected. In pristine populations of the species, there were 10 rams for every 10 ewes (Hansen, 1967). Currently, there are no bighorn sheep populations that maintain this ram:ewe ratio because in all their areas of distribution the species is exploited both legally (sport hunting) and illegally (poaching). In the coastal region of the Sierra Santa Isabel, the local community recognizes the incidence of poaching on their lands (Ruiz-Mondragón *et al*., 2023). This situation explains the ram:ewe ratio recorded at the site (8:10), which indicates that this is a population from which rams are extracted. On the other hand, bighorn sheep populations inhabiting desert ecosystems are characterized by low proportions of lambs and yearlings because recruitment occurs in boom and bust cycles linked to periods of drought and because these age classes have the highest mortality (Hansen, 1967).

The bighorn sheep population (129 individuals) was higher than estimated in six of the thirteen mountain ranges in Baja California where the species is distributed (Romero-Figueroa *et al*., 2024): Cucapá (31), Las Tinajas (27), San Pedro Mártir (65), San Francisquito (11), La Asamblea (111), and Las Ánimas (114). Furthermore, it is comparable to that reported in the El Peloncillo (140–160), Fra Cristóbal (150–200), and San Andrés (174) mountain ranges in New Mexico, USA (Ruhl and Rominger, 2021). Likewise, the ram:ewe ratio recorded in the coastal region of the Sierra Santa Isabel (8:10) was higher than that reported for the entire state of Baja California (6:10; Romero-Figueroa *et al*., 2024) and in the states of Arizona (5:10; Murphy, 2021) and Nevada (5:10; Cox, 2021). The bighorn sheep population in the coastal region of the Sierra Santa Isabel is one of the most abundant in the state of Baja California (Romero-Figueroa *et al*., 2024) and is comparable in size to those recorded in the mountain ranges of New Mexico, where several management measures are currently being implemented to increase the population of the species (Ruhl and Rominger, 2021). Furthermore, the number of rams per ten ewes is higher than reported in states such as Arizona and Nevada, where bighorn sheep populations are currently stable (Cox, 2021; Murphy, 2021).

In the coastal region of the Sierra Santa Isabel, as in other desert areas where bighorn sheep are distributed (Jaeger *et al*., 1991; Perry *et al*., 2010), a higher frequency of photography was observed during the hottest and driest months of the year. This is due to the fact that during the summer, the water consumption of sheep increases, and they require a minimum water intake equivalent to 4 % of their body weight (Monson and Sumner, 1980). This is why, at this time of the year, the surface area of the home range of sheep is reduced and concentrated near available water bodies (Longshore and Douglas, 1995; Hoglander *et al*., 2015).

The largest number of photographs was recorded at Tinaja del Miramar, which is the largest waterhole in the coastal region of the Sierra Santa Isabel. The same occurred on the western slope of the Sierra Santa Isabel, where the most commonly used water body is found (Escobar-Flores *et al.*, 2016). The species' preference for water holes with the highest water volume is explained by the concentration of dissolved solids, the increase of which reduces water quality. In the Sierra Santa Isabel, smaller water holes have a higher concentration of dissolved solids that increases in the dry season when water volume is reduced (Escobar-Flores *et al*., 2016). The decrease in records on the trail is attributed to the fact that, in June and July, the sheep concentrated their activities around the troughs that have water year-round. As for the Cinco Islas watering hole, its use decreased in the hottest months, as the amount of water in the hole during April and May decreased considerably by June and July.

CONCLUSIONS

The bighorn sheep population estimate calculated with the Lincoln-Petersen method using trail cameras deployed at waterholes during the summer and with independent samples separated by one week was comparable to that previously reported for the area using aerial monitoring. Likewise, the population structure obtained from this estimate was consistent with that expected for a free-living desert bighorn sheep population. Capture periods with independent sampling separated by one hour and one day yielded lower abundances than previously reported for the area, along with an age and sex class ratio that did not reflect the population structure of the species, but rather the use that each of these groups made of the sites where trail cameras were deployed. The abundance of the bighorn sheep population in the coastal region of the Sierra Santa Isabel was 129 ± 9 animals, and the ram:ewe:yearling:lamb ratio was 8:10:1:2. These results suggest that the population of the species at this site is in a good state of conservation.

ACKNOWLEDGMENTS

To the Autonomous University of Baja California for funding project no. 400/2975. To the UABC Foundation for arranging funding for this research. To the Secretariat of Science, Humanities, Technology, and Innovation (SECIHTI) for the postgraduate scholarship awarded to the first author. To the members of the Matomí Ejido for allowing us to carry out this research on their property. To Mr. Agustín Ramírez for sharing his knowledge of the study area. To the anonymous reviewers and associate editor whose comments enriched the manuscript.

REFERENCES

Alonso R, McClintock B, Lyren L, Boydston E, Crooks K. 2015. Mark-recapture and mark-resight methods for estimating abundance with remote cameras: A carnivore case study. PLoS ONE 10 (3): e0123032. https://doi.org/10.1371/journal.pone.0123032

Bolen EG, Robinson WL. 2003. Wildlife ecology and management (Fifth edition). Prentice Hall Inc: Upper Saddle River, NJ, USA. 605 p.

Chapman D. 1951. Some properties of the hypergeometric distribution with applications to zoological censuses. University of California Publications in Statistics 1: 131–160.

Conroy MJ, Harris G, Stewart DR, Butler MJ. 2018. Evaluation of desert bighorn sheep abundance surveys, southwestern Arizona, USA. The Journal of Wildlife Management 82 (6): 1149–1160. https://doi.org/10.1002/jwmg.21463

Cox M. 2021. Status of bighorn sheep in Nevada, 2019-2020. Desert Bighorn Council Transactions 56: 98–104.

Douglass C, Longshore K. 1995. Costs and effectiveness of methods used for population estimates of desert bighorn sheep in Death Valley National Park. Desert Bighorn Council Transactions 39: 1–9.

Escobar-Flores JG, Valdez R, Álvarez-Cárdenas S, Díaz-Castro S, Castellanos-Vera A, Torres J, Delgado-Fernández M. 2016. Utilización de aguajes por el borrego cimarrón (*Ovis canadensis cremnobates*) y análisis de calidad del agua en Sierra Santa Isabel, Baja California, México. Acta Universitaria 26 (1): 12–19. https://doi.org/10.15174/au.2016.822

Gallina-Tessaro S. 2015. Manual de técnicas del estudio de la fauna. Instituto de Ecología A.C.: Xalapa, México. 210 p.

Gastelum-Mendoza FI, Lozano-Cavazos EA, González-Saldívar FN, Uvalle-Sauceda JI, Romero-Figueroa G, Serna-Lagunes R, Tarango-Arámbula LA, Cantú-Ayala CM. 2024. Estrategias forrajeras del borrego cimarrón (*Ovis canadensis mexicana*) en el noreste de México. Ecosistemas y Recursos Agropecuarios 11 (1): e3921. https://doi.org/10.19136/era.a11n1.3921

García E. 2004. Modificaciones al sistema de clasificación climática de Köppen (Cuarta edición). Universidad Nacional Autónoma de México: Ciudad de México, México. 217 p.

Geist V. 1968. On the interrelation of external appearance, social behaviour, and social structure of mountain sheep. Zeitschrift für Tierpsychologie 25 (2): 119–215.

Hammer Ø, Harper D, Ryan P. 2001. PAST: Paleontological statistics software package for education and data analysis. Paleontologia Electronica 4: 9.

Hansen C. 1967. Bighorn sheep populations of the desert game range. The Journal of Wildlife Management 31 (4): 693–706. https://doi.org/10.2307/3797972

Harris G, Butler M, Stewart D, Rominger E, Ruhl C. 2020. Accurate population estimation of Caprinae using came traps and distance sampling. Scientific Reports 10 (1): 17729. https://doi.org/10.1038/s41598-020-73893-5

Hoglander C, Dickson B, Rosenstock S, Anderson J. 2015. Landscape models of space use by desert bighorn sheep in the Sonoran Desert of southwestern Arizona. The Journal of Wildlife Management 79 (1): 77–91. https://doi.org/10.1002/jwmg.818

Jaeger J, Wehausen J, Bleich V. 1991. Evaluation of time-lapse photography to estimate population parameters. Desert Bighorn Council Transactions 35: 5–8.

Kuvlensky W, Henke S, Brennan L, Ballard B, Cherry M, Hewitt D, Campbell T, Deyoung R, Anderson C, Hernández F. 2022. Managing populations. *In* Krausman PR, Cain III JW. (eds.), Wildlife Management and Conservation: Contemporary Principles and Practices (Second edition). Johns Hopkins University Press: Baltimore, MD, USA, pp: 383–414.

Lee R. 2011. Economic aspects of and the market for desert bighorn sheep. Desert Bighorn Council Transactions 51: 46–49.

López G, Ruiz-Campos G, Rodríguez-Meraz M. 1995. Population density of desert bighorn in northern Baja California, Mexico (cañadas Arroyo Grande and Jaquejel). Desert Bighorn Council Transactions 39: 42–49.

Longshore K, Douglas C. 1995. Home ranges of desert bighorn sheep inhabiting the black mountains, Death Valley National Park, California. Desert Bighorn Council Transactions 39: 26–35.

Miranda F, Hernández E. 1963. Los tipos de vegetación de México y su clasificación. Boletín de la Sociedad Botánica de México 28: 29–179. https://doi.org/10.17129/botsci.1084

Monson G, Sumner L. 1980. The desert bighorn: Its life history, ecology, and management. The University of Arizona Press: Tucson, AZ, USA. 370 p.

Murphy R. 2021. Status of bighorn sheep in Arizona, 2020. Desert Bighorn Council Transactions 56: 83–86.

Palencia P, Rowcliffe J, Vicente J, Acevedo P. 2021. Assessing the camera trap methodologies used to estimate density of unmarked populations. Journal of Applied Ecology 58 (8): 1583–1592. https://doi.org/10.1111/1365-2664.13913

Perry T, Newman T, Thibault K. 2010. Evaluation of methods used to estimate size of a population of desert bighorn sheep (*Ovis canadensis mexicana*) in New Mexico. The Southwestern Naturalist 55 (4): 517–524. https://doi.org/10.1894/SGM-07.1

Pollock K, Nichols J, Brownie C, Hines J. 1990. Statistical inference for capture-recapture experiments. Wildlife Monographs 107: 1–98.

Romero-Figueroa G, Ruiz-Mondragón EJ, Shahriary E, Yee-Romero C, Guevara-Carrizales AA, Paredes-Montesinos R, Corrales-Sauceda JM, Guerrero-Cárdenas I, Valdez R. 2024. Population and conservation status of bighorn sheep in the state of Baja California, Mexico. Animals 14 (3): 504. https://doi.org/10.3390/ani14030504

Rosas-Rosas O, Valdez R, Bender LC, Daniel D. 2003. Food habits of pumas in Northwestern Sonora, Mexico. Wildlife Society Bulletin 31 (2): 528–535.

Ruhl C, Rominger E. 2021. Status of desert bighorn sheep in New Mexico, 2019-2020. Desert Bighorn Council Transactions 56: 105–108.

Ruiz-Mondragón EdJ, Romero-Figueroa G, Paredes-Montesinos R, Tapia-Cabazos LA, Méndez-Rosas LA, Venegas-Barrera CS, Arrellano-García ME, Guerrero-Cárdenas I, Lozano-Cavazos EA. 2023. Community-based workshops to involve rural communities in wildlife management case study: Bighorn sheep in Baja California, Mexico. Animals 13 (20): 3171. https://doi.org/10.3390/ani13203171

Sandoval A, Valdez R, Espinosa-T A. 2019. Desert bighorn sheep in Mexico. *In* Valdez R, Ortega A. (ed.), Wildlife ecology and management in Mexico. Texas AyM University Press: College Station, TX, USA, pp: 350–365.

SEMARNAT (Secretaría de Medio Ambiente y Recursos Naturales). 2019. MODIFICACIÓN del Anexo Normativo III, Lista de especies en riesgo de la Norma Oficial Mexicana NOM-059-SEMARNAT-2010, Protección ambiental-Especies nativas de México de flora y fauna silvestres-Categorías de riesgo y especificaciones para su inclusión, exclusión o cambio-Lista de especies en riesgo, publicada el 30 de diciembre de 2010. 93 p.

Vidal R. 1990. Precipitación media anual. Comisión Nacional para el Conocimiento y Uso de la Biodiversidad. Ciudad de México, México. http://www.conabio.gob.mx/informacion/gis/?vns=gis_root/clima/precip/preci4mgw (Retrieved: June 2024).

VOLUME 59, NUMBER 3 | April 01 - May 15, 2025 | MEXICO